



PHD

**Biomechanical Analysis of Cervical Spine Injury Mechanisms in Rugby through Computational and Modelling Techniques**

Silvestros, Pavlos

*Award date:*  
2020

*Awarding institution:*  
University of Bath

[Link to publication](#)

**Alternative formats**

If you require this document in an alternative format, please contact:  
[openaccess@bath.ac.uk](mailto:openaccess@bath.ac.uk)

**General rights**  
Unspecified

Copyright of this thesis rests with the author. Access is subject to the above licence, if given. If no licence is specified above, original content in this thesis is licensed under the terms of the Creative Commons Attribution-NonCommercial 4.0 International (CC BY-NC-ND 4.0) Licence (<https://creativecommons.org/licenses/by-nc-nd/4.0/>). Any third-party copyright material present remains the property of its respective owner(s) and is licensed under its existing terms.

**Take down policy**

If you consider content within Bath's Research Portal to be in breach of UK law, please contact: [openaccess@bath.ac.uk](mailto:openaccess@bath.ac.uk) with the details. Your claim will be investigated and, where appropriate, the item will be removed from public view as soon as possible.

# Biomechanical Analysis of Cervical Spine Injury Mechanisms in Rugby through Computational and Modelling Techniques

submitted by

Pavlos Silvestros

for the degree of Doctor of Philosophy

of the

University of Bath

Department for Health

August 2020

## **COPYRIGHT**

Attention is drawn to the fact that copyright of this thesis rests with the author. A copy of this thesis has been supplied on condition that anyone who consults it is understood to recognise that its copyright rests with the author and that they must not copy it or use material from it except as permitted by law or with the consent of the author.

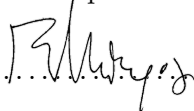
Access to this thesis in print or electronically is  
restricted until ..... (date). Signed on behalf on the  
Doctoral College ..... (print name).





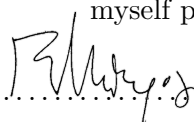
**DECLARATION OF ANY PREVIOUS SUBMISSION OF THE WORK**

The material presented here for examination for the award of a higher degree by research has not been incorporated into a submission for another degree.

Candidate's signature:  .....

**DECLARATION OF AUTHORSHIP**

I am the author of this thesis, and the work described therein was carried out by myself personally.

Candidate's signature:  .....



«Χαρά στὸν ἄνθρωπο, συλλογίζουμαι, ποὺ ἀξιώθηκε, προτοῦ πεθάνει, ν' αρμενίσει τὸ Αἰγαῖο.»

ΒΙΟΣ ΚΑΙ ΠΟΛΙΤΕΙΑ ΤΟΥ ΑΛΕΞΗ ΖΟΡΜΠΑ

Νίκος Καζαντζάκης



## Acknowledgements

First and foremost, I would like to thank my supervisors for their constant guidance and support throughout the last three years. Dario, who would have thought a first year undergraduate helping you set up the lab for data collection almost seven years ago would have led to this? Your enthusiasm and passion for research has motivated me to achieve all I have over the last few years. You are a mentor and a friend, thank you. Richie, your knowledge of the field always amazed me as after every meeting we shared I realised there is so much more to learn. Thank you for taking the time to guide me through topics I lacked experience in. Ezio, you have been my academic guide since I arrived at the University in 2013. Your calm and collectiveness always made me see aspects of academic and research choices from another viewpoint. If it wasn't for you in my undergraduate, I would likely not have been introduced to this research the way I was. Thank you for giving me the opportunity to make the most of it. Without the support from the RFU IPF I would not have been able to have this amazing experience, thank you for the funding of this work.

I would like to also thank Dr Claudio Pizzolato and Prof David Lloyd who hosted me at Griffith University. You provided an environment where it was easy to learn and enjoy an experience I never thought I was likely to have. Also my thanks to Dr Sabina Gheduzzi and Dr Tim Holsgrove for their guidance with experimental aspects of my work. Everyone at the ABS for providing a happy environment to work in, and especially to those that I shared the PhD office with for the light-heartedness and fun along the way as well as putting up with my idiocies towards the end. To my friends and housemates Alex and Will who I have shared countless laughs with over the years and instilled that "life is all about the banter". Especially Alex that made it easy to come home and relax and has put up with me the last couple of years. And of course to everyone at Oldfield Old Boys RFC who helped me fall in love with the game of rugby but also gain an applied aspect on my studies.

Finally, and I doubt my words will do them justice, to my family. Giles and Vic you have given me a base since I came to the UK for whenever I needed comfort or a break, thank you. Most of all however to my parents and sister. Mum, dad I don't need to put it on paper – you know everything I feel. You are the hardest working people I know and you have given me values which have sculpted me into who I am, I could never have asked for anything more. Eleni, I will always be there for you. This is for the three of you.



## Ευχαριστίες

Αρχικά θα ήθελα να ευχαριστήσω τους καθηγητές μου για την συνεχής καθοδήγηση και υποστήριξη τους κατά την διάρκεια των περασμένων τριών ετών. Ντάριο, ποιος θα γνώριζε πώς ένας πρωτοετής προπτυχιακού που σε βοήθησε να προετοιμάσεις το εργαστήριο πριν από επτά χρόνια θα οδηγούσε έως εδώ; Ο ενθουσιασμός και το πάθος σου για την έρευνα μου έδωσε το κίνητρο για να κατορθώσω όλα όσα έχω τα περασμένα χρόνια. Είσαι ο μέντορας και φίλος μου, σε ευχαριστώ. Ρίτσυ, οι γνώσεις σου για το πεδίο της μελέτης πάντα με εντυπωσίαζαν καθώς μετά από κάθε συζήτηση που μοιραζόμασταν κατανοούσα πως υπάρχουν τόσα πολλά ακόμα να μάθω. Ευχαριστώ για την υπομονή σου να με καθοδηγήσεις στα θέματα που οι γνώσεις μου ήταν ελλιπείς. Έτζιο, με έχεις καθοδηγήσει ακαδημαϊκά από τότε πού έφτασα στο πανεπιστήμιο το 2013. Η ηρεμία και ο συλλογισμός σου πάντα με βοηθούσαν να δω ακαδημαϊκές και ερευνητικές αποφάσεις από άλλη γωνία. Εάν δεν ήταν για εσένα στο προπτυχιακό μου πιθανόν να μην είχα παρουσιαστεί στην κόσμο της έρευνας με τον τρόπο πού είχα. Ευχαριστώ που μου έδωσες μια ευκαιρία που μπορούσα να αξιοποιήσω. Χωρίς την υποστήριξη του RFU IPF δεν θα μπορούσα να έχω αυτήν την απίστευτη εμπειρία, ευχαριστώ για την χορήγηση της έρευνας.

Θα ήθελα να ευχαριστήσω επίσης τον Δρ. Κλαούντιο Πιτζολάτο και τον Δρ. Ντάβιντ Λόϊντ που με φιλοξένησαν στο Πανεπιστήμιο του Γκρίφιθ. Προσφέρατε ένα περιβάλλον στο οποίο ήταν εύκολο να μελετήσω και να απολαύσω μια εμπειρία που δεν πίστευα να ήταν εφικτή. Επιπλέον ευχαριστώ την Δρ. Σαμπίνα Γκεντούτσι και Δρ. Τιμ Χόλσγκρουουβ για την καθοδήγηση τους σε πτυχές της εργαστηριακής μου μελέτης. Όλους στα γραφεία του Α.Μ.Σ. που πρόσφεραν ένα ευτυχισμένο περιβάλλον για εργασία και ειδικά σε αυτούς με τους οποίους μοιράστηκα το γραφείο τον μεταπτυχιακών σπουδών για την ανοιχτόκαρδη ατμόσφαιρα. Στους φίλους και συγκατόικους μου Άλεξ και Ουίλ με τους οποίους μοιράστηκα αμέτρητα γέλια και χαβαλέ. Ειδικά τον Άλεξ με τον οποίο ήταν εύκολο να ησυχάσω στο σπίτι και με επέμενε τα τελευταία δύο χρόνια. Αλλά βέβαια και σε όλους στην ομάδα Όλντφιελντ Όλντμποϊς που με βοήθησαν να αγαπήσω το ράγκμπι και να αποκτήσω μία επιπλέον εφαρμοσμένη κατανόηση για την έρευνα μου.

Τελικά - και πιστεύω πώς τα λόγια μου δεν θα είναι επαρκή - στην οικογένεια μου. Τζάιλζ και Βίκυ ήσασταν η βάση μου από την στιγμή που ήρθα στην Αγγλία όποτε χρειαζόμουν φροντίδα ή ένα διάλειμμα, σας ευχαριστώ. Πάνω από όλα όμως στους γονείς και την αδερφή μου. Μπαμπά, μαμά δεν χρειάζεται να το γράψω κάτω - ξέρετε ακριβώς πώς νιώθω. Δουλεύετε πιο σκληρά από οποιονδήποτε άλλον ξέρω και με έχετε δώσει αξίες που με γαλούχησαν στον άνθρωπο ο οποίος είμαι τώρα, δεν θα μπορούσα ποτέ να ζητήσω για τίποτε παραπάνω. Ελένη, ξέρεις πως θα είμαι πάντα δίπλα σου. Αυτό είναι για τους τρεις σας.





## Abstract

In this thesis an integrated biomechanical framework was developed and applied for the investigation of catastrophic cervical spine injuries in rugby. The main aims of the thesis were to identify the primary injury mechanism of the commonly observed bilateral facet dislocations and secondly highlight the implications of technique on cervical spine injury risk during misdirected impacts. The integrated framework combined experimental *in vitro* and *in vivo* data that guided *in silico* methodologies to provide the most realistic representation of the injurious events. Firstly impact specific passive joint parameters (stiffness and damping) were estimated that described the cervical spine's response to axial loads representative of misdirected rugby impacts. Results showed a larger increase in axial joint stiffness compared to damping which was representative of the rate dependant loading response of intervertebral discs. Secondly a MRI-informed musculoskeletal model was developed and used for the estimation of neck muscle recruitment patterns experienced by players prior to rugby contact events. Knowledge of how muscles activate prior to impacts is crucial to describe the dynamic response of the cervical spine to misdirected loading. An EMG-assisted optimisation methodology was applied for the analysis of *in vivo* staged tackles and scrums in order to estimate neck muscle activations using the MRI-informed model. The EMG-assisted method tracked experimental neck joint moments (RMSE = 0.95-1.07 Nm;  $R^2 = 0.90-0.95$ ) whilst generating physiological muscle activation patterns (RMSE < 0.1;  $R^2 > 0.8$ ) and maintaining experimental co-contraction ratios. Finally and in order to answer the original research questions the passive parameters were included in the MRI-informed musculoskeletal model which was then used in theoretical simulations. Estimated *in vivo* neck muscle activations and kinematics during rugby tackles were prescribed to the model and *in vitro* impact forces were applied to seven skull locations. The initial neck angle of the model was changed through  $5^\circ$  increments to investigate the effect of tackling technique. Results showed that initial neck flexion angles and cranial head impact locations had the largest effects on maximal compression, anterior shear and flexion moment loads. The pattern and combination of these loads in the lower cervical support buckling as the primary injury mechanism for rugby injuries and highlights the importance of correct tackling technique to reduce injury risk. In conclusion, this thesis provided the first evidence-based biomechanical evaluation of rugby spinal injuries within an injury prevention research model. This framework can inform future neck and head injury prevention policies in rugby and other impact sports.

## Dissemination of thesis and other research during period of studies:

### Research articles

**Silvestros P**, Pizzolato C, Lloyd DG, Preatoni E, Gill HS and Cazzola D (2020). EMG-assisted models estimate physiological muscle activations and moment equilibrium across the neck before impacts. *Annals of Biomedical Engineering*.

(Under Review)

Lenihan JN, Pascual SR, **Silvestros P**, Beak P, Miles AW and Trompeter A (2020). Novel techniques demonstrate superior fixation of simple transverse patella fractures - A biomechanical study. *Injury* 51(6): 1288-1293. <https://doi.org/10.1016/j.injury.2020.03.010>.

(NB Work not associated with this thesis.)

**Silvestros P**, Preatoni E, Gill HS, Gheduzzi S, Hernandez BA, Holsgrove TP and Cazzola D (2019). Musculoskeletal modelling of the human cervical spine for the investigation of injury mechanisms during axial impacts. *PLOS ONE* 14(5): e0216663. <https://doi.org/10.1371/journal.pone.0216663>

### Conference podium presentations

**Silvestros P**, Pizzolato C, Lloyd DG, Preatoni E, Gill HS and Cazzola D (2020). Estimation of neck muscle activation state using EMG-assisted methods in pre-impact events. *CAMS OpenSim Workshop*. ETH Zurich (CH). February 2020.

**Silvestros P**, Pizzolato C, Lloyd DG, Preatoni E, Gill HS and Cazzola D (2019). Estimation of neck muscle forces and function in the preparatory phase of rugby contact events. *Bath Biomechanics Symposium*. University of Bath (UK). September 2019.

Lenihan JN, Pascual SR, **Silvestros P**, Beak P, Miles AW and Trompeter A (2019). Novel techniques for Superior Fixation of Simple Transverse (34C) Patella Fractures - A Biomechanical Study. *X British Orthopaedic Association Congress*. Liverpool (UK). September 2019.

(NB Work not associated with this thesis.)

**Silvestros P**, Cremen E, Preatoni E, Seminati E and Cazzola D (2019). Measurement of head forces magnitude and location during live scrummaging. *XXVII Congress of the International Society of Biomechanics*. Calgary (CAN). August 2019.

(NB Work not included in this thesis.)

**Silvestros P**, Preatoni E, Gill HS and Cazzola D (2019). Evaluation of optimised cervical spine viscoelastic elements for sport injury analysis. *XVII International Symposium on Computer Simulation in Biomechanics*. Canmore (CAN). July 2019.

**Silvestros P**, Preatoni E, Gill HS, Gheduzzi S, Hernandez BA, Holsgrove TP and Cazzola D (2018). Development of a musculoskeletal cervical spine model for the use in the biomechanical analysis of axial impacts. *Bath Biomechanics Symposium*. University of Bath (UK). September 2018.

Boyd S, **Silvestros P**, Hernandez BA, Cazzola D, Preatoni E, Gill HS and Gheduzzi S (2018). Comparison of vertebral body displacements obtained by DIC and motion capture in a cervical spine impact experiment. *British Orthopaedic Research Society Conference*. Leeds (UK). September 2018.

**Silvestros P**, Boyd S, Hernandez BA, Gheduzzi S, Gill HS, Preatoni E and Cazzola D (2018). Estimation of viscoelastic bushing parameters of a musculoskeletal cervical spine model in impact scenarios. *British Orthopaedic Research Society Conference*. Leeds (UK). September 2018.

**Silvestros P**, Preatoni E, Gill HS, Gheduzzi S, Hernandez BA, Holsgrove TP and Cazzola D (2018). Estimation of cervical spine internal loads with the use of validated bushing elements for sport collisions. Application in the analysis of head impacts in rugby contact events. *VIII World Congress of Biomechanics*. Dublin (IRE). July 2018.

### Acquired funding

University of Bath Research Staff and Postgraduate Research Conference Funding (2020)	£500
University of Bath Research Staff and Postgraduate Research Conference Funding (2019)	£1000
University of Bath International Research Funding Scheme (2018)	£5000
ESA Academy Sponsorship (2018)	£200

### Public Engagement

Walking With Scientists (European Researchers' Night)	2019
Images of Research (University of Bath)	2018

### Accolades

Student committee member of the ISB Technical Group on Computer Simulation	2017-19
Winning Team of MultiSim Modellathon - INSIGNEO (University of Sheffield)	2017

# List of Figures

1-1	Contact events in the game of rugby (union). Scrum set-piece (left) and open play tackling (right) during professional (above) and community (below) levels of the game. . . . .	2
1-2	Incidence rates of rugby injuries by location (above) and inciting event (below). Recreated from a meta-analysis by <i>Williams et al. (2013) [159]</i> . . . . .	3
1-3	The van Mechelen (above) and TRIPP (below) injury prevention models. Dashed lines represent the practice usually observed in injury prevention research where Stage 2 is often skipped. Recreated and adapted from <i>van Mechelen et al. (1992) [149]</i> and <i>Finch (2006) [45]</i> . . . . .	5
1-4	Flowchart illustrating the structure of the research chapters in thesis including the main research questions and outputs of each chapter. . . . .	8
2-1	The human spinal column is comprised of the cervical, thoracic, lumbar and sacral regions. The lordotic curvature of the cervical and lumbar regions as well as the kyphotic curvature of the thoracic region can be identified. From Gray (1918). . . . .	10
2-2	Transverse cross-section at the level of the C6 vertebrae. From Gray (1918). . . . .	11
2-3	Skeletal anatomy of the C1 (top), C2 (middle) and C7 (bottom) vertebrae. From Gray (1918). . . . .	12
2-4	Passive structures of the ligaments and intervertebral discs across two spinal vertebrae (functional spinal unit). From Gray (1918). . . . .	13
2-5	Lateral view of the neck with superficial musculature (left) and anterior view of the cervical spine with deep musculature of the neck (right). From Gray (1918). . . . .	15
2-6	Jefferson fracture of the atlas (C1) (above) and Hangman's fracture of the axis (C2) (below). Adapted from Gray (1918). . . . .	17

2-7	MRI stills of C7 burst fracture caused by a motor-bike fall (left) and severe anterior dislocation with fracture caused by automotive roll-over crash (right). Damage to the spinal cord (dark grey shade) can be seen in both accidents. Images obtained from <i>radiopedia.org</i> . . . . .	19
2-8	Acute cervical spine injury during a rugby tackle sustained by the ball carrier (blue jersey). Images obtained from <i>dailymail.co.uk</i> . . . . .	20
2-9	Theorised mechanisms that occur in rugby cervical spine injuries. Adapted from <i>Dennison et al. (2012) [40]</i> . . . . .	22
2-10	The initial posture of the cervical spine together with its configuration after first order buckling occurred during experimental drop tests (above). An example of the variation in local forces as result of continued load acceptance after buckling occurs (below). The compressive impact force ( $P$ ) is shown as components of compression ( $P_c$ ) and shear ( $P_s$ ) on the end plates of C3 and C7 vertebrae. Adapted from <i>Kuster et al. (2012) [67]</i> . . . . .	24
3-1	Musculoskeletal models used for injury and functional movement analysis. Adapted from <i>de Bruijn et al. (2016) [37]</i> ; <i>Nightingale et al. (2016) [96]</i> ; <i>Vasavada et al. (1998) [152]</i> ; <i>Cazzola et al. (2017) [23]</i> and <i>Mortensen et al. (2018) [86]</i> . . . . .	33
3-2	Hill-type muscle model (above) with the muscle force-length (below - left), force-velocity (below - centre) and tendon-strain (below - right) curves. CE = contractile element; springs = passive elements; $l^M$ = muscle length; $l^T$ = tendon length; $l^{MT}$ = muscle-tendon unit length; $\alpha$ = pennation angle; $F_0^M$ = muscle force; $F_0^T$ = tendon force. Adapted from <i>Thelen (2003) [136]</i> . . . . .	35
3-3	Wrapping surfaces applied to the line of action for the semispinalis capitis (above - left) and sternocleidomastoid (above - right) muscles in Vasavada et al. (2008). Original linear (below - left) and curvilinear muscle paths (below - right) generated by moving muscle via-points in Suderman and Vasavada (2017). Adapted from <i>Vasavada et al. (2008) [151]</i> and <i>Suderman and Vasavada (2017) [133]</i> . . . . .	37
3-4	Axial MRI images and photographs showing differences in neck muscle volume and fat depositss (C6-C7 level) between matched controls (A) and former international forward (above) and back (below) rugby player. Adapted from <i>Brauge et al. (2015) [16]</i> . . . . .	39

4-1	Experimental set up of the spinal specimen positioned in the impact rig (left) and digital representation as a specimen specific model with virtual registered markers (right). Markers secured to the anterior aspect of the specimen and the cranial and caudal pots were used for the registration process during model creation. The markers of the cranial pot and the clusters secured to the C3, C4 and C5 vertebrae were used as tracking markers in the optimisation . . . . .	55
4-2	Joint and coincident 6 DOF viscoelastic bushing element locations. Only axial ( $F_y$ - left) and anteroposterior ( $F_x$ - right) viscoelastic elements were optimised, the parameters of the remaining four degrees of freedom remained at their initialised values. . . . .	56
4-3	Optimisation pipeline used to estimate specimen specific model viscoelastic joint parameters. Literature values [37] ( $k_1$ and $b_1$ ) were used to initialise the 6 DoF viscoelastic bushing elements of the specimen-specific models (SSM). A total of 16 optimised stiffness ( $k_{opt}$ ) and damping ( $b_{opt}$ ) for axial and shear degrees of freedom were estimated. . . . .	57
4-4	Axial loads measured at the cranial load cell during the experiments. The initial 5 ms (segmented vertical line) of the load traces were used to drive the forward dynamics simulations by applying them to the centre of mass of the C2 segments of the models. The legend denotes specimens S1 to S5. . . . .	59
4-5	Parameter values identified by the optimisation procedure. Axial stiffness (top left), shear stiffness (top right), axial damping (bottom left) and shear damping (bottom right). Values are shown for each of the cervical spine joints identified by the two red coloured vertebrae on the horizontal axis and for each of the five specimens identified by the legends. The legend denotes specimens S1 to S5. . . . .	60
4-6	Results of the 1000 sample Monte Carlo sensitivity analysis for the five specimen-specific models. Results are presented in order of their effect on the $\Delta RMSE = RMSE_{per}$ (largest to smallest). The axonometric view (central column) shows the response of the five models as the interpolated 3rd degree polynomial surfaces between the six possible parameter combinations. Left and right columns show the projection of each axis of the parameter variation against the $\Delta RMSE = RMSE_{per}$ on their respective sides for specimen S1 as an example of the response. . . . .	65

4-7	Forward dynamic results of theoretical injurious sporting scenario. Comparison of internal joint loads (Row 2) and resulting joint displacements (Row 3) calculated from the three versions of the musculoskeletal model and across three loading conditions (Row 1). Only joint loads are displayed for the Rugby Model (RM) as the kinematic constraints do not allow for joint translation which is displayed for Impact Specific (IS) and Quasi-Static (QS) versions of the model. . . . .	65
5-1	Representation of the three main steps to update the OpenSim Rugby Model's muscles paths: <b>A)</b> high resolution (1 mm isotropic) MRI scans of a rugby forward player's neck and upper-shoulder region were segmented yielding muscle and bone geometries together with muscle volume and centreline information; <b>B)</b> musculoskeletal geometries ( $\alpha$ ) and muscle centroid paths ( $\beta$ ) were imported into Matlab and parametric surfaces ( $\gamma$ ) were estimated based on [151]; <b>C)</b> parameters were used for the generation of wrapping surfaces in the OpenSim model (here only the muscles constrained by the defined wrapping surfaces are presented in the model and the scapulae removed for better visualisation of muscles).	81
5-2	Schematic overview of computational pipeline used in the study. The scaled musculoskeletal model was used in the analysis of calibration and execution trials with Inverse Kinematic, Inverse Dynamic and Muscle Analysis in OpenSim 3.3. The outputs of these analyses were then used in the CEINMS framework for all Static Optimisation (SO) and EMG-assisted (EMGa and EMGaMRI) neural solutions. For both the EMG-assisted solutions the model underwent the same calibration procedures with the exception of the EMGaMRI that derived muscle maximal isometric forces from the segmentation of muscles identifiable in the MRI. Calibration was completed on a set of dynamic and functional trials that was distinct from the execution trials (tackling and scrummaging) that were analysed with the three neural solutions. . . . .	83
5-3	Flowchart showing the inputs and resulting outputs for the two calibrations via a three stage process used for the EMGa and EMGaMRI solutions. For both EMGa and EMGaMRI the calibration procedure was the same apart from EMGaMRI where in Stage 1 $F_{max}^{iso}$ of the model's MTUs (n=44) were updated from segmented muscles volumes (n=26). .	86



5-4	Representation of how the 96 muscles of the model were separated into functional quadrants of left flexion (16 muscles), right flexion (16 muscles), left extension (32 muscles) and right extension (32 muscles). The separation of the muscles into functional quadrants allowed for the prescription of the experimental EMG signals (right/left sternocleidomastoid, right/left upper trapezius) to the respective functional muscle groups in the EMG-assisted methods. . . . .	87
5-5	RMSE (top) and $R^2$ (bottom) from the neuromusculoskeletal model with different neural solutions tracking inverse dynamics (ID) flexion/extension joint moments across different joints and trials. These are shown in violin plots that present individual (solid marker), mean (white marker) and density (coloured area shape) trial performance for SO (blue), EMGa (orange) and EMGaMRI (green) solutions. RMSE of each estimated joint moment is normalised to the range of the experimental joint moment (ID) of the respective joint and trial. . . . .	90
5-6	RMSE (top) and $R^2$ (bottom) from the neuromusculoskeletal model with different neural solutions when tracking inverse dynamics (ID) lateral bending joint moments across different joints and trials. These are shown in violin plots that present individual (solid marker), mean (white marker) and density (coloured area shape) trial performance for SO (blue), EMGa (orange) and EMGaMRI (green). RMSE of each estimated joint moment is normalised to the range of the experimental joint moment (ID) of the respective joint and trial. . . . .	91
5-7	RMSE (top) and $R^2$ (bottom) of neck different neural solutions when tracking experimental EMG signals (right trapezius, left trapezius, right sternocleidomastoid, left sternocleidomastoid) across different trials. These are shown in violin plots that present individual (solid marker), mean (white marker) and density (coloured area shape) trial performance for SO (blue), EMGa (orange) and EMGaMRI (green). Naming of MTUs is consistent with the OpenSim model. . . . .	92

5-8 Left: mean of 5 tackling trials' co-contraction index ( $CCI_{FE}$  and  $CCI_{LB}$  of the four experimental EMG signals (solid black) and estimated for SO (top - blue), EMGa (middle - orange) and EMGaMRI (bottom - green) for the 0.5 s before impact. Subplots show the muscle group activations used to calculate the estimated CCI values during an individual tackling trial (flexors and extensors ( $CCI_{FE}$ ; left and right lateral flexors for ( $CCI_{LB}$ . The 86 MTUs that had no measured experimental EMG and were either synthesised (SO) or adjusted (EMGa and EMGaMRI) from their input signal (mapped from the left and right sternocleidomastoid and upper trapezius muscles EMG) are shown in grey, the 10 for which experimental EMG was measured (constrained to the left and right sternocleidomastoid and upper trapezius muscles) in solid black and average activations for each muscle group are plotted as dashed lines for each solution. Centre: snapshots of the musculoskeletal model at the point of impact (depicted right) with MTUs coloured to matched the level of estimated excitations for each neural solution (red - high; blue - low). Right: still of the experimental set-up with the participant simulating a tackle during EMG and kinematic measurements. . . . . 94

6-1 A) Close up view of the scaled MRI informed OpenSim model's head and neck region with reference views of maximal ranges of motion tested in the simulations (muscles and wrapping surfaces removed for clarity of the cervical spine structure). Anteroposterior shear and Lateral Bending are defined by the X axis. Compression and Axial Rotation are defined by the Y axis. Lateral Shear and Flexion/Extension are defined by the Z axis. B) Neck muscle activation pattern estimated using EMG-assisted optimisation from staged experimental tackling and used across all simulations. During the staged experimental trials, the tackle was taken on the right shoulder which can be seen by the different levels of the model's muscle activations (red - maximum, blue - minimum). . . 108

6-2	<p><u>A)</u> Resultant impact force signals collected at two different impact speeds between the tackle simulator (mass = 40 kg) and the ATD. <u>B)</u> Cranial (left) and lateral (right) loading conditions applied to the skull (CA – Cranial Anterior; CC – Cranial Central; CA – Cranial Anterior; LP – Lateral Posterior; LMP – Lateral Mid Posterior; LMA – Lateral Mid Anterior; LA – Lateral Anterior). These were identified in Matlab by defining a grid of parallel transverse (n=2) and frontal (n=5) planes at 30 mm intervals to the skull segment’s geometry. The intersecting locations of the planes with the skull’s geometry defined four rectangular regions on the right side of the skull. Each parallelogram can be thought of an impact area on the musculoskeletal model skull to which a new plane was fitted. The point of impact force application for each of the four areas defined by the rectangular regions was the projected midpoint of the fitted plane onto the skull geometry. The directional vector was the normal vector of the fitted plane directed into the skull. . . . .</p>	109
6-3	<p>Workflow of integrated experimental and theoretical framework used to investigate cervical spine injury mechanism in rugby tackles. <u>Experimental:</u> <i>in vivo</i> data (neck muscle EMG and joint angles and velocities) were collected during stage tackling laboratory trials using a tackle simulator (mass= 40 kg; velocity = 2.0-2.5 and 3.1-3.6 m/s). <i>in vitro</i> data (force magnitude and loading rate) was collected from the Anthropometric Test Device (ATD) during simulated misdirected impacts to the head. <u>Theoretical:</u> for each of the 1638 simulations an initial neck angle configuration combining Flexion/Extension, Lateral Bending and Axial Rotation angles (<math>q_i</math>, n=117) taken from ranges in the literature was prescribed to the model. <i>in vivo</i> data at the time of impact were used to inform then initial neck joint angular velocities (<math>\dot{q}</math>) and joint angles of the torso and upper limbs. Level of neck muscle activations (<math>\alpha</math>) at the time of impact derived from EMG-assisted analysis of the staged tackling trial were applied to the model’s muscles to be constant throughout the 50 ms simulations. For each initial neck angle configuration (<math>q_i</math>) external loading conditions were applied (<math>\vec{F}_j^{Imp}</math>, n=14) replicating different impact locations on the head at two different speeds. The points of application and direction of the loading conditions were defined using the model’s skull geometry in Matlab. The magnitude and loading rate characteristics were taken from the first 50 ms of the <i>in vitro</i> ATD impact forces . . . . .</p>	111

- 6-4 Patterns of maximal compression (left) and anteroposterior shear (right) loading sustained during the 50 ms simulations across all simulated initial neck angles for cranial loading conditions. Column represents an individual loading condition (Cranial Posterior – left columns; Cranial Central – centre columns and Cranial Anterior – right columns). Rows represent the cervical spine levels from C3-C4 (top) to C6-C7 (bottom). The cubic grids of each subplot represents the initial neck angle ( $^{\circ}$ ) in Flexion/Extension (FE), Lateral Bending (LB) and Axial Rotation (AR). Magnitude of maximal loading (Newton) in the 50 ms simulations is represented with the colour bars. Note compression are only positive values and anteroposterior shear positive and negative values to represent direction with anterior and posterior respectively. . . . . 113
- 6-5 Maximal compressive joint loads (Newton) of C3-C4 (top row) to C6-C7 (bottom row) intervertebral joints plotted against  $5^{\circ}$  changes in Flexion(-)/Extension(+) (left column), Lateral Bending (centre column) and Axial Rotation (right column) during the cranial loading conditions (Cranial Posterior, Cranial Central and Cranial Anterior). First order polynomial lines of best fit are plotted to highlight the effect of joint angle on compressive joint loads for each loading condition (dashed lines). In each subplot data points are spread slightly in each  $5^{\circ}$  bin on the horizontal axes for better visualisation. . . . . 114
- 6-6 Maximal anteroposterior shear joint loads (Newton) of C3-C4 (top row) to C6-C7 (bottom row) intervertebral joints plotted against  $5^{\circ}$  changes in Flexion(-)/Extension(+) (left column), Lateral Bending (centre column) and Axial Rotation (right column) during the cranial loading conditions (Cranial Posterior, Cranial Central and Cranial Anterior). First order polynomial lines of best fit are plotted to highlight the effect of joint angle on compressive joint loads for each loading condition (dashed lines). In each subplot data points are spread slightly in each  $5^{\circ}$  bin on the horizontal axes for better visualisation. . . . . 115

6-7	Mean and standard deviation values for maximal compression (left column), anteroposterior (centre column) and flexion moment (right column) of all initial neck angle conditions plotted against changes in neck flexion (negative) and extension (positive) angles for cranial loading conditions. Estimated injury thresholds from the literature for the entire cervical spine are also presented with the horizontal lines for compression and anteroposterior shear and subjective thresholds of “ <i>maximum voluntary contraction</i> ” are presented for flexion moment. . . . .	117
6-8	Mean and standard deviation values for maximal compression, anteroposterior and flexion moment of all initial neck angle conditions plotted against changes in neck flexion (negative) and extension (positive) angles for lateral loading conditions. Estimated injury thresholds from the literature are presented with horizontal lines. . . . .	118
A-1	Changes in model MTU maximal isometric force values ( $F_{max}^{iso}$ ) informed from segmented muscle volumes. Grey bars represent individual MTU $F_{max}^{iso}$ values and black bars estimated values from MRI information. Multiple MTU under brackets are sub regions of an individual anatomical muscle (e.g. trap_acr and trap_cleid are both constituents of the <i>trapezius</i> ). Naming of MTUs consistent with OpenSim models. . . . .	137
B-1	Maximal flexion moment joint loads (Newton-meter) of C3-C4 (top row) to C6-C7 (bottom row) intervertebral joints plotted against 5° changes in Flexion(-)/Extension(+) (left column), Lateral Bending (centre column) and Axial Rotation (right column) during the cranial loading conditions (Cranial Posterior, Cranial Central and Cranial Anterior). In each subplot data points are spread slightly in each 5° bin on the horizontal axes for better visualisation. . . . .	144
B-2	Maximal compressive joint loads (Newton) of C3-C4 (top row) to C6-C7 (bottom row) intervertebral joints plotted against 5° changes in Flexion(-)/Extension(+) (left column), Lateral Bending (centre column) and Axial Rotation (right column) during the cranial loading conditions (Lateral Posterior, Lateral Mid Posterior, Lateral Mid Anterior and Lateral Anterior). In each subplot data points are spread slightly in each 5° bin on the horizontal axes for better visualisation. . . . .	145

B-3	Maximal anteroposterior shear joint loads (Newton) of C3-C4 (top row) to C6-C7 (bottom row) intervertebral joints plotted against 5° changes in Flexion(-)/Extension(+) (left column), Lateral Bending (centre column) and Axial Rotation (right column) during the cranial loading conditions (Lateral Posterior, Lateral Mid Posterior, Lateral Mid Anterior and Lateral Anterior). In each subplot data points are spread slightly in each 5° bin on the horizontal axes for better visualisation. . . . .	146
B-4	Maximal flexion moment joint loads (Newton-meter) of C3-C4 (top row) to C6-C7 (bottom row) intervertebral joints plotted against 5° changes in Flexion(-)/Extension(+) (left column), Lateral Bending (centre column) and Axial Rotation (right column) during the cranial loading conditions (Lateral Posterior, Lateral Mid Posterior, Lateral Mid Anterior and Lateral Anterior). In each subplot data points are spread slightly in each 5° bin on the horizontal axes for better visualisation. . . . .	147

# List of Tables

3.1	Multibody models used for functional and injury analysis . . . . .	34
3.2	Stiffness values of cervical spine segments about their six degrees of freedom	45
4.1	Descriptive data of porcine cervical spine segments (C2-C6). . . . .	54
4.2	Axial stiffness (k) and damping (b) parameter values identified for each specimen specific model of the spinal specimens (S1-S5). . . . .	61
4.3	Shear stiffness (k) and damping (b) parameter values identified for each specimen specific model of the spinal specimens (S1-S5). . . . .	62
4.4	Root mean square errors ( $RMSE_{opt}$ – Column 2) across the 15 tracking markers between measure and simulated kinematics during the optimisation procedure. Errors are also presented for the five-fold cross validation ( $RMSE_{val}$ – Column 3) and model evaluations using joint viscoelastic values from the literature [37] that were used to initialise the models at the start of each optimisation ( $RMSE_{lit}$ – Column 4). The calibration error of the motion capture system for each experimental measurement is presented for comparison (Column 5). . . . .	63
5.1	Neuromuscular parameters optimised in CEINMS calibration stage. For detailed explanation on these musculotendon and activation dynamics parameters refer to Lloyd and Besier [72] and Pizzolato et al. [103]. . .	84
6.1	Stiffness and damping parameter values used in bushing elements of the musculoskeletal model cervical spine joints (C2-C3 to C7-T1). . . . .	106

A.1	The 96 muscletendon units (MTUs) used in the model with indication to which functional quadrant they were assigned to, experimental excitation signal they received as initial input(SCM = <i>Sternocleidomastoid</i> and UT = <i>Upper Trapezius</i> ), if the mapped excitation signal was constrained (n=10) or adjusted (n=86) during the solution, if wrapping surfaces constrained the MTUs paths and the 44 MTUs' $F_{max}^{iso}$ were scaled from MRI measurements. . . . .	139
-----	---	-----



# Contents

<b>1</b>	<b>Introduction</b>	<b>1</b>
1.1	The game of rugby . . . . .	1
1.2	Injury prevention in sport . . . . .	3
1.3	Aims . . . . .	6
1.4	Thesis structure . . . . .	7
<b>2</b>	<b>Background</b>	<b>9</b>
2.1	Anatomy of the cervical spine . . . . .	9
2.2	The neck . . . . .	10
2.2.1	Skeletal anatomy . . . . .	11
2.2.1.1	Cervical vertebrae . . . . .	11
2.2.1.2	Intervertebral discs and ligaments . . . . .	12
2.2.2	Intervertebral joints . . . . .	14
2.2.3	Musculature . . . . .	14
2.2.4	Neurology . . . . .	15
2.3	Cervical spine injuries . . . . .	16
2.3.1	Types of cervical spine injuries . . . . .	16
2.3.1.1	Upper cervical spine (C1 and C2) . . . . .	16
2.3.1.2	Lower cervical spine (C3 to C7) . . . . .	17
2.3.1.3	Acute cervical spine injuries in rugby . . . . .	18
2.4	Injury mechanisms of the lower cervical spine . . . . .	21
<b>3</b>	<b>Computational methods for the investigation of cervical spine biomechanics</b>	<b>27</b>
3.1	Introduction . . . . .	28
3.2	Computational pathways for biomchanical investigation . . . . .	28
3.3	Computational models of the cervical spine . . . . .	30
3.3.1	Finite element models . . . . .	30

3.3.2	Musculoskeletal models . . . . .	33
3.3.2.1	Muscle modelling . . . . .	35
3.3.2.2	Redundancy problem . . . . .	40
3.3.2.3	Representation of passive joint properties . . . . .	42
3.4	Summary . . . . .	46
<b>4</b>	<b>Musculoskeletal modelling of the human cervical spine for the investigation of injury mechanisms during axial impacts</b>	<b>48</b>
4.1	Abstract . . . . .	50
4.2	Introduction . . . . .	51
4.3	Materials and Methods . . . . .	53
4.3.1	<i>In vitro</i> experiments . . . . .	53
4.3.2	Musculoskeletal model creation . . . . .	54
4.3.3	Optimisation Pipeline . . . . .	56
4.3.4	Validation and sensitivity analysis . . . . .	56
4.3.5	Application to an injurious sporting scenario . . . . .	58
4.4	Results . . . . .	59
4.5	Discussion . . . . .	66
4.5.1	Viscoelastic parameter estimation . . . . .	66
4.5.2	Model comparisons and application to injury prevention analysis	69
4.5.3	Limitations . . . . .	70
4.6	Conclusion . . . . .	71
4.7	Acknowledgements . . . . .	71
4.8	Competing Interests . . . . .	71
<b>5</b>	<b>EMG-assisted models estimate physiological muscle activations and moment equilibrium across the neck before impacts</b>	<b>72</b>
5.1	Abstract . . . . .	75
5.2	Introduction . . . . .	76
5.3	Materials and Methods . . . . .	77
5.3.1	Participant . . . . .	78
5.3.1.1	Medical imaging . . . . .	78
5.3.2	Experimental methods . . . . .	78
5.3.3	Musculoskeletal modelling . . . . .	79
5.3.4	Neuromuscular modelling . . . . .	82
5.3.5	Calibration . . . . .	82
5.3.6	Data analysis . . . . .	88
5.4	Results . . . . .	89

5.5	Discussion . . . . .	95
5.5.1	Limitations . . . . .	97
5.6	Conclusion . . . . .	98
5.7	Acknowledgements . . . . .	98
5.8	Conflict of interest . . . . .	98
<b>6</b>	<b>An integrated experimental and modelling approach indicates that buckling is the primary mechanism of cervical spine injury in rugby tackling</b>	<b>99</b>
6.1	Abstract . . . . .	102
6.2	Introduction . . . . .	103
6.3	Materials and Methods . . . . .	104
6.3.1	Experimental data . . . . .	104
6.3.1.1	<i>In vivo</i> . . . . .	104
6.3.1.2	<i>In vitro</i> . . . . .	105
6.3.2	Musculoskeletal simulations . . . . .	105
6.3.2.1	Musculoskeletal model . . . . .	105
6.3.2.2	Neck angle conditions . . . . .	106
6.3.2.3	Muscle activations . . . . .	106
6.3.2.4	Loading conditions . . . . .	107
6.3.2.5	Forward dynamic simulations . . . . .	110
6.4	Results . . . . .	112
6.5	Discussion . . . . .	119
6.5.1	Neck muscle forces . . . . .	120
6.5.2	Rugby tackling and injury mechanisms . . . . .	120
6.5.3	Limitations . . . . .	121
6.6	Conclusion . . . . .	123
<b>7</b>	<b>Epilogue</b>	<b>124</b>
7.1	Summary . . . . .	125
7.1.1	Contribution to the field of research . . . . .	129
7.2	Future outlook . . . . .	131
7.3	Conclusion . . . . .	134
<b>A</b>	<b>Appendix to Chapter 5</b>	<b>136</b>
A.1	Estimation of maximal isometric force and definition of musculoskeletal model wrapping surfaces from MRI measurements . . . . .	136

A.2 Mapping of experimental excitations to muscle tendon unit (MTUs) in CEINMS . . . . .	139
<b>B Appendix to Chapter 6</b>	<b>143</b>
B.1 Supplementary results . . . . .	143



# Chapter 1

## Introduction

This thesis investigates the biomechanics of cervical spine injuries observed in the game of rugby during contact events. An integrated methodological framework is presented that combines *in vivo*, *in vitro* and *in silico* biomechanical analyses, with the final aim of providing the best representation of injurious events, specifically during tackling. The framework allows for the prediction of potential "*what if*" injurious scenarios and their effect on internal loads experienced by the cervical spine joints that are impossible to investigate through experimental methods alone. The overarching goal of this work is to provide quantitative information that can be used to inform injury prevention policies and practices in the game of rugby.

### 1.1 The game of rugby

The game of Rugby union, commonly known as rugby, is a full contact field-based team sport. The latest annual report by the game's international governing body (World Rugby) stated that rugby is played across 124 countries (105 member unions and 19 associate unions) with a total of 9.6 million participating players across member unions. This was a 0.5 million increase from the previous year which included 0.3 million female players (World Rugby 2019 Annual Report [160]). The traditional form of the game is comprised by two teams of 15 players that run with the ball in hand with the aim of gaining territory on the field of play and scoring points through tries and kicks at goal. One of the key features of rugby is the physical contest for possession of the ball between players of the two opposing teams (Figure 1-1). Contests occur throughout the 80 minutes of play in different forms such as in tackles during open play and during scrums, lineouts, kick-offs and kicks to restart play.



Figure 1-1: Contact events in the game of rugby (union). Scrum set-piece (left) and open play tackling (right) during professional (above) and community (below) levels of the game.

The physically demanding nature of the game requires frequent exertions of high intensity activity in open play, such as running, sprinting, jumping and change of direction, as well as during contact, such as tackling, scrummaging, rucking and mauling. This combination of high physical demands and exposure to contact events during the game of rugby carries with it an inherent risk of injury. Rugby has one of the highest reported incidences of match injuries amongst any professional sport, comparable however to other contact sports such as ice hockey and American football [48, 111]. The incidence of rugby injuries differs by factors such as the type (e.g. neural, musculotendinous, structural and laceration), the location (head and neck, trunk, lower and upper limb etc.) and the inciting event (tackle, scrum, collision, ruck, maul, lineout etc.) where the injury occurred [159] (Figure 1-2). Understandably different combinations of these factors will lead to varying levels of injury severity for the players involved. This thesis will investigate the biomechanical mechanisms of acute catastrophic injuries sustained by the neck, specifically by the cervical spine, for the purposes of injury prevention strategies during rugby tackling. The epidemiology of catastrophic cervical spine in-

juries will be discussed in Chapter 2.

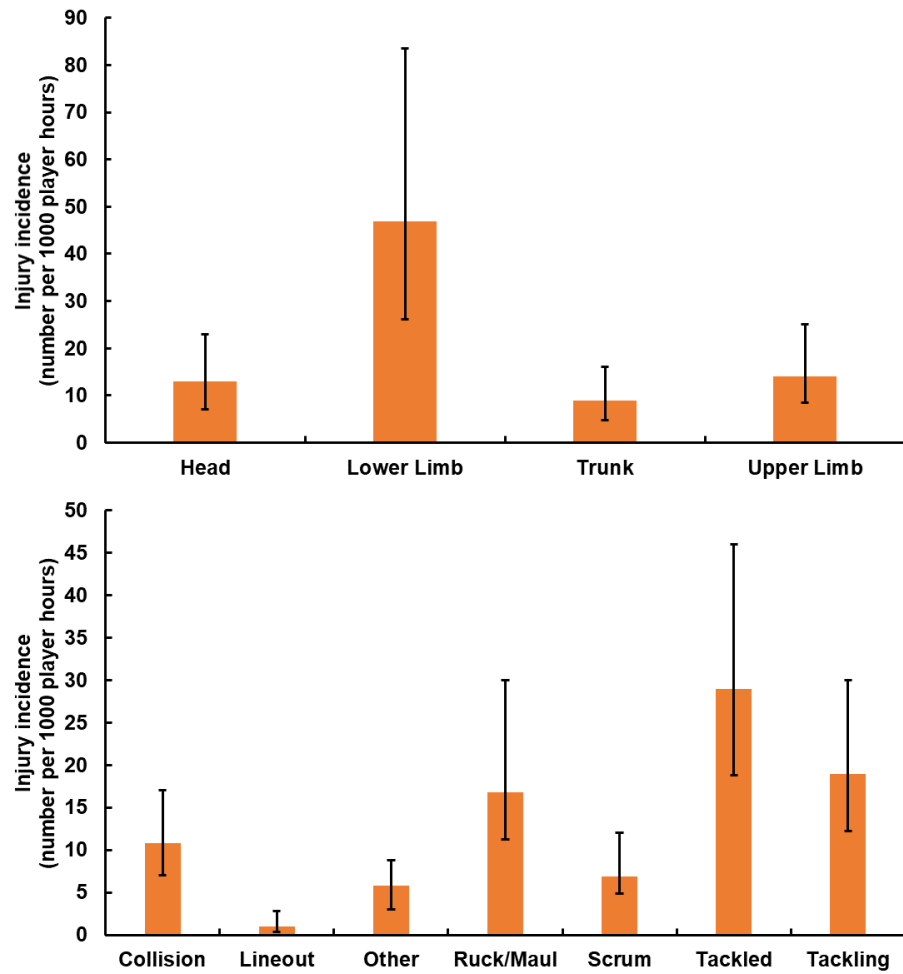


Figure 1-2: Incidence rates of rugby injuries by location (above) and inciting event (below). Recreated from a meta-analysis by *Williams et al. (2013) [159]*.

## 1.2 Injury prevention in sport

Injuries are, and are likely to forever be, an inherent risk associated with sporting participation and physical activity. Injury prevention strategies aim to understand their causes and mitigate the risk of injury to within acceptable levels. Models of sport injury prevention provide a research framework where theorised strategies that aim to reduce an identified injury risk can be translated into practice. The first widely adopted sport specific injury prevention model was the four stage model by van Mechelen et al. in



1992 [149]. In 2006 two more stages were proposed by Finch (2006) [45] through the TRIPP six-staged approach. The four main features of both of these models are first the identification of the problem (injury surveillance), establishment of the aetiology and mechanisms of injury, development of preventative measures and their final introduction into practice and evaluation. Injury surveillance data is largely based on the statistical evaluation of observed injuries which is crucial for informing and guiding the appropriate response needed to mitigate the associated injury risks. Too often than not however injury prevention strategies are tested or trialled in gameplay situations without adequate consideration for the underlying biomechanical mechanisms of the injury or the possible unintended consequences of the proposed interventions. This effectively bypasses Stage 2 of the van Mechelen [149] and the TRIPP models [45] (Figure 1-3). Biomechanical research is highlighted as an important aspect of these multidiscipline stages as such research can provide quantitative information for the external and resulting internal loads experienced by athletes [153]. Importantly correct biomechanical analysis can provide a detailed description of the inciting injury event which is a key element in the understanding of the situations injuries occur in [9]. In the past this area of research has been expensive, time consuming and often not highly representative of the situations in which these injuries occur due to necessary experimental simplifications. Unfortunately, these challenges have often detracted injury prevention researchers from investing in biomechanical research.

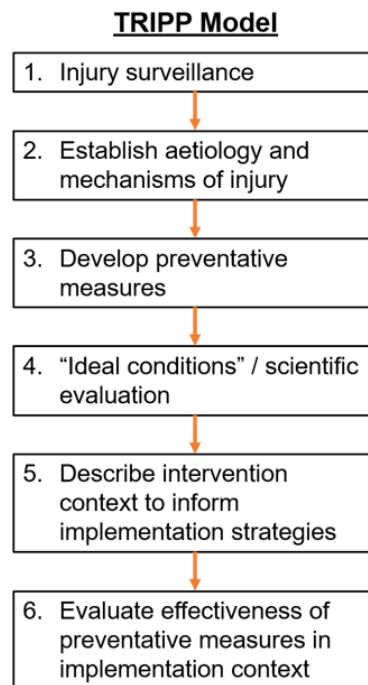
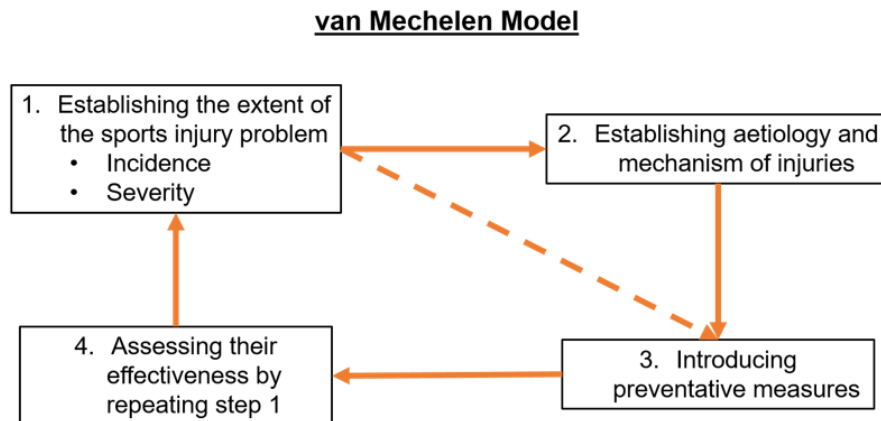


Figure 1-3: The van Mechelen (above) and TRIPP (below) injury prevention models. Dashed lines represent the practice usually observed in injury prevention research where Stage 2 is often skipped. Recreated and adapted from *van Mechelen et al. (1992) [149]* and *Finch (2006) [45]*.

68 In the case of cervical spine injuries biomechanical studies have been critical in sport  
 69 policy changes to increase player safety. For example, in 1976 and 2012 sporting law  
 70 changes took place to reduce incidence rates of severe cervical spine injuries during  
 71 spear tackling in American football [142] and rugby scrummaging [24, 104] respec-

tively. These events are characterised by impulsive impacts to the head and neck area of the athletes. Biomechanical research of impact injuries is regarded as an essential element in the prevention of acute trauma [153]. Therefore injuries of the complex cervical spine system within the dynamic rugby environment emphasise the necessity of correct biomechanical research inform the second stage of injury prevention models and complete the cycle. With the advent of increased computational power, applied questions in the context of sporting injuries regarding injury mechanisms, biomechanical responses to impact and impact tolerance levels can be investigated to a deeper degree than pure experimental methods through validated computational models. Biomechanical models can inform injury prevention strategies by identifying possible cause and effect relationships that may predispose or shield athletes from injuries [45]. The use of biomechanical models through computer simulations therefore provides an added advantage that cannot be obtained through experimental biomechanical, epidemiological or cohort studies alone.

### 1.3 Aims

The aim of this thesis is to develop, validate and utilise an integrated framework that utilises experimental and computational biomechanical methodologies. The framework will be used to profile internal cervical spine joint loads experienced during misdirected rugby impacts in order to understand the injury mechanisms commonly observed during these events. This will be attempted through answering the following research questions (Figure 1-4):

- How does the multi-level cervical spine respond to dynamic axial loads representative of misdirected rugby impacts. What are the structural parameters that can characterise the passive response of cervical spine joints to such loads in a musculoskeletal biomechanical model?
- What are the neck muscle recruitment patterns experienced by a rugby player before making contact during a tackle or a scrum?
- What are the implications to injury risk during misdirected or mistimed rugby tackles and what is the primary mechanism that causes them?
- How are specific aspects of technique associated with internal loads experienced by the cervical spine during these misdirected or mistimed impacts and how can this knowledge be translated into coaching?

## 1.4 Thesis structure

*Chapter 1*, provided an introduction to the topic of rugby and injury prevention research. The aims and objectives of this thesis were stated which will be answered through the investigation of acute cervical spine injuries observed in rugby.

*Chapter 2*, presents an anatomical overview of the human neck and cervical spine injuries. The theorised mechanisms that cause the acute neck injuries observed in rugby are presented and the biomechanical research used to investigate them is discussed.

*Chapter 3*, reviews available biomechanical methods used to investigate cervical spine injury mechanisms and identifies aspects of models and biomechanical methods that influence the development of computational models in injury prevention research.

*Chapter 4*, investigates how the multi-level cervical spine responds to impact loads representative of those experienced in rugby contact events. Novel structural viscoelastic parameters are identified through an optimisation methodology that characterise the passive response of the intervertebral joints to axial impulses. A sensitivity analysis is also performed on these parameters and a verification procedure is carried out.

*Chapter 5*, investigates how neck muscles are activated prior to rugby contact events. The first MRI-informed musculoskeletal model of a rugby athlete is developed and used in an EMG-assisted framework. The incorporation of the model within the EMG-assisted framework provides the first physiological estimates of neck muscle recruitment strategies prior to impact events (tackling and scrummaging) that match experimental net joint moment equilibrium across the cervical spine.

*Chapter 6*, examines the internal loading experienced by the cervical spine during mis-directed impacts representative of the conditions expected during rugby tackling. This is the first study within an injury prevention context to provide a complete biomechanical evaluation of injury mechanism analysis that is representative of the events under investigation. The impact specific viscoelastic parameters from *Chapter 4* are implemented within the MRI-informed model and the neck muscle activations from *Chapter 5* to investigate the injury mechanisms and how tackling technique can affect internal loads.

*Chapter 7*, provides a summary and discussion of the work completed in this thesis that investigated acute cervical spine injuries in the game of rugby. Future recommendations for further injury prevention research are made based on the novel methods and results of the thesis and their potential impact on rugby injury prevention policies.

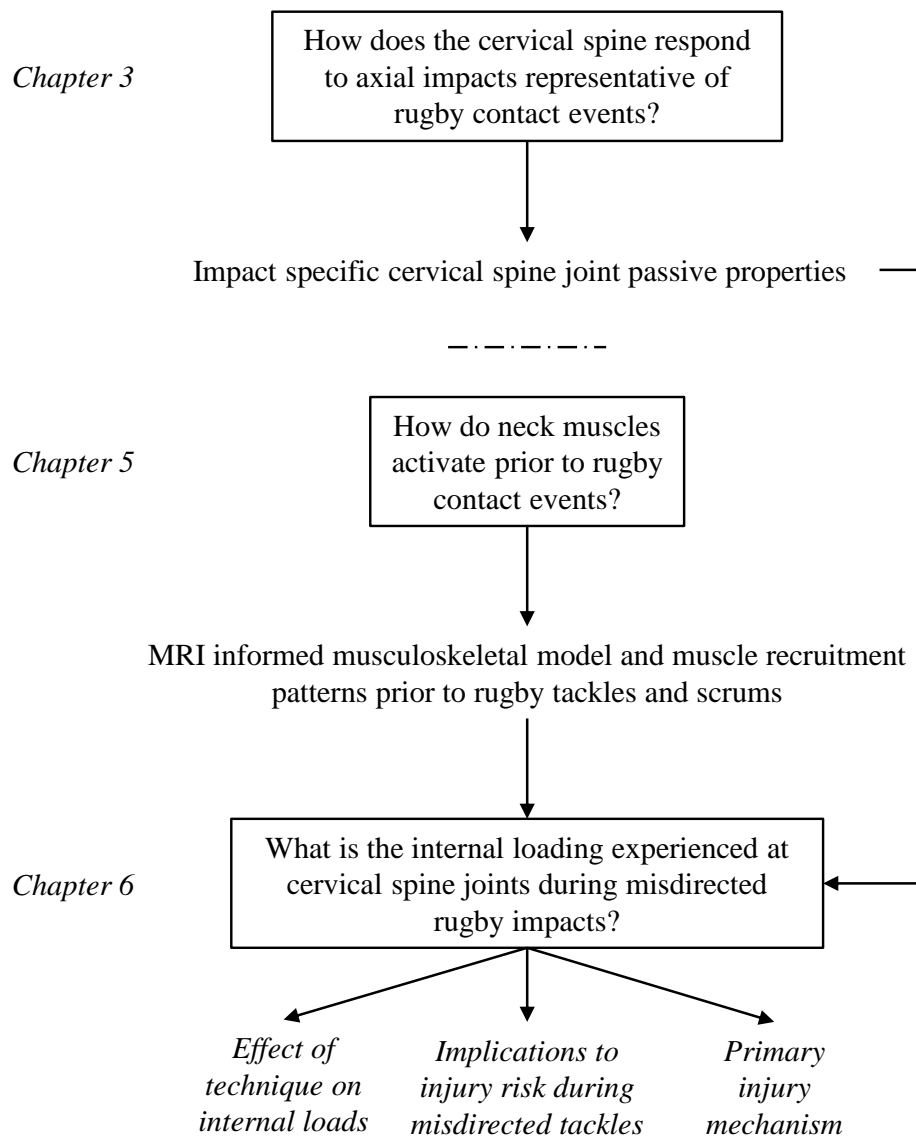


Figure 1-4: Flowchart illustrating the structure of the research chapters in thesis including the main research questions and outputs of each chapter.

## 137 Chapter 2

# 138 Background

139 This chapter will provide a brief anatomical overview of the osteology, myology and  
140 neurology of the human neck after which cervical spine injuries caused by acute trauma  
141 will be discussed together with the research that has aimed to identify causal injury  
142 mechanisms.

### 143 2.1 Anatomy of the cervical spine

144 The human spine extends from the neck to the coccyx and is one the most complex  
145 neuromusculoskeletal systems in the human body. As part of the axial skeleton it  
146 supports the weight of the head, torso and upper limbs by providing attachment points  
147 for many muscles and bones, its large flexibility allows for the generation of movement  
148 and it also houses and protects the spinal cord. The spinal column is comprised,  
149 cranially to caudally, of seven cervical, twelve thoracic, five lumbar, five fused sacral  
150 and three to four coccyx vertebrae (Figure 2-1).

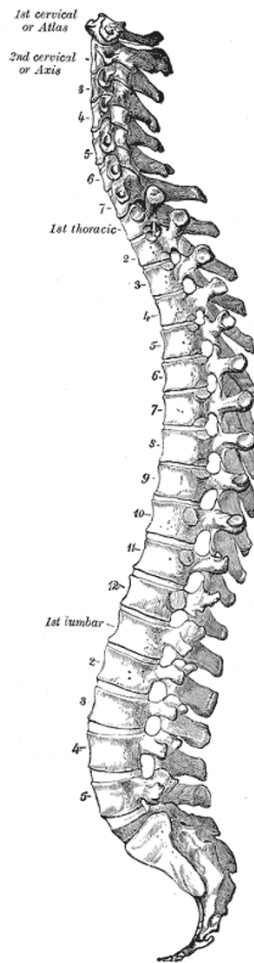


Figure 2-1: The human spinal column is comprised of the cervical, thoracic, lumbar and sacral regions. The lordotic curvature of the cervical and lumbar regions as well as the kyphotic curvature of the thoracic region can be identified. From Gray (1918).

## 2.2 The neck

151

The neck extends from the base of the head, caudally to the thorax, and laterally to the shoulders. It has four compartments housed by an outer musculofacial collar. These are the vertebral compartment containing the cervical vertebrae and musculature, the visceral compartment containing parts of the respiratory and digestive tracts and endocrine system and two vascular compartments bilaterally containing major neurovascular vessels (Figure 2-2). This thesis studies the biomechanics of sporting injuries to components of the vertebral compartment.

152

153

154

155

156

157

158

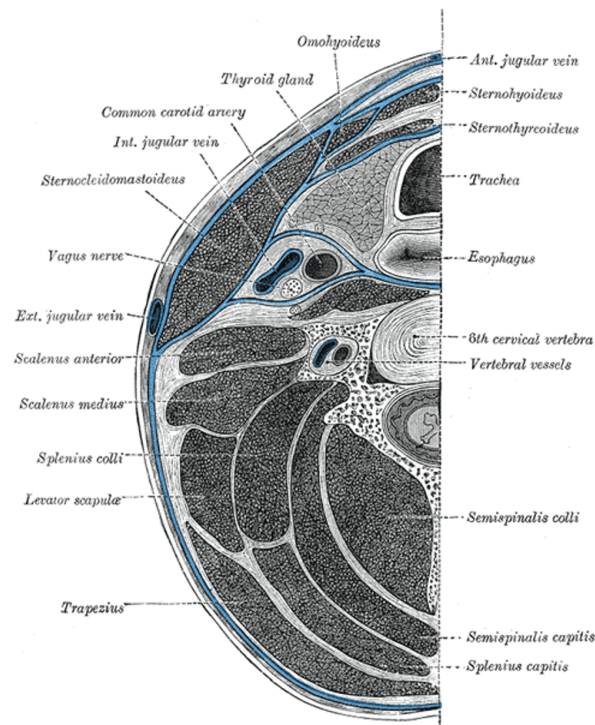


Figure 2-2: Transverse cross-section at the level of the C6 vertebrae. From Gray (1918).

## 159 2.2.1 Skeletal anatomy

### 160 2.2.1.1 Cervical vertebrae

161 The seven cervical vertebrae (C1 to C7) form the main skeletal structure of the neck  
 162 (Figure 2-3). Each vertebra, other than C1, consists anteriorly of the vertebral body  
 163 and posteriorly of the vertebral arch. The vertebral body is the major load bearing  
 164 element of the cervical vertebrae. Their size increases inferiorly representing the in-  
 165 creased load bearing in the lower cervical spine. The vertebral arch forms the lateral  
 166 and posterior parts of the vertebral foramen through which the spinal cord passes. Con-  
 167 nection between the vertebral arch and the vertebral body is made via the pedicles.  
 168 From the region of the pedicles superior and inferior articular processes are projected  
 169 that articulate with the inferior and superior articular processes of the adjacent ver-  
 170 tebrae respectively. The laminae are flat sheets of bone that extend posteriorly from  
 171 the pedicles and converge to form a junction from which the spinous process projects  
 172 posteriorly and inferiorly.



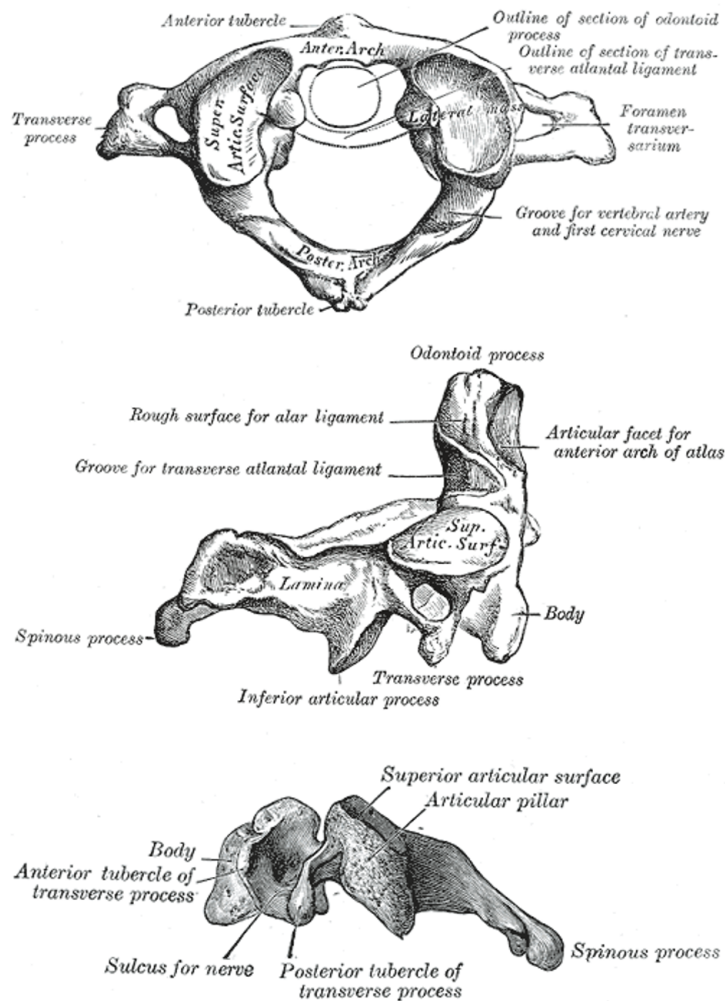


Figure 2-3: Skeletal anatomy of the C1 (top), C2 (middle) and C7 (bottom) vertebrae. From Gray (1918).

### 2.2.1.2 Intervertebral discs and ligaments

173

Between two adjacent cervical vertebrae (except between C1 and C2) lies an intervertebral disc. The role of the intervertebral discs is primarily to support the weight of adjacent vertebrae by absorbing compression forces and to a lesser degree to allow for intervertebral motion. Intervertebral discs consist of an outer annulus fibrosus which surrounds the central nucleus pulposus. The annulus fibrosus consists of an outer ring of collagen that surrounds fibrocartilage layers arranged in a lamellar configuration. The nucleus pulposus is a gelatinous substance that fills the area within the two adja-

174  
175  
176  
177  
178  
179  
180

cent vertebrae and the outer annulus fibrosus. Each disc is connected to the superior and inferior vertebral bodies via thin layers of hyaline cartilage called vertebral cartilaginous endplates which help maintain disc homeostasis.

Numerous ligaments provide support to intervertebral joints by spanning two or more cervical vertebrae. The anterior and posterior longitudinal ligaments are attached to the anterior and posterior aspects of the vertebral bodies respectively and span the length of the spinal column. Attaching to the posterior tips of the cervical spinous processes the ligamentum nuchae is an anatomically distinct portion of the supraspinal ligament that, like the longitudinal ligaments, spans the length of the spine. The ligamentum flavum and interspinous ligaments pass between the laminae and spinous processes of adjacent vertebrae. The intervertebral discs and ligaments together provide the passive structural stability of the cervical spine (Figure 2-4).

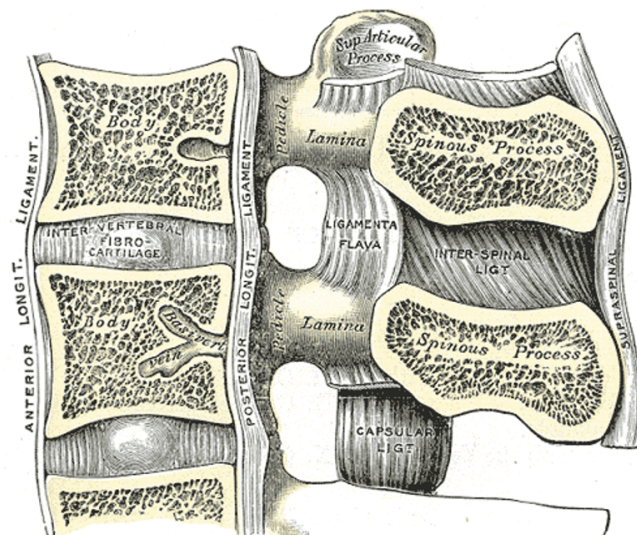


Figure 2-4: Passive structures of the ligaments and intervertebral discs across two spinal vertebrae (functional spinal unit). From Gray (1918).

### 2.2.2 Intervertebral joints

193

Vertebrae of the sub-axial cervical spine (C3 to C7) articulate with their adjacent  
vertebrae through two major types of joints. These are the symphyses between vertebral  
bodies as well as synovial joints between superior and inferior articular surfaces of  
adjacent vertebrae. For each joint the symphysis includes the intervertebral discs and  
is located anteriorly to the synovial joints. The synovial joints between the superior  
and inferior articular processes are the zygapophysial joints, also called facet joints.  
In the cervical spine the facet joints are inclined inferiorly from anterior to posterior  
allowing for a large range of motion in the sagittal plane. The atlas (C1) and axis  
(C2) differ from the sub-axial vertebrae (C3 to C7) and allow for head movement. The  
atlas lacks a vertebral body and articulates with the head via the atlanto-occipital  
joint. From the axis a bony projection called the dens articulates with the atlas via the  
atlanto-axial joint. Each intervertebral joint from C1-C2 to C7-T1 which includes the  
two adjacent vertebrae and their intermediate intervertebral disc is characterised as a  
functional unit.

207

### 2.2.3 Musculature

208

The vertebral compartment of the neck includes over 25 pairs of muscles organised into  
superficial and deep groups (Figure 2-5). Muscles unlike the aforementioned structures  
of the vertebrae, intervertebral discs and ligaments are active structures of the neck.  
Their functional role is to produce head movement and also stabilise the head and  
cervical spine column. Motion and stabilisation of the cervical spine is produced by  
muscles crossing single or multiple intervertebral joint levels generating complex lines of  
action to actuate the joints. Superficial neck muscles include the trapezius and levator  
scapulae that attach the head and cervical spine to the shoulder girdle to produce neck  
extension, lateral bending and shoulder elevation. Anteriorly the sternocleidomastoid  
muscle originates from the sternum and clavicle. It inserts into the mastoid process  
and the superior nuchal line to produce neck flexion, lateral bending and axial rotation.  
These superficial muscles are multiarticulate, have large moment arms about the joints  
and have large force generating capacities. Deep muscles are smaller and have less force  
generating capacity but provide stability and control to the intervertebral joints whilst  
also mobilising them. Larger deep muscle groups include the splenius capitis, semispinal  
capitis, semispinalis cervical, longus capitis and longus colli that are multiarticulate.  
The smaller muscle bundles of the multifidus can span one to three intervertebral  
joint levels. The suboccipital muscles are a small group of deep muscles in the upper  
cervical spine region that connect the atlas (C1) to the axis (C2) and both to the

227

base of the skull to extend the head. The neck musculature also helps to maintain the natural lordosis of the cervical spine and through passive muscle tone contributes to its structural stability.

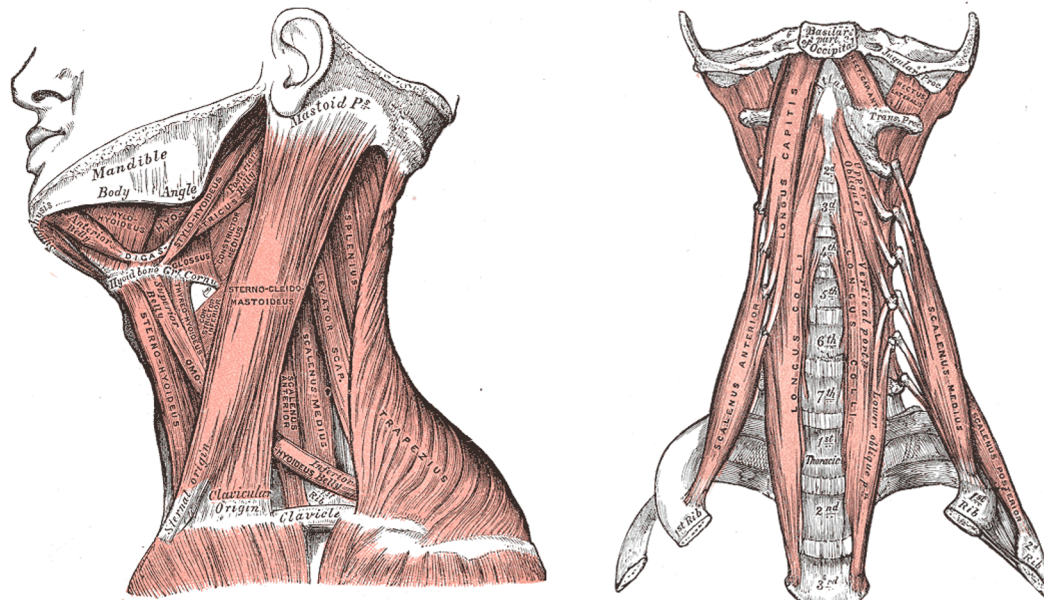


Figure 2-5: Lateral view of the neck with superficial musculature (left) and anterior view of the cervical spine with deep musculature of the neck (right). From Gray (1918).

#### 2.2.4 Neurology

The spinal cord passes through the vertebral canal formed by the vertebral foramina of all the spinal vertebrae. Its function is to transmit efferent and afferent nerve signals from the central nervous system to the peripheral nervous system and receive sensory stimuli respectively. It is also the centre for reflex generation. The spinal cord is not uniform in diameter across the length of the spine but has two enlargements. A cervical enlargement occurs between the regions where the C5 and T1 spinal nerves originate which innervate the upper limbs. The second enlargement is in the lumbar region.

Eight cervical nerves (C1 to C8) emerge from the vertebral canal above their respective vertebrae. In the cases of the C8 nerves emerge from the vertebral canal between the C7 and T1 vertebrae. The C1 to C4 nerves form the cervical plexus that supplies the neck musculature and diaphragm. The C5 to C8 nerves form the brachial plexus that innervate the upper limb and parts of the cervical musculature. Musculoskeletal injuries that damages the spinal cord or cervical nerves in the neck region can result

in the complete or partial impairment of motor and sensory function below the level of injury. The extent of the impairments depends on the severity of the injury to the spinal cord or cervical nerves. Injuries to the neural tissue do not allow nerve signals to pass beyond the level of injury and prohibit efferent commands reaching their targets or afferent stimuli to be processed in the brain.

## 2.3 Cervical spine injuries

Spinal cord injuries in the cervical spine area can occur during leisure, automotive and sporting accidents. These accidents may happen during diving, riding, surfing, motor vehicle rollovers, underbody blasts in the military, and sporting events such as American football, gymnastics, martial arts and rugby.

Spinal cord injuries are relatively rare, with total global prevalence of cases ranging between 28 and 130 per 100,000 of the population [99]. Although not all injuries are fatal they are life altering and can lead to dramatic reduction in the individual's quality of life. Furthermore, the direct and indirect socioeconomic costs to the injured and the immediate society are considerable. A recent collaborative report from the World Health Organisation and the International Spinal Cord Society [99] reported direct costs of approximately 750,000 to 1,000,000 USD during the first year of tetraplegic spinal cord injury and 110,000 to 180,000 USD for subsequent years. Life time indirect costs of all spinal cord injuries are estimated to be much greater with conservative estimates of 3.0 to 6.0 billion USD in the United States [46] and 1.4 billion GBP in the United Kingdom [74]. These values do not include cost estimates due to loss of productivity which is considerable as injuries predominantly occur in earlier age groups [99].

### 2.3.1 Types of cervical spine injuries

Common fracture and dislocation patterns differ between the upper (Skull to C2) and lower (C3 to C7) cervical spine. The main classifications are outlined below.

#### 2.3.1.1 Upper cervical spine (C1 and C2)

Damage to the spinal cord at this level affects neurological pathways to the upper limbs and vital organs resulting in severe loss of function, such as tetraplegia, or death. A Jefferson fracture is often described as the multipart fracture of the atlas (C1) [62] (Figure 2-6). The spinal instability at this level of the spinal cord caused by these fractures results in high levels of fatality [157]. The Hangman's fracture refers to

277 the traumatic posterior motion of the axis (C2) over the subjacent C3 (Figure 2-6).  
 278 Posterior spondylolisthesis of the C2 results in the fracture of the C2 pedicles disrupting  
 279 the vertebral arch of the C2. This injury also is linked with instability and as its name  
 280 suggests has historically been linked to fatal outcomes. An odontoid fracture is an  
 281 injury to the on odontoid or dens of the C2. These are also inherently unstable fractures  
 282 that can lead to atlanto-axial joint (C1-C2) dislocations and impingement of the spinal  
 283 cord. Depending on the severity of damage to the C2 vertebra they are classified into  
 284 three groups.

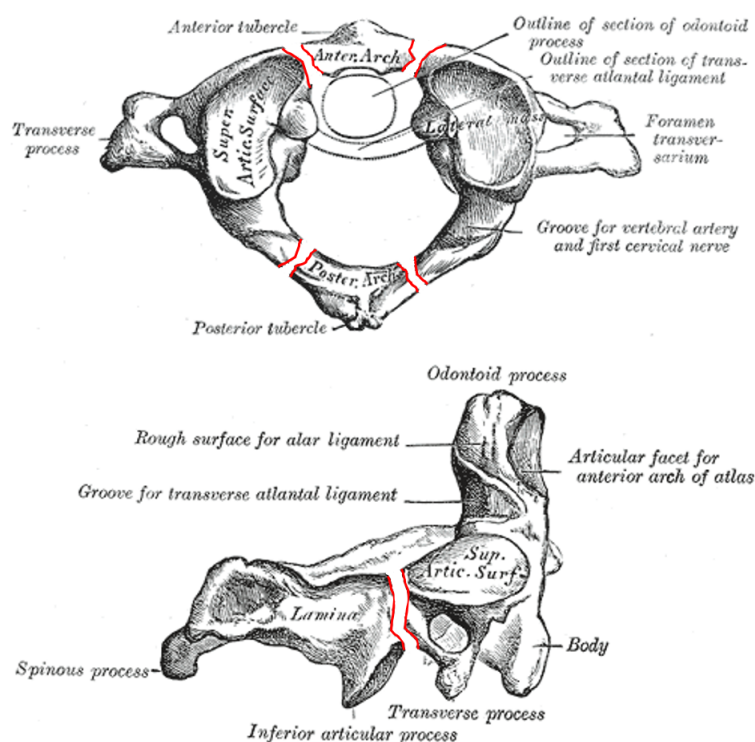


Figure 2-6: Jefferson fracture of the atlas (C1) (above) and Hangman's fracture of the axis (C2) (below). Adapted from Gray (1918).

#### 285 2.3.1.2 Lower cervical spine (C3 to C7)

286 Spinal cord injuries at this level do not typically result in fatalities however can cause  
 287 complete or partial impairment of lower limb motor control (paraplegia) and physiolog-  
 288 ical functions of the lower body, partial impairment of the upper limbs can also result  
 289 from these injuries. Dislocations of lower cervical spine joints occur when the verte-  
 290 bral body of a vertebra is subluxed anteriorly relative to the inferior vertebral body

(anterolisthesis) (Figure 2-7). Anterior translation of the superior body results in the dislocation of the inferior facet joints as the inferior articular processes of the vertebra is moved anteriorly over the superior articular process of the inferior vertebra. This dislocation of the facet joints results in the locking of the articular processes between each other which can occur on a single side, called a unilateral facet dislocation, or both sides called a bilateral facet dislocation.

Burst fractures are caused by the failure of the posterior and anterior cortices of the vertebral body and often accompanied with loss of disc height (Figure 2-7). Fracture through both cortices of the vertebral body often results in damage to the lamina and facet joints. The posterior expulsion of cortical bone fragments caused by vertebral body fractures can damage the spinal cord. Complete failure of the vertebral structure and disruption of the facet joints results in these being unstable injuries. Teardrop fractures are the avulsion of the superior or inferior edges of the anterior aspect of the vertebral body. If in isolation and not in conjunction with burst fractures the risk of posterior expulsion of vertebral fragments into the spinal canal is reduced. However due to the observed variation in the severity of teardrop fractures their relation to cervical spine stability and risk to spinal cord injury is unclear [141].

### 2.3.1.3 Acute cervical spine injuries in rugby

The most recent review of the literature compiled fourteen clinical observation studies from 1952 to 2010 and concluded that lower cervical spine (C4-C5 and C5-C6 level) bilateral facet dislocations were the most common catastrophic injuries in rugby [67] (Figure 2-8). The average incidence rates for these acute cervical spine injuries have been reported to range from 0.89 to 13 per 100,000 players per year [47]. Incidence rates range between countries and epidemiological studies due to differences in clinical reporting of the injuries and methods of statistical reporting respectively [18, 47, 48]. Although the absolute number of the incidence rates fall within the "acceptable risk" (2-100 per 100,000 per year) of the United Kingdom's Health and Safety Executive [47] the resulting effects of a cervical spine injury have major detrimental impact on the individual, wider society and the reputation of the sport. For example, for individuals injured at the age of 25 resulting in quadraplegia life-time care and treatment costs can reach 4.6 million US\$ [105, 99]. Other than secondary societal costs due to lack of productivity neurological damage can lead to secondary factors such as physical and mental health issues, discrimination and in cases suicide [105]. Therefore, sporting governing bodies should ensure player welfare and safety during rugby participation by providing players adequate protection through rules and laws. The van Mechelen



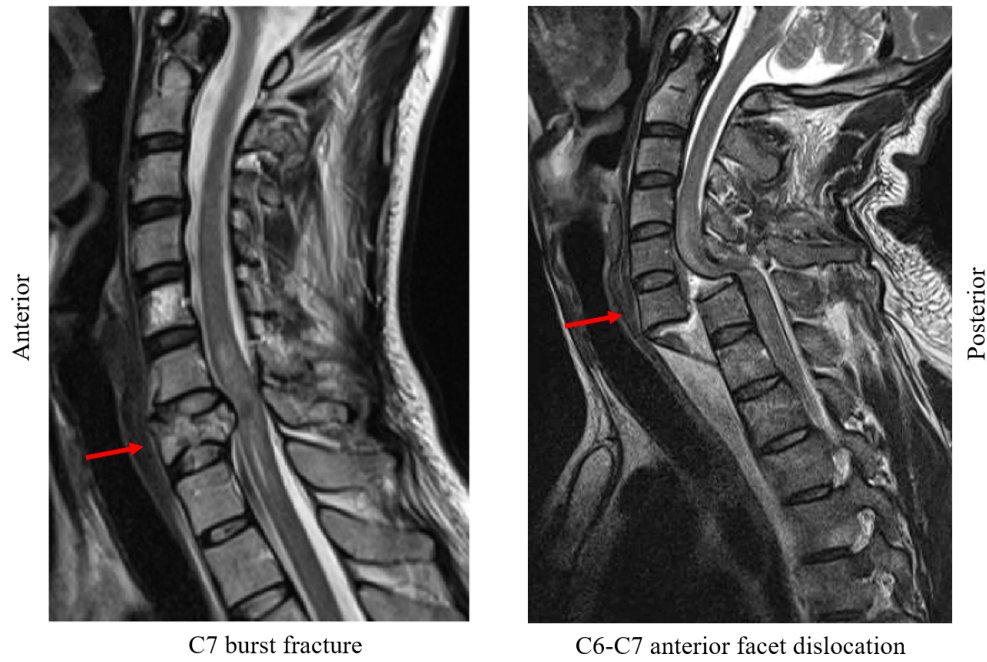


Figure 2-7: MRI stills of C7 burst fracture caused by a motor-bike fall (left) and severe anterior dislocation with fracture caused by automotive roll-over crash (right). Damage to the spinal cord (dark grey shade) can be seen in both accidents. Images obtained from *radiopedia.org*.

326 and TRIPP injury prevention models (*Chapter 1.2*; Figure 1-3) which are informed  
 327 by biomechanical data (Stage 2) aim to support the development of sport safety. The  
 328 reduction of catastrophic injuries is crucial for maintaining rugby’s popularity and  
 329 participation in nations where it is a premier sport (i.e. England, New Zealand, Fiji  
 330 and South Africa) but also expanding the sport’s reach to other nations (e.g. Japan  
 331 and Argentina).

332 Cervical spine injuries were most common in the scrum (42%) and tackle (38%) phases  
 333 on play followed by the ruck, maul and unclear impacts [18, 67]. However a recent  
 334 epidemiological analysis of cervical spine injuries in France stated that since 2010 “sig-  
 335 nificantly more catastrophic cervical spine injuries have occurred in backs (player po-  
 336 sition in rugby), notably during tackling or tackled activities” [109]. The increase of  
 337 these injuries during tackling had also been noted in the review by Kuster et al. (2012)  
 338 [67]. The review by Kuster et al. (2012) [67] and the subsequent editorial response of  
 339 Dennison et al. (2012) [40] has since lead to the debate as to what injury mechanism  
 340 causes the bilateral facet dislocations observed during acute cervical spine injuries in



rugby. The cause for the debate is due to the discrepancy between an intuitive ex- 341  
 planation of the observed injuries, which is often supported by qualitative information 342  
 of the inciting events (e.g. video footages and testimonies), and quantitative experi- 343  
 mental evidence which is explained bellow. One of the aims of the thesis is to help 344  
 settle the debate using an approach that brings together as much information as possi- 345  
 ble from currently available methods in an integrated experimental and computational 346  
 biomechanical framework. 347



Figure 2-8: Acute cervical spine injury during a rugby tackle sustained by the ball carrier (blue jersey). Images obtained from *dailymail.co.uk*.

## 2.4 Injury mechanisms of the lower cervical spine

Injury mechanisms describe the mechanical changes that result in anatomical and functional damage to systems and structures of the human body [153]. Knowledge of cervical spine injury mechanisms is crucial to reduce their occurrence by correctly informing specific interventions or policy changes. The importance of correctly identifying injury mechanisms and their aetiology is an integral part of injury prevention models (van Mechelen and TRIPP - *Chapter 1.2*). Unfortunately, injury prevention research rarely investigates in depth the biomechanical mechanisms as their study can be difficult, time consuming and often not representative of the injurious events due to experimental and computational limitations. Since our ability to closely predict failure of the cervical spine is not possible, the study of injury mechanisms can help characterise the circumstances under which cervical spine injuries occur.

In the case of bilateral facet dislocations, which are predominant causes of spinal cord injury in rugby [67], the two main theorised injury mechanisms are hyperflexion and buckling of the cervical spine (Figure 2-9). Hyperflexion is the isolated flexion of the neck that results in the forward rotation of the head towards the torso, exceeding the physiological range of cervical spine motion. This theory is an intuitive explanation of the injury it describes, which has led to its adoption into clinical and epidemiological literature. Additionally, case studies based on video analysis, eye witness accounts and injured player reports of the injurious event have supported hyperflexion as the predominant injury mechanism in rugby [117, 67]. However, as also described in a recent review of bilateral facet dislocations these injuries have been difficult to produce by applying pure flexion moments to the cervical spine [92].

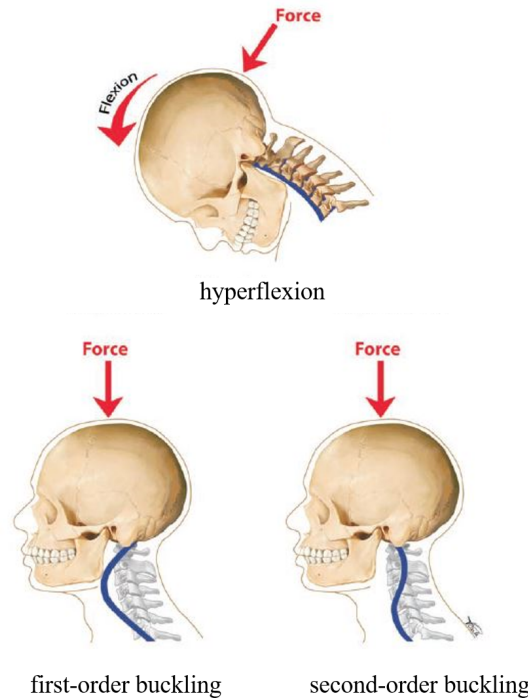


Figure 2-9: Theorised mechanisms that occur in rugby cervical spine injuries. Adapted from *Dennison et al. (2012) [40]*.

Anterior bilateral facet dislocations of the lower cervical spine have been primarily reproduced in experiments where the spinal column is loaded in axial compression. Early studies of human cadavers observed that local flexion was produced in the lower region of the intact cervical spine column by compression loads generated when the head impacts a rigid surface [11, 56]. These studies however did not produce bilateral facet dislocation injuries but theorised that compression-flexion type injuries, such as anterior facet dislocations, could occur without hyperflexion based on the resulting pre-injury kinematics of the spine. During cranial impacts the momentum of the head is arrested by the impact surface and the cervical spine is forced to handle the momentum of the following body which leads to buckling of the cervical spine column. Buckling is the rapid transition from an initial spinal configuration of equilibrium to another through a combination of local flexion and extension in the cervical spine column [94, 95] (Figure 2-10). First order buckling results in extension of the mid cervical spine region (C3-C4 to C4-C5) and flexion of the lower cervical spine (C5-C6 to C7-T1). Second order buckling is an unstable state that has been observed to occur prior

386 to first order buckling and usually observed in the straightened cervical spine. Similar  
387 to first order buckling second order buckling exhibits flexion in the lower cervical spine  
388 and extension in the mid region but also flexion in the upper cervical spine (Skull-C1  
389 to C2-C3). These studies showed that the buckled cervical spine does not necessitate  
390 structural failure (fracture or dislocation) and can still accept load which can result in  
391 local injuries that are representative of the local spinal configuration generated by the  
392 buckling [11, 56].

393 The buckling phenomenon is theorised to be the reason why a poor relationship has  
394 existed between head motion caused by impacts and clinically observed injuries. During  
395 cadaveric drop tests of 22 specimens by Nightingale et al. (1997) [94] bilateral facet  
396 dislocations and burst fractures occurred within the first 30 ms of impact. It was  
397 reported that neck flexion angles greater than  $20^\circ$  were produced between 20 and 100  
398 ms after impact and flexion angles larger than  $90^\circ$  after 90 ms. Ivancic (2012) [59]  
399 also reproduced anterior bilateral facet dislocations within 20 ms of axial compression  
400 impacts. It should be noted that these experimental studies did not include initial  
401 angular or translational velocities other than the 3.14 m/s vertical velocity of the drop  
402 test [94] and 4.10 m/s horizontal velocity of the sled test [59]. In contact sports (e.g.  
403 rugby) and leisure activities (e.g. diving) players likely duck or rotate their heads to  
404 shield their face away from the oncoming impacts. Initial angular velocities of the head  
405 at the time of impact could alter the dynamic response of the head and produce large  
406 angular displacements of the neck earlier. The effects of initial angular velocities during  
407 impacts however have not yet been investigated. To summarise, these experiments have  
408 shown the complex kinematic response of the cervical spine column to dynamic loading  
409 and why variations exist in clinically observed injuries.

410 Investigations of cervical spine injury mechanisms have also shown that the response  
411 of the cervical spine to dynamic axial loading is affected by neck pre-flexion angle on  
412 impact, impact load characteristics, endpoint constraints and simulated muscle forces.  
413 Saari et al. (2013) [113] applied experimental follower loads to cadaveric drop tests  
414 and observed increased cervical column stiffness and closer axial coupling between  
415 measured head and neck loads. The follower loads were applied by tensioned cables  
416 (101 N) placed bilaterally to the the specimens. Although replication of muscle forces  
417 experimentally is a gross simplification of the physiological loading experienced *in vivo*  
418 this study verified the hypothesis that muscles play a crucial role in compressive injury  
419 mechanisms by stiffening the cervical spine. The role of muscles was further supported  
420 by a computational study that applied forces from 23 pairs of active neck muscles  
421 during simulated drop tests [96], and found that the critical buckling load of the cervical

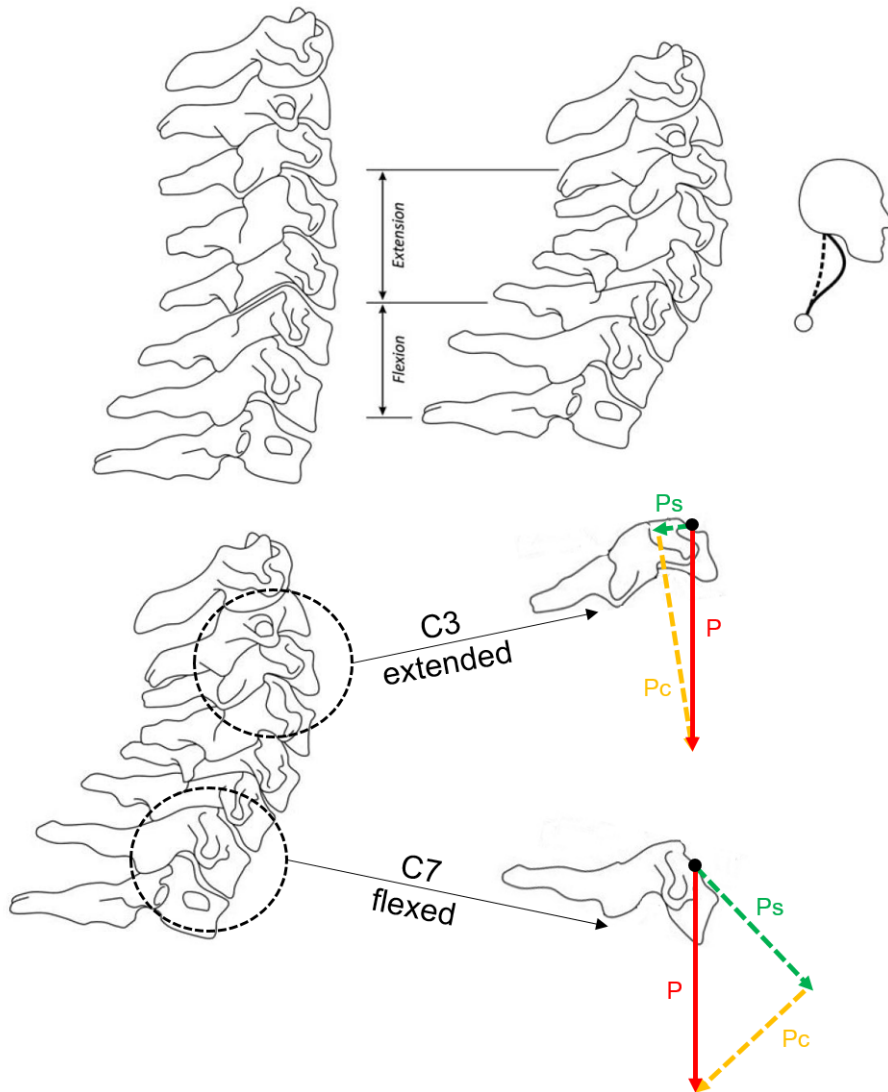


Figure 2-10: The initial posture of the cervical spine together with its configuration after first order buckling occurred during experimental drop tests (above). An example of the variation in local forces as result of continued load acceptance after buckling occurs (below). The compressive impact force ( $P$ ) is shown as components of compression ( $P_c$ ) and shear ( $P_s$ ) on the end plates of C3 and C7 vertebrae. Adapted from *Kuster et al. (2012) [67]*.

column increased which resulted in larger peak compressive forces than when no muscles 422  
 forces were simulated. Experimental studies identified that padded surfaces [94] and 423  
 head endpoint conditions [93] increased the risk of cervical spine injury. Compliant 424  
 impact surfaces apply shear loads at the contact interface with the head that resist head 425

426 deflection, which results in the neck being axially loaded by arresting the momentum of  
427 the oncoming torso. The ability of the head to escape (i.e. no endpoint constraint) has  
428 been shown to significantly reduce the axial loading of the spine during compression  
429 [93]. Energy dissipation properties and reductions in surface friction of the impact  
430 surface could allow the head to be deflected during impacts near or posterior to the  
431 vertex of the head. This was shown in a parametric computational study by Camacho  
432 et al. (2001) [22]. Finally neck flexion angles that align the head, neck and torso with  
433 the impact force vector direction, usually when the neck is flexed and the head impacted  
434 posterior to the vertex, increase the risk of sustaining bilateral facet dislocation and  
435 compression injuries [92, 95]. This can also be understood by the level of eccentricity  
436 between the impact force vector and the cervical spine column.

437 In the context of rugby impacts, such as tackles or scrums, surface interactions between  
438 a player's head and the impact surface (another player or the playing field) as well as  
439 players' technique, classified as neck and torso angles, are modifiable risk factors of  
440 cervical spine injuries. These factors can be linked to mechanistic parameters affecting  
441 injury such as the effects of impact padding as well as the alignment of the head, neck  
442 and torso through the angular configuration of the body. A player's tackling technique  
443 affects the positioning of their head with respect to the oncoming ball carrier. Correct  
444 technique would allow for the tackle impact to be accepted onto the tackler's shoulder,  
445 whilst poor technique could misdirect the impact onto the tackler's head. Technique  
446 also relates to the tackler's body position in the tackle with the alignment of the head,  
447 neck and torso. This will be dependent of relative direction of the tackle (e.g. front-on,  
448 oblique etc.) and the approach speeds of the colliding players. These technique factors  
449 will affect the direction, magnitude and loading rate of the impact force onto the head  
450 as well as the transfer of the force through the cervical spine. Another factor includes  
451 the interaction between the head and the impact surface that will affect the constraints  
452 applied to the head during the impact. Misdirected impacts onto soft tissue areas such  
453 as the stomach, an area commonly targeted in the tackle, could pocket the tackler's head  
454 and not allow the head to be deflected away from the oncoming torso. Additionally, use  
455 of equipment (e.g. head gear) and weather conditions could also alter the interaction  
456 between the head and impact surface. For example, whilst scrummaging front row  
457 players' head and neck are constrained by other players' bodies which restricts their  
458 mobility and forces players' necks into flexion. If in the event of a collapsed scrum  
459 a front row player's neck impacts the surface of the playing field factors such as the  
460 condition of the field (e.g. muddy, hard packed) are likely to place additional end  
461 condition constraints on the head other than those imposed by other players' bodies.

It is clear that as the field's fundamental understanding of spinal injuries is increasing 462  
the questions that spinal injury research is being asked to answer are becoming more 463  
applied. These applied questions, as shown in the context of rugby injuries, are in- 464  
fluenced by many factors and parameters which are challenging to directly investigate 465  
experimentally without losing the transferability and practical application of the re- 466  
sults to the question at hand. The reason being that although experimental studies are 467  
essential in providing fundamental knowledge of biomechanical principles they include 468  
inherent limitations that may reduce their real-world validity. Computational biome- 469  
chanical models, which also include their own limitations, have helped improve the 470  
field of injury biomechanics to better understand the fundamental principles of injury 471  
and explore more applied settings by providing an alternative to and complimenting 472  
experimental research respectfully. In the following Chapter computational models will 473  
be discussed as well as their validity and applicability to answer applied rugby injury 474  
analysis questions. 475

## 476 Chapter 3

# 477 Computational methods for the 478 investigation of cervical spine 479 biomechanics



### 3.1 Introduction

Rugby is a full contact sport interspersed by game specific contact events [112]. Studies have analysed the external loads placed on players during scrummaging and tackling through *in vivo* [25, 24, 53, 64, 104, 119, 130, 135], *in vitro* [57] and *in silico* methodologies [137, 138, 139, 140]. These studies have quantified the kinematics and biomechanical loads placed on players during simulated gameplay but also offer insight into situations with potential for injury. However, such experimental studies are unable to reliably determine the internal loading placed on anatomical structures of the cervical spine that may lead to injuries. Therefore, there is the need for an integrated approach and more specifically of a computational method that allows for the establishment of cause-effect relationships between external and internal loading.

Computational models are often used in injury prevention research for conducting biomechanical analysis and evaluating how external forces and segmental motions affect internal loads of the body's structures. Such models are also used in forward simulations with the final aim of exploring how external loads and muscles contribute to intervertebral joint loading experienced during "*what if*" scenarios. The reason for utilising these methodologies is to determine the internal loads of the cervical spine during normal and injurious scenarios representative of rugby gameplay. By understanding the physiological demands and risks to the neck under rugby specific external loads necessary precautions can be taken by governing bodies for player conditioning and injury risk reduction.

### 3.2 Computational pathways for biomchanical investigation

The main pathways used in biomechanical research to investigate the dynamics of the human musculoskeletal system are inverse analyses and forward simulations using computational models. Inverse kinematic analyses are performed when a model tracks experimental motion data to generate model generalised coordinates which are differentiated to obtain velocities and accelerations. Experimental motion data of body segments are commonly obtained from marker based motion capture systems (MoCap) or markerless wearable sensors such as inertial measurement units (IMUs). The inverse kinematic procedure tracks experimental motion data by calculating generalised coordinates which pose the model in a specific kinematic configuration that best matches the experimental data whilst satisfying the model's kinematic constraints. This inverse kinematic procedure is executed through a weighted least squares quadratic optimisa-

tion problem which minimises both marker and coordinate errors (Equation 3.1):

$$\text{minimise: } \sum_i^{\text{markers}} w_i \|x_i^{\text{exp}} - x_i(q)\|^2 + \sum_j^{\text{coordinates}} \omega_j (q_j^{\text{exp}} - q_j)^2 \quad (3.1)$$

Where  $q$  is the vector of the model's generalised coordinates being solved for,  $w_i$  is the weight factor for the  $i^{\text{th}}$  marker error term,  $x_i^{\text{exp}}$  is the experimental motion marker position,  $x_i(q)$  is the corresponding model motion marker position depending on the coordinate values,  $\omega_j$  is the weight factor for the  $j^{\text{th}}$  coordinate error term,  $q_j^{\text{exp}}$  is the experimental coordinate and  $q_j$  is the corresponding model coordinate. Marker error is the three dimensional difference between the experimental and model markers. Coordinate error is the difference between experimental coordinate values (only if known *a priori* and the calculated model coordinates by the inverse kinematic procedure.

With knowledge of the kinematics and the external loads applied to the model from experimental measurements, the multibody dynamics equations of the modelled system can be solved for the unknown generalised joint forces using inverse dynamics (Equation 3.2):

$$M(q)\ddot{q} + C(q, \dot{q}) + G(q) = \tau \quad (3.2)$$

Where  $M(q)$  is the system mass matrix,  $C(q, \dot{q})$  is the vector of Coriolis and centrifugal forces,  $G(q)$  is the vector of gravitational forces,  $q$  are the generalised positions,  $\dot{q}$  are the generalised velocities  $\ddot{q}$  are the generalised accelerations and  $\tau$  are the generalised joint forces.

The kinematics of the model resulting from the generalised coordinates outputted by the inverse kinematics algorithm aim to be dynamically consistent with the external load applied to the system during inverse dynamics analyses. However, due to experimental errors and modelling assumptions which reflect the inconsistencies between the kinematics, external loads, and the modelled system dynamic consistency does not always exist producing force and moment residuals. For these reasons, kinematic and kinetic data has historically been collected in a laboratory environment to ensure accuracy, whilst biomechanical models must undergo validation and verification procedures before use [54]. With the advancement of wearable sensors, such as inertial measurement units, more representative data collections in real world scenarios are beginning to be used for these analyses.

In contrast to inverse dynamics where experimental body kinematics are used to estimate the generalised joint forces, forward dynamic simulations generate new kinematics given the internal and external forces applied to the system. Forward simulations achieve this by integrating the system dynamics equations forward through time to generate the new body segment motion (Equation 3.3):

$$\ddot{q} = [M(q)]^{-1} \{C(q, \dot{q}) + G(q) + F\} \quad (3.3)$$

Where  $[M(q)]^{-1}$  is the inverse mass matrix of the system,  $C(q, \dot{q})$  is the vector of Coriolis and centrifugal forces,  $G(q)$  is the vector of gravitational forces,  $q$  are the generalised positions,  $\dot{q}$  are the generalised velocities  $\ddot{q}$  are the generalised accelerations and  $F$  are the forces applied to the model.

The resulting motion of the model is dynamically consistent with the applied loads and constraints of the multibody system under investigation. However, forward dynamics simulation are sensitive to the initial conditions. For this reason, careful application of initial positions, velocities, loads and integrator settings must be completed to avoid unstable and divergent results. In injury biomechanics forward dynamic simulations are a valuable tool for injurious scenarios that are often challenging to replicate experimentally.

### 3.3 Computational models of the cervical spine

Computational modelling of biomechanical systems is an advanced method that allows for the estimation of *in vivo* internal loads when direct measurements are not viable. These models, which are a mechanical representation of the investigated physiological system using mathematical formulations, can be used in an inverse and forward sense as previously described. Currently the two modelling approaches that aim to describe the mechanics of a biomechanical system are the discrete multibody mechanics method often termed musculoskeletal (MSK) models, and the continuum mechanics method using finite element (FE) models. It is often regarded that the benefits of one approach are the limitations of the other.

#### 3.3.1 Finite element models

Finite element models can represent with a high level of detail the anatomy (i.e. geometry) and tissue (i.e. material) properties of the neck. These FE models have allowed for the study of cervical spine injury mechanisms during dynamic impacts representative

compressive [22, 50, 58] and inertial loading [43, 33]. Material properties can be specified for individual structures of the cervical spine (e.g. ligaments, annulus fibrosus, nucleus pulposus, cortical and cancellous bone) which provide high resolution stress and strain patterns on the structures under load. Individualised and high resolution material responses therefore can be helpful for the investigation of injury mechanisms and the identification of structures likely to be injured.

Investigations of compression head-first impacts using FE models have been limited [22, 50, 58, 96] compared to the many computational studies of whiplash related injuries. Camacho et al. (1997) [22] developed a FE model of the head-neck system to study the dynamic response of the cervical spine to near vertex head impacts. This model simplified the vertebrae as rigid bodies and used non-linear spring and damper elements to represent the lumped behaviour of the intervertebral joints. The multibody neck was connected to a finite element head model and validated against human cadaveric experiments of near vertex head impacts [95]. The model predicted similar resultant neck forces, head impact forces and resulting neck kinematics. An updated version of this model which included muscle elements was used by Nightingale et al. (2016) [96] to investigate the effects of muscle forces and neck pre-flexion angles during head-first impacts. Although these models could not identify sites of possible injury (i.e. material failure) as they included simplified rigid vertebrae and lumped dynamic intervertebral elements they did reproduced cervical spine buckling representative of experimental head-first drop tests. Halldin et al. (2000) [50] developed a linear elastic finite element model of the head and cervical spine that was able to predict injury in the cervical spine by local stress thresholds during compressive impacts of vehicle rollovers. This was the first *in silico* study to reproduce *in vitro* experimental injuries sustained during compressive axial impacts. However they were able to only predict Hangmans' fractures just prior to buckling of the cervical column unlike injuries in the lower cervical spine which were also reported in the experimental tests being validated against. The results of Halldin et al. (2000) were able to inform the design of car roofs that would cause head and neck flexion upon head impact in a vehicle rollover that reduced the neck loads by 27%. A similar study investigating factors affecting cervical spine injuries in rollover crashes by Hu et al. (2008) [58] used a non-linear finite element model of the head and neck. Simulations varied impact velocity, impact surface angles as well as surface padding thickness, stiffness and coefficient of friction. By comparing the maximal principal strain in regions of the cervical spine they were able to identify that the coefficient of friction had the largest influence on neck fracture injury risk followed by impact velocity. Through their results they were able to recommend seatbelt design that reduced head-to-roof impacts and minimising the coefficient of friction of vehicle

roof padding would reduce cervical spine injury risk in vehicle rollover crashes. 609

Although finite element studies investigating compressive injury mechanisms have also 610  
included muscle elements [58, 96] they are limited to applying muscle forces that may 611  
not be representative of the situations they are simulating. This is because unlike front 612  
or rear vehicle collisions [33], where the neuromuscular response can be measured ex- 613  
perimentally with volunteers at low impact speeds, muscle recruitment strategies used 614  
in simulations investigating compressive neck loading during rollover are challenging 615  
to validate. Recent highly controlled experiments [90, 91] on human participants in- 616  
verted to simulate the alignment of the cervical spine and the response of the muscles 617  
*in vivo* could provide valuable insight into their function during in these events. How- 618  
ever extracting information regarding the configuration of the neck and muscle forces 619  
directly from *in vivo* experimental or even real-world situations and applying them 620  
directly as input for finite element boundary conditions is challenging. Therefore to 621  
provide information that is representative of the state of the neck system (i.e. vertebral 622  
kinematics and muscle forces) prior to injury during impacts, such as rugby tackles, an 623  
initial analysis stage should be undertaken that can better utilise information gathered 624  
*in vivo*. Musculoskeletal models, as discussed in the following section, are capable of 625  
performing inverse analyses of data collected in experimental or real world settings. 626  
Outputs from these inverse analyses such as neck joint positions and accelerations as 627  
well as neck muscle forces that cause the kinematics can then be used forward dy- 628  
namic simulations to investigate theoretical injurious situations. Another approach 629  
is the combination of finite element and musculoskeletal models to generate hybrid 630  
finite element-multibody (musculoskeletal) models. Hybrid approaches maintain the 631  
relatively low computational cost and higher stability of multibody musculoskeletal 632  
models whilst incorporating detailed finite element components for areas of the system 633  
where higher accuracy is required. This powerful approach allows for complex anatomic 634  
structures, such as the intervertebral discs, ligaments and facet joints, to be analysed 635  
using accurate representations of their material properties during dynamic simulations 636  
of the entire system [63]. Such multi-scale [154, 155] couplings can provide valuable 637  
information on the complex biomechanical response of non-linear spinal tissues (such 638  
as intervertebral discs) or vertebral areas of interest during injurious events. The re- 639  
mainder of this chapter will focus primarily on multibody musculoskeletal models and 640  
the following studies presented in this thesis will utilise musculoskeletal models. In- 641  
verse analyses will be executed to obtain neck joint kinematics and muscle forces from 642  
experimental *in vivo* data which will then be used in forward simulations to investigate 643  
the kinematic and dynamic response of the cervical spine to compressive impacts to 644  
identify cervical spine injury mechanisms in rugby. 645

### 3.3.2 Musculoskeletal models

Musculoskeletal models are multi-body systems made up of rigid anatomical segments, which are interconnected by joints actuated by Hill-type muscles, and constrained by kinematic couplings or viscoelastic elements representing passive internal structures (e.g. ligaments and intervertebral discs). Musculoskeletal models of the cervical spine have been created for the biomechanical analysis of functional neck movements [146, 23, 38, 133, 152] and cervical spine injuries during impact events [21, 37, 51, 66, 96].

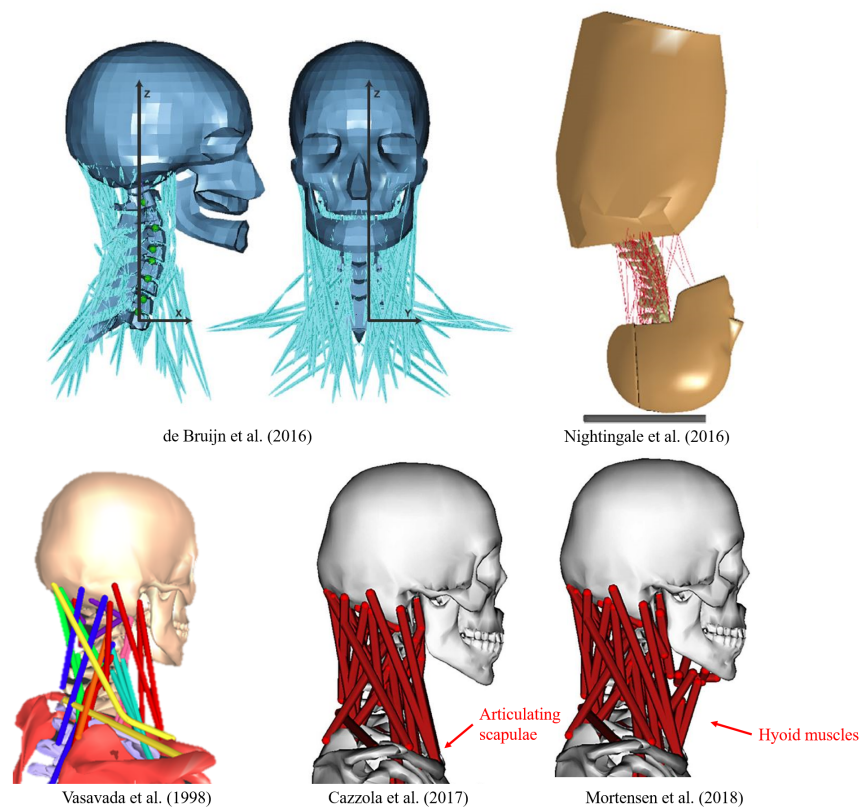


Figure 3-1: Musculoskeletal models used for injury and functional movement analysis. Adapted from *de Bruijn et al. (2016) [37]*; *Nightingale et al. (2016) [96]*; *Vasavada et al. (1998) [152]*; *Cazzola et al. (2017) [23]* and *Mortensen et al. (2018) [86]*.

Table 3.1: Multibody models used for functional and injury analysis

Study	Model type	Muscle elements	Muscle geometry	Passive joint elements	Analysis
<i>Vasavada et al. (1998) [152]</i>	MSK - Kinematic	52	Linear	N/A - kinematic coupling	Functional
<i>Suderman and Vasavada (2017) [133]</i>	MSK - Kinematic	52	Curvilinear	N/A - kinematic coupling	Functional
<i>Cazzola et al. (2017) [23]</i>	MSK - Dynamic	78	Linear	N/A - kinematic coupling	Functional
<i>Mortensen et al. (2018) [86]</i>	MSK - Dynamic	72	Linear	Lumped parameter	Functional/Injury
<i>Kuo et al. (2019) [66]</i>	MSK - Dynamic	84	Linear	Individual elements	Injury
<i>de Bruijn et al. (2016) [37]</i>	Hybrid MSK/FE - Dynamic	258	Linear	Lumped parameter	Injury
<i>Nightingale et al. (2016) [96]</i>	Hybrid MSK/FE - Dynamic	81	Curvilinear	Lumped parameter	Injury

### 3.3.2.1 Muscle modelling

The Hill-type muscle is a phenomenological non-dimensional model of muscle contractile dynamics [164]. It consists of a contractile element connected in parallel and in series with two elastic elements (Figure 3-2). The contractile element aims to replicate the muscle's active behaviour whilst the parallel and in series elastic elements represent the passive properties of the muscle and the tendon respectively.

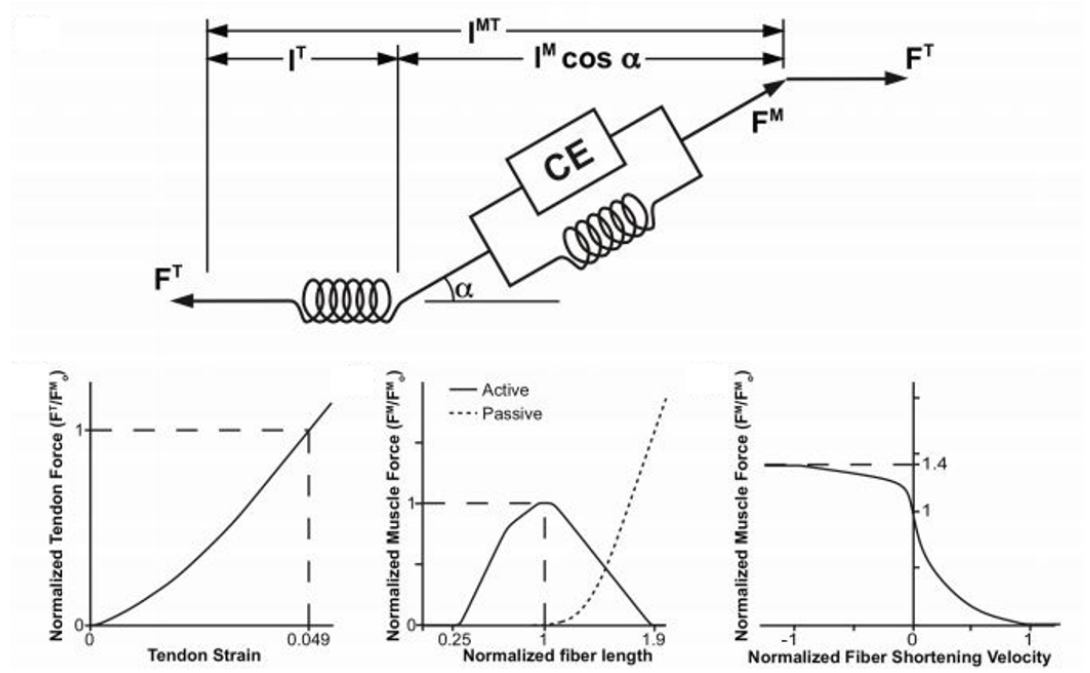


Figure 3-2: Hill-type muscle model (above) with the muscle force-length (below - left), force-velocity (below - centre) and tendon-strain (below - right) curves. CE = contractile element; springs = passive elements;  $l^M$  = muscle length;  $l^T$  = tendon length;  $l^{MT}$  = muscle-tendon unit length;  $\alpha$  = pennation angle;  $F_0^M$  = muscle force;  $F_0^T$  = tendon force. Adapted from *Thelen (2003) [136]*.

Physiological neck muscle paths better represent muscle function through correct moment arms and generate appropriate muscle force estimation which results in more physiological intervertebral joint loads. Earlier functional and impact specific models represented muscle lines of action as linear elements with static path constraints (via points) between origin and insertion points on model segments [37, 38, 152]. Via points aim to maintain physiological muscle moment arms about the neck joints as the origin



and insertion points of the muscle translate with the range of motion of the neck [3]. More recently dynamic path constraints (wrapping surfaces) have been utilised to better represent the complicated muscle paths of the neck [66, 132, 133, 151]. Wrapping surfaces are frictionless parametric geometries (spheres and cylinders) that generate curvilinear muscle paths if a muscle line of action crosses them as the head and neck move through their range of motion. The first study to use wrapping surfaces for neck musculature in MSK models was Vasavada et al. (2008) [151] and later extended by Suderman and Vasavada (2017) [133] with moving muscle points linked to each vertebra. They defined wrapping surfaces in their neck model that generated curvilinear muscle paths (sternocleidomastoid and semispinalis) that minimised the deviation from segmented muscle centroid paths from magnetic resonance imaging (MRI) of participants. These surfaces maintained extension moment arms for the semispinalis muscle and ipsilateral lateral bending moment arms for the sternocleidomastoid during sagittal and frontal plane neck rotations respectively. This was a significant contribution as the moment arms of linear muscles in the model significantly differ from the physiological moment arms observed *in vivo*, however the use of these wrapping surfaces has not been adopted in models since. Recently Kuo et al. [66] defined a wrapping surface between the caudal region of the sternocleidomastoids and the lower cervical spine to maintain the muscles' flexion moment arms about the lower cervical joints during large neck extension movements.

Biofidelic muscle representations in MSK models of the cervical spine is critical as neck musculature is also an important structural element of the cervical spine. This has been clearly shown also in experimental studies where the application of forces simulating the effect of muscles increased the spine's structural stability and altered its failure mechanisms [96, 95, 113]. The force a Hill-type muscle model can generate in a given state is dependent on parameters such as the maximal isometric force (force generating capacity), length, contraction velocity and level of activation [2, 72, 78, 136]. Maximal isometric force, force-length and force-velocity relationships are muscle model parameters than can be scaled linearly based on a subject's anthropometry or estimated using measurements obtained from medical imaging (Figure 3-2). Both approaches can be also be calibrated with numerical optimisation strategies guided by experimental data to allow for more accurate joint moment predictions during inverse and forward simulations [79, 103, 122]. The ability of neck MSK models to generate sufficient moments to match experimental values is sensitive to correct definition of these muscle elements and maximal isometric force in particular [152, 150]. This however introduces a trade-off between either increasing maximal isometric forces of functional muscle groups (e.g. extensors, flexors etc.) to represent the strength of other muscles not

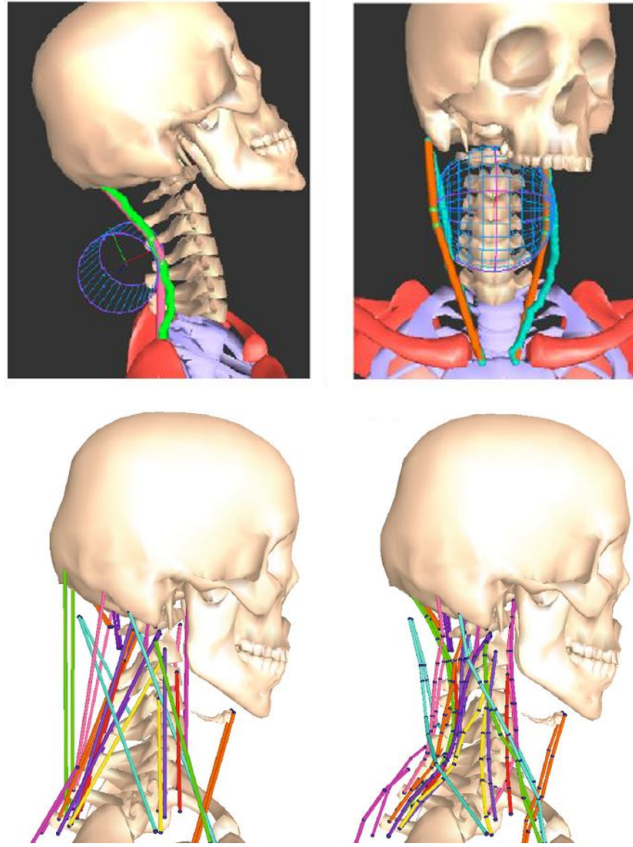


Figure 3-3: Wrapping surfaces applied to the line of action for the semispinalis capitis (above - left) and sternocleidomastoid (above - right) muscles in Vasavada et al. (2008). Original linear (below - left) and curvilinear muscle paths (below - right) generated by moving muscle via-points in Suderman and Vasavada (2017). Adapted from Vasavada et al. (2008) [151] and Suderman and Vasavada (2017) [133].

702 modelled or including those muscles as new elements. Although the first method is  
 703 not an accurate physiological representation of the system it does not increase the  
 704 complexity of the system by including more muscle elements. This was reported by  
 705 Cazzola et al. (2017) [23] who generated a rugby population specific MSK model and  
 706 used maximal force scaling factors for extensor (1.9) and flexor (2.7) muscle groups in  
 707 order to match experimental isometric neck strength measurements. A similar problem  
 708 in an average population model [23] which built upon the original Vasavada et al. (1998)  
 709 [152] neck model was accounted for by including the hyoid muscle group [86]. The  
 710 inclusion of the hyoids, which are small anterior neck muscles attached to the hyoid bone  
 711 with large moment arms, improved the flexion moment generating capacity in dynamic

simulations of the head and neck. A later investigation using this model showed that increasing the maximal isometric strength of the muscles significantly reduced head accelerations during impacts replicating concussion events in American football [87]. However, it should be considered that although stronger muscles can generate moments that reduce inertial loading (accelerations and decelerations) they also increase the intervertebral joint loads which in the case of compressive impacts could overestimate proximity to critical injury thresholds. Therefore correct identification of model muscle parameters is important for the appropriate estimation of internal joint loads during cervical spine injury analysis.

As previously mentioned a process used to overcome limitations associated to scaling models is the utilisation of medical imaging data, such as magnetic resonance imaging (MRI) and computed tomography (CT). Such imaging approaches are key for the measurement and definition of subject specific parameters in MSK models [115, 144]. MRI has been frequently used when creating MSK models based on subject specific skeletal geometry and muscle parameters in the lower limbs [13, 14, 79] and cervical spine [132, 133, 151] due to better muscle structure visibility and no radiation exposure compared to CT imaging. The majority of studies adopting the use of subject specific modelling focuses on the lower limbs and clinical populations (e.g. cerebral palsy, osteoarthritis). Despite the increase of computational power and accessibility to medical imaging a standardised methodology of creating subject specific models has not been established. This is due to the difficulty of developing a standardised pipeline that can efficiently overcome bottlenecks relating to execution time but also be flexible enough for a variety of applications across research centres. The lack of reproducibility and high expertise needed is also reflected by the low adoption rates in clinical musculoskeletal practices.

Studies evaluating the sensitivity of subject specific musculoskeletal models to measurements associated with model creation have concluded that they are more accurate than generic scaled models for the investigation of joint function and pathological conditions [115, 134, 145]. Others however have not found any increased model performance with MRI informed maximal isometric force [36]. Due to the nature of rugby and its physical demands it is key to realistically model the anatomical and physiological characteristics of players' necks, something that is currently missing in the field of sport injury biomechanics. A cross sectional radiographic study of recently retired (5.8 years) rugby players and matched controls showed significant skeletal (foraminal stenosis and vertebral canal narrowing) geometric differences between the two groups [16]. Additionally, former rugby players displayed significantly larger physiological cross sectional areas of

748 the neck muscles compared to the general population. The physiological cross sectional  
 749 area of a muscle is typically used for estimates of maximal isometric strength [97]. In  
 750 rugby and other impact events, where high dynamic perturbations risk to destabilise the  
 751 cervical spine, the importance of correctly estimating muscle moment arms and maxi-  
 752 mal force generating capacity based on correct physiological measurements is therefore  
 753 emphasised. This thesis will aim to address the lack of a detailed musculoskeletal model  
 754 of a rugby player through the creation of one with MRI information.

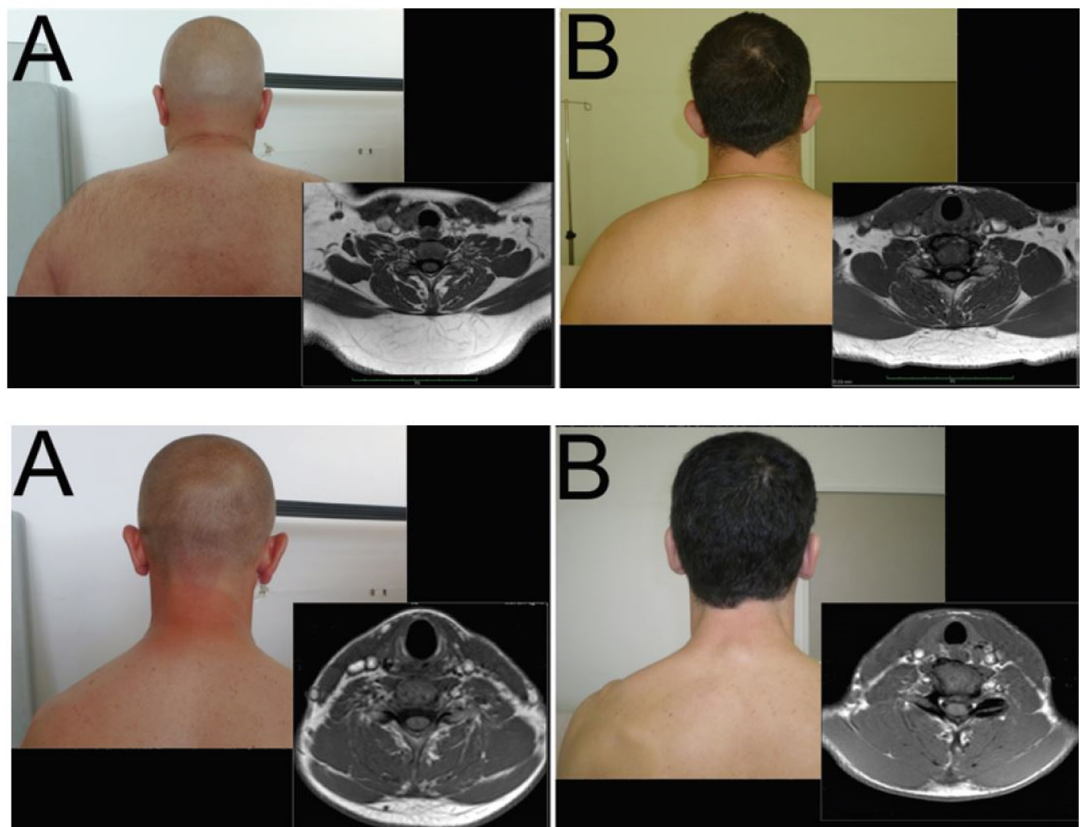


Figure 3-4: Axial MRI images and photographs showing differences in neck muscle volume and fat deposits (C6-C7 level) between matched controls (A) and former international forward (above) and back (below) rugby player. Adapted from *Brauge et al. (2015) [16]*.

### 3.3.2.2 Redundancy problem

The force distribution problem of the musculoskeletal system, resulting from “motor redundancy” as first described by Bernstein (1967) [12] or “motor abundance” being termed more recently [68, 69], only allows for muscle force estimation using computational strategies. At present two methods have been utilised in MSK models to estimate neck muscle forces during inverse analyses [4]. These are pure optimisations and electromyography (EMG) informed methods.

Pure optimisation methods (Equation 3.4) estimate neck muscle activations needed to produce the required muscle forces that generate moments that satisfy the generalised joint forces of the model from the inverse dynamics by minimising or maximising an objective criterion (cost function).

$$\begin{aligned} &\text{minimise or maximise: } J = f(a_m) \\ &\text{subject to: } f_m(F_m^0, l_m, v_m, a_m) r_m^j = \tau^j \\ &0 \leq \alpha_m \leq 1 \end{aligned} \tag{3.4}$$

Where  $f(a_m)$  is the linear or non-linear function being minimised or maximised,  $f_m(F_m^0, l_m, v_m, a_m)$  is the vector of muscle forces at a given level of activation ( $a_m$ ), maximal isometric force ( $F_m^0$ ), fibre length ( $l_m$ ) and contraction velocity ( $v_m$ ),  $r_m^j$  is the vector of muscle moment arms that cross the  $j^{th}$  joint and  $\tau^j$  is the generalised force acting about the  $j^{th}$  joint. The criterion ( $J$ ) can be mechanical (e.g. maximal force production, maximal joint stiffness etc.) or metabolic (e.g. minimisation of energy expenditure). Estimated activations produced from these optimisation techniques however are frequently characterised by poor agreement with experimental muscle EMG measures and lack the stabilising effect of muscle co-contraction [15, 28] observed in neck musculature during flexion/extension and lateral bending motions [126]. Additionally, the resulting muscle forces are highly dependent on the chosen objective criterion of the optimisation [85]. EMG-informed methods combine experimental EMG signals with optimisation procedures to estimate muscle activations and subsequent muscle forces. These methods can provide estimations representative of measured experimental EMG signals and co-contraction estimates as the estimates are implicitly guided by the experimental measures. A limitation for the use of EMG-informed estimations of spinal muscle activation however is the inaccessibility to deep muscle layers to obtain experimental EMG measurements. For this reason, EMG-assisted approaches have generated deep muscle activation patterns with the combination of optimisation meth-

ods [27, 28, 29, 30]. In situations such as sporting collisions when the neuromuscular objective is not clear EMG-assisted approaches could help provide an initial insight on muscle recruitment strategies. For example, a player may want to tense their neck enough to brace for impact whilst maintaining adequate mobility to position their head correctly and maintain good technique by avoiding a misdirected impact to the head. This thesis will investigate the use of EMG-assisted models to investigate their applicability to rugby specific impact situations in order to gain physiological estimations muscle recruitment strategies.

During forward simulations that investigate injury scenarios, muscles can be constrained to follow activation signals determined *a priori* to generate desired internal loading conditions in the neck. These predetermined activation patterns are usually derived from estimation methods, such as EMG-assisted or pure optimisation methods, during non-injurious events [26, 41, 96]. For example, Nightingale et al. (2016) [96] applied activation patterns to the muscles of a model during drop test simulations which were derived from maintaining the head in equilibrium under the effect of gravity [41]. However, the application of these relaxed muscle activations during head first drops could be questioned as larger contractions in some muscles would be expected in a fall as a protective or reflex mechanism. A more physiological solution could be generated with the incorporation of closed-loop feedback controllers or optimal control theory. Happee et al. (2017) [51] showed that vestibulocollic and cervicocollic reflexes, which physiologically originate from the inner ear and neck muscle spindles respectively, could maintain the stability of a MSK model's cervical spine when tracking head oscillations between 0.3 and 8 Hz. This approach however has not been attempted in forward simulations. Recent advancements in optimal control theory have been able to produce predictions of human gait from neuropathological conditions such as cerebral palsy [42, 102]. Optimal control methods are used to identify optimal control signals that cause the modelled system to behave in a way that minimises or maximises a performance criterion whilst satisfying task requirements and model constraints. Such techniques could be valuable in spinal research to determine if certain muscle activation patterns can maintain stability after a perturbation and even predispose or protect the neck from injury.

Additionally, stability of the cervical spine is likely not only contributed to by point loads, simulated by muscle elements in musculoskeletal models, but also surface pressures generated between skeletal and muscular tissues in the neck. Modelling the interactions between muscle surfaces would also allow for better representation of neck muscle moment arms and reduce the need for wrapping surfaces. Such models have

begun to emerge using FE methods in the lower limbs [110]. However, their validation and application to the cervical spine has not been attempted possibly due to the complicated geometry of neck structures and very advanced methods needed.

### 3.3.2.3 Representation of passive joint properties

The kinematics of the multilevel cervical spine are inherently complex and pose a considerable modelling challenge. As well as the geometry of the cervical spine structures their passive properties highly influence the resulting kinematics. For MSK models investigating functional movements [23, 86, 152] total neck motion is defined by six rotational degrees of freedom describing the relative position of the head with respect to the trunk. These allow for independent motion of the upper (skull-C1 and C1-C2) and lower (C2-C3 to C6-T1) cervical spine in the three planes of motion. Each intervertebral joint motion is specified about three fixed instantaneous rotational axes as a percentage of the total neck motion (head with respect to the trunk). These percentages represent how the total neck angle in each plane is partitioned into intervertebral joint motions [125, 152] based on cadaveric experiments [157]. This method provides a stable kinematic solution for intervertebral joint angles during head and neck movements as the passive properties of the entire cervical spine are implicitly accounted for in the percentage distribution of the total neck angles to the intermediate intervertebral joints. Although such kinematic couplings with fixed instantaneous centres of rotation are valuable for stable kinematic solutions of functional neck motions (predominantly during inverse analyses), they may not best represent the effects of high dynamic loading. Dynamic loading such as impacts can result in non-linear responses of intervertebral rotations and translations which cannot be accounted for with kinematic couplings and fixed centres of rotation. Viscoelastic elements are implemented into MSK models to better understand the resulting intervertebral forces and motions during these events. However parameter values for viscoelastic elements representative of the dynamic loading of the entire cervical spine column, which would happen in misdirected rugby tackles, are not available. Finally, it should be noted that these kinematic coupling constraints should not be used in conjunction with viscoelastic elements (discussed in the next paragraph) as the resulting joint kinetics will not be dynamically consistent. The correct practise of removing the constraints whilst adding viscoelastic elements was observed in Kuo et al. (2019) [66] but not in the study by Mortensen et al. (2018) [85].

Musculoskeletal models used for cervical spine injury analysis of impact scenarios have incorporated two methods for representing intervertebral joint passive properties using

viscoelastic elements. Lumped parameter models use a single six degree of freedom viscoelastic element, or bushing, at each intervertebral joint [31, 37, 96]. These represent the passive contribution of the ligaments, intervertebral disc and facet joints along and about the three translational and three rotational degrees of freedom respectively of each intervertebral joint (Equations 3.5 and 3.6). Passive stiffness and damping properties are represented mechanically via 6-by-6 stiffness and damping matrices which generate forces based on the generalised positions and and velocities of the joint.

$$F_i^J = Kq_i + B\dot{q}_i, \text{ or} \quad (3.5)$$

$$F_i^J = \begin{bmatrix} f_i^x \\ f_i^y \\ f_i^z \\ \mu_i^x \\ \mu_i^y \\ \mu_i^z \end{bmatrix} = \begin{bmatrix} k_{11} & k_{12} & k_{13} & k_{14} & k_{15} & k_{16} \\ k_{21} & k_{22} & k_{23} & k_{24} & k_{25} & k_{26} \\ k_{31} & k_{32} & k_{33} & k_{34} & k_{35} & k_{36} \\ k_{41} & k_{42} & k_{43} & k_{44} & k_{45} & k_{46} \\ k_{51} & k_{52} & k_{53} & k_{54} & k_{55} & k_{56} \\ k_{61} & k_{62} & k_{63} & k_{64} & k_{65} & k_{66} \end{bmatrix} \begin{bmatrix} q_i^{tx} \\ q_i^{ty} \\ q_i^{tz} \\ q_i^{rx} \\ q_i^{ry} \\ q_i^{rz} \end{bmatrix} + \begin{bmatrix} b_{11} & b_{12} & b_{13} & b_{14} & b_{15} & b_{16} \\ b_{21} & b_{22} & b_{23} & b_{24} & b_{25} & b_{26} \\ b_{31} & b_{32} & b_{33} & b_{34} & b_{35} & b_{36} \\ b_{41} & b_{42} & b_{43} & b_{44} & b_{45} & b_{46} \\ b_{51} & b_{52} & b_{53} & b_{54} & b_{55} & b_{56} \\ b_{61} & b_{62} & b_{63} & b_{64} & b_{65} & b_{66} \end{bmatrix} \begin{bmatrix} \dot{q}_i^{tx} \\ \dot{q}_i^{ty} \\ \dot{q}_i^{tz} \\ \dot{q}_i^{rx} \\ \dot{q}_i^{ry} \\ \dot{q}_i^{rz} \end{bmatrix} \quad (3.6)$$

Where  $F_i^J$  is the vector of the generalised forces ( $f_i^x$ ,  $f_i^y$  and  $f_i^z$ ) and moments ( $\mu_i^x$ ,  $\mu_i^y$  and  $\mu_i^z$ ) for the  $i^{th}$  joint,  $K$  and  $B$  are the 6-by-6 stiffness and damping matrices respectively with  $q_i$  and  $\dot{q}_i$  being the 6-by-1 vectors of generalised joint positions and velocities for the  $i^{th}$  joint's translational (superscripts  $tx$ ,  $ty$  and  $tz$ ) and rotational (superscripts  $rx$ ,  $ry$  and  $rz$ ) degrees of freedom.

Additionally, coupled spinal motions observed between intervertebral joint degrees of freedom can be represented using this method [31, 84, 98]. Spinal motion coupling is achieved by including off-diagonal elements in the bushing stiffness matrix. The stiffness and dampening parameters of the bushings which characterise the passive properties of the joint, are derived from static, quasi-static or in some instances dynamic loading tests using *in vitro* spinal specimens (Table 3.2) [34, 84, 108]. These *in vitro* tests have identified large variations in measured joint stiffness values. Moroney et al. (1988) [84] found cervical spine motion segment (vertebra-disc-vertebra) stiffness ranges of 116-3924 kN/m and 29-631 kN/m for compression and anterior shear respectively. The same study observed a decrease up to 50% in all degrees of freedom once the posterior elements of the vertebrae were removed. Variability observed in this and similar studies is theorised to be caused by differences in applied loading rates, age and levels of degeneration of the *in vitro* specimens. Furthermore differences in specimen



preparation (multi-level, motion segment or isolated disc) and the spinal level tested 881  
also seem to affect stiffness calculations [84]. Due to the variability of stiffness and 882  
damping parameters caused by their specificity to testing protocols their incorporation 883  
into musculoskeletal models has to be representative of the task under analysis. For 884  
this reason, in the development of new models often direct validation of viscoelastic 885  
parameters is undertaken which are specific to the task or event being analysed. This 886  
was one of the rationales for the identification of new parameters representative of the 887  
cervical spine's response to loading representative of rugby impacts. 888

Table 3.2: Stiffness values of cervical spine segments about their six degrees of freedom

Study	NS	Loading Rate	Max (N)	Max (Nm)	Preload (N)	Specimen Type	Spinal Level	CMP (kN/m)	SHR (kN/m)	FL (N/°)	EX (N/°)	LB (N/°)	AR (N/°)
Moroney et al. (1988) [84]	35	Static	73.6 (CMP)	2.16	49	C2-C3 (n=9)	FSU	116-3924	29-631 (Ant.)	0.10-0.83	0.26-1.80	0.19-1.58	0.64-2.02
						C3-C4 (n=6)			25-96 (Post.)				
			C4-C5 (n=6)			Disc segment	58-2060	28-226 (Lat.)					
			C4-C5 (n=4)										
			C6-C7 (n=6)					12-317 (Ant.)					
C7-T1 (n=4)	13-169 (Post.)	0.05-0.65	0.06-0.78	0.09-0.91	0.23-0.93								
C7-T1 (n=4)	17-267 (Lat.)												
Shea et al. (1991) [124]	27	Quasi-static (5 mm/s 5 °/s)	500 (CMP)	5 (FL)	N/A	C2-C5	Two FSUs	957 ± 244	1230 ± 350 (Ant.)	1.13 ± 0.68	1.74 ± 0.93	N/A	N/A
			100 (SHR)	3.5 (EX)		C5-T1			1140 ± 690 (Post.)				
Panjabi et al. (1986) [100]	18	Static	approx. 25	N/A	N/A	C2-C3	FSU	141	34 (Ant.)	N/A	N/A	N/A	N/A
						to C7-T1			53 (Post.)				
									53 (Post.)				

NS: Number of specimens tested

CMP: Compression

SHR: Shear

FL: Flexion

EX: Extension

LB: Lateral Bending

AR: Axial Rotation

N/A: Data not Available

NB: Data ranges reported as presented in original manuscripts

A second method to represent the passive properties of cervical spine intervertebral joints in MSK models is to define ligaments and intervertebral discs as separate viscoelastic elements [66]. In Kuo et al. (2019) eleven cervical spine ligament groups were represented using 80 individual linear elements. The non-linear toe, linear and yield regions of the ligaments' force-length relationship were defined using piecewise linear functions used to fit their model to previous experimental values from the literature. Additionally, the annulus fibrosus of each the intervertebral disc was attempted to be represented with two elements. The study reported that the passive elements significantly contributed in the reduction of head angular accelerations after impulses were applied to the head. Although it is clear that a significant volume of work was completed for this study the question of parameter overfitting in the MSK model's passive parameters could be accounted for directly with the use of an FE or hybrid FE-MSK model. Thus the decision to represent the passive properties of each cervical spine intervertebral joint as either a lumped parameter or individual elements (i.e. intervertebral discs and ligaments) in musculoskeletal models should be made with caution. As the complexity of the representation increases the inclusion of additional parameters could lead to overfitting or generate multiple solutions when identifying their values that make the practical interpretation of the results difficult. For this reason this thesis will focus on the use of lumped parameter models (i.e. bushings) for the representation of the intervertebral joint passive properties.

### 3.4 Summary

The aim of this chapter was to provide an overview of available musculoskeletal methods used to investigate cervical spine injury mechanisms. Aspects of models and methods that influence the development of computational injury prevention research were also identified. The main aspects of the review are summarised below:

- Multibody musculoskeletal and finite element models can be used for cervical spine injury analysis. Each provide different scales of resolution with their respective benefits and limitations. Their use in hybrid multi-scale models would be beneficial in future research to investigate intervertebral disc responses. However, at the present the relative ease of muscle representation in musculoskeletal over finite element models during dynamic simulations and their integration with experimental data due to fewer boundary conditions remains a strong argument for their use. This thesis will use musculoskeletal models to investigate cervical spine injuries during axial compressive impacts in the applied setting of rugby. The musculoskeletal modelling approach was not only chosen for the above rea-

son to link it with experimental data to obtain initial conditions but also that previous computational neck injury studies have utilised similar musculoskeletal approaches. Camacho et al. (1998) and Nightingale et al. (2016) had a combined finite element model of the head connected to rigid vertebrae with six degree of freedom bushing elements to investigate similar head first axial compressive impacts. As the kinematic response of the cervical spine column to this loading modality which is theorised to precede the observed lower cervical spine anterior dislocations in catastrophic rugby accidents musculoskeletal models were deemed an appropriate tool for the investigation.

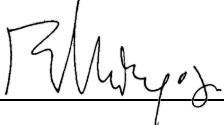
- Inverse analyses can provide information during measurable non-injurious neck experiments whereas forward simulations can be used to investigate theoretical impact scenarios. The studies presented in this thesis will utilise inverse analyses to gain estimates of neck joint motion and muscle activation that cannot be measured directly through experiments. This data will then be used to inform forward simulations of injurious events of misdirected impacts to the head that are not ethically or experimentally feasible.
- Biofidelic representation of neck muscle paths and maximal isometric strength are important in simulating the cervical spine's response to impacts. This is emphasised in athletic populations, such as rugby or American football players, where muscle morphology can be significantly different from the average population. For this reason, MRI data of a rugby player will be used to inform the creation of musculoskeletal model.
- Pure optimisation methodologies can estimate neck muscle activation patterns however EMG-assisted methods can be used to better elucidate muscle recruitment strategies during impacts as the neuromuscular recruitment objective is not clear. The exploration of if pure optimisation or EMG-assisted methods are best suited for the analysis of rugby impacts will be completed.
- Variability in the measurement of intervertebral joint passive properties necessitates appropriate selection of model viscoelastic or kinematic coupling parameters whilst considering the type of computational investigation being conducted with the model. For this reason, novel intervertebral joint viscoelastic properties will be estimated that are representative of the loads experienced during rugby impacts. Kinematic coupling and passive parameters will be used appropriately within the integrated framework presented in this thesis to estimate and predict the response of the cervical spine to external and internal loads.

## Chapter 4 959

# Musculoskeletal modelling of the 960 human cervical spine for the 961 investigation of injury 962 mechanisms during axial impacts 963

### *Pre-chapter commentary* 964

This chapter includes an investigation into the passive response of the multi-level cervical spine to axial impacts. Correct description of the cervical spine's intervertebral joints response to impacts representative of loads experience during rugby tackling is an important step in being able to create a musculoskeletal model to investigate injury mechanisms. This first study of the thesis describes an *in vitro* and *in silico* investigation to estimate viscoelastic joint parameters that can be used in impact specific musculoskeletal models. 965  
966  
967  
968  
969  
970  
971

<b>This declaration concerns the article entitled:</b>			
Chapter 4: <i>"Musculoskeletal modelling of the human cervical spine for the investigation of injury mechanisms during axial impacts"</i> 972			
<b>Publication status (tick one)</b>			
Draft manuscript <input type="checkbox"/> Submitted <input type="checkbox"/> In review <input type="checkbox"/> Accepted <input type="checkbox"/> Published <input checked="" type="checkbox"/>			
<b>Publication details (reference)</b>	Silvestros P, Preatoni E, Gill HS, Gheduzzi S, Hernandez BA, Holsgrove TP and Cazzola D (2019) Musculoskeletal modelling of the human cervical spine for the investigation of injury mechanisms during axial impacts. PLoS ONE 14(5): e0216663. <a href="https://doi.org/10.1371/journal.pone.0216663">https://doi.org/10.1371/journal.pone.0216663</a>		
<b>Copyright status (tick the appropriate statement)</b>			
I hold the copyright for this material <input checked="" type="checkbox"/> Copyright is retained by the publisher, but I have been given permission to replicate the material here <input type="checkbox"/>			
<b>Candidate's contribution to the paper (provide details, and also indicate as a percentage)</b>	<p>The candidate considerably contributed to and predominantly executed the:</p> <p><b>Formulation of ideas: 75%</b> PS contributed to: Background research, proof of concept theoretical study on existing data and presentation of the combined methodology to supervisors and co-investigators</p> <p><b>Design of methodology: 60%</b> PS made the decision for the use of experimental methods initially developed by TPH, contributed fully in the choice of computational methodology this study used</p> <p><b>Experimental work: 60%</b> Experimental work was carried out by PS together with BAH and a MEng student for joint use of the dataset under the supervision of SG</p> <p><b>Formal data analysis: 90%</b> PS performed the computational simulations and the analysis on the input and output data</p> <p><b>Presentation of data in journal format: 75%</b> PS wrote the first draft of the paper, draft revisions, submitted the manuscript to the journal and made amendments required for publication.</p>		
<b>Statement from Candidate</b>	This paper reports on original research I conducted during the period of my Higher Degree by Research candidature.		
<b>Signed</b>		<b>Date</b>	20 <sup>th</sup> June 2020

## 4.1 Abstract

973

Head collisions in sport can result in catastrophic injuries to the cervical spine. Muscu- 974  
loskeletal modelling can help analyse the relationship between motion, external forces 975  
and internal loads that lead to injury. However, impact specific musculoskeletal models 976  
are lacking as current viscoelastic values used to describe cervical spine joint dynamics 977  
have been obtained from unrepresentative quasi-static or static experiments. The aim 978  
of this study was to develop and validate a cervical spine musculoskeletal model for 979  
use in axial impacts. Cervical spine specimens (C2-C6) were tested under measured 980  
sub-catastrophic loads and the resulting 3D motion of the vertebrae was measured. 981  
Specimen specific musculoskeletal models were then created and used to estimate the 982  
axial and shear viscoelastic (stiffness and damping) properties of the joints through 983  
an optimisation algorithm that minimised tracking errors between measured and sim- 984  
ulated kinematics. A five-fold cross validation and a Monte Carlo sensitivity analysis 985  
were conducted to assess the performance of the newly estimated parameters. The 986  
impact-specific parameters were integrated in a population specific musculoskeletal 987  
model and used to assess cervical spine loads measured from Rugby union impacts 988  
compared to available models. Results of the optimisation showed a larger increase of 989  
axial joint stiffness compared to axial damping and shear viscoelastic parameters for all 990  
models. The sensitivity analysis revealed that lower values of axial stiffness and shear 991  
damping reduced the models performance considerably compared to other degrees of 992  
freedom. The impact-specific parameters integrated in the population specific model 993  
estimated more appropriate joint displacements for axial head impacts compared to 994  
available models and are therefore more suited for injury mechanism analysis. 995

## 4.2 Introduction

The worldwide reported incidence for traumatic cervical spine injuries is 15 to 39 cases per million [35, 71]. Spinal injuries associated with permanent neurological damage have devastating consequences on the quality of life of the individual and can result in individual lifetime costs rising to \$3 million [105]. Neurological damage can reduce quality of life and lead to secondary factors such as discrimination, depression, and suicide [105] with wider societal costs of up to \$9.7 billion [1]. In sporting activities, cervical spine injuries are more common during high energy contact sports such as American football and Rugby union, where the incidence rates of catastrophic cervical spine injuries range from 2 to 10 per 100,000 players per year for American football [111] and Rugby union [18] respectively. A better understanding of injury mechanisms is key to educate coaching and conditioning as well as to inform possible changes to the governing rules of contact sports. *In silico* approaches allow the estimation of measures such as internal joint loads and muscle forces that are extremely difficult and impractical to safely measure in sporting conditions. Also, they give the opportunity to explore ranges of theoretical scenarios [40] and thus understand how changes in impact conditions (e.g. external load, movement technique) and neuromusculoskeletal characteristics (e.g. muscle activation patterns) may affect injury factors. The reliability of such computational approaches is strongly dependent on the models used and their rigorous validation [54]. Although a lot of work has been produced to investigate the mechanisms of cervical spine injury in impact events, such as motor vehicle accidents and falls [37, 96], application of musculoskeletal models in sporting neck injury research is lacking.

Musculoskeletal models of the cervical spine have been created for the biomechanical analysis of functional neck movements [38, 133, 152] and impacts [21, 37, 51, 96]. Multibody musculoskeletal modelling can estimate system dynamics during sport impact events and, if rigorously validated, provide a viable approach to test fundamental principles and investigate their injury mechanisms [54]. This approach also enables a practical and direct use of experimental data as inputs for musculoskeletal analyses [123], and allows simulations to be run at low computational cost compared to detailed finite element models. Furthermore, musculoskeletal simulation results can be used as boundary conditions to finite element models [154], which can then provide a more detailed description of the stress and strain patterns experienced by specific spinal structures [63]. Musculoskeletal models of the cervical spine have incorporated biomechanical properties of the intervertebral disc to investigate and better understand head and neck injury mechanisms during dynamic loading scenarios such as motor vehicle



collisions and falls [21, 37, 41, 51, 96, 148]. By approximating the complex dynamic be- 1032  
haviour of spinal joints the resulting joint motions can be estimated providing valuable 1033  
information for injury mechanism analysis. 1034

The viscoelastic behaviour of the intervertebral disc [34, 108] in musculoskeletal mod- 1035  
els has been represented with the Kelvin-Voight model of a parallel arrangement of a 1036  
spring and a damper, which is referred to as a “bushing element” in the automotive 1037  
sector [5, 70]. The stiffness and damping values of the bushings are obtained from 1038  
*in vitro* experimental studies on human and animal (e.g. porcine, bovine) specimens 1039  
which are implemented in musculoskeletal models [21, 37, 41, 51, 83, 96, 131]. Some 1040  
of these musculoskeletal models have been used to analyse the internal loading of the 1041  
cervical spine during axial compressive loading [21, 96], however the *in vitro* experi- 1042  
mental procedures used to extract cervical joint stiffness values [93] were not conducted 1043  
under conditions that correctly reflect the scenarios the models are used to evaluate 1044  
[21, 96]. For example, the model initially developed by Camacho et al. (1997) [21] and 1045  
later updated and used by Nightingale et al. [96] is used in the analyses of axial head 1046  
impacts with peak forces of 2 kN being reached within 5 to 10 ms of loading. These 1047  
values are an order of magnitude higher to what the study of Nightingale et al. (1991) 1048  
[93] used, with peak loads of near 200 N reached in 2 s, to calculate joint stiffnesses 1049  
and are not representative of high energy collisions occurring in sport. In fact, cervical 1050  
spine injuries experienced during sport impacts are often caused by loads characterised 1051  
by a high rate and magnitude of loading [40, 67]. 1052

From an experimental point of view, *in vitro* tests have often investigated the loading 1053  
response of intervertebral discs using single motion segments (vertebra-disc-vertebra) 1054  
under static or quasi-static loading conditions [84, 101, 124, 157]. However, the be- 1055  
haviour of the entire cervical spine as a multi-segmented beam with interactions be- 1056  
tween joints is too complex to be modelled as the sum of individual joint responses 1057  
to loading [93, 113]. The lack of a model that is representative of the cervical spine 1058  
behaviour under impulsive axial loads is likely to be due to technical limitations in 1059  
both experimental and computational approaches. The reliable estimation of individ- 1060  
ual joint stiffness of a multi-level cervical spine under such conditions would require 1061  
experimental rigs capable of applying high load-controlled impulses whilst measuring 1062  
individual vertebral motion. Currently experimental designs that can load a multi- 1063  
level cervical spine specimen and measure individual joint displacements mechanically 1064  
is challenging. However, combining subject specific modelling with high speed motion 1065  
capture [59, 113] can be used to measure vertebral motion without the need for highly 1066  
technical experimental rigs. 1067

Therefore, the aim of this study was to: (a) estimate the viscoelastic properties of individual joints of multi-jointed cervical spines under loading conditions representative of sport impacts; (b) create and validate the first musculoskeletal model of the cervical spine that efficiently and reliably enables the estimation of compressive and shear joint forces and resulting motions via linear bushing (Kelvin-Voight) elements during impulsive loads; and (c) evaluate the newly developed model’s behaviour during an injurious sporting scenario.

## 4.3 Materials and Methods

*In vitro* experimental data and *in silico* methods were used to estimate the viscoelastic properties of the cervical spine’s joints. Representative loads of sub-catastrophic sporting impacts were applied to porcine cervical spine specimens (C2-C6) which were used as human specimen surrogates during experimental testing.

### 4.3.1 *In vitro* experiments

Six porcine cervical spine specimens (C2-C6) were excised from pigs aged between 8 and 12 months at the time of slaughter (Larkhall Butchers, Bath, UK). Surrounding musculature was removed, facet capsules and ligaments were maintained apart from the anterior longitudinal ligament. Specimens were secured in a neutral position into nylon pots with bone cement (CMW, DePuy Int. Ltd., Leeds, UK). Motion capture markers (9 mm diameter) were glued using epoxy adhesive and allowed to become secure (approximately 10 minutes) in a non-collinear arrangement to the anterior surface of the vertebral bodies. Specimens were then wrapped in paper towels, sprayed with 0.9% saline solution, sealed in plastic bags and frozen at  $-24^{\circ}\text{C}$ . Each frozen specimen underwent 0.1 mm resolution micro-computed tomography ( $\mu\text{CT}$ ) scans (XT225 ST, Nikon Metrology, UK) prior to impact testing. The mass and height of each specimen were recorded and are presented in Table 4.1.

On the day of testing each specimen was left to thaw at room temperature ( $21 \pm 2^{\circ}\text{C}$ ) whilst kept hydrated by applying saline solution to the surface of the wrapped specimens. The specimens did not undergo any preconditioning prior to impact testing. Motion capture tracking clusters were placed posteriorly to each transverse process of the C3, C4 and C5 vertebrae (Figure 4-1) and rigidly secured to the bony segments by means of a self-tapping screw. The specimen was mounted in an impactor [57] and was preloaded with 152 N via two constant force springs (51 N bilateral to the specimen) and the weight of the impact plate (50 N cranial to the specimen) [57, 113]. The

Table 4.1: Descriptive data of porcine cervical spine segments (C2-C6).

Specimen number	Mass (kg)	Height (m)
<b>S1</b>	0.378	0.203
<b>S2</b>	0.444	0.215
<b>S3</b>	0.396	0.202
<b>S4</b>	0.375	0.199
<b>S5</b>	0.358	0.202
<b>S6*</b>	0.570	0.223
<b>Mean <math>\pm</math> SD</b>	<b>0.390 <math>\pm</math> 0.033</b>	<b>0.204 <math>\pm</math> 0.006</b>

\* The mass and height of Specimen 6 (S6) are only shown for comparison and not included in the average values of the specimens as it sustained fractures at the C2, C3 and C4 vertebral levels.

experimental configuration constrained C2 to one DoF (axial translation) and C6 to zero DoF. This left the C3 to C5 vertebrae (C3-C4 and C4-C5 joints) unconstrained and able to move in a more physiologically manner.

A load of 80 N was dropped from a height of 0.5 m to the impact plate on the cranial aspect of the specimen to simulate peak forces measured during sub-catastrophic rugby tackles [104, 119]. Two 22 kN load cells (Model SLC41/005000, RDP Electronics Ltd., UK) were used to collect cranial and caudal force data at 1 MHz using an analogue to digital converter (TiePie Handyscope HS5 USB Oscilloscope, TiePie Engineering, Koperslagersstraat, Netherlands). Synchronised kinematic data were recorded by a five-camera motion capture system (Oqus, Qualisys, Sweden) at 4 kHz. Following impact testing specimens were  $\mu$ CT scanned to ensure the impact was sub-catastrophic.

Impact force data were filtered with a zero-lag fourth-order low-pass Butterworth filter with a cut-off frequency of 5 kHz (Matlab 2017a, The Mathworks, Natick, MA, USA). Kinematic marker data were filtered using the same filter with a cut-off frequency of 150 Hz after a power density analysis was performed on the raw kinematic data. For both sets of data the time of impact was identified when the cranial load cell measurement exceeded 200 N [57, 113].

#### 4.3.2 Musculoskeletal model creation

The pre-impact  $\mu$ CT images were segmented (ScanIP M-2017.06, Simpleware, UK) to obtain specimen specific geometries of the cervical spine vertebrae. The MeshLab v2016.12 [32], NMSBuilder 2.0 [144] and OpenSim 3.3 [39] software packages were used to create specimen specific musculoskeletal models analogous to conventional methods used [80].

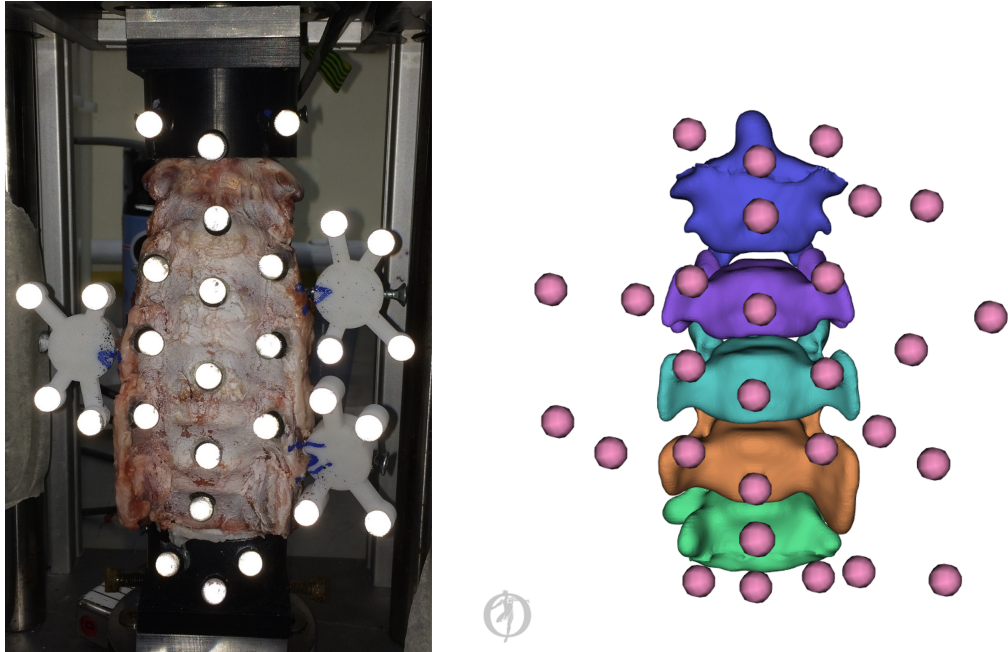


Figure 4-1: Experimental set up of the spinal specimen positioned in the impact rig (left) and digital representation as a specimen specific model with virtual registered markers (right). Markers secured to the anterior aspect of the specimen and the cranial and caudal pots were used for the registration process during model creation. The markers of the cranial pot and the clusters secured to the C3, C4 and C5 vertebrae were used as tracking markers in the optimisation

1124 Joint frame origins were located at the center of the intervertebral mid-planes between  
 1125 the inferior surface of the cranial segment and superior surface of the caudal segment  
 1126 for each of the four joints [121]. The anterior-posterior (x-axis) and medio-lateral (z-  
 1127 axis) axes were defined parallel to the superior surface of the caudal vertebrae with  
 1128 the superior-inferior (y-axis) axis normal to this plane Figure 4-2. Six degree of free-  
 1129 dom viscoelastic bushing elements comprised of a linear spring and damper in parallel  
 1130 (Kelvin-Voight model) were defined through the OpenSim 3.3 Matlab API to be coin-  
 1131 cident with the joint frames origins to overcome dynamic errors [31]. Reference values  
 1132 from the literature [37] were used to initialise all degrees of freedom of the four bushing  
 1133 elements. The OpenSim models were then constrained to replicate the experimental  
 1134 set up. Virtual markers were created in the same relative position as the experimental  
 1135 tracking markers to the cervical vertebrae by registering their position to the segmented  
 1136 static marker positions measured from the  $\mu$ CT scans.

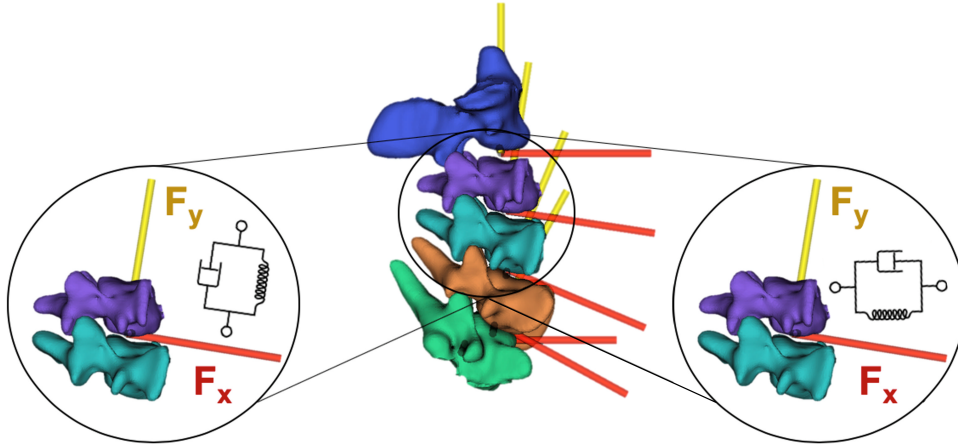


Figure 4-2: Joint and coincident 6 DOF viscoelastic bushing element locations. Only axial ( $F_y$  - left) and anteroposterior ( $F_x$  - right) viscoelastic elements were optimised, the parameters of the remaining four degrees of freedom remained at their initialised values.

### 4.3.3 Optimisation Pipeline

1137

A dynamic optimisation pipeline Figure 4-3 was developed to identify the optimal compressive (superior-inferior) and shear (anterior-posterior) viscoelastic bushing parameters. Simulations were performed up to 5 ms after the time of impact, which contained the cranial load peaks. A genetic algorithm (Matlab 2017a) was used to investigate the parameter space and identify the optimal viscoelastic bushing parameters ( $n=16$ ) by minimising the root mean square error (RMSE) between measured and simulated 3D marker kinematics over the 5 ms simulation window.

1138

1139

1140

1141

1142

1143

1144

### 4.3.4 Validation and sensitivity analysis

1145

A five-fold cross validation was completed by applying the median value of the identified parameters obtained from four of the five spines to the model of the fifth spine iteratively a total of five times. The new combination of model and parameters was then used in the forward dynamic section of the previous pipeline Figure 4-3 and evaluated against the experimental kinematic data of remaining fifth model, which was not included in the calculation of the parameters median value.

1146

1147

1148

1149

1150

1151

The 16 optimised parameters of each spine were grouped into four sets of four parameters dependent on their functionality: axial stiffness ( $k_y = [k_y^{C2C3}, k_y^{C3C4}, k_y^{C4C5}, k_y^{C5C6}]$ ), axial damping ( $b_y = [b_y^{C2C3}, b_y^{C3C4}, b_y^{C4C5}, b_y^{C5C6}]$ ), shear stiffness ( $k_x = [k_x^{C2C3}, k_x^{C3C4}, k_x^{C4C5}, k_x^{C5C6}]$ ) and shear damping ( $b_x = [b_x^{C2C3}, b_x^{C3C4}, b_x^{C4C5}, b_x^{C5C6}]$ ), where  $k$  is stiff-

1152

1153

1154

1155

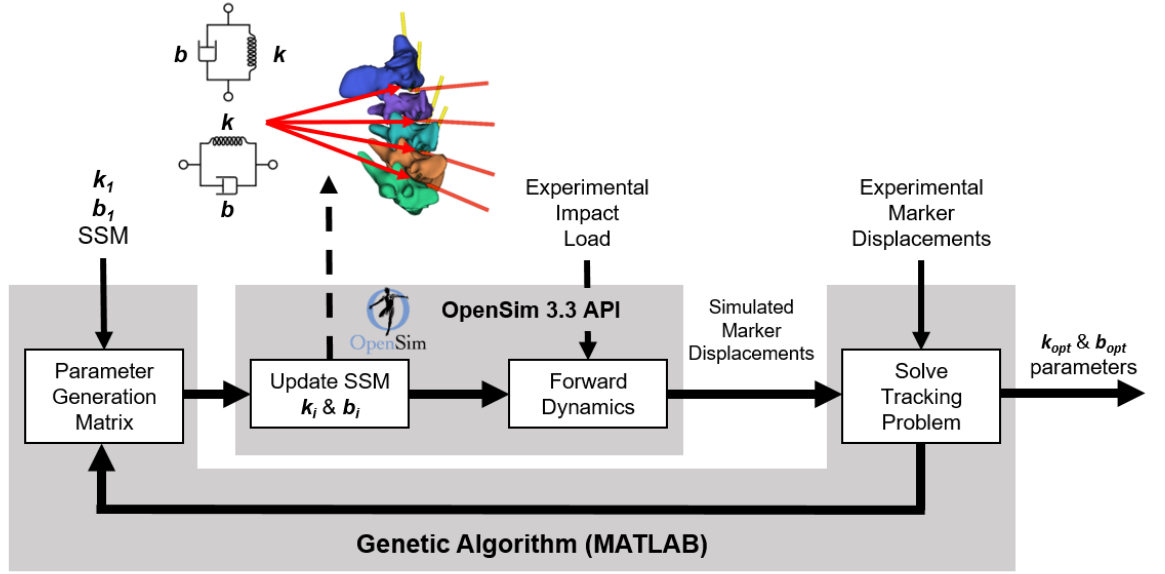


Figure 4-3: Optimisation pipeline used to estimate specimen specific model viscoelastic joint parameters. Literature values [37] ( $k_1$  and  $b_1$ ) were used to initialise the 6 DoF viscoelastic bushing elements of the specimen-specific models (SSM). A total of 16 optimised stiffness ( $k_{opt}$ ) and damping ( $b_{opt}$ ) for axial and shear degrees of freedom were estimated.

ness,  $b$  is damping, subscripts indicate direction ( $y$  compressive and  $x$  shear) and superscripts show the joint level. Model sensitivity to individual parameter set uncertainty was also assessed by varying individual sets from 50% to 150% of their identified optimum value.

To assess model sensitivity to combined changes in the four parameter sets a 1000 sample Monte Carlo analysis (Matlab 2017a) was performed by randomly perturbing axial stiffness, axial damping, shear stiffness and shear damping simultaneously with a uniform distribution between 50% and 150% of their identified optimum value (Equation 4.1):

$$p_i = p + rp \quad (4.1)$$

Where  $p$  is the entire set of optimised parameters  $p = [k_y, b_y, k_x, b_x]$ ,  $r = [-0.5, 0.5]$  is the coefficient used to induce the parameter perturbations and  $p_i$  is the  $i^{th}$  set of perturbed parameters of the sensitivity analysis. Third degree polynomial surfaces

were then fitted to the six pairs of parameter combinations to better asses their effect  
on RMSE change. Changes in the RMSE during the perturbations were evaluated as  
(Equation 4.2):

$$\Delta RMSE = RMSE_{per} - RMSE_{opt} \quad (4.2)$$

Where  $RMSE_{per}$  and  $RMSE_{opt}$  are the RMSE between experimental and simulated  
marker kinematics of the  $i^{th}$  parameter set perturbation simulation of the Monte Carlo  
analysis and identified optimum parameter sets respectively.

Similarly, the joint frame position (JFP) on the intervertebral mid-planes was program-  
matically varied between -0.02 m and 0.02 m in the anteroposterior direction on all four  
joints simultaneously (Equation 4.3):

$$JFP_i^x = JFP^x + dx \quad (4.3)$$

Where  $JFP^x$  is the anteroposterior joint frame positions for the four cervical spine  
joints C2-C3, C3-C4, C4-C5, C5-C6,  $dx = [-0.02, 0.02]$  is the displacement in meters  
applied to the joint frame locations and  $JFP_i^x$  is the newly defined anteroposterior  
position of the joint frames.

#### 4.3.5 Application to an injurious sporting scenario

The viscoelastic parameters estimated in this study, and previously used viscoelastic  
parameters from the literature [37] were then integrated in a population specific model  
(i.e. “Rugby Model”, [23]) to evaluate their behaviour during a sporting injurious  
scenario. This analysis was based on the comparison between three different models: i)  
the original “Rugby Model” [23] that utilises kinematic constraints [152], ii) a version  
implemented with the 6 DoF bushings from de Bruijn et al. (2016) [37] updated  
with the median values of the C3-C4 and C4-C5 joints for axial and shear viscoelastic  
parameters estimated in this study (hence referred to as impact-specific), and iii) the  
“Rugby Model” integrated with the original de Bruijn et al. (2016) [37] viscoelastic  
parameters (hence referred to as quasi-static).

The models response was compared during a simulated head-first impact in rugby,  
and consisted in the analysis of the cervical spine joint kinematics and reaction forces.  
Forward dynamic simulations (OpenSim 3.3) were used for the analysis and driven by  
a set of pure axial loads applied to the skull segment (Figure 4-7: 1<sup>st</sup> row). Existing

1196 muscle actuators of the “Rugby Model” were included but no activation was prescribed  
 1197 to them. The external load profile used as input for the forward dynamics simulations  
 1198 was taken from dummy head forces (Hybrid III, Humanetics, Germany) measured  
 1199 during live scrum trials against an instrumented scrum machine [128].

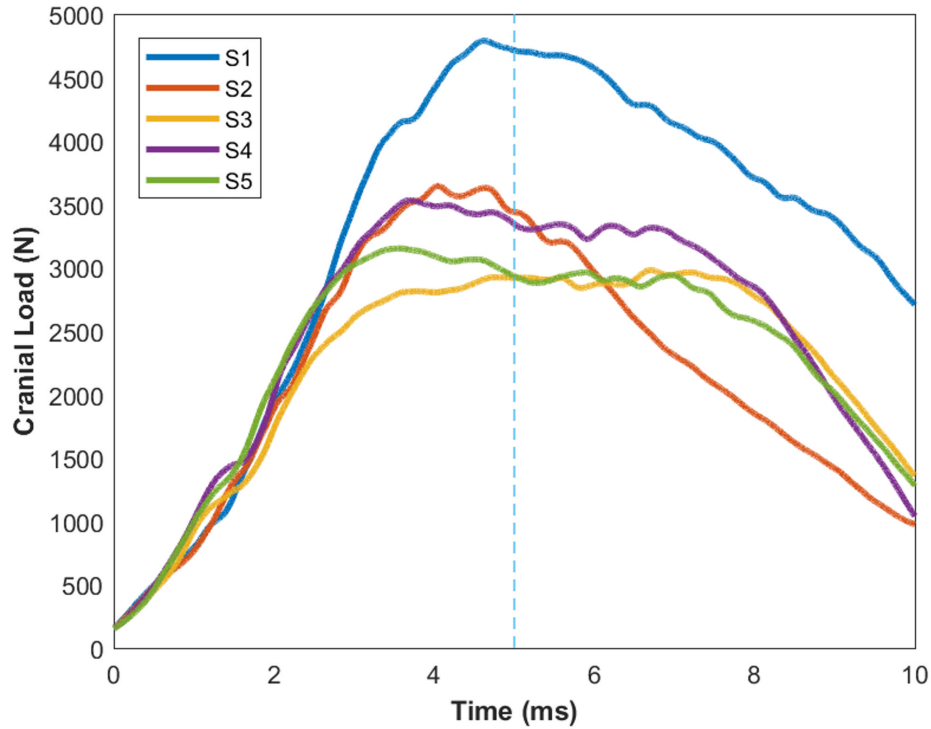


Figure 4-4: Axial loads measured at the cranial load cell during the experiments. The initial 5 ms (segmented vertical line) of the load traces were used to drive the forward dynamics simulations by applying them to the centre of mass of the C2 segments of the models. The legend denotes specimens S1 to S5.

## 1200 4.4 Results

1201 Peak cranial loads measured experimentally ranged from 3.0 to 4.8 kN (Figure 4-4)  
 1202 with maximal axial displacements of 1.2 to 7.5 mm. One of the six tested specimens  
 1203 (S6) suffered vertebral body fractures at the C2, C3 and C4 levels and was not included  
 1204 in the report of the final parameter values. The genetic algorithm evaluated 100 sample  
 1205 populations over 15 generations of the parameter space with an approximate run time  
 1206 of 10 hours (real-time) per model on a 3.00 GHz v6 Xeon processor with 32 GB RAM.

1207 Overall, the estimated values for axial stiffness, axial damping shear stiffness and shear



damping across the four joints increased with respect to the initialised values taken from the literature, and ranged between 2.2 to 26.6 MN/m, 2.4 to 6.1 kNs/m, 28.4 to 91.2 kN/m and 0.6 to 1.5 kNs/m respectively (Figure 4-5, Tables 4.2 and 4.3). The average RMSE of the five models was 0.46 mm across the 5 ms between the simulation and measured kinematics. The five-fold cross validation showed that interchanging bushing parameter values between models closely replicated model kinematics as tracking errors increasing by 2.5 to 6.4% for specimens S1, S3, S4 and S5, whilst specimen S2 showed a 35.4% increase compared to optimised tracking errors (Table 4.4).

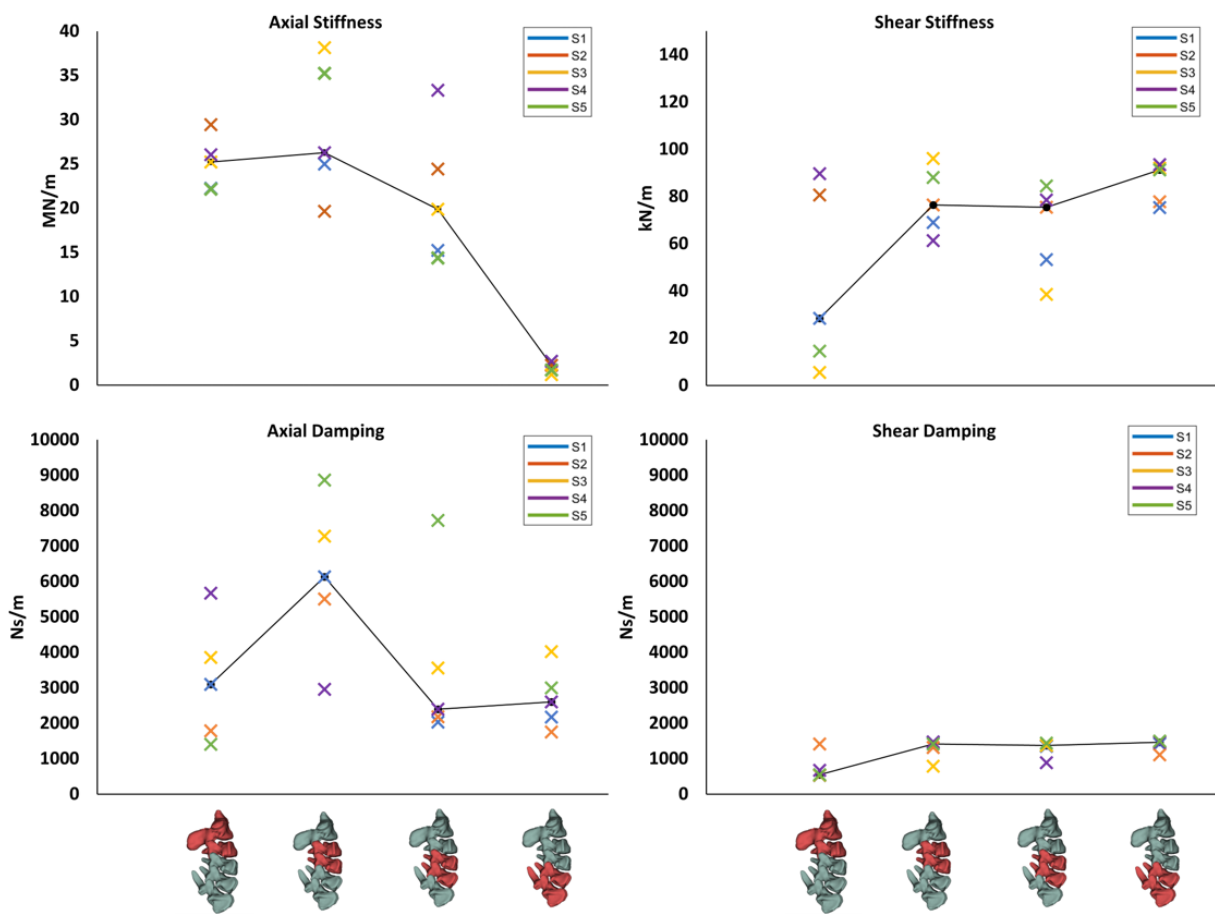


Figure 4-5: Parameter values identified by the optimisation procedure. Axial stiffness (top left), shear stiffness (top right), axial damping (bottom left) and shear damping (bottom right). Values are shown for each of the cervical spine joints identified by the two red coloured vertebrae on the horizontal axis and for each of the five specimens identified by the legends. The legend denotes specimens S1 to S5.

Table 4.2: Axial stiffness (k) and damping (b) parameter values identified for each specimen specific model of the spinal specimens (S1-S5).

Axial	C2-C3		C3-C4		C4-C5		C5-C6	
	Stiffness (k) N/m	Damping (b) Ns/m	Stiffness (k) N/m	Damping (b) Ns/m	Stiffness (k) N/m	Damping (b) Ns/m	Stiffness (k) N/m	Damping (b) Ns/m
<b>Initialised values</b>	$1.1 \times 10^6$	$10^3$	$1.1 \times 10^6$	$10^3$	$1.1 \times 10^6$	$10^3$	$1.1 \times 10^6$	$10^3$
<b>S1</b>	$22.2 \times 10^6$	$3.1 \times 10^3$	$25.0 \times 10^6$	$6.1 \times 10^3$	$15.2 \times 10^6$	$2.0 \times 10^3$	$2.7 \times 10^6$	$2.2 \times 10^3$
<b>S2</b>	$29.4 \times 10^6$	$1.8 \times 10^3$	$19.7 \times 10^6$	$5.5 \times 10^3$	$24.4 \times 10^6$	$2.2 \times 10^3$	$2.2 \times 10^6$	$1.8 \times 10^3$
<b>S3</b>	$25.2 \times 10^6$	$3.9 \times 10^3$	$38.2 \times 10^6$	$7.3 \times 10^3$	$19.9 \times 10^6$	$3.6 \times 10^3$	$1.2 \times 10^6$	$4.0 \times 10^3$
<b>S4</b>	$26.0 \times 10^6$	$5.7 \times 10^3$	$26.3 \times 10^6$	$3.0 \times 10^3$	$33.3 \times 10^6$	$2.4 \times 10^3$	$2.7 \times 10^6$	$2.6 \times 10^3$
<b>S5</b>	$22.2 \times 10^6$	$1.4 \times 10^3$	$35.2 \times 10^6$	$8.9 \times 10^3$	$14.4 \times 10^6$	$7.7 \times 10^3$	$1.7 \times 10^6$	$3.0 \times 10^3$
<b>Median</b>	$25.2 \times 10^6$	$3.1 \times 10^3$	$26.3 \times 10^6$	$6.1 \times 10^3$	$19.9 \times 10^6$	$2.4 \times 10^3$	$2.2 \times 10^6$	$2.6 \times 10^3$

Initialised values used at the start of the optimisation are presented in the first row.

Table 4.3: Shear stiffness (k) and damping (b) parameter values identified for each specimen specific model of the spinal specimens (S1-S5).

	C2-C3		C3-C4		C4-C5		C5-C6	
Shear	Stiffness (k) N/m	Damping (b) Ns/m	Stiffness (k) N/m	Damping (b) Ns/m	Stiffness (k) N/m	Damping (b) Ns/m	Stiffness (k) N/m	Damping (b) Ns/m
<b>Initialised values</b>	$63.0 \times 10^3$	$10^3$	$63.0 \times 10^3$	$10^3$	$63.0 \times 10^3$	$10^3$	$63.0 \times 10^3$	$10^3$
<b>S1</b>	$28.4 \times 10^3$	$0.5 \times 10^3$	$69.0 \times 10^3$	$1.5 \times 10^3$	$53.3 \times 10^3$	$1.4 \times 10^3$	$75.3 \times 10^3$	$1.4 \times 10^3$
<b>S2</b>	$80.6 \times 10^3$	$1.3 \times 10^3$	$76.4 \times 10^3$	$1.3 \times 10^3$	$75.5 \times 10^3$	$1.4 \times 10^3$	$77.8 \times 10^3$	$1.1 \times 10^3$
<b>S3</b>	$5.5 \times 10^3$	$0.5 \times 10^3$	$96.1 \times 10^3$	$0.8 \times 10^3$	$38.5 \times 10^3$	$1.4 \times 10^3$	$92.0 \times 10^3$	$1.5 \times 10^3$
<b>S4</b>	$89.7 \times 10^3$	$0.7 \times 10^3$	$61.3 \times 10^3$	$1.5 \times 10^3$	$78.6 \times 10^3$	$0.9 \times 10^3$	$93.5 \times 10^3$	$1.5 \times 10^3$
<b>S5</b>	$14.5 \times 10^3$	$0.6 \times 10^3$	$88.0 \times 10^3$	$1.4 \times 10^3$	$84.5 \times 10^3$	$1.4 \times 10^3$	$91.2 \times 10^3$	$1.5 \times 10^3$
<b>Median</b>	<b><math>28.4 \times 10^3</math></b>	<b><math>0.5 \times 10^3</math></b>	<b><math>76.4 \times 10^3</math></b>	<b><math>1.4 \times 10^3</math></b>	<b><math>75.5 \times 10^3</math></b>	<b><math>1.4 \times 10^3</math></b>	<b><math>91.2 \times 10^3</math></b>	<b><math>1.5 \times 10^3</math></b>

Initialised values used at the start of the optimisation are presented in the first row.

Table 4.4: Root mean square errors ( $RMSE_{opt}$  – Column 2) across the 15 tracking markers between measure and simulated kinematics during the optimisation procedure. Errors are also presented for the five-fold cross validation ( $RMSE_{val}$  – Column 3) and model evaluations using joint viscoelastic values from the literature [37] that were used to initialise the models at the start of each optimisation ( $RMSE_{lit}$  – Column 4). The calibration error of the motion capture system for each experimental measurement is presented for comparison (Column 5).

<b>Specimen number</b>	<b><math>RMSE_{opt}</math> (mm)</b>	<b><math>RMSE_{val}</math> (mm)</b>	<b><math>RMSE_{lit}</math> (mm)</b>	<b>Calibration error (mm)</b>
<b>S1</b>	0.46	0.47	2.59	0.24
<b>S2</b>	0.33	0.45	2.28	0.12
<b>S3</b>	0.58	0.59	2.08	0.17
<b>S4</b>	0.51	0.53	2.60	0.50
<b>S5</b>	0.44	0.46	2.30	0.29

1217 The models showed a similar response to individual and combined parameter variations  
1218 during the sensitivity analysis (Figure 4.4). Changing shear damping and axial stiffness  
1219 parameters in isolation resulted in the largest increases of RMSE by 0.2 to 0.4 mm.  
1220 When shear damping and axial stiffness were concurrently perturbed models showed  
1221 the largest combined effect on RMSE ranging between 0.4 and 0.6 mm (Figure 4.4:  
1222 1st and 2nd rows). Perturbations in anteroposterior joint locations resulted in RMSE  
1223 increases  $<0.1$  mm.

1224 The model comparison showed a similar response during the sub-injurious scenarios,  
1225 whilst the injurious scenario highlighted a different behaviour. The impact specific  
1226 model and the original “Rugby Model” yielded similar peak joint loads, whilst the  
1227 quasi-static model estimated 13 to 15% higher compressive loads for the three tested  
1228 impact conditions (Figure 4-7: 2nd row). The resulting joint compressions of the  
1229 bushing model with the new parameters allowed smaller displacements ( $<0.1$  mm)  
1230 compared to the model implemented with the previous parameters (0.4 to 1.5 mm)  
1231 (Figure 4-7 3rd row).

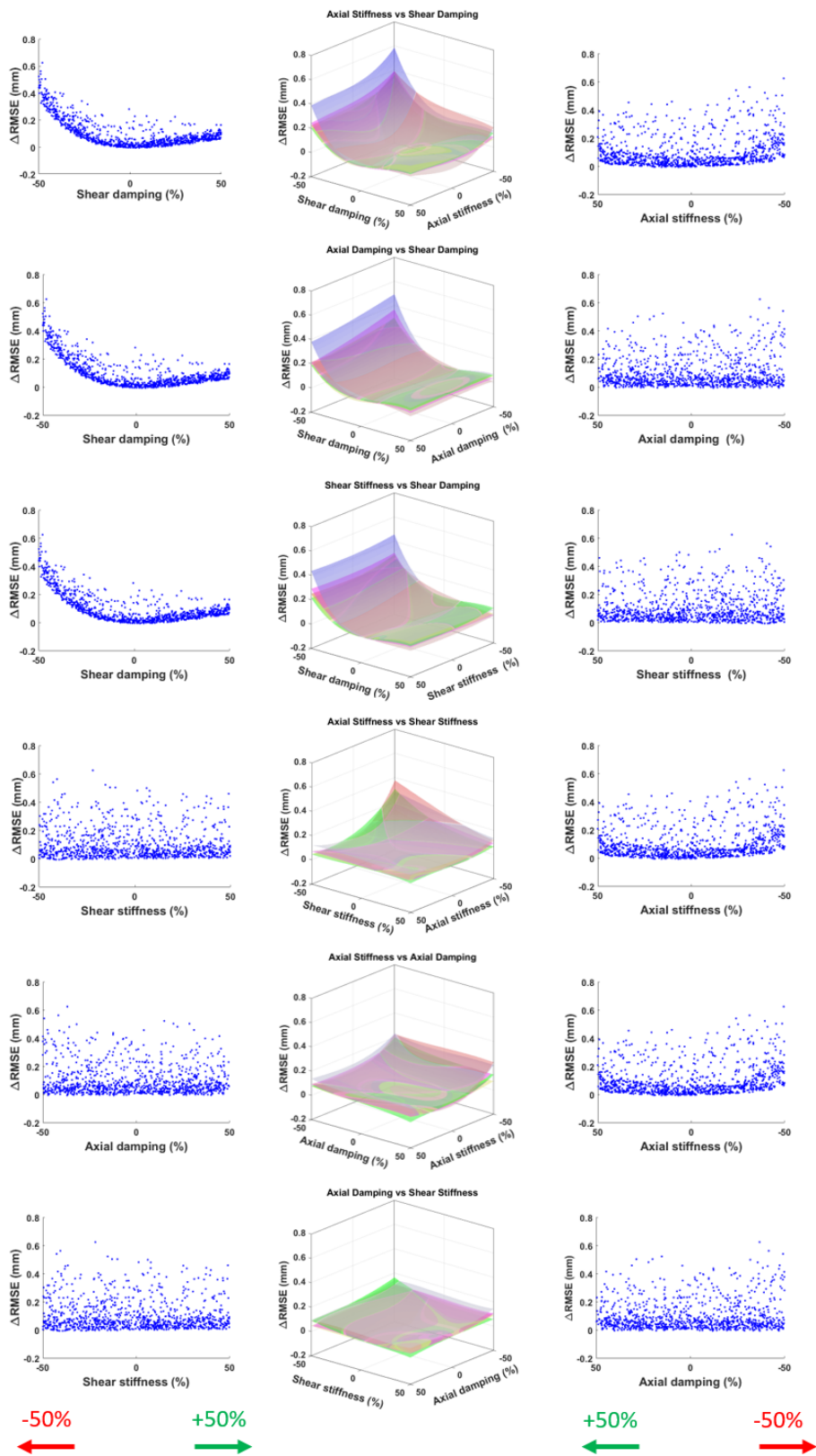


Figure 4-6: Results of the 1000 sample Monte Carlo sensitivity analysis for the five specimen-specific models. Results are presented in order of their effect on the  $\Delta RMSE = RMSE_{per}$  (largest to smallest). The axonometric view (central column) shows the response of the five models as the interpolated 3rd degree polynomial surfaces between the six possible parameter combinations. Left and right columns show the projection of each axis of the parameter variation against the  $\Delta RMSE = RMSE_{per}$  on their respective sides for specimen S1 as an example of the response.

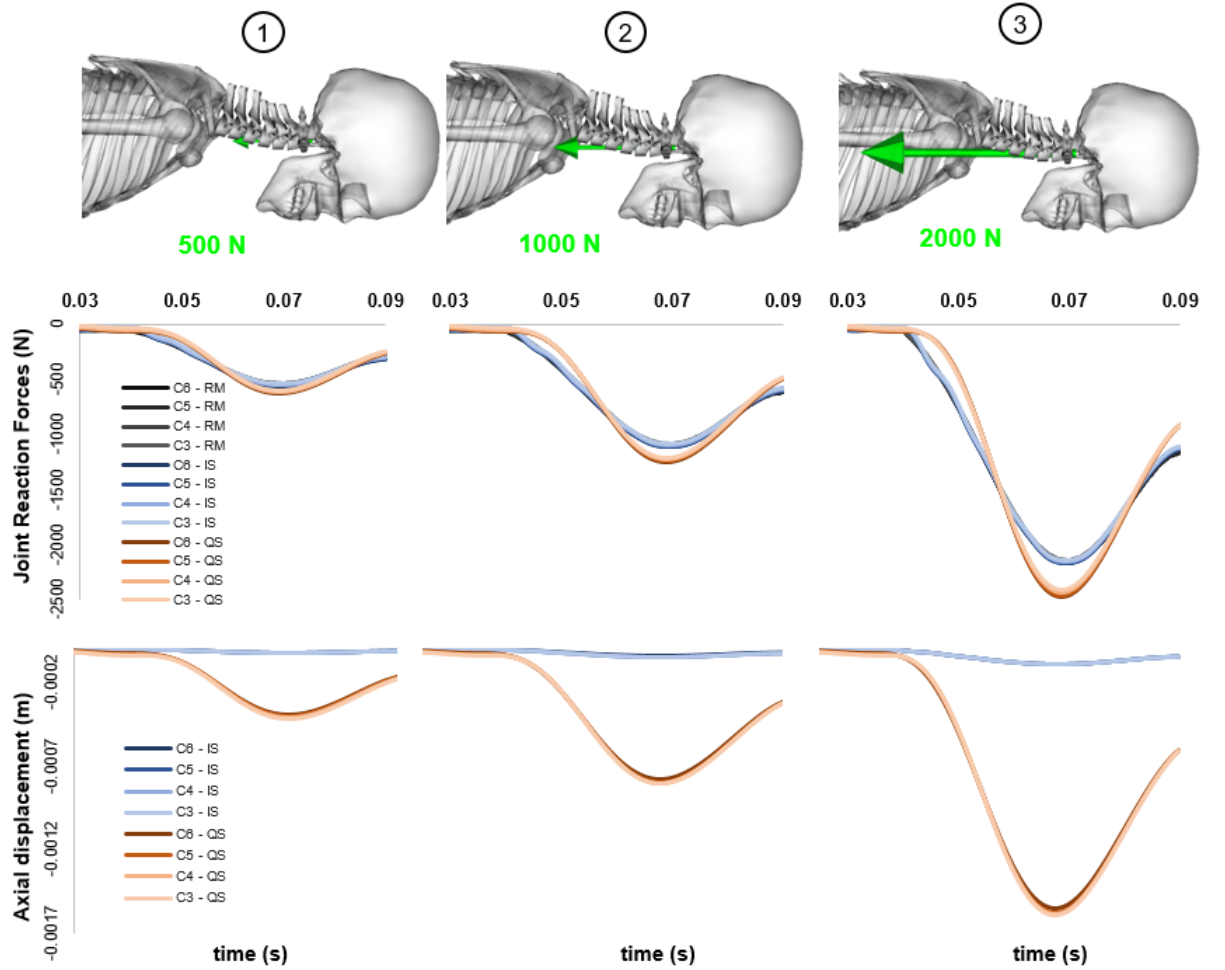


Figure 4-7: Forward dynamic results of theoretical injurious sporting scenario. Comparison of internal joint loads (Row 2) and resulting joint displacements (Row 3) calculated from the three versions of the musculoskeletal model and across three loading conditions (Row 1). Only joint loads are displayed for the Rugby Model (RM) as the kinematic constraints do not allow for joint translation which is displayed for Impact Specific (IS) and Quasi-Static (QS) versions of the model.

## 4.5 Discussion

1232

The purpose of this study was to identify and validate cervical spine viscoelastic joint parameters under impulsive axial impact conditions, and integrate them in a musculoskeletal model for the analysis of injury mechanisms. Specimen specific musculoskeletal models of porcine cervical spines were used as surrogates to human specimens to estimate joints' axial and shear viscoelastic values. Combined *in vitro* and *in silico* approaches allowed to identify the parameters that describe the viscoelastic response of individual cervical joints, and successfully apply them for the analysis and simulation of sporting scenarios.

1233  
1234  
1235  
1236  
1237  
1238  
1239  
1240

### 4.5.1 Viscoelastic parameter estimation

1241

The estimated stiffness values for axial compression increased by one order of magnitude from the initialisation values for all joints except the most caudal (C5-C6). Compressive damping as well as shear stiffness and damping also showed an increasing trend but remained within the same order of magnitude as the initialising values [37]. The large increase of axial stiffness values is likely to be related to the high impulsive load applied to the spine. The viscoelastic behaviour of the intervertebral disc has been characterised by its non-linear response to loading especially in axial compression which is a degree of freedom highly affected by the poroelastic properties of the disc [34, 108, 124, 161]. *In vitro* studies have measured increased apparent stiffness of intervertebral discs and functional units when subjected to higher loading rates indicating greater energy storage than energy dissipation under these conditions [34, 108].

1242  
1243  
1244  
1245  
1246  
1247  
1248  
1249  
1250  
1251  
1252

The musculoskeletal models of the presented study used a parallel arrangement of linear stiffness and damping elements (Kelvin-Voight model) to approximate the dynamics of the spine. This representation of the intricate dynamic behaviour of the intervertebral disc has been utilised previously [37, 96] and its ease of implementation into musculoskeletal models provides an added benefit for their use. More complex viscoelastic models of the intervertebral disc may be used in musculoskeletal models, however the inclusion of additional parameters over multiple levels of the spinal structure could lead to overfitting or generate multiple solutions that make the interpretation of the results difficult. There is potential that in future studies more detailed viscoelastic models can be explored however this initial use of a simple Kelvin-Voight model resulted in good estimation of the general intervertebral disc properties under dynamic loads.

1253  
1254  
1255  
1256  
1257  
1258  
1259  
1260  
1261  
1262  
1263

Linear bushings, however, only approximate regions of the inherent non-linear behaviour of the intervertebral disc's force-displacement curves. Thus, the higher esti-

1264  
1265

1266 mated values represent a steeper portion of the force-displacement curve of the interver-  
 1267 tebral discs caused by the high loading rate of sporting collisions. Median compressive  
 1268 stiffness values of the C2-C3 to C4-C5 joints were within similar values of 19.9 to 26.3  
 1269 MN/m compared to the stiffness for the C5-C6 joint of 2.2 MN/m. The lower axial  
 1270 stiffness values found at the most caudal joint (C5-C6) are attributed to the experi-  
 1271 mental and computational constraints during the experiments as well as the relative  
 1272 position of the joint with respect to the axial force vector applied at the C2 vertebra  
 1273 of the specimen. Full kinematic constraints on the C6 body of the models may have  
 1274 neglected small motions experienced in the experiment, and thus underestimated the  
 1275 joint stiffness. Additionally, the caudal section of the cervical spine displays greater  
 1276 lordosis which cause a rotation of the joint reference system in the sagittal plane (Fig-  
 1277 ure 4-2) and directs the vector of the axial force at a more of a shear angle to the  
 1278 C5-C6 joint. The effect of such anatomical change would be to transfer the load in  
 1279 a more anterior direction with respect to the joint. Similarly, optimal values in the  
 1280 shear direction were within closer ranges for the C3-C4 to C5-C6 joints compared to  
 1281 the C2-C3 joint. The constraints of the most cranial (C2) and caudal (C6) segments  
 1282 of the specimens allowed the intermediate vertebrae to be loaded in a more physiologic  
 1283 manner as they were experimentally unconstrained. This resulted in two joint levels  
 1284 C3-C4 and C4-C5 to be displaced with no experimental constraints acting on any of  
 1285 their segments. Therefore, due to the large sagittal angle of the C5-C6 joint to the ax-  
 1286 ial force vector, it is suggested that the median values of the C3-C4 and C4-C5 joints'  
 1287 axial and shear viscoelastic parameters estimated in this study, should be used across  
 1288 cervical spine joints in multibody models investigating impulsive axial impacts to the  
 1289 head. This strategy was adopted in the analysis of joint loads by implementing the  
 1290 stiffness and damping values in bushing parameters at the cervical spine joints of the  
 1291 validated "Rugby Model" [23].

1292 Investigations on the dynamic stiffness of individual joint levels of multi-jointed cervical  
 1293 spines have been limited. The increased compressive stiffness estimated for these speci-  
 1294 mens under the large impulsive loads logically follow results from static and quasi-static  
 1295 experiments on single joint units [84, 100, 124]. The studies by Panjabi et al. (1986)  
 1296 [100] and Moroney et al. (1988) [84] used incremental static loads up to a physiological  
 1297 loading range of 50 N to study the stiffness of cervical motion segments. Stiffness val-  
 1298 ues from the two studies differed substantially with 141 vs 1318 kN/m and 34 vs 131  
 1299 kN/m for axial compression and anteroposterior shear respectively. The static results  
 1300 of Moroney et al. (1988) [84], however, closely matched the quasi-static stiffnesses by  
 1301 Shea et al. (1991) [124] obtained from loads up to 2000 N. Both of these studies re-  
 1302 ported large variability in stiffness between specimens. This suggests that the range



of viscoelastic parameter values found in this study could be caused primarily by the physiological inter- and intra-specimen variability rather than the optimisation search. Musculoskeletal models of the human neck used in automotive research [37, 61, 147] have used the compressive stiffness values of these experimental studies when investigating injuries during collisions. However, the applicability of these values from static and quasi-static experiments to analyses of dynamic events remains an open question. Damping values of 1000 Ns/m were selected to sufficiently attenuate head acceleration, however it was believed these values may still be too low [61], which supports the larger damping values estimated in this study.

The experimental set-up of this study applied a higher compressive preload (152 N) to the physical specimens compared to previous experiments of 10 N and 42 N [84, 100]. A larger preload, more representative of that experienced *in-vivo*, does stiffen the cervical spine specimen prior to impact compared to specimens impacted without a preload/follower-load [113]. The higher preload [57, 113] together with the impulsive loading would support the significantly higher compressive stiffness increase compared to damping of the intervertebral discs that was estimated. This was supported by the sensitivity analysis where lower axial stiffness values resulted in higher tracking errors. Investigations of intervertebral disc mechanical response over increased loading rates have demonstrated that energy dissipation decreases at higher rates compared to energy storage caused by the fluid-solid phase of the disc [34, 108, 161]. However, the fluid-solid phase of the disc as a function of disc deformation is difficult to examine due to its complex tissue matrix structure, internal and peripheral fluid flow and end-plate diffusion. The significantly increased compressive stiffness over shear stiffness is supported because the axial compression degree of freedom is a disc deformation mode where fluid flow effects are greater than in shear [34].

An acceptable parameter fit tested by the five-fold cross validation displayed significantly closer tracking results ( $RMSE_{val}$ ) compared to when the models were evaluated using parameter values from the literature ( $RMSE_{lit}$ ) [37] (Table 4.4). The smaller increase of  $RMSE_{val}$  compared to  $RMSE_{lit}$  from  $RMSE_{opt}$  supports previous findings that during impulsive axial loading the cervical spine responds in a stiffer manner. The Monte Carlo analysis also showed that models' responses were sensitive to decreases in axial stiffness ( $k_y$ ). Perturbations in shear damping ( $b_x$ ) combined with axial stiffness (Figure 4.4: Row 1) resulted in the largest relative increases in tracking errors ( $\Delta RMSE$ ). Lower shear damping appears to have a large effect on the models' performance (Figure 4.4: Row 1). During these impulsive axial impacts the cervical spines showed a rapid but non-injurious anterior buckling response as previously observed by

Nightingale et al. (1996) [95]. The anterior shear motion of the vertebrae caused by the buckling of the specimens, however, did not lead to injuries because the applied load was chosen to be sub-catastrophic. This also indicates that the energy transmitted from the axial impact causing the anterior vertebral motion was dissipated quickly. These results highlight the importance of anterior-posterior joint damping parameters used in musculoskeletal models analysing cervical spine injury mechanisms of axial impacts. In fact, the inclusion of lower values of shear damping in the models may result in an excessive anterior motion of the vertebrae, and in a subsequent erroneous prediction of the injurious events (i.e. joint dislocation).

#### 4.5.2 Model comparisons and application to injury prevention analysis

A reliable estimation of joint loads and resulting joint kinematics during impacts is key for the analysis of the injury mechanisms and estimation of injury risk. This becomes extremely important in sporting scenarios where real-world interventions, which aim to minimise injury occurrence, are informed by the output of injury mechanisms analyses. There is therefore a pressing need to use accessible computational tools, such as musculoskeletal models, capable of estimating internal joint loading and simulating injurious scenarios without adding excessive complexity. In fact, it is very challenging to directly integrate conventional *in vivo* measurements of sporting activities with finite element analyses. Currently more detailed finite element analyses are often driven by *in vitro* experimental loads and kinematics that do not adequately describe the *in vivo* behaviour during these impact events. Therefore musculoskeletal modelling is a valuable link between real-world measurements and more complex structural analyses and provides appropriate boundary conditions for finite element analyses [63].

The viscoelastic parameters estimated in this study, and their integration in a previously validated musculoskeletal model (i.e. the “Rugby Model”), provide a valid and accessible tool for such analyses. In fact, the comparison with previous models clearly shows the importance of using impact-specific bushing parameters to estimate realistic joint loads and simulate injurious events. The three versions of the “Rugby Model” tested under axial impacts revealed differences in their simulated kinematics but comparable loading patterns. Similar peaks of compressive load between the impact-specific “Rugby Model” and the original “Rugby Model” are expected. This is due to the high axial stiffness value mimicking the response of the translationally constrained joints of the “Rugby Model”. The higher peak loads showed by the non-impact-specific “Rugby Model” could be attributed to a larger effect of the damping component and lower

stiffness values. This illustrates the benefit of using impact-specific parameters compared to bushings validated in quasi-static conditions when used in impulsive events. From a joint displacement perspective, the model using quasi-static bushing parameters showed joint displacements which were near failure values of 0.84 mm [106]. As a result, the use of bushing parameters not validated for the analysis of impact events can misrepresent the resulting joint kinematics due to lower stiffness values, and therefore indicating erroneous injury mechanisms.

### 4.5.3 Limitations

The experimental and modelling assumptions of this study must be highlighted. Firstly, the simulations were driven only by a compressive axial load applied at the C2 vertebrae as the experimental load cell was uniaxial and the applied load was delivered primarily in the axial direction via the impactor. This may have neglected anteroposterior or medio-lateral shear loads that were not measured by the load cell. Cyclic preconditioning, such as series of lower magnitude axial loads, was not performed in case of specimen damage. Such preconditioning would affect the fluid content of the intervertebral discs and possibly influence the response of the spine under axial load. Preconditioning is commonly done under similar loads to the ones used for testing, however in the presented experiment a series of lower magnitude axial loads would have the potential to weaken the specimens prior to testing. Another source of error was potentially introduced by the natural resonant frequency of the tracking clusters due to their lever arms. The virtual markers were positioned at constant distances from the geometry of the models however, the experimental clusters may have experienced lag between the vertebral movement and the tracking cluster displacement during impact. The genetic algorithm minimised the tracking errors between the measured and simulated marker kinematics by optimising the 16 axial and shear joint stiffness and damping parameters of the models (Table 4.4). The similarity of this problem with automotive suspension design problems [10, 88] and the genetic algorithm's ability to search the parameter space for solutions was the reason the algorithm was chosen. Finally, porcine specimens have been evaluated as surrogates to human specimens in injury mechanism studies [20, 116, 158]. Furthermore, they provide a more homogeneous sample allowing for a better controlled experimental design without the effect of confounding factors such as age and level of degradation [161]. This is important for injury mechanism analysis as these factors can influence the effects of rapidly applied loads experienced by a young sporting population. However, the use of porcine specimens for the investigation may not be entirely representative of the functional joint behaviour of human specimens.

## 1410 4.6 Conclusion

1411 This is the first study providing cervical spine joints (C2-C6) viscoelastic parameters for  
1412 the analysis of injury mechanisms during axial impacts. The bushing (Kelvin-Voight)  
1413 parameters were estimated via combined *in vitro* experimental and *in silico* muscu-  
1414 loskeletal modelling approaches. Specimen-specific cervical spine models were created  
1415 and validated against *in vitro* 3D kinematic data of high impact loading situations.  
1416 Results showed higher values of axial stiffness in unconstrained joints compared to pre-  
1417 vious values found in the literature derived from static and quasi-static experiments.  
1418 Researchers should also be aware of the sensitivity of spinal models to low values of  
1419 axial stiffness and shear damping when investigating axial impacts to the spine. Fi-  
1420 nally, this study provides the first proof-of-concept that a musculoskeletal modelling  
1421 approach can be used to analyse cervical spine injury mechanisms by allowing the  
1422 estimation of internal joint loads and simulating realistic joint kinematics during in  
1423 sporting scenarios.

## 1424 4.7 Acknowledgements

1425 The authors would like to thank the Rugby Football Union Injured Player Foundation  
1426 charity for funding this project. Furthermore, the authors would like to thank Mr  
1427 Stuart Boyd who assisted in the data collection of this study as well as the labora-  
1428 tory technicians, Mr Jack Howell and Mr Andreas Wallbaum, for excellent technical  
1429 guidance.

## 1430 4.8 Competing Interests

1431 The authors have declared that no competing interests exist.

## Chapter 5

1432

# EMG-assisted models estimate physiological muscle activations and moment equilibrium across the neck before impacts

1433

1434

1435

1436

### *Pre-chapter commentary*

1437

This chapter explores the use of EMG-assisted models to estimate neck muscle activations during dynamic pre-impact rugby events (tackling and scrummaging). Experimental studies investigating cervical spine injury mechanisms *in vitro* have shown that the application of representative muscle forces (i.e. follower loads) to the specimens changes their dynamic response. Musculoskeletal models include muscle elements that produce force dependant in part on the level of their activation. Complete descriptions of neck muscle activations during dynamic motions are infeasible to measure experimentally *in vivo*. For this reason computational methods are regularly needed to estimate the neuromuscular state of the neck system guided by experimental muscle activation data during the analysed tasks. This second study of the thesis conducts an *in vivo* and *in silico* investigation to quantify levels of neck muscle activations based on physiological measurements of rugby tackles and scrums. Estimation of neck muscle activations was achieved through a combined inverse-forward modelling approach. Firstly *in vivo* experimental kinematics were analysed through inverse kinematics and inverse dynamics using a MRI-informed musculoskeletal model to obtain generalised joint coordinates and joint moments. An EMG-assisted optimisation is then used to

1438

1439

1440

1441

1442

1443

1444

1445

1446

1447

1448

1449

1450

1451

1452

1453

1454 compute muscle excitations that generate muscle forces and thus moments about joints  
1455 that match generalised joint moments computed through inverse dynamics. The EMG-  
1456 assisted optimisation computes the levels of excitations of muscles that could not be  
1457 collected *in vivo* providing physiological constraints based on EMG measurements. The  
1458 computed excitations are then integrated in a forward at each timestep through an ac-  
1459 tivation dynamic model to provide muscle activations which are sequentially used in a  
1460 musculotendon dynamics model to produce muscle force and moments about the joints.  
1461 The levels of activation and subsequent muscle forces can be used to provide a complete  
1462 dynamic representation of the cervical spine prior to impacts.

**This declaration concerns the article entitled:**

Chapter 5: "EMG-assisted models estimate physiological muscle activations and moment equilibrium across the neck before impacts"

1463

**Publication status (tick one)**

Draft manuscript

☐

Submitted

☐

In review

☒

Accepted

☐

Published

☐**Publication details (reference)**

Silvestros P, Pizzolato C, Lloyd DG, Preatoni E, Gill SH and Cazzola D (2020). EMG-assisted models estimate physiological muscle activations and moment equilibrium across the neck before impacts. *Annals of Biomedical Engineering*. (Under Review)

**Copyright status (tick the appropriate statement)**

I hold the copyright for this material

☒

Copyright is retained by the publisher, but I have been given permission to replicate the material here

☐**Candidate's contribution to the paper (provide details, and also indicate as a percentage)**

The candidate considerably contributed to and predominantly executed the:

**Formulation of ideas: 75%**

PS contributed to: Background research and identification of suitable methodologies

**Design of methodology: 60%**

PS utilised an experimental methodology previously developed by DC and EP and adapted a computational methodology developed by CP and DGL

**Experimental work: 40%**

Experimental work was carried out by PS together with DC and EP

**Formal data analysis: 90%**

PS performed the computational simulations and the analysis on the input and output data

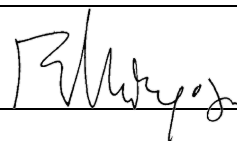
**Presentation of data in journal format: 75%**

PS wrote the first draft of the paper, draft revisions and submitted the manuscript to the journal.

**Statement from Candidate**

This paper reports on original research I conducted during the period of my Higher Degree by Research candidature.

Signed



Date

20<sup>th</sup> June 2020

## 1464 5.1 Abstract

1465 Understanding neck muscle activation strategies prior to automotive and contact sport  
1466 impacts is crucial for investigating mechanisms of severe neck injuries. However, mea-  
1467 surement of muscle activations during impacts is experimentally challenging and com-  
1468 putational estimations are often not guided by experimental measurements. We aimed  
1469 to investigate neck muscle activations prior to impacts with the use of electromyography  
1470 (EMG)-assisted models. Kinematic data and EMG recordings from four major neck  
1471 muscles of a rugby player were experimentally measured during rugby activities. A  
1472 musculoskeletal model was updated with hyoid muscles, wrapping surfaces and muscle  
1473 strengths from MRI measurements. The model was used in the Calibrated EMG-  
1474 Informed Neuromusculoskeletal Modelling toolbox to compare three neural solutions:  
1475 i) static optimisation (SO), ii) calibrated EMG-assisted (EMGa) and iii) calibrated  
1476 MRI-informed EMG-assisted (EMGaMRI) in tracking experimental cervical joint mo-  
1477 ments (C0-C1 to C6-C7) and muscle excitation patterns. EMGaMRI outperformed  
1478 EMGa when tracking joint moments (RMSE range: 0.95 – 1.07 vs 1.35 – 2.07 Nm;  $R^2$   
1479 range: 0.90 – 0.95 vs 0.67 – 0.84) with both generating physiological muscle activation  
1480 patterns (RMSE:<0.10;  $R^2$  >0.8) whilst maintaining experimental co-contraction ra-  
1481 tios. SO tracked moments correctly (RMSE range: 0.84 – 2.32 Nm;  $R^2$  range: 0.87 –  
1482 0.89) however generated activations characterised by saturation and non-physiological  
1483 “on-off” patterns (RMSE:0.15 - 0.62;  $R^2$  >0.25). This study showed for the first time  
1484 that physiological neck muscle activations can be estimated without assumed *a priori*  
1485 mechanical objective criteria during impact events whilst maintaining moment equilib-  
1486 rium for all cervical spine joints.



## 5.2 Introduction

1487

The human cervical spine is a highly complex neuromusculoskeletal system that is susceptible to injuries under various loading conditions. Severe cervical spine injuries are commonly caused during automotive [118, 162] and sporting incidents [40]. Accidents that lead to neurological impairment at the level of the cervical spine are relatively rare, 40 to 80 per million annually [99], but associated with large socioeconomic burdens [105]. Lifetime costs can rise to between 2.3 and 4.6 million US\$ for those injured at the age of 25 [99]. Therefore, to reduce these injuries biomechanical investigations are of principal importance to inform and develop injury prevention strategies.

1488

1489

1490

1491

1492

1493

1494

1495

Experimental [57, 95] and computational [37, 96] investigations have analysed cervical spine injury mechanisms identifying the importance of muscles in injury analysis. Neck muscles not only mobilise the head and neck, but also alter vertebral alignment and loading [91]. Experimental in-vitro studies have underlined the importance of replicating the contribution of the neck muscles as these can alter the ultimate load and load transmission across vertebrae [95]. Similarly, the inclusion of muscle forces in numerical models of the neck has been shown to affect both intervertebral loading [96] and the resulting kinematics [41, 85] caused by impacts. These studies provide a strong rationale for considering muscle contribution when investigating neck injury mechanisms, but little is still known about how neck muscles are activated *in-vivo* before impacts. This is an important consideration as understanding the effect of muscle forces prior to impacts is critical to fully inform neck injury mechanism research and design preventative measures.

1496

1497

1498

1499

1500

1501

1502

1503

1504

1505

1506

1507

1508

Intramuscular electrodes for electromyography (EMG) have been used to investigate static and quasi-static tasks [15, 91], but the invasive nature of the measurement has so far limited investigations of dynamic movements (e.g. collisions) to highly controlled conditions neck [126, 127]. These studies have highlighted that muscle groups work synergistically, and that, prior to collisions, muscles are unlikely to activate maximally, which is instead frequently prescribed in modelling studies as an *a priori* criterion to estimate muscle forces. From a sports biomechanics perspective, the use of EMG on the neck region during dynamic events is even more limited due to ethical and experimental constraints (i.e. invasiveness of intra-muscular electrodes or interference with task performance). Thus, a combination of experimentally viable and computationally valid methods is currently the only practicable strategy to gain insight into the function of neck musculature during dynamic events.

1509

1510

1511

1512

1513

1514

1515

1516

1517

1518

1519

1520

In neuromusculoskeletal modelling, EMG-assisted methods combine experimental EMG

1521

1522 signals with optimisation procedures to generate muscle excitation patterns that sat-  
 1523 isfy both experimental muscle EMG signals and joint moments [29, 103, 114]. These  
 1524 methods have primarily been applied successfully to single intervertebral joint lev-  
 1525 els (e.g. C4-C5 or L5-Sacrum) of the spine region during static and functional tasks  
 1526 [27, 28, 29, 30, 82]. However, the use of calibrated EMG-assisted methods for the  
 1527 entire cervical spine and intervertebral joints to model dynamic tasks representative  
 1528 of contact sports associated with traumatic neck injuries have not been investigated.  
 1529 Importantly, EMG-assisted methods, to a certain extent, can circumvent the challenge  
 1530 of defining objective criteria adopted by the neuromuscular system during these events,  
 1531 and assist in the identification of muscle recruitment strategies that are not constrained  
 1532 to *a priori* defined physiological or mechanical criteria.

1533 The aims of this study were twofold. First, we created a calibrated EMG-assisted  
 1534 neuromusculoskeletal model with MRI-informed neck musculoskeletal anatomy. This  
 1535 model would permit the estimation of physiologically plausible neck muscle excitations  
 1536 and moments across all intervertebral joints of the cervical spine in rugby impacts. Sec-  
 1537 ond, we assessed the effects of level of subject-specificity (personalised musculoskeletal  
 1538 anatomy and muscle activation patterns) on the model’s ability to generate physiolog-  
 1539 ically plausible results, i.e. reproduce experimental joint moments and muscle activa-  
 1540 tions. It was hypothesised that increasing subject-specificity by using EMG-assisted  
 1541 neural solutions and/or MRI derived muscle strengths generates simulated activations  
 1542 that successfully replicated the experimental EMG data and net joint moments, whilst  
 1543 methods that purely use mathematical optimisation would provide less physiologically  
 1544 acceptable muscles activation patterns but better match the experimental net joint  
 1545 moments.

### 1546 5.3 Materials and Methods

1547 A case study comprising multiple trials on a single rugby athlete was used. A neu-  
 1548 romusculoskeletal modelling pipeline was created wherein the ability of the model to  
 1549 reproduce experimental joint moments and muscle activation patterns was tested. Two  
 1550 neuromuscular solution modalities were assessed: static optimisation and EMG-assisted  
 1551 methods. Additionally, the level of subject specificity of the model and its performance  
 1552 was assessed by incorporating MRI derived information into the model when using the  
 1553 EMG-assisted methods.

### 5.3.1 Participant

One professional academy-level front-row rugby player (male, 22 years, 1.824 m, 113.7 kg) participated in this study. Ethical approval was obtained from the Research Ethics Approval Committee for Health of the University of Bath and the participant provided written informed consent prior to data collection.

#### 5.3.1.1 Medical imaging

The participant underwent isotropic T1-weighted magnetic resonance imaging (MRI) (Skyra, SIEMENS, Germany) scans of the neck and upper shoulders (occiput to T1 level) with a slice thickness of 1 mm. Musculoskeletal structures (skull to C7 vertebrae and muscles) were identified to inform the creation of the subject specific musculoskeletal model used in the study. Thirteen bilateral muscle pairs (Figure S1 – Supplementary Material) that were clearly identifiable in the MRI images were semi-automatically segmented in Mimics (v22 ,Materialise, Belgium) guided by musculoskeletal atlases[7, 81].

Segmented muscle volumes and 3D centroid paths were then derived from the identified muscles using existing Mimics v22 algorithms. Muscle maximal isometric forces were calculated from the segmented muscle volumes based on the relationship (Equation 5.1):

$$F_{max}^{iso} = \sigma \frac{v^m}{l_o^m} \quad (5.1)$$

Where  $\sigma$  is the muscle's specific tension set to 55 N/cm<sup>2</sup> [97],  $v^m$  is the segmented muscle volume and  $l_o^m$  is the muscle's optimal fibre length from the scaled model [23] subsequently discussed. Further details are presented in the Supplementary Material.

### 5.3.2 Experimental methods

To test the performance of the proposed neuromusculoskeletal method in pre-impact events the participant performed laboratory-based machine scrummaging [24, 104] and staged tackling [119] trials on the same day as the MRI scans. Neck functional movement in the three cardinal planes of motion against no resistance were also performed. Three successful trials were collected for each dynamic condition (i.e., scrummaging, front and side on tackling) as a best compromise between representativeness, exposure to multiple impacts and reducing the effects of fatigue. Full body kinematics [23] (Oqus, Qualysis, Sweden) and bilateral EMG (Trigno, Delsys, USA) of the sternocleidomastoid and upper trapezius muscles [23, 119] were collected at 250 Hz and 2500 Hz,

1584 respectively. Maximum voluntary isometric contractions (MVIC) were also performed  
1585 following established methods [25]. Due to the large hypertrophy of rugby athletes'  
1586 neck musculature, radiographically observed by Brauge et al. [16] and in this study,  
1587 only the two major bilateral flexors and extensors could be reliably measured with sur-  
1588 face electromyography without crosstalk from other. Additionally, the dynamic nature  
1589 of the simulated rugby tasks involves direct forceful contact with participants' neck area  
1590 making the use of intra-muscular electrodes considerably challenging and unadvisable  
1591 for ethical reasons (risk for the participant).

1592 Experimental marker trajectories were low-pass filtered with a fourth-order zero-lag  
1593 Butterworth filter at 6 Hz in Matlab R2017a (The Mathworks Inc., Natick MA, USA).  
1594 EMG signals were band-pass filtered (10-250 Hz), full wave rectified, low-pass filtered  
1595 at 6 Hz [72] with the same filter, then amplitude normalised to the maximum recorded  
1596 value identified in the MVIC or dynamic trials prior to impact to create EMG linear  
1597 envelopes

### 1598 **5.3.3 Musculoskeletal modelling**

1599 The population specific Rugby Model [23] was updated and used as the baseline model  
1600 for this study. The hyoid muscle group was added to the Rugby Model to improve its  
1601 physiological fidelity [86] increasing the number of MTUs that actuated the cervical  
1602 spine to 96 (64 extensors and 32 flexors). The musculoskeletal model was then linearly  
1603 scaled in OpenSim 3.3 [39] to the participant's dimensions using anatomical markers  
1604 and vertebrae measurements from the segmented MRI images. MTU attachment sites  
1605 were not changed due to difficulties identifying muscle attachment locations in the  
1606 MRI.

1607 Six parametric muscle wrapping surfaces (Figure 5-1) were also included in the mus-  
1608 culoskeletal model to better replicate muscle line of action in the cervical spine: i)  
1609 a cylinder anterior to the lower cervical spine registered to the C6 vertebra [66]; ii)  
1610 a sphere originating and registered to the C2 vertebra; iii) two bilateral cylinders at  
1611 the posterior of the upper cervical spine also registered to the C2 vertebra; iv) lastly  
1612 two bilateral tori at the lower cervical spine registered to the C7 vertebra. All wrap-  
1613 ping surfaces were constrained to move with their registered bodies. The choice of  
1614 parameters and position used to define the model's wrapping surfaces were informed  
1615 by Vasavada et al. (2008) [151] and measurements taken from the segmented MRI  
1616 images of the rugby player participant. Further details of these procedures are given in  
1617 the Supplementary Material. The Rugby Model is available from the SimTK repository  
1618 (<https://simtk.org/projects/csibath>).

Functional movement and dynamic rugby trials (500 ms preceding impact) were analysed via inverse kinematics, inverse dynamics and muscle analyses using the OpenSim 3.3 Matlab API to calculate joint kinematics, net joint moments (hence called experimental joint moments), as well as MTU kinematics and moment arms during the experimental. During inverse kinematics the model's intervertebral joint motions were driven by coordinate coupler constraints [125] that partitioned the measured relative angle of head with respect to the trunk to the internal coordinates [152]. Kinematic constraints were only used during inverse kinematics to obtain intervertebral joint angles. The kinematic coupler constraints were not applied for inverse dynamics and muscle analysis as they would interfere with the estimation of experimental joint moments and MTU kinematics in OpenSim. No reserve actuators were included in the model during the inverse dynamics stage.

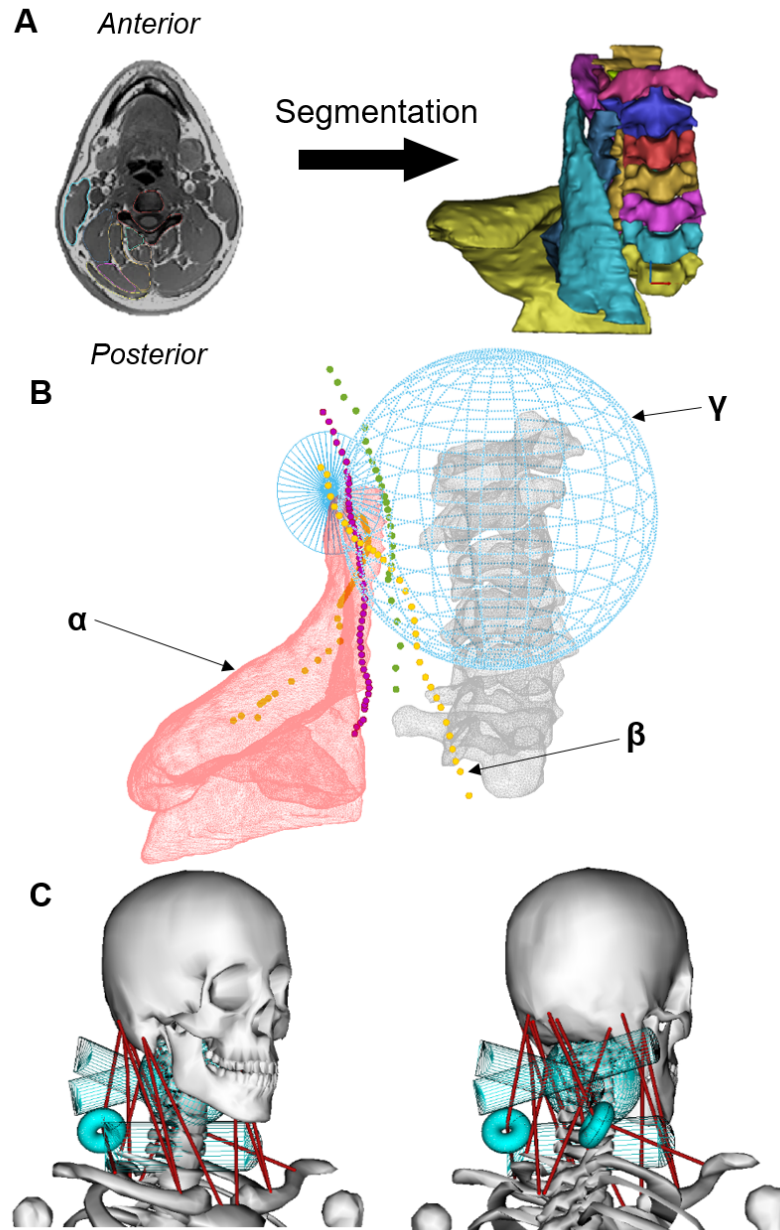


Figure 5-1: Representation of the three main steps to update the OpenSim Rugby Model's muscles paths: **A)** high resolution (1 mm isotropic) MRI scans of a rugby forward player's neck and upper-shoulder region were segmented yielding muscle and bone geometries together with muscle volume and centreline information; **B)** musculoskeletal geometries ( $\alpha$ ) and muscle centroid paths ( $\beta$ ) were imported into Matlab and parametric surfaces ( $\gamma$ ) were estimated based on [151]; **C)** parameters were used for the generation of wrapping surfaces in the OpenSim model (here only the muscles constrained by the defined wrapping surfaces are presented in the model and the scapulae removed for better visualisation of muscles).

### 5.3.4 Neuromuscular modelling

The estimation of the model's 96 muscle activation patterns was solved using the Calibrated EMG-Informed Neuromusculoskeletal Modelling (CEINMS) OpenSim Toolbox [103, 114] that minimised the following cost function (Equation 5.2):

$$F = \alpha E_M + \beta E_{\Sigma e^2} + \gamma E_e \quad (5.2)$$

Where  $E_M$  was the sum of the squared differences between the estimated and experimental net joint moments from the inverse dynamics (sagittal and frontal plane moments of the C0-C1 through to C6-C7 joints),  $E_{\Sigma e^2}$  was the sum of the squared synthesised excitations for all MTUs, and  $E_e$  was the sum of the differences between the adjusted model excitations and experimental excitations. Factors  $\alpha$ ,  $\beta$  and  $\gamma$  were non-negative weightings for each term of the cost function. Activation dynamics were characterised by a critically damped linear second-order differential system [72, 103]. It was assumed that the MTU tendons of the model were stiff due to their short length and function in the neck.

Three neural solution methodologies were assessed in their ability to track experimental neck net joint moments and EMG excitation signals of the experimental trials (Figure 5-2):

- *Static optimisation (SO)*: an uncalibrated model was used through a static optimisation algorithm to estimate muscle activation patterns by minimising both the net joint moments errors and the sum of activations squared;
- *EMG-assisted (EMGa)*: a calibrated model was used along with an EMG-assisted approach to estimate muscle activation patterns;
- *MRI-informed EMG-assisted (EMGaMRI)*: EMG-assisted approach was used to estimate muscle activation patterns and included MRI derived  $F_{max}^{iso}$  values within the calibration;

### 5.3.5 Calibration

Calibration in CEINMS was completed through an EMG-driven procedure, where experimental muscle excitations (i.e. EMG linear envelopes) were prescribed to the model's MTUs that generate moments about the cervical joints for a set of calibration trials [103]. Musculotendon and activation dynamic parameters [72, 103] were optimised within chosen physiological bounds (Table 5.1) by minimising the sum of

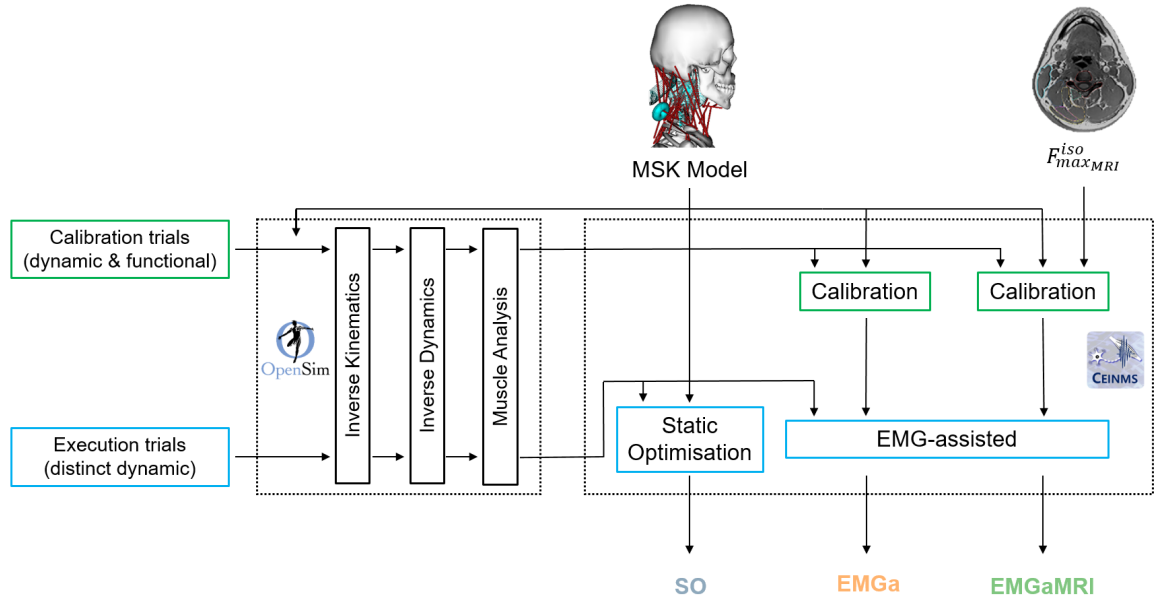


Figure 5-2: Schematic overview of computational pipeline used in the study. The scaled musculoskeletal model was used in the analysis of calibration and execution trials with Inverse Kinematic, Inverse Dynamic and Muscle Analysis in OpenSim 3.3. The outputs of these analyses were then used in the CEINMS framework for all Static Optimisation (SO) and EMG-assisted (EMGa and EMGaMRI) neural solutions. For both the EMG-assisted solutions the model underwent the same calibration procedures with the exception of the EMGaMRI that derived muscle maximal isometric forces from the segmentation of muscles identifiable in the MRI. Calibration was completed on a set of dynamic and functional trials that was distinct from the execution trials (tackling and scrummaging) that were analysed with the three neural solutions.

squared differences between the predicted and the experimentally measured joint moments for all analysed degrees of freedom (DoF) across the calibration trials. Calibrated musculotendon parameters included tendon slack length ( $l_s^t$ ), optimal fibre length ( $l_o^m$ ), a strength coefficient to scale the  $F_{max}^{iso}$  of the MTU whilst activation dynamics parameters were two recursive coefficients ( $C_1$  and  $C_2$ ) and a non-linear shape factor ( $A$ ) [72, 103].

To overcome the high level of redundancy present in the model's neck region, the model underwent two calibrations (intermediate and final) in a three-stage process in CEINMS (5-3). This allowed for an intermediate stage where unknown MTU excitations could be estimated using the four available EMG linear envelopes. Two functional movement trials (flexion/extension and left/right lateral bending), one scrummaging



Table 5.1: Neuromuscular parameters optimised in CEINMS calibration stage. For detailed explanation on these musculotendon and activation dynamics parameters refer to Lloyd and Besier [72] and Pizzolato et al. [103].

Parameter	Range
$C_1$	[-0.95 0.05]
$C_2$	[-0.95 0.05]
Shape Factor ( $A$ )	(-3 0)
Tendon Slack Length ( $l_s^t$ )	[0.8 1.2]*
Optimal Fibre Length ( $l_o^m$ )	[0.8 1.2]*
Strength Coefficient	[0.6 2.6]

\* Indicates the range was relative to the model's initial parameter value.

and one tackling trial were selected for the calibration process. This combination of movements was considered to mobilise the model through a sufficient range of motion. Only the 14 DoF's corresponding to flexion/extension and left/right lateral bending of the intervertebral neck joints were considered when minimising the error between experimental (i.e. inverse dynamics) and estimated net joint moments.

The three stages of the calibration process (Figure 5-3) for the EMGa and EMGaMRI were:

*Stage 1* calibrated neuromuscular parameters (Table 5.1) of the model resulting in an intermediate calibrated model. The 96 MTUs of the uncalibrated musculoskeletal model were separated into functional quadrants (right/left flexion, right/left extension) (Figure 5-4 and Table A.1 [Appendix A]). The MTUs of each quadrant were mapped and constrained to their respective experimental EMG signals (right/left sternocleidomastoid, right/left upper trapezius). This assumed that MTUs of each functional quadrant were activated identically to the experimental excitation signals. For the EMGa solution, the strength coefficient of all MTUs ranged between the minimum (60%) and maximum (260%) differences identified between the MRI derived and baseline model  $F_{max}^{iso}$  values (Figure A-1). In the EMGaMRI solution, the  $F_{max}^{iso}$  of the 44 MTUs that constituted the 26 segmented muscles were updated to the MRI derived values. The strength coefficients of these 44 MTUs were set equal to 1 and not varied during the calibration process. The strength coefficients of the remaining MTUs could range between 60 and 260%.

*Stage 2* estimated the 86 unknown muscle excitations of the calibration trials using the intermediate calibrated model. For each trial the MTUs were again separated into functional quadrants and mapped with their respective experimental EMG signals as

1696 in *Stage 1*. However, this differed by only constraining excitation signals to the flexion  
1697 (n=6) and extension (n=4) MTUs corresponding to measured muscle EMGs (Table  
1698 S1). The remaining 86 unknown MTU excitations were estimated by adjusting their  
1699 mapped initial excitation input to generate joint moments that matched experimental  
1700 joint moments whilst minimising the estimated excitations' deviation from their input  
1701 signals.

1702 *Stage 3* further calibrated the intermediate model's parameters by mapping and con-  
1703 straining each MTU with excitation signals. This time initial excitation signals of all  
1704 model MTUs were mapped from either measured excitations, again constrained to the  
1705 ten corresponding MTUs (as in *Stage 1*), or individual estimated excitations (from  
1706 *Stage 2*), constrained to the remaining 86 MTUs in the EMG-driven calibration.

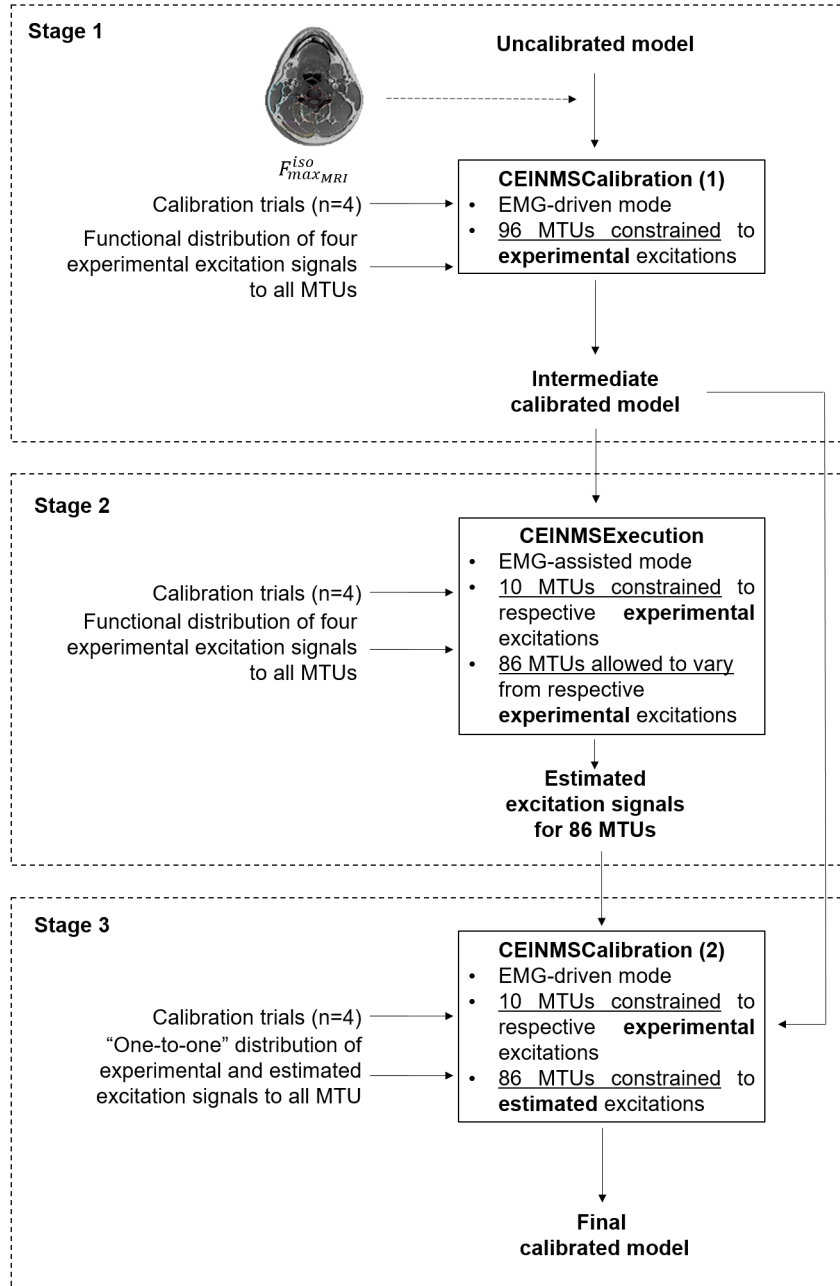


Figure 5-3: Flowchart showing the inputs and resulting outputs for the two calibrations via a three stage process used for the EMGa and EMGaMRI solutions. For both EMGa and EMGaMRI the calibration procedure was the same apart from EMGaMRI where in Stage 1  $F_{max}^{iso}$  of the model's MTUs (n=44) were updated from segmented muscles volumes (n=26).

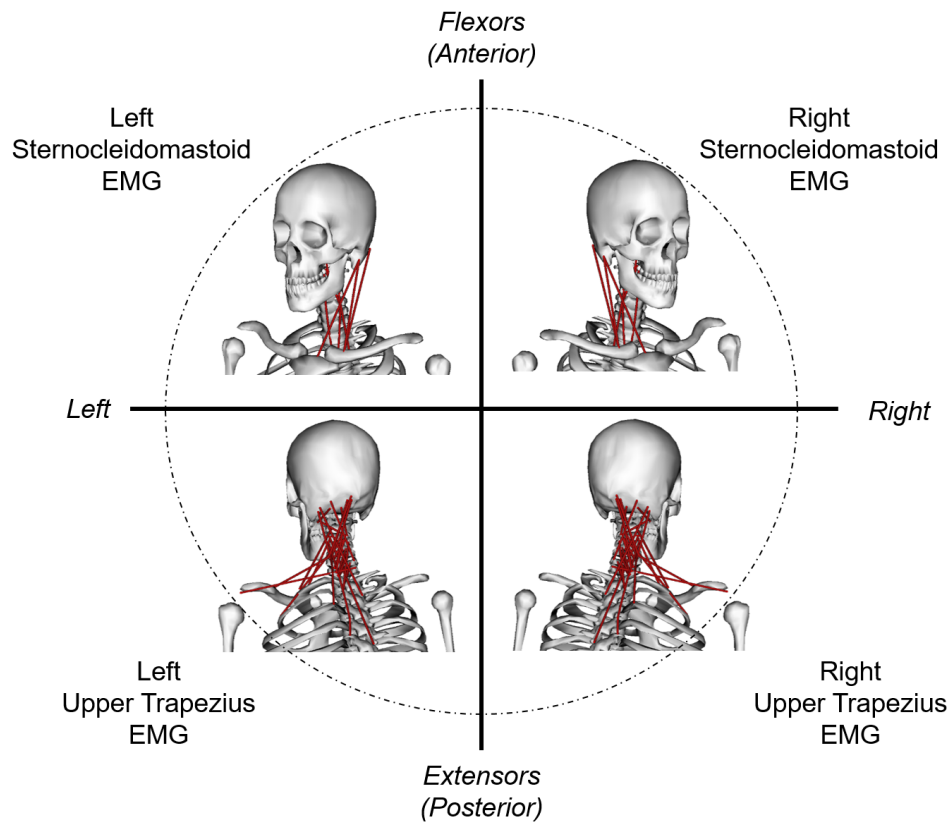


Figure 5-4: Representation of how the 96 muscles of the model were separated into functional quadrants of left flexion (16 muscles), right flexion (16 muscles), left extension (32 muscles) and right extension (32 muscles). The separation of the muscles into functional quadrants allowed for the prescription of the experimental EMG signals (right/left sternocleidomastoid, right/left upper trapezius) to the respective functional muscle groups in the EMG-assisted methods.

### 5.3.6 Data analysis

1707

Experimental trials (distinct from the calibration trials) were analysed with the SO 1708 method by setting the CEINMS weighting factors of Equation 2 to  $\alpha=1$ ,  $\beta=1$  and 1709  $\gamma=0$ . This equally weighed the tracking of estimated intervertebral joint moments 1710 ( $\alpha=1$ ) and the minimisation of the excitations squared term ( $\beta=1$ ) whilst neglecting 1711 the estimation of muscle excitations from experimental EMG measurements ( $\gamma=0$ ). For 1712 EMGa and EMGaMRI methods, the excitations squared term was neglected ( $\beta=0$ ) and 1713 the measured excitations tracking term engaged ( $\gamma > 0$ ). In this muscle excitations were 1714 either constrained or adjusted from measured EMG linear envelopes depending on their 1715 function and if experimental measurements existed (Table A.1) in order to minimise 1716 errors between experimental and estimated intervertebral joint moments. For this the 1717  $\alpha$  and  $\gamma$  factor values were optimised to balance the error between the minimisation 1718 of tracking experimental joint moments and EMG linear envelopes [114] then slightly 1719 adjusted to increase weighting on moment tracking ( $\alpha=50$  and  $\gamma=50$ ). To evaluate the 1720 performance and the level of physiological agreement of the three neural solutions (SO, 1721 EMGa and EMGaMRI), experimental and simulated net joint moments and muscle 1722 excitations were compared using the root mean squared error (RMSE) and coefficient 1723 of determination ( $R^2$ ). Net joint moments RMSE were normalised to the range of 1724 their respective experimental joint moment (from Inverse Dynamics) as the magnitude 1725 of moments increased from C0-C1 to C6-C7. Co-contraction indices [52] of estimated 1726 excitations were calculated and compared to experimental EMG signals for flexion- 1727 extension (Equation 5.3) and lateral bending (Equation 5.4). For flexion-extension 1728 the excitations of the model' flexors ( $A_f$ ) and extensors ( $A_e$ ) were separately grouped 1729 and averaged then compared to the average flexor (sternocleidomastoids) and extensor 1730 (upper trapezius muscles) EMG. Similarly for lateral bending left ( $A_{llb}$ ) and right 1731 ( $A_{rlb}$ ) lateral bending excitation averages were calculated and compared respectively 1732 to the left (sternocleidomastoid and upper trapezius) and right (sternocleidomastoid 1733 and upper trapezius) EMG signals: 1734

$$CCI_{FE} = \begin{cases} 1 - \frac{A_f}{A_e}, & A_f < A_e \\ \frac{A_e}{A_f} - 1, & A_f \leq A_e \end{cases} \quad (5.3)$$

$$CCI_{LB} = \begin{cases} 1 - \frac{A_{llb}}{A_{rlb}}, & A_{llb} < A_{rlb} \\ \frac{A_{rlb}}{A_{llb}} - 1, & A_{rlb} \leq A_{llb} \end{cases} \quad (5.4)$$

These ratios provide the relative amount of muscle co-contraction for flexion-extension 1735

1736 and lateral bending across the whole cervical spine. A value near 0 represents higher  
1737 levels of co-contraction, near 1 is higher extension or right lateral bending and near -1  
1738 higher flexion or left lateral bending excitations.

## 1739 5.4 Results

1740 The average moment RMSE across all trials and joint levels showed that EMGaMRI  
1741 ( $\text{RMSE} = 0.95 \pm 0.75 \text{ Nm}$ ) neuromuscular solutions tracked experimental flexion/extension  
1742 net joint moments more accurately than SO ( $\text{RMSE} = 2.32 \pm 1.84 \text{ Nm}$ ) and EMGa  
1743 ( $\text{RMSE} = 1.35 \pm 1.05 \text{ Nm}$ ) (Figure 5-5). In lateral bending SO had lower RMSE than  
1744 EMGaMRI ( $0.84 \pm 0.60 \text{ Nm}$  vs.  $1.07 \pm 0.90 \text{ Nm}$ ) with EMGa showing the largest  
1745 errors ( $\text{RMSE} = 2.07 \pm 1.38 \text{ Nm}$ ). Normalised RMSE and  $R^2$  values showed net joint  
1746 moments in the upper cervical spine region (C0-C1 through to C3-C4 level) were not  
1747 tracked as well as the lower cervical spine (C4-C5 through to C6-C7) for all methods  
1748 (Figures 5-5 and 5-6).

1749 Tracking of experimental excitations for the ten MTUs corresponding to the four mea-  
1750 sured muscles was better with EMGa and EMGaMRI ( $\text{RMSE}: < 0.10$  and  $R^2: > 0.82$ )  
1751 than SO ( $\text{RMSE}: 0.15 - 0.65$  and  $R^2: < 0.25$ ) (Figure 5-7). The activations of the re-  
1752 maining 86 MTUs maintained a similar pattern to the initial prescribed signals (Figure  
1753 5-8). In contrast SO was not able to reproduce the experimental signal patterns across  
1754 MTUs with low  $R^2$  average values (Figure 5-7).

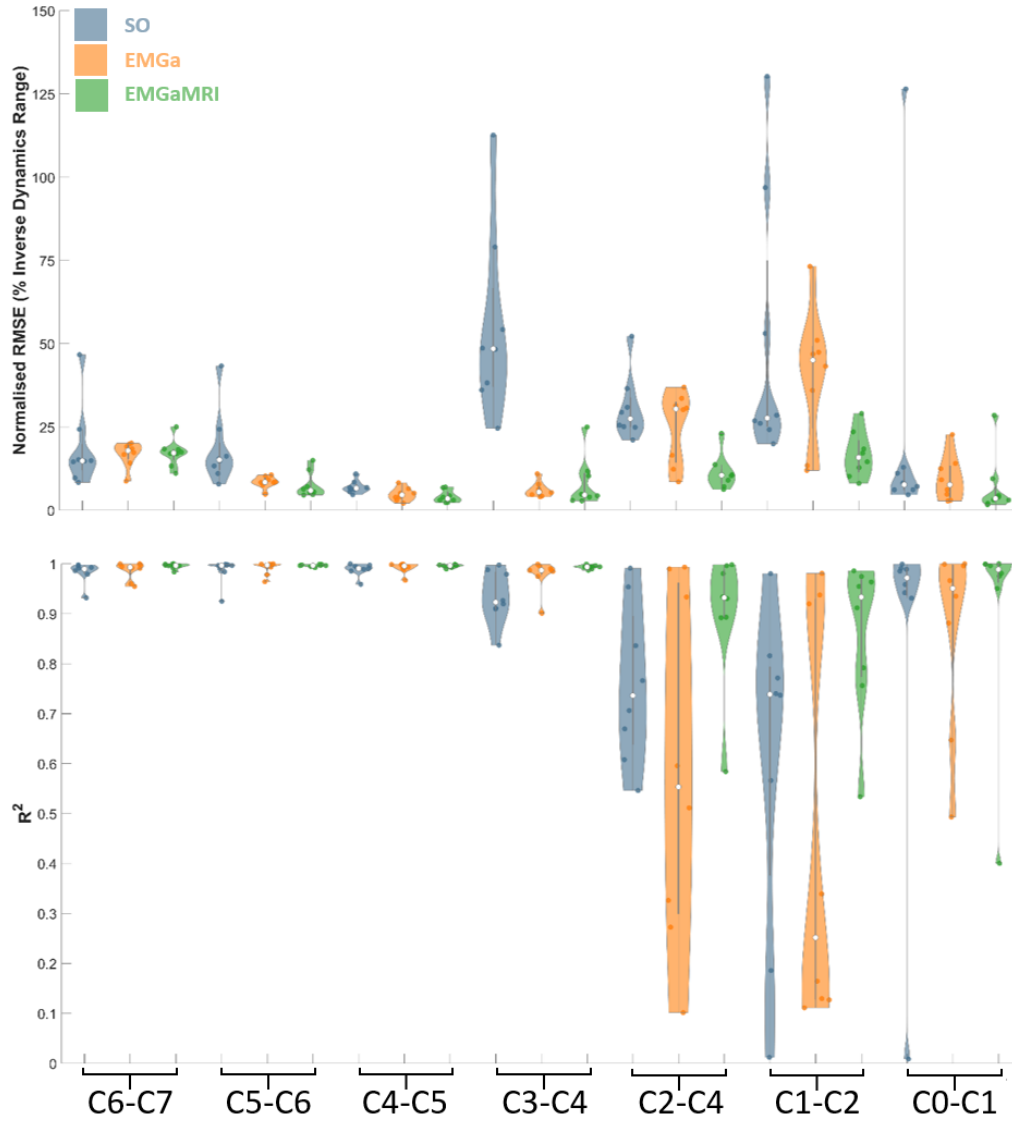


Figure 5-5: RMSE (top) and  $R^2$  (bottom) from the neuromusculoskeletal model with different neural solutions tracking inverse dynamics (ID) flexion/extension joint moments across different joints and trials. These are shown in violin plots that present individual (solid marker), mean (white marker) and density (coloured area shape) trial performance for SO (blue), EMGa (orange) and EMGaMRI (green) solutions. RMSE of each estimated joint moment is normalised to the range of the experimental joint moment (ID) of the respective joint and trial.

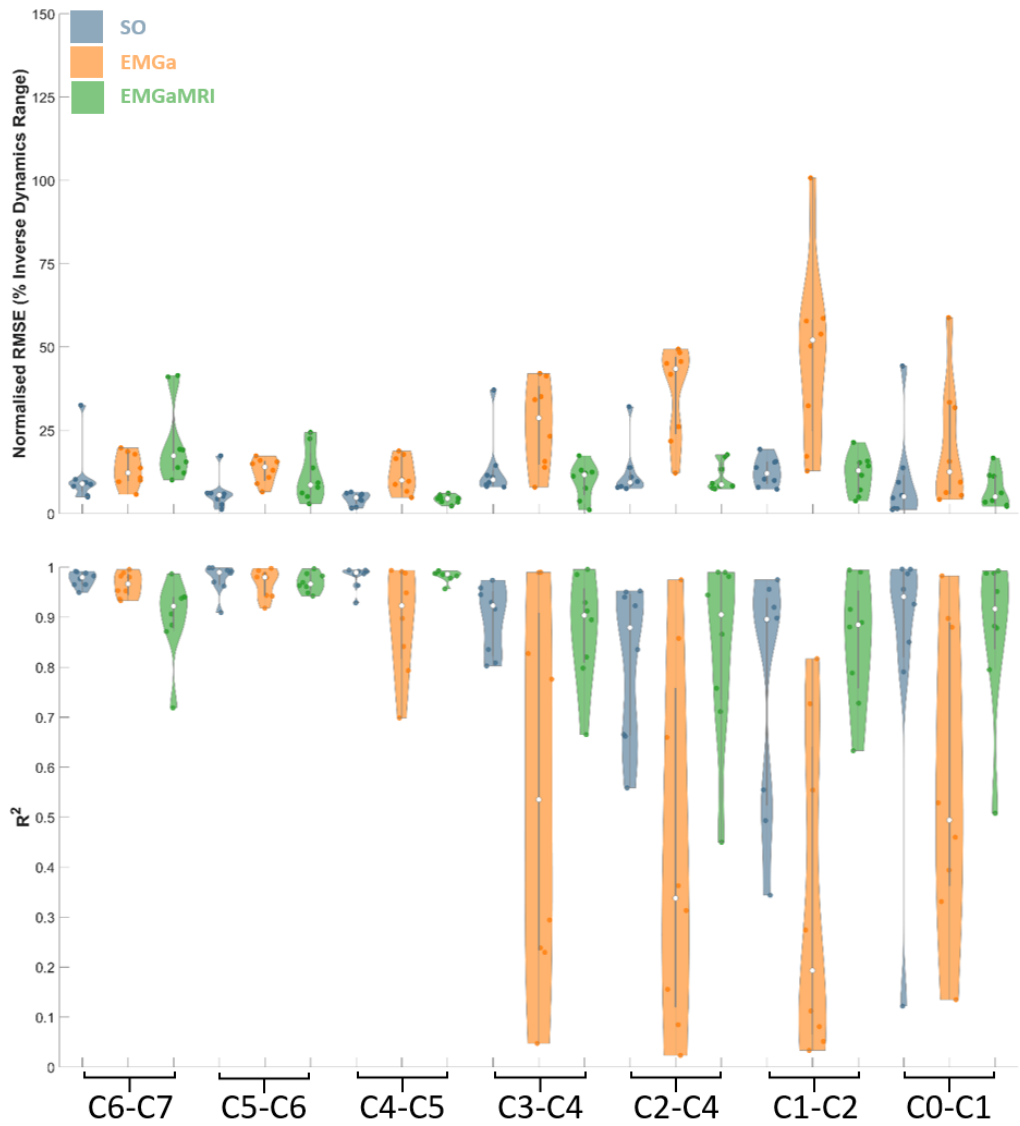


Figure 5-6: RMSE (top) and  $R^2$  (bottom) from the neuromusculoskeletal model with different neural solutions when tracking inverse dynamics (ID) lateral bending joint moments across different joints and trials. These are shown in violin plots that present individual (solid marker), mean (white marker) and density (coloured area shape) trial performance for SO (blue), EMGa (orange) and EMGaMRI (green). RMSE of each estimated joint moment is normalised to the range of the experimental joint moment (ID) of the respective joint and trial.



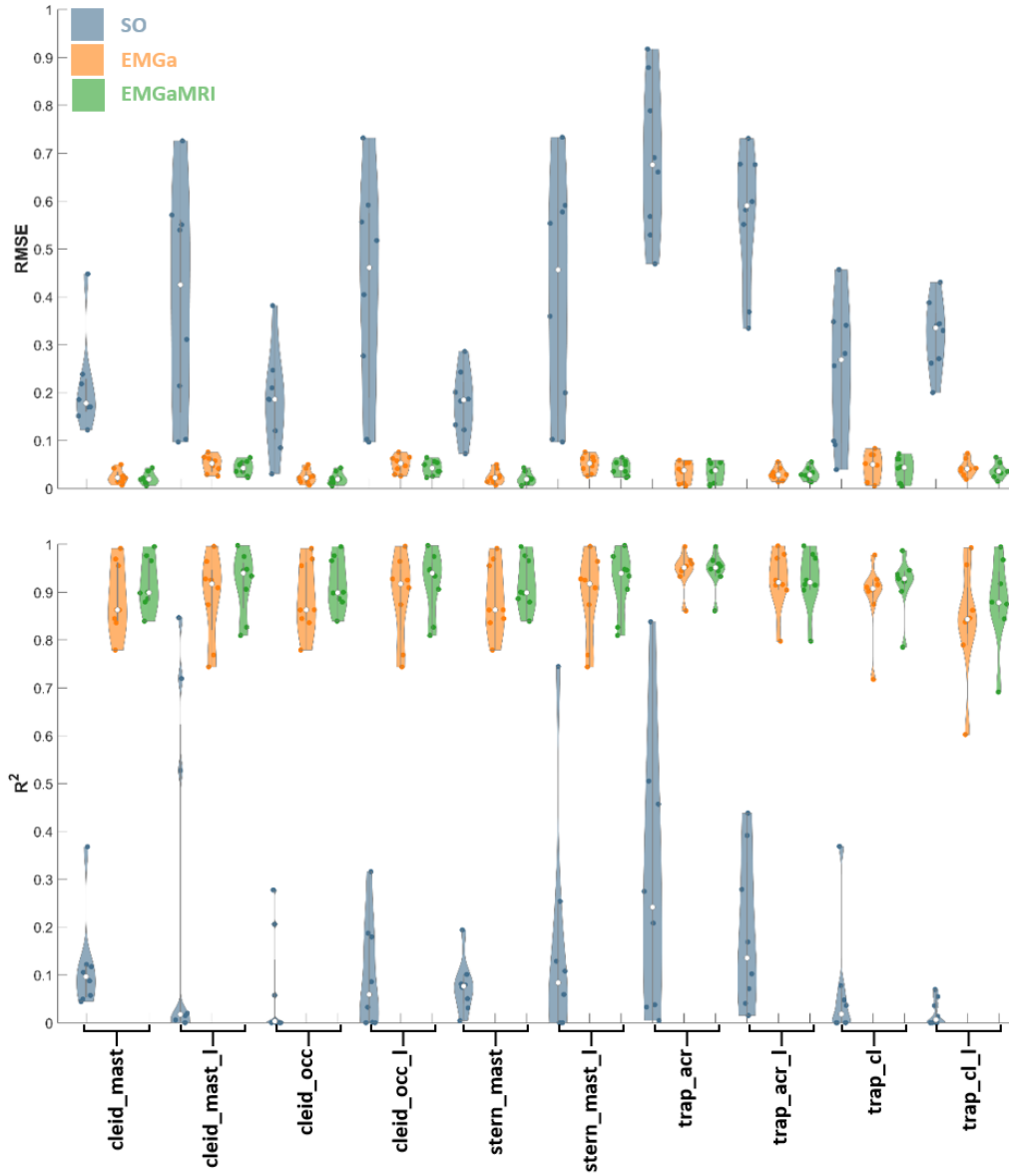


Figure 5-7: RMSE (top) and  $R^2$  (bottom) of neck different neural solutions when tracking experimental EMG signals (right trapezius, left trapezius, right sternocleidomastoid, left sternocleidomastoid) across different trials. These are shown in violin plots that present individual (solid marker), mean (white marker) and density (coloured area shape) trial performance for SO (blue), EMGa (orange) and EMGaMRI (green). Naming of MTUs is consistent with the OpenSim model.

1755 There were clear differences in the MTU recruitment patterns between the SO and  
1756 the two EMG-assisted solutions (Figure 5-8). The SO solution created high frequency  
1757 transitions in activation levels with distinguishable “*on-off*” phases and frequent satu-  
1758 ration. The estimates from the two EMG-assisted solutions showed muscle activations  
1759 followed the pattern of experimental EMG input signals with individual muscle groups  
1760 (e.g. *multifidus*, *erector spinae*) varying the signal for their constituent MTUs. This  
1761 resulted in a closer approximation of experimental co-contractions nearer to the time  
1762 of impact in both flexion-extension and lateral bending.

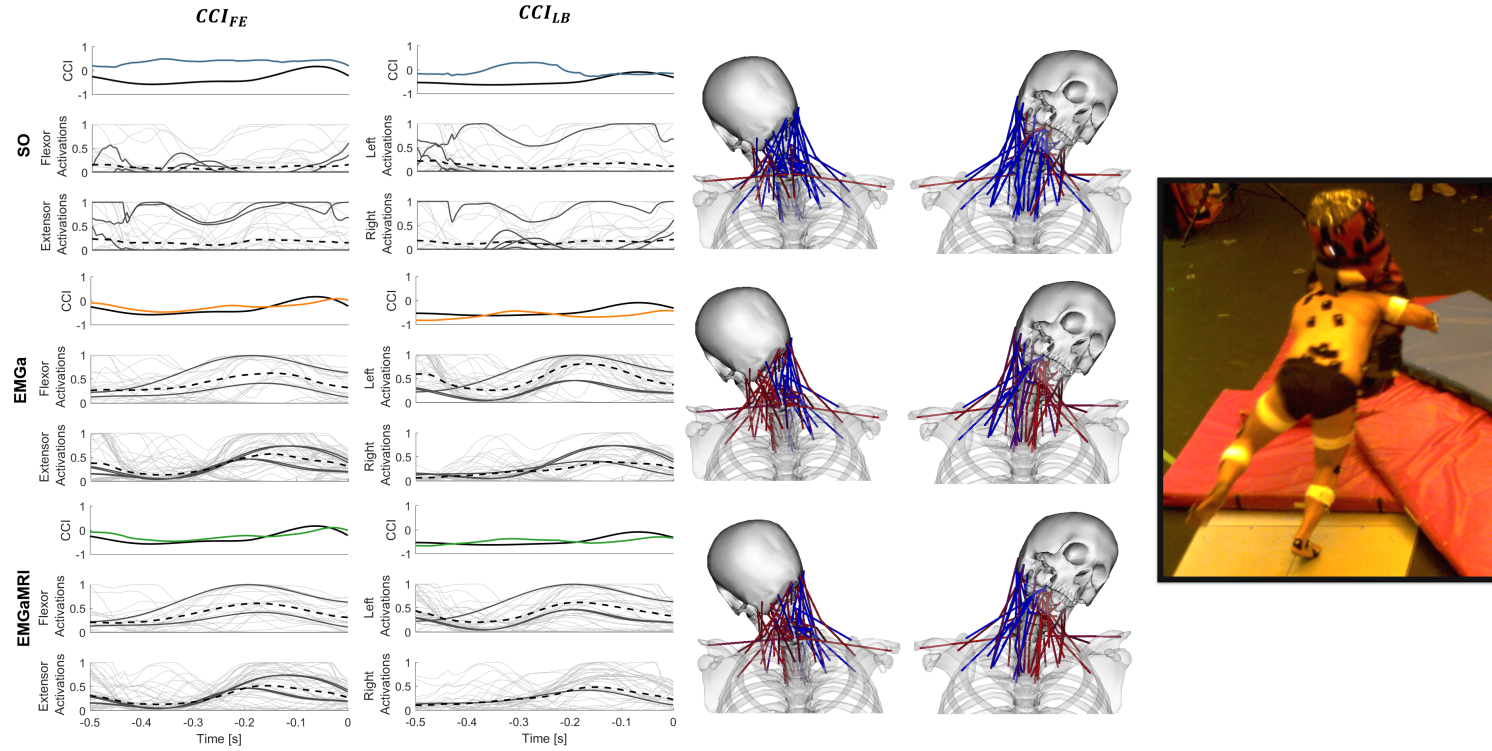


Figure 5-8: Left: mean of 5 tackling trials' co-contraction index ( $CCI_{FE}$  and  $CCI_{LB}$  of the four experimental EMG signals (solid black) and estimated for SO (top - blue), EMGa (middle - orange) and EMGaMRI (bottom - green) for the 0.5 s before impact. Subplots show the muscle group activations used to calculate the estimated CCI values during an individual tackling trial (flexors and extensors ( $CCI_{FE}$ ; left and right lateral flexors for ( $CCI_{LB}$ ). The 86 MTUs that had no measured experimental EMG and were either synthesised (SO) or adjusted (EMGa and EMGaMRI) from their input signal (mapped from the left and right sternocleidomastoid and upper trapezius muscles EMG) are shown in grey, the 10 for which experimental EMG was measured (constrained to the left and right sternocleidomastoid and upper trapezius muscles) in solid black and average activations for each muscle group are plotted as dashed lines for each solution. Centre: snapshots of the musculoskeletal model at the point of impact (depicted right) with MTUs coloured to matched the level of estimated excitations for each neural solution (red - high; blue - low). Right: still of the experimental set-up with the participant simulating a tackle during EMG and kinematic measurements.

## 1763 5.5 Discussion

1764 This study created a cervical spine neuromusculoskeletal model and assessed how the  
1765 level of model subject-specificity affected the generation of physiologically plausible  
1766 neck muscle activation patterns in the preparatory phase of rugby impacts. Rugby  
1767 activities were chosen as a case study and a combination of experimental and modelling  
1768 approaches were adopted to provide physiological and reliable estimation of neck muscle  
1769 activation patterns during impact events. A musculoskeletal model of a rugby forward  
1770 player was created and its ability to generate required neck joint moments was assessed  
1771 through three neural solutions with increasing levels of subject-specificity. For the  
1772 first time, we showed that an MRI-informed EMG-assisted solution can both generate  
1773 neck muscle activations that closely match experimental excitations, and replicate the  
1774 required mechanical demands across the cervical spine (i.e. net joint moments) of an  
1775 impact event.

1776 The ability of neuromuscular models to simulate physiological muscle activation pat-  
1777 terns and concurrently reproduce the experimental net joint moments is key to accu-  
1778 rately estimate joint internal loading and investigate injury mechanisms. As shown in  
1779 our study, a pure optimisation method (SO) was able to accurately track the net joint  
1780 moments, but poorly replicated the physiological muscle activation patterns (Figures  
1781 5-5, 5-6, 5-7, 5-8). In fact, the assumption of *a priori* criteria in objective functions  
1782 used to guide the estimation of muscle activations may not be the best approach due  
1783 to our current lack of understanding of how the muscles behave to control the neck in  
1784 preparation of impacts. Mortensen et al. (2018) [85] illustrated that metabolic and  
1785 mechanical static optimisation objective functions produced different neck kinematics  
1786 under the effect of gravity. The objective criteria used in that study maximised joint  
1787 stiffness or joint moment generation capacity which resulted in the smallest neck angle  
1788 displacement. Although this may be favourable during a direct perturbation to the  
1789 head, it may not be applicable in situations where adequate neck mobility is required  
1790 to safely position the head in preparation for impact, such as the preparatory phase of  
1791 rugby tackling (Figure 5-8). In our study, the use of EMG-assisted solutions success-  
1792 fully tracked experimental net joint moments whilst concurrently estimating unknown  
1793 muscle activations from experimental muscle excitations. The ability of the EMG-  
1794 assisted solutions to reproduce two experimental variables (i.e. net joint moments and  
1795 muscle excitations) and reach physiologically acceptable solutions across the cervical  
1796 spine with no assumption of *a priori* objectives (metabolic or mechanical) supports the  
1797 validity of the presented methods during dynamic neck motions. Our study extends  
1798 these EMG-assisted methods to the entire cervical spine as the results are in line with

previous studies investigating the upper [65] and lower [36, 55] limbs as well as a single joint level of the lumbar spine [82].

The additional incorporation of MRI derived neck muscle strengths in the EMGaMRI solution further improved the tracking of experimental net joint moments especially in the upper cervical spine compared to the EMGa solution. Assigning accurate muscle strength values for the set of 44 MTUs in EMGaMRI assisted the calibration and illustrates the importance of future detailed models describing the complexity of the neck region. The incorporation of personalised musculoskeletal anatomy information with EMG-assisted neural solutions was shown to improve tracking of net moments and experimental excitations in the lower limbs of children [36]. This may suggest that in populations where musculoskeletal characteristics (e.g. strength and anatomy) are significantly different than the average populations, such as rugby athletes [16] and children [36], personalised models used for investigations can improve the accuracy of the results.

For the first time our neuromusculoskeletal models concurrently generated moment equilibrium across all the cervical spine joints (C0-C1 through to C6-C7), in two motion planes for different dynamic neck motions. This is an advancement over previous studies that solved for moments across a single cervical or lumbar joint level [6, 27, 28, 82] which has also been supported in the lumbar region [49]. Solving moment equilibrium across cervical spine levels is important as many major spinal muscles are multi-articulate (span multiple joint levels), and apply loads to multiple cervical joint levels. Characterisation of the entire cervical spine's internal loading caused by muscles is paramount in injury mechanism analysis during dynamic events (e.g. inertial loading or direct impacts) as it influences the propagation of external forces down the intervertebral joint levels which has already been highlighted in the literature [37].

Muscle co-contraction is an important neural strategy used to stabilise spinal joints [15, 28]. We found that the SO did not track the experimental co-contraction indices, whereas the EMG-assisted solutions preserved neck muscle co-contraction by replicating experimental co-contraction indices. This is an important factor for the analysis of spinal injury mechanism as muscle forces highly influence net joint loading [96]. Previous studies have shown that EMG-assisted models replicate muscle co-contractions when assessed against experimental measures [49, 55, 65]. Models that correctly reproduce muscle co-contractions have been shown to produce more physiologically valid estimates of muscle forces and resulting joint loads [156]. Our findings support the use of EMG-assisted approaches as a starting point to estimate neck muscle function during dynamic tasks of the head and neck until viable experimental methods are identified

1835 or computational estimations using *a priori* cost functions are verified further.

### 1836 5.5.1 Limitations

1837 The following limitations of this study should be considered. Firstly, our musculoskeletal  
1838 model of the cervical spine is still a simplification of the anatomical complexity  
1839 of the physical system. The addition of wrapping surfaces, updated muscle strengths  
1840 and region-specific scaling of the cervical vertebrae based on the participant's MRI  
1841 measurements aimed to address this issue. The availability of four measured excitation  
1842 signals as inputs for the EMG-assisted analyses, when 96 MTUs were included  
1843 in the model, required a number of assumptions that may oversimplify the contribution  
1844 of individual muscles, especially in deep areas. The positive results provided in  
1845 Moroney et al. (1988) [75], that also grouped neck muscles, along with our findings,  
1846 suggest that such a grouping method is a viable initial approach given the limitations  
1847 associated with applied studies of the neck during impacts. Additionally McGill et  
1848 al.[75] have shown that surface EMGs could represent deeper muscle excitations within  
1849 15% degree of error in the lumbar spine. In our study the muscle activations that  
1850 were measured experimentally could be modulated in order to generate the required  
1851 forces. Similar approaches have been used previously [6, 28, 75] which we deemed as  
1852 a reasonable approach based on these assumptions. The single subject EMG-assisted  
1853 analysis provided subject and task specific muscle excitation estimates that matched  
1854 experimental moment and EMG measures during representative rugby scrummaging  
1855 and tackles. The estimated excitations are not intended to provide a definite characterisation  
1856 of the recruitment pattern the nervous system adopts during these rugby  
1857 tasks but gives an indication of what can be expected based on available experimental  
1858 data. However, this consideration has not been seen as a major limitation in previous  
1859 research estimating spinal muscle activations [6, 146]. Finally experimental EMG measurements  
1860 were conducted in a single data collection on a single subject. The inherent  
1861 variability of EMG measurements poses a risk of inconsistency and misrepresentation  
1862 of the neural state on neck muscles during simulated rugby contact events. To account  
1863 for this familiarisation trial were conducted during the participant warm-up during  
1864 which EMG electrode positions were adjusted to obtain the clearest signal to noise  
1865 ratio. Additionally multiple trials of three different impact conditions were collected  
1866 (scrummaging, side-on and frontal tackling) whose EMG signals were normalised to  
1867 the maximal level of muscle excitation which accounts for intra-subjected variability  
1868 of EMG signals. Future studies could apply this method to neck EMG measurements  
1869 from multiple participants to assess further the effect of EMG variability and investigate  
1870 the EMG-assisted estimations of neck muscle activations by including mechanical ob-

jective criteria, such as load protection mechanisms [146], based on observations from  
experimental studies.

## 5.6 Conclusion

In conclusion, this study shows for the first time that both experimental net joint  
moments across the entire cervical spine and neck muscle activation patterns during  
dynamic tasks can be reproduced using MRI-informed EMG-assisted models. The abil-  
ity of the EMG-assisted models to reproduce net joint moments with MTU activations  
that i) track experimental EMG measurements, ii) do not saturate, iii) do not dis-  
play high frequency activation and deactivation phases, iv) closely follow experimental  
co-contraction ratios and v) are estimated with no *a priori* objective function, is a  
key step forward to investigate cervical spine injury mechanisms during impact events.  
The results presented here are not intended to provide a definitive answer on how the  
neck neuromuscular system functions during dynamic tasks as further investigation is  
needed for these scenarios. They do, however, illustrate that the presented methods  
better estimate the neuromuscular state of the entire neck prior to impacts based solely  
on experimental data (kinetics and muscle excitations) compared to previous numerical  
methods.

## 5.7 Acknowledgements

The authors would like to thank the Rugby Football Union Injured Player Founda-  
tion for funding the PhD scholarship for PS and the University of Bath International  
Funding Scheme for helping to fund the international collaboration.

## 5.8 Conflict of interest

No conflicts of interest to declare from the authors

## Chapter 6

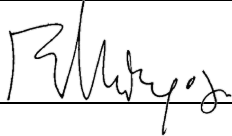
# An integrated experimental and modelling approach indicates that buckling is the primary mechanism of cervical spine injury in rugby tackling

### *Pre-chapter commentary*

This final investigative chapter of the thesis studies the effects of theoretical head impacts on cervical spine loading as a result of misdirected rugby tackles. For understandable ethical reasons injurious scenarios cannot be studied directly through *in vivo* experiments involving athletes. On the other hand *in vitro* experiments allow for the direct study of injuries but can lack the representation of the system and environment in which they occur. Applied *in silico* investigations however, can combine *in vivo* and *in vitro* data to create and drive computational models circumventing some of the limitations associated with each separate approach. Such applied *in silico* investigations require validated models appropriate for the event or task being study and careful replication of the environment and initial conditions of the injurious event. This study integrates the impact specific viscoelastic joint parameters from Chapter 4 into the MRI-informed rugby player musculoskeletal model from Chapter 5. Forward dynamic simulations using the new model are driven by muscle activation, joint kinematic and impact force data from Chapter 5 representative of misdirected rugby tackles. These



closely representative simulations of misdirected tackle are used to investigate the ef- 1915  
fect of specific tackling technique on intervertebral joint loading and the primary injury 1916  
mechanism that caused lower cervical spine dislocations in these events. 1917

<b>This declaration concerns the article entitled:</b>			
Chapter 6: "An integrated experimental and modelling approach indicates that buckling is the primary mechanism of cervical spine injury in rugby tackling" 1918			
<b>Publication status (tick one)</b>			
Draft manuscript <input checked="" type="checkbox"/> Submitted <input type="checkbox"/> In review <input type="checkbox"/> Accepted <input type="checkbox"/> Published <input type="checkbox"/>			
<b>Publication details (reference)</b>	Silvestros P, Preatoni E, Gill SH and Cazzola D (2020) An integrated experimental and modelling approach indicates that buckling is the primary mechanism of cervical spine injury in rugby tackling. <i>(Draft manuscript in preparation)</i>		
<b>Copyright status (tick the appropriate statement)</b>			
I hold the copyright for this material <input checked="" type="checkbox"/> Copyright is retained by the publisher, but I have been given permission to replicate the material here <input type="checkbox"/>			
<b>Candidate's contribution to the paper (provide details, and also indicate as a percentage)</b>	The candidate considerably contributed to and predominantly executed the:  <b>Formulation of ideas: 75%</b> PS contributed to: Background research, identification of suitable methodologies and initial proof of concept theoretical simulations  <b>Design of methodology: 75%</b> PS developed the integrated framework and computational pipelines under the supervision of DC,EP and HSG  <b>Experimental work: N/A</b> N/A  <b>Formal data analysis: 90%</b> PS performed the computational simulations and the analysis on the input and output data  <b>Presentation of data in journal format: 75%</b> PS wrote the first draft of the paper and draft revisions		
<b>Statement from Candidate</b>	This paper reports on original research I conducted during the period of my Higher Degree by Research candidature.		
<b>Signed</b>		<b>Date</b>	20 <sup>th</sup> June 2020

## 6.1 Abstract

1919

Catastrophic neck injuries in rugby tackling are rare (2 per 100,000 players per year) with 38% of these injuries occurring in the tackle. The aim of this study was to determine the primary mechanism of cervical spine injury during rugby tackling and to highlight the effect of tackling technique on intervertebral joint loads. *In vivo* and *in vitro* experimental data were integrated to generate realistic computer simulations representative of misdirected tackles. MRI images were used to inform the creation of a musculoskeletal model. *In vivo* kinematics and neck muscle excitations were collected during lab-based staged tackling of the player. Impact forces were collected *in vitro* using an instrumented anthropometric test device during experimental simulations of rugby collisions. Experimental kinematics and muscle activations were prescribed to the model and impact forces applied to seven skull locations (three cranial and four lateral). To examine the effects of technique on intervertebral joint loads the model's neck angle was altered in steps of  $5^\circ$  about each rotational axis resulting in a total of 1,623 experimentally informed simulations of misdirected tackles. Neck flexion angles and cranial impact locations had the largest effects on maximal compression, anterior shear and flexion moment loads. During posterior cranial impacts compression and flexion moments increased from 1500 to 3200 N and 30 to 60 Nm respectively between neck angles of  $30^\circ$  extension and  $30^\circ$  flexion. This was more evident at the C5-C6 and C6-C7 joints. Anterior shear loads remained stable throughout neck angle ranges however in anterior loading conditions they were directed posteriorly in flexed neck angles. The combination of estimated joint loads in the lower cervical spine support buckling as the primary injury mechanism of anterior bilateral facet dislocations observed in misdirected rugby tackles and highlights the importance of adopting a correct tackling technique.

1943

## 1944 6.2 Introduction

1945 Rugby is a full contact field sport with the tackle resulting in a high proportion of head,  
1946 neck and shoulder injuries [17, 48, 143]. Recently epidemiological and biomechanical  
1947 injury prevention research has focused on the reduction of concussion risks in rugby  
1948 with the primary suggestion being reducing the legal tackle height [137, 140, 143].  
1949 Tackling however carries with it a high proportion ( $>30\%$ ) of all catastrophic cervical  
1950 spine injuries in rugby [19]. Although the likelihood of sustaining a catastrophic injury  
1951 is rare (2-10 per 100,000 players per year) compared to that of concussion in the tackle  
1952 (8.9 per 1000 hours), the reduction on quality of life as well as associated financial  
1953 costs are far greater [99]. There is, therefore, a pressing need to accurately and reliably  
1954 investigate neck injury mechanism with the final aim to appropriately inform injury  
1955 prevention interventions to increase the safety of rugby [9].

1956 The main theorised cervical spine injury mechanisms in rugby are buckling [67] and  
1957 hyperflexion [40]. Buckling is caused by a compressive axial load applied to the cer-  
1958 vical spine column that results in the combination of flexion and extension across the  
1959 intervertebral joints [95, 163]. Hyperflexion is the excessive posterior to anterior head  
1960 motion resulting in intervertebral joints exceeding their physiological flexion range. The  
1961 catastrophic cervical spine dislocations observed in rugby accidents are predominately  
1962 anterior bilateral facet dislocations in the lower cervical spine (C4-C5 to C6-C7) [67].  
1963 Hyperflexion was maintained as the primary injury mechanism during rugby activities  
1964 by Dennison et al. (2012) [40], supported by player recollections [8] and video analysis  
1965 of the inciting events. Such evidences were used to draw a cause-effect relationship  
1966 with clinically observed spinal injuries and together with a lack of *in vivo* evidence led  
1967 the authors to believe that buckling was not likely to occur *in vivo*. However, cervical  
1968 spine buckling had been recreated during quasi-static and dynamic *in vitro* cadaveric  
1969 experiments [60, 59, 93, 95]. These experimental studies showed that cervical spine  
1970 buckling is sensitive to neck pre-flexion angles (geometric alignment), simulated muscle  
1971 forces (internal stability), impact load characteristics and interaction with impacted  
1972 surface (endpoint constraint) [92, 93, 94, 95, 113]. The rationale for questioning buck-  
1973 ling as the primary injury mechanism in rugby was firstly that highly controlled *in vitro*  
1974 experiments differ greatly from the real *in vivo* dynamics of rugby tackles. Secondly  
1975 qualitative data from video analysis and personal accounts of injured players supported  
1976 hyperflexion as the mechanism of injury.

1977 Computer simulations have since proven a valuable method in being able to recre-  
1978 ate with high fidelity the internal (i.e. muscle forces) and external loading condi-

tions during which cervical spine injuries occur under inertial and compressive loading [26, 37, 41, 51, 96]. In-silico simulations using musculoskeletal and finite element models have strengthened the theory that muscle forces affect resulting head and neck dynamics during injurious scenarios (whiplash and axial impacts). Furthermore, neck models validated for dynamic loading have been able to characterise the internal loading patterns of cervical spine structures sustained during impacts which is not achievable *in vitro* and *in vivo*. Computational investigations [96] have supported the theorised decoupling between externally observed head and neck kinematics and the internal dynamic response of the spine during axial loading injuries [60, 95, 163]. These have supported buckling over hyperflexion as the main injury mechanism under compressive impacts to the head [96, 92].

However, a rugby tackle is a very dynamic event, characterised by extremely variable and intense external loading conditions and a high-level of spinal muscle co-contraction [120]. Also, it is very challenging to measure accurate rugby tackling forces *in vivo* to inform and drive computational studies. For these reasons, a rugby-specific theoretical modelling study has not yet been conducted to specifically evaluate if buckling is the predominant cervical spine injury mechanism observed during tackling. A rugby-specific theoretical study would aim to replicate high risk impact scenarios associated with catastrophic neck injuries occurring in gameplay situations and relate them to applied aspects such as players technique and governing laws of the game.

Therefore, we conducted an *in silico* investigation, informed and driven by a combination of *in vitro* and *in vivo* data, to examine the dynamic response of the cervical spine to loading conditions representative of misdirected rugby tackles. The aims of the study were firstly to determine the primary cervical spine injury mechanism during rugby tackling, and secondly to highlight the effect of tackling technique on the intervertebral loading experienced during high fidelity musculoskeletal simulations.

## 6.3 Materials and Methods

### 6.3.1 Experimental data

#### 6.3.1.1 *In vivo*

One professional academy-level front-row rugby player (male, 22 years, 1.824 m, 113.7 kg) participated in this study. Ethical approval was obtained from the Research Ethics Approval Committee for Health of the University of Bath and the participant provided written informed consent prior to data collection. Full body kinematics (Oqus, Qualy-

sis, Sweden) and bilateral EMG (Trigno, Delsys, USA) of the sternocleidomastoid and upper trapezius muscles were collected at 250 Hz and 2500 Hz, respectively during laboratory-based staged tackling trials with a tackle simulator (mass = 40 kg) [23, 120] as described in Study 2 (5.3.2). Kinematics and EMG signals at the instant of tackle impact were used to inform the initial conditions of the model during the *in silico* simulations.

#### 6.3.1.2 *In vitro*

A head and neck assembly of an anthropometric test device (ATD) (Hybrid III 50<sup>th</sup> percentile male, Human Kinetics, Germany) was attached to a steel frame 1.5 m from a ground anchoring and used to simulate misdirected rugby tackle impacts to the head [73]. A six-axis load cell was instrumented at the head and neck interface of the ATD to measure forces caused by the impacts of the tackle simulator with the ATD assembly. Impacts were generated by the tackle simulator (mass = 40 kg) contacting the ATD assembly at two different speeds 2.0-2.5 m/s and 3.1-3.6 m/s. These impacts aimed to represent the momentum change experienced during live tackles [53]. The resultant impact force magnitudes and loading rates were used to inform theoretical impact conditions applied during the *in silico* simulations.

### 6.3.2 Musculoskeletal simulations

#### 6.3.2.1 Musculoskeletal model

A MRI-informed musculoskeletal model of the participant [23] (*Chapter 5.3.3*) was implemented with impact specific 6 degrees of freedom linear bushing elements [129] (*Chapter 4.5*) at each of the sub-axial cervical spine joints (C2-C3 to C7-T1) in OpenSim 3.3 [39] (6.1). The model included anatomically measured muscle paths for 13 bilateral pairs of neck muscles (*Chapter 5.3.1*). The bushing elements were defined coincident with each cervical joint's reference system to replicate their viscoelastic behaviour of the intervertebral joints during impacts. The model was posed to match the participants body configuration at the moment of impact using the joint angles outputted via inverse kinematic analysis in OpenSim. The pelvis and trunk bodies were then rigidly attached to the inertial reference frame prohibiting any motion other than the skull and cervical vertebrae.

Table 6.1: Stiffness and damping parameter values used in bushing elements of the musculoskeletal model cervical spine joints (C2-C3 to C7-T1).

	Stiffness	Damping
<b>Anteroposterior shear</b>	75.9 kN/m	1400 Ns/m
<b>Axial compression</b>	23100 kN/m	4300 Ns/m
<b>Lateral shear</b>	73.0 kN/m	1000 Ns/m
<b>Lateral bending</b>	18.91 Nm/rad	1.5 Nms/rad
<b>Axial rotation</b>	18.58 Nm/rad	1.5 Nms/rad
<b>Flexion/Extension</b>	24.06 Nm/rad	1.5 Nms/rad

### 6.3.2.2 Neck angle conditions

2042

To examine the effect of initial neck positioning during impacts in misdirected tackles the model's sub-axial neck angles (C2-C3 to C7-T1) about the three axes of rotation (Flexion/Extension; Lateral Bending and Axial Rotation) were compared in steps of 5°. In the sagittal plane: from 30° degrees of extension to -30° of flexion (13 conditions), frontal plane: from 0° (neutral) to -10° of lateral bending (3 conditions) and in the transverse plane: 5° to 15° of axial rotation (3 conditions). This resulted in 117 unique initial neck angle configurations. The angle ranges selected were informed by kinematic measurements of one-on-one experimental tackling trials of university/professional level rugby players [64]. The initial angle of the upper cervical spine (C0-C1 to C1-C2) was kept the same as the *in vivo* experimental trials, which was in the extended position (18°) to replicate a more forward looking gaze of the tackler. Neck and head angular velocities from an *in vivo* experimental tackling trial at the moment of tackle impact were prescribed to the model for all unique initial neck angle configurations.

2055

### 6.3.2.3 Muscle activations

2056

For all the simulations the model's muscles were prescribed the same activation scheme (Figure 6-1). This activation scheme was estimated using an EMG-assisted neuro-musculoskeletal model (*Chapter 5.5*) to minimise the error between experimental and simulated joint moments and muscle activations during the same *in vivo* experimental trial used for informing initial angular velocities. This provides a reasonable and physiologically plausible muscle recruitment pattern for a player expecting a correct tackle to the shoulder. Muscle activation values were selected from instant of tackle impact during the staged tackle trial and remained constant for the duration of the 50 ms simulations. Constant activations were selected to represent muscle pre-activation as cervical spine reflex times exceed 50-60 ms [44, 90, 127] reducing the effect of active neck muscle modulation during short impact events.

2067

#### 2068 **6.3.2.4 Loading conditions**

2069 To replicate the possible head impact locations during misdirected tackles seven loading  
2070 conditions were defined for the simulations (Figure 6-2). As the location and direction  
2071 of contact forces cannot be generated with great validity in multibody musculoskeletal  
2072 models, an approximation was adopted to calculate these parameters based on the  
2073 skull's geometry in Matlab. Three points of impact force application were defined on  
2074 the cranial midline of the model's skull segment. These were at the vertex, posterior to  
2075 the vertex (near the skull lambda or crown) and anterior to the vertex. The directional  
2076 vector of these three loading conditions was defined from the points of application to  
2077 the base of the skull to simulate misdirected tackles resulting in "*head on*" impacts.  
2078 Four remaining points of impact were defined on the right lateral side of the skull with  
2079 an inferolatateral direction representing more oblique impacts. All points of application  
2080 and directional vectors were constant with respect to the model's skull reference system.  
2081 The magnitude and loading rate of each condition was acquired from the *in vitro*  
2082 experimental trials simulating misdirected rugby tackle impacts to the head using the  
2083 ATD and tackle simulator at two different speeds. The loading rate of these tests  
2084 (80 kN/s) were one order of magnitude lower than what the bushing elements were  
2085 validated against (800 kN/s). However it has been shown that the stiffness response  
2086 of intervertebral discs does not change considerably after a rate of 75-90 N/s [108, 89]  
2087 therefore the bushings used in the model were deemed valid for the loading conditions  
2088 tested.



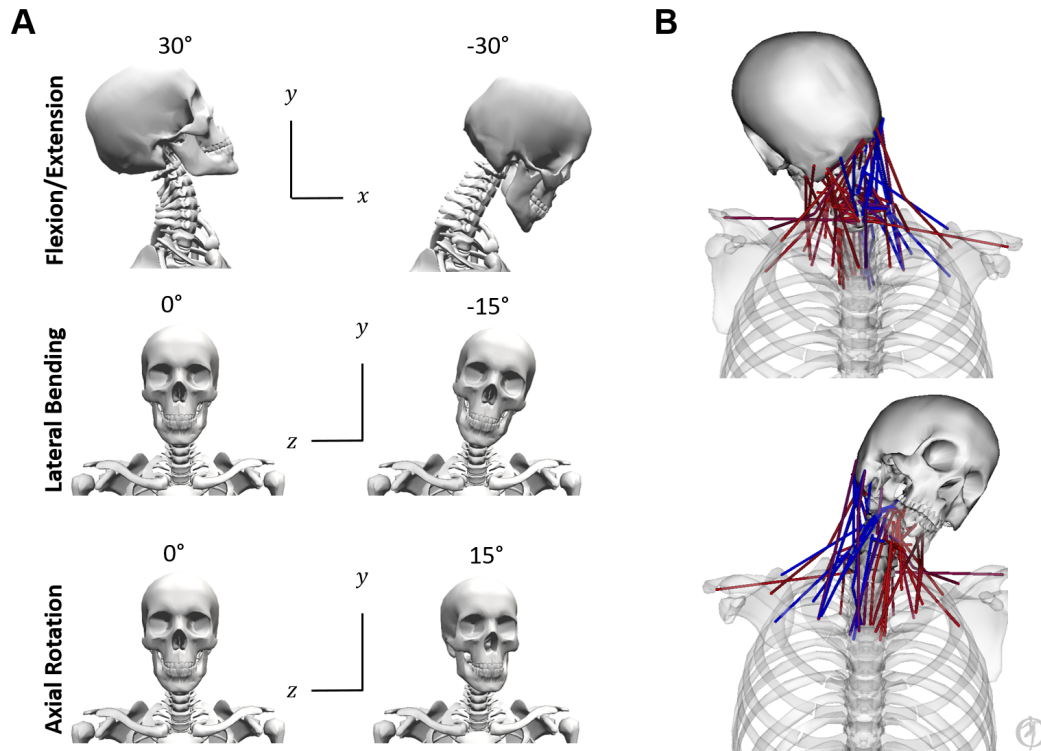


Figure 6-1: A) Close up view of the scaled MRI informed OpenSim model's head and neck region with reference views of maximal ranges of motion tested in the simulations (muscles and wrapping surfaces removed for clarity of the cervical spine structure). Anteroposterior shear and Lateral Bending are defined by the X axis. Compression and Axial Rotation are defined by the Y axis. Lateral Shear and Flexion/Extension are defined by the Z axis. B) Neck muscle activation pattern estimated using EMG-assisted optimisation from staged experimental tackling and used across all simulations. During the staged experimental trials, the tackle was taken on the right shoulder which can be seen by the different levels of the model's muscle activations (red – maximum, blue – minimum).

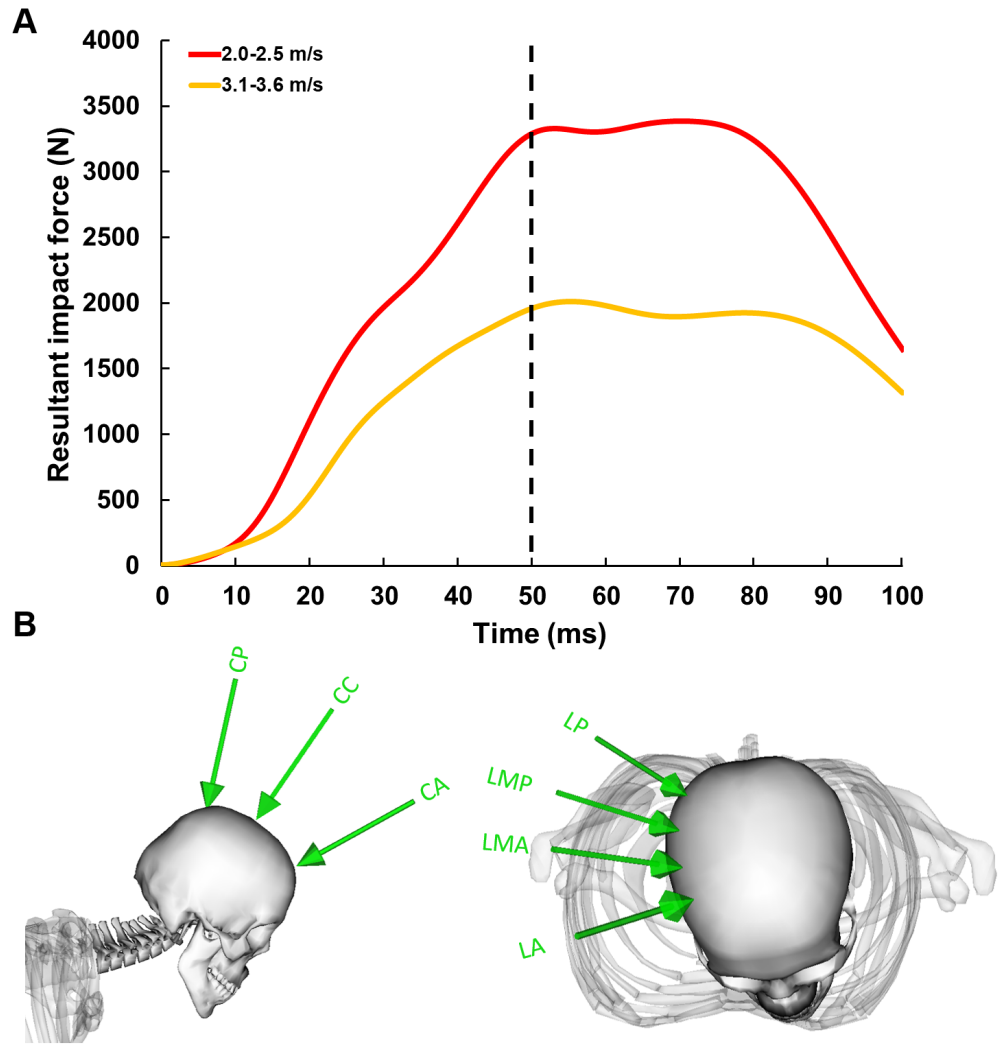
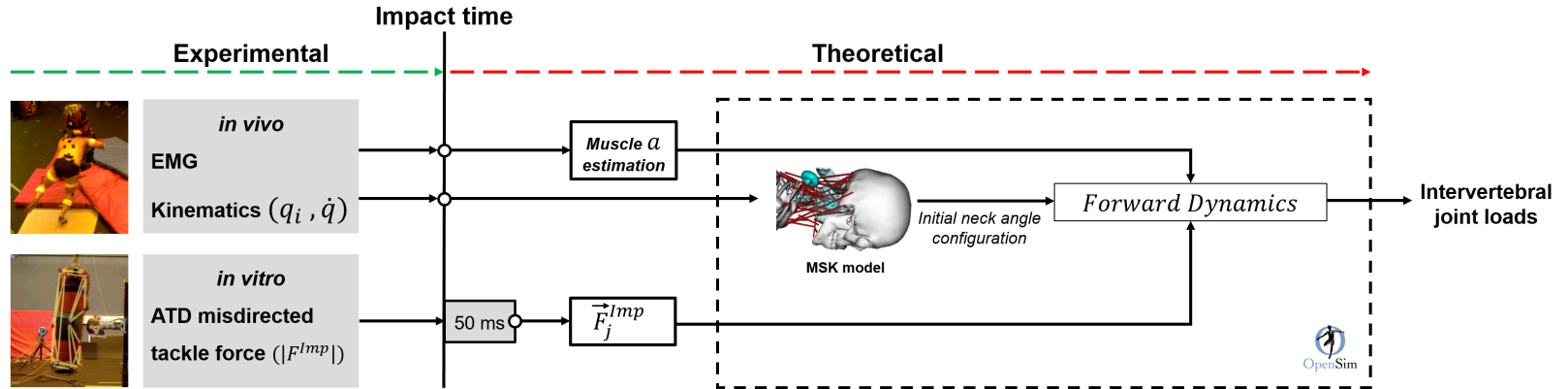


Figure 6-2: A) Resultant impact force signals collected at two different impact speeds between the tackle simulator (mass = 40 kg) and the ATD. B) Cranial (left) and lateral (right) loading conditions applied to the skull (CA – Cranial Anterior; CC – Cranial Central; CA – Cranial Anterior; LP – Lateral Posterior; LMP – Lateral Mid Posterior; LMA – Lateral Mid Anterior; LA – Lateral Anterior). These were identified in Matlab by defining a grid of parallel transverse (n=2) and frontal (n=5) planes at 30 mm intervals to the skull segment’s geometry. The intersecting locations of the planes with the skull’s geometry defined four rectangular regions on the right side of the skull. Each parallelogram can be thought of an impact area on the musculoskeletal model skull to which a new plane was fitted. The point of impact force application for each of the four areas defined by the rectangular regions was the projected midpoint of the fitted plane onto the skull geometry. The directional vector was the normal vector of the fitted plane directed into the skull.

### 6.3.2.5 Forward dynamic simulations

2089

For each initial neck angle configuration, the model was loaded under the seven different 2090  
loading conditions at two loading rates resulting in a total of 1,638 simulations (117 2091  
neck angles configurations  $\times$  7 loading conditions  $\times$  2 loading rates). Each simulation 2092  
was performed for 50 ms from the time of initial force application and initialisation of 2093  
muscle forces. This time duration for the simulations was chosen as it contained the 2094  
initial measured force peak and in in-vitro cadaveric head drop experiments [95] injury 2095  
was reported to occur within 20 ms. The simulations were not performed past the peak 2096  
of the applied load as multibody models are unable to simulate tissue deformation and 2097  
thus are not expected to reliably predict the injury in such conditions. The effects 2098  
of initial neck angle and loading conditions were evaluated by analysing the maximal 2099  
compressive loading, anteroposterior shear loading and flexion bending moment at the 2100  
C3-C4 to C6-C7 joints sustained during the 50 ms impact simulations. 2101



111

Figure 6-3: Workflow of integrated experimental and theoretical framework used to investigate cervical spine injury mechanism in rugby tackles. Experimental: *in vivo* data (neck muscle EMG and joint angles and velocities) were collected during stage tackling laboratory trials using a tackle simulator (mass= 40 kg; velocity = 2.0-2.5 and 3.1-3.6 m/s). *in vitro* data (force magnitude and loading rate) was collected from the Anthropometric Test Device (ATD) during simulated misdirected impacts to the head. Theoretical: for each of the 1638 simulations an initial neck angle configuration combining Flexion/Extension, Lateral Bending and Axial Rotation angles ( $q_i$ ,  $n=117$ ) taken from ranges in the literature was prescribed to the model. *in vivo* data at the time of impact were used to inform then initial neck joint angular velocities ( $\dot{q}$ ) and joint angles of the torso and upper limbs. Level of neck muscle activations ( $\alpha$ ) at the time of impact derived from EMG-assisted analysis of the staged tackling trial were applied to the model's muscles to be constant throughout the 50 ms simulations. For each initial neck angle configuration ( $q_i$ ) external loading conditions were applied ( $\vec{F}_j^{Imp}$ ,  $n=14$ ) replicating different impact locations on the head at two different speeds. The points of application and direction of the loading conditions were defined using the model's skull geometry in Matlab. The magnitude and loading rate characteristics were taken from the first 50 ms of the *in vitro* ATD impact forces

## 6.4 Results

2102

Initial neck angles and loading conditions affected intervertebral joint loading patterns across the cervical spine (Figure 6-4). Joint loads were more sensitive to initial neck flexion angles compared to changes in lateral bending and axial rotation across the loading conditions and vertebral levels (Figure 6-5 and 6-6). Average compressive joint loads were larger in the lower cervical spine whereas anteroposterior shear and flexion moments showed more complex loading patterns across intervertebral joints (Figure 6-7 and 6-8).

2103  
2104  
2105  
2106  
2107  
2108  
2109

Lateral bending and axial rotation of the neck did not significantly affect the magnitudes of compressive joint loading across the loading conditions (Figure 6-5). Maximal compressive joint loads during the 50 ms simulations on increased as initial neck position transitioned from an extended ( $30^\circ$ ) to a flexed position ( $-30^\circ$ ) with largest loads experienced when the neck was initially flexed. The largest increase was seen in the posterior cranial impacts (CP) during which lower cervical spine compressive loading increased by approximately 50% (from 2100 to 3200 N) in the  $-30^\circ$  flexed condition compared to neutral ( $0^\circ$ ) (Figure 6 – Column 1 Rows 3 and 4). Lateral posterior impacts (LP and LMP) also resulted in increased compressive joint loading of up to 30% (from 2200 to 2900 N). In anterior loading conditions (CA, LMA and LA) initial neck flexion had a smaller effect with compression increasing less than 500 N (20%) from when the neck was extended (Figure 6-6 and 6-7 – Column 1).

2110  
2111  
2112  
2113  
2114  
2115  
2116  
2117  
2118  
2119  
2120  
2121

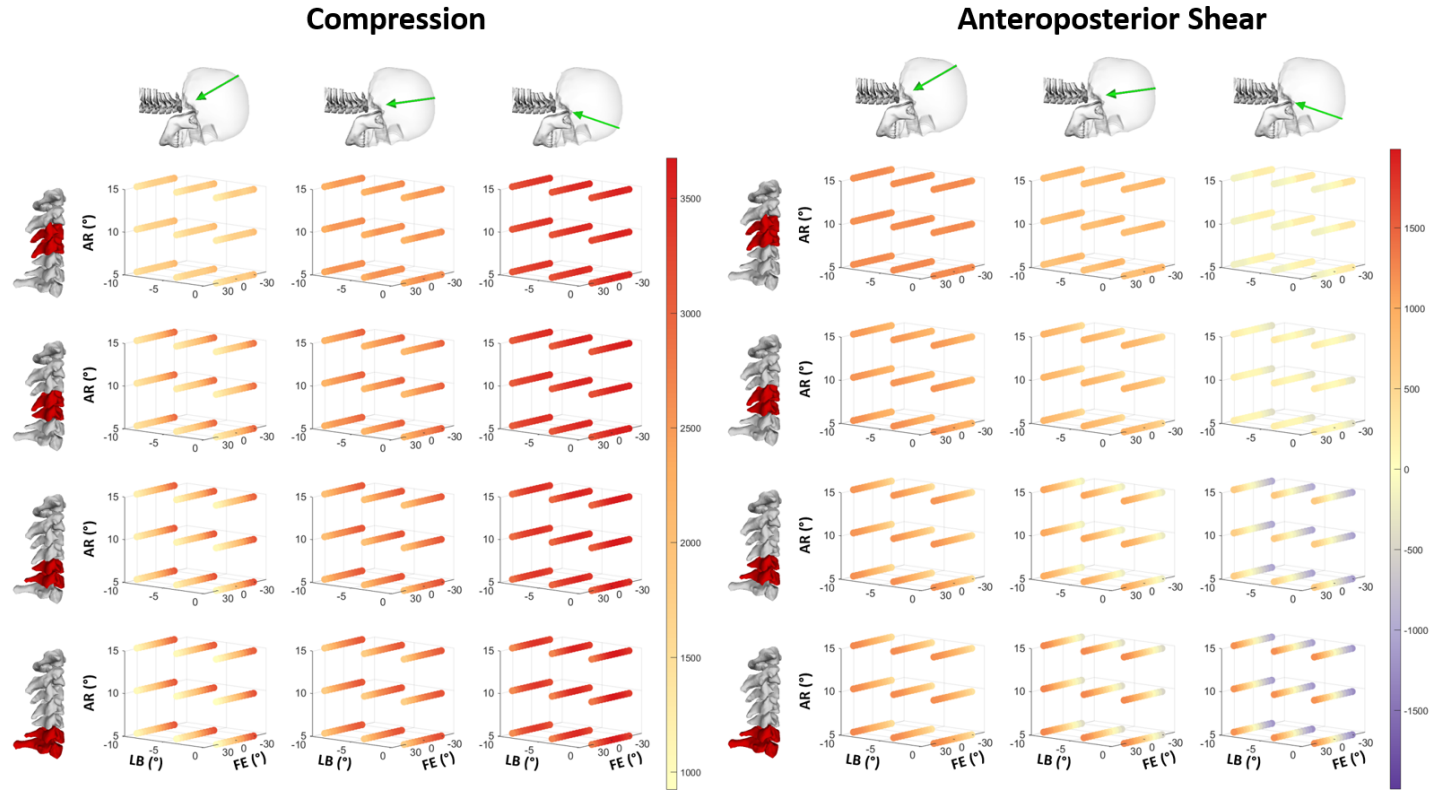


Figure 6-4: Patterns of maximal compression (left) and anteroposterior shear (right) loading sustained during the 50 ms simulations across all simulated initial neck angles for cranial loading conditions. Column represents an individual loading condition (Cranial Posterior – left columns; Cranial Central – centre columns and Cranial Anterior – right columns). Rows represent the cervical spine levels from C3-C4 (top) to C6-C7 (bottom). The cubic grids of each subplot represents the initial neck angle ( $^{\circ}$ ) in Flexion/Extension (FE), Lateral Bending (LB) and Axial Rotation (AR). Magnitude of maximal loading (Newton) in the 50 ms simulations is represented with the colour bars. Note compression are only positive values and anteroposterior shear positive and negative values to represent direction with anterior and posterior respectively.

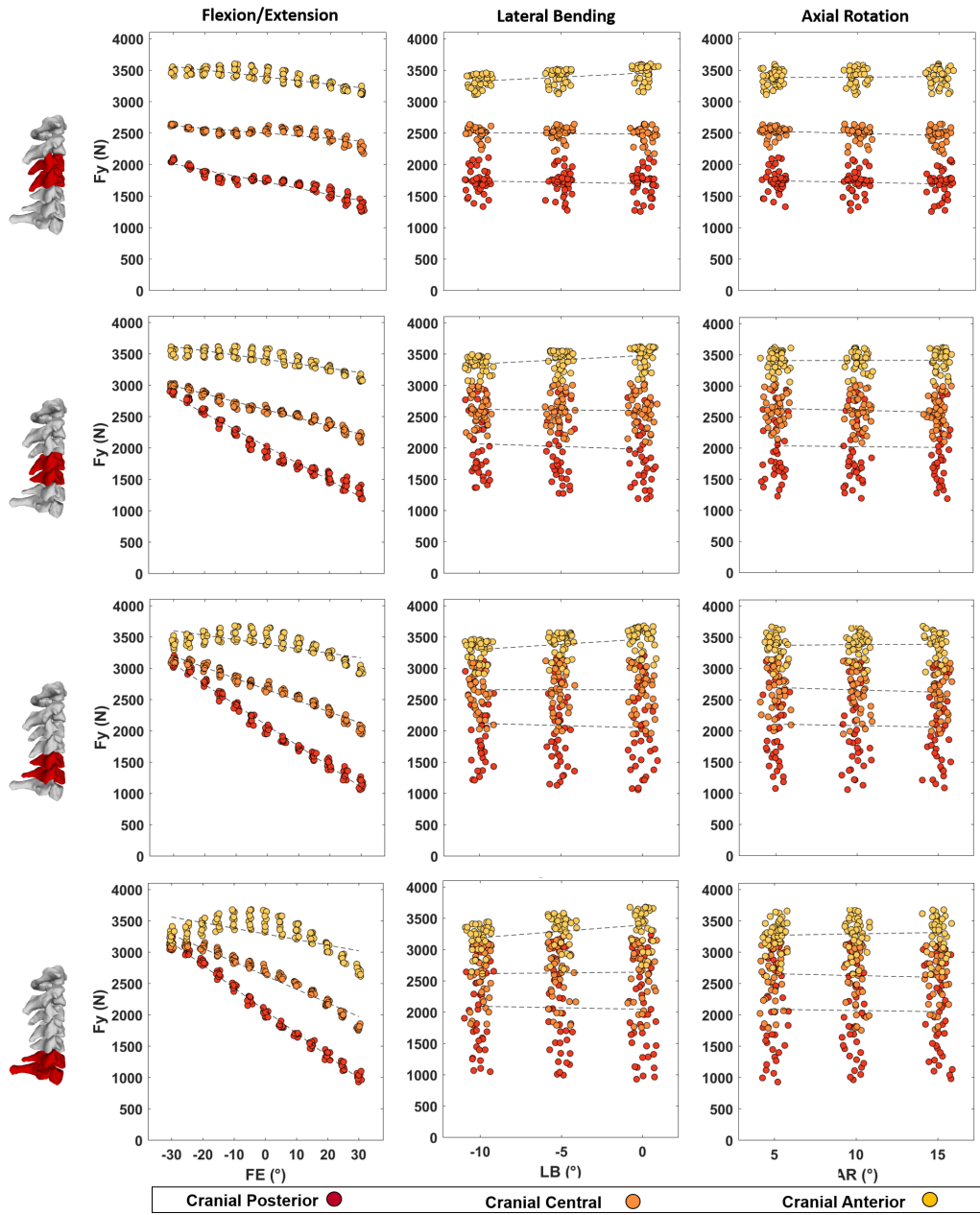


Figure 6-5: Maximal compressive joint loads (Newton) of C3-C4 (top row) to C6-C7 (bottom row) intervertebral joints plotted against  $5^\circ$  changes in Flexion(-)/Extension(+) (left column), Lateral Bending (centre column) and Axial Rotation (right column) during the cranial loading conditions (Cranial Posterior, Cranial Central and Cranial Anterior). First order polynomial lines of best fit are plotted to highlight the effect of joint angle on compressive joint loads for each loading condition (dashed lines). In each subplot data points are spread slightly in each  $5^\circ$  bin on the horizontal axes for better visualisation.

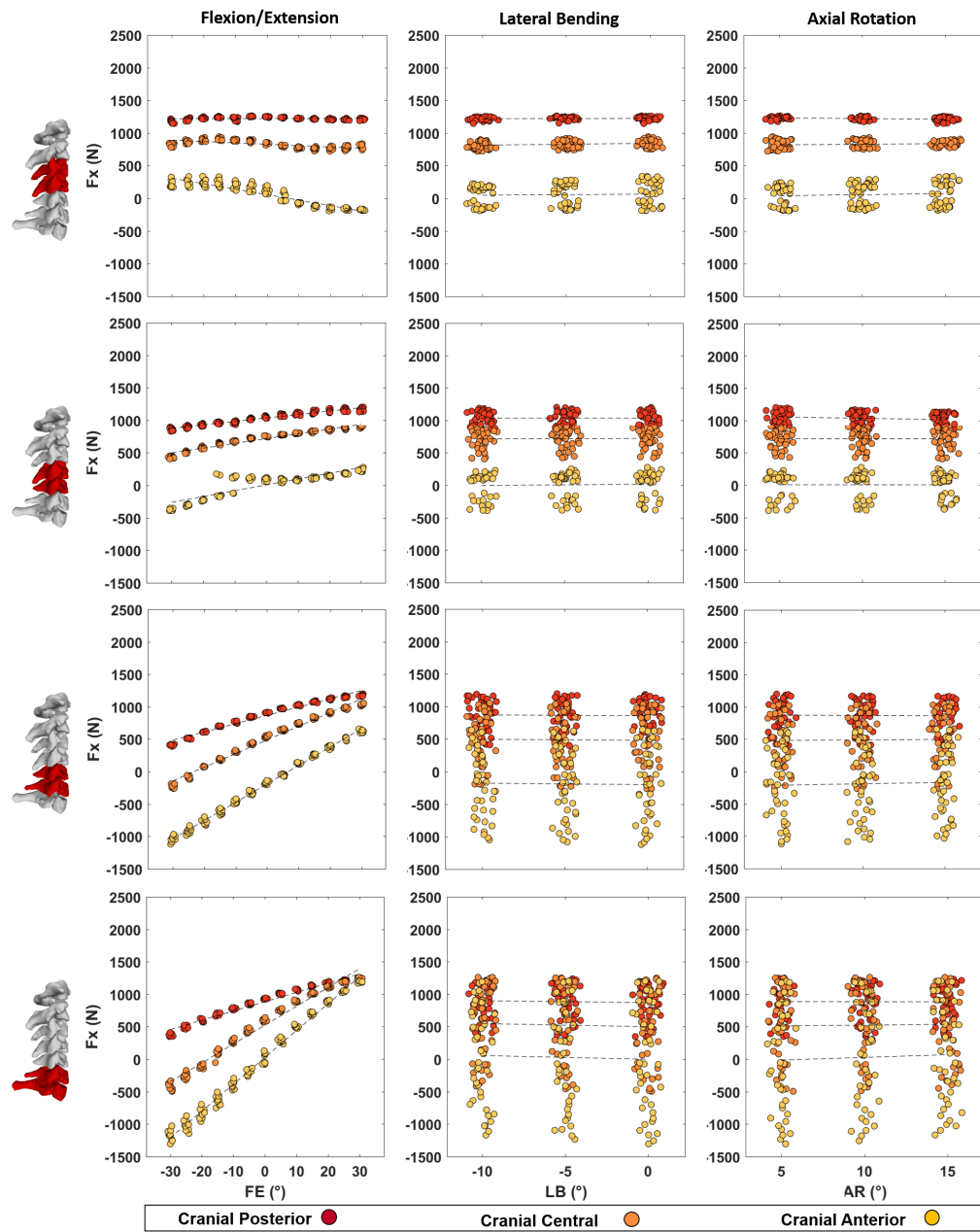


Figure 6-6: Maximal anteroposterior shear joint loads (Newton) of C3-C4 (top row) to C6-C7 (bottom row) intervertebral joints plotted against 5° changes in Flexion(-)/Extension(+) (left column), Lateral Bending (centre column) and Axial Rotation (right column) during the cranial loading conditions (Cranial Posterior, Cranial Central and Cranial Anterior). First order polynomial lines of best fit are plotted to highlight the effect of joint angle on compressive joint loads for each loading condition (dashed lines). In each subplot data points are spread slightly in each 5° bin on the horizontal axes for better visualisation.



Lateral bending and axial rotation of the neck did not affect the magnitudes of antero- 2122  
posterior loading across the loading conditions (Figure 6-6). Maximal anteroposterior 2123  
shear loads changed direction from anterior to posterior as the initial neck flexion angle 2124  
increased (Figures 6-7 and 6-8 – Column 2). This was more evident at the C5-C6 and 2125  
C6-C7 joint levels and during anterior loading of the skull (CA, LMA and LA), here 2126  
anterior shear loads of approximately 600 N changed to posterior loads of 1000 N from 2127  
when the neck was extended to when it neck was flexed. Posterior loading conditions 2128  
(CP, CC, LP and LMP) resulted in anterior shear loading across the initial neck angles 2129  
and all vertebral joint levels other than C6-C7 in the most flexed conditions (Figures 2130  
6-7 and 6-8 – Column 2). 2131

Flexion moments increased up to 60 Nm (Figures 6-7 and 6-8 – Column 3) as the 2132  
initial neck flexion angle approached -30°. This flexion moment pattern across neck 2133  
flexion angles was more visible during the posterior loading conditions (CP and LP). 2134  
Other loading conditions did not affect neck joint flexion moments across the initial 2135  
neck angles. Flexion moments were larger in the lower cervical spine when the spine 2136  
was loaded at the posterior (CP and LP) and across initial neck angles. However, in 2137  
other loading conditions lower cervical spine flexion moments reduced as neck flexion 2138  
angles increased. Supplementary simulation results for compression, anteroposterior 2139  
shear and flexion moment loads are presented in Appendix B. 2140

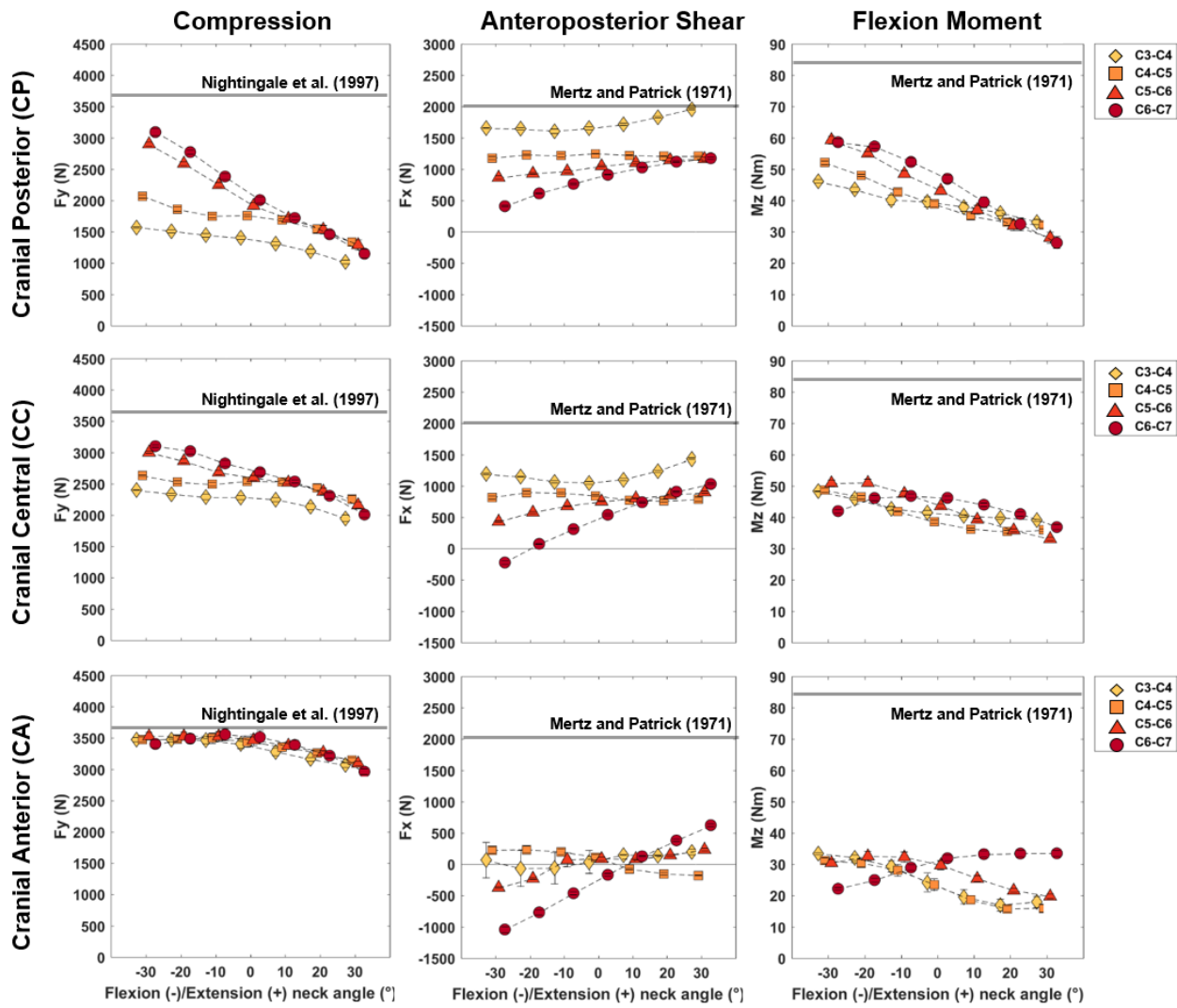


Figure 6-7: Mean and standard deviation values for maximal compression (left column), anteroposterior (centre column) and flexion moment (right column) of all initial neck angle conditions plotted against changes in neck flexion (negative) and extension (positive) angles for cranial loading conditions. Estimated injury thresholds from the literature for the entire cervical spine are also presented with the horizontal lines for compression and anteroposterior shear and subjective thresholds of “*maximum voluntary contraction*” are presented for flexion moment.

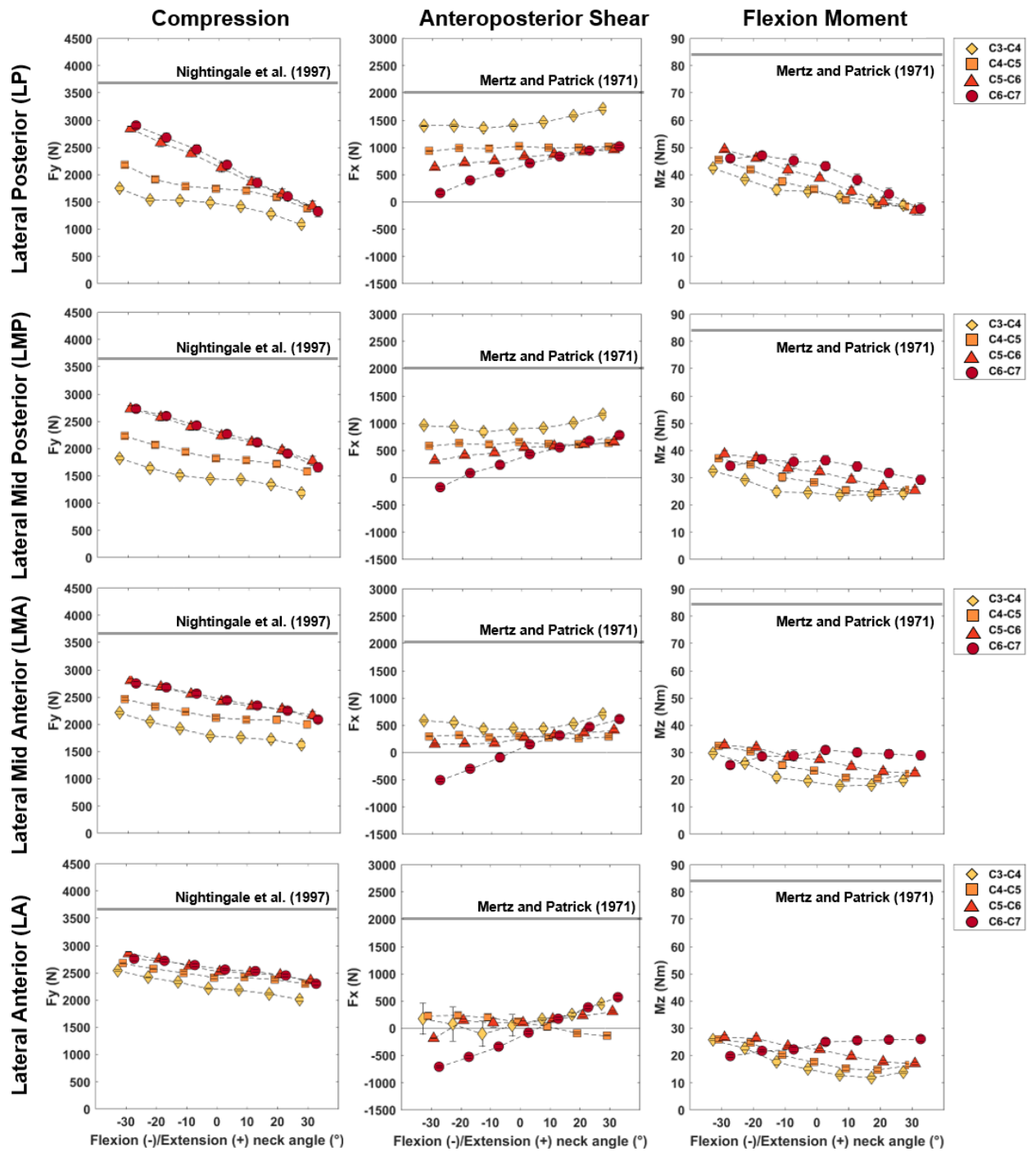


Figure 6-8: Mean and standard deviation values for maximal compression, anteroposterior and flexion moment of all initial neck angle conditions plotted against changes in neck flexion (negative) and extension (positive) angles for lateral loading conditions. Estimated injury thresholds from the literature are presented with horizontal lines.

2141 Lateral shear displayed the lowest joint load magnitudes ( $< 1000$  N). As left lateral  
 2142 bending angle increased left shear loads in the lower cervical spine (C5-C6 and C6-  
 2143 C7) also increased during cranial impacts. Lateral loading conditions (which were on  
 2144 the right side of the skull) increased the left lateral loading. The higher loading rate  
 2145 resulted in larger loads across all initial head angle and loading conditions. Individual  
 2146 values for maximal compressive loading and lateral shear during only cranial impacts  
 2147 are presented in the graphs for brevity. The equivalent graphs for lateral head impacts  
 2148 (LA, LMA, LMP and LP) are available in the supplementary material.

## 2149 6.5 Discussion

2150 The aim of this study was to simulate the dynamic response of the cervical spine to  
 2151 loading conditions representative of misdirected rugby tackles injurious, informed by  
 2152 experimental *in vivo* and *in vitro* data collected representing realistic rugby tackling  
 2153 conditions. We investigated the cervical spine injury mechanisms occurring in misdi-  
 2154 rected rugby tackles, where impact forces are applied to the head instead of the antic-  
 2155 ipated shoulder, and assessed the effect of tackling technique (neck angle) on cervical  
 2156 spine internal loading.

2157 Neck flexion angle at the time of impact had the largest effect on neck internal loading  
 2158 during misdirected tackle simulations. The important role of neck flexion on spinal  
 2159 loading during impacts has been previously shown with *in vitro* and *in silico* exper-  
 2160 iments [96, 95]. Our results confirmed that compressive loading increased with neck  
 2161 flexion also in rugby tackling, whilst anterior shear was reduced or directed posteriorly  
 2162 primarily in the lower cervical spine (C5-C6 and C6-C7). A more flexed position causes  
 2163 the neck to lose its natural lordosis resulting in an axial alignment of the vertebrae and  
 2164 a stiffer configuration of the cervical spine. This is a very hazardous situation that  
 2165 alters the transmission of head impact forces through the cervical spine and the way in  
 2166 which the impact energy is dissipated [96]. Our results supported this loading modality  
 2167 as compressive joint loads were highly dependent on the relative alignment of the im-  
 2168 pact force vector with the cervical spine column axis as neck flexion increased. This is  
 2169 also in line with the experiments reported by Nightingale et al. [94] who showed higher  
 2170 risk for injury when the impact is aligned within  $15^\circ$  of the neck axis. Additionally,  
 2171 the inverse loading pattern between compression and shear observed for the posterior  
 2172 loading conditions was likely caused by the change in relative alignment of the neck  
 2173 and impact force axes.

2174 The inverse loading pattern between compression and shear during posterior loading

conditions is also likely to be caused by the change in relative alignment of the neck and impact force axes. For individual joints as compression increased anterior shear loading decreased in flexion and vice versa in extension. For instance, during posterior cranial impacts (Figure 6-6 row 1), when the neck is extended by  $15^\circ$  compared to flexed by  $-15^\circ$ , proximity to compression tolerances is reduced from 65 to 40% (reduction of 1000 N) whilst increasing shear loading from 17 to 30% of shear tolerance values (increase of 400 N). This inversely proportional effect could be a beneficial trade-off between loading modalities when the head is impacted with the neck in a more extended position.

### 6.5.1 Neck muscle forces

The important role of active and passive neck muscle forces to load the cervical spine during impacts has been previously investigated [37, 41, 51, 96]. Neck musculature provides a compressive preload that increases the stability of the spinal column but also bring the intervertebral loads closer to their critical failure limits [113]. Our study is the first one in which task specific muscle forces are estimated from simulated *in vivo* rugby tackling and applied to analysis of spinal injury mechanisms. Activation levels derived using EMG-assisted methods for the analysis of staged laboratory rugby tackling provided an internal loading condition that would be expected in a tackle where the anticipated impact was to the right shoulder. This approach allowed for the use of physiologically plausible neck muscle forces at the time of impact, as they were not derived from any *a priori* assumptions. Such assumptions could result in the overestimation of intervertebral joint loads if maximal joint stiffness was the objective [85]. Our proposed approach increased the fidelity of the simulations as neural recruitment strategies during impacts are still not well understood in order to apply explicit *a priori* objective criteria to estimate muscle activations [44, 127].

### 6.5.2 Rugby tackling and injury mechanisms

Video analysis has estimated energy transfer during rugby tackle events can vary between 1.4 kJ and 3.0 kJ [53] which is considerably more energy than the 82 J needed to cause neck injury *in vitro* [93] and *in silico* [96] during axial impacts. This highlights the importance of correct tackling technique to position the head away from the oncoming ball carrier to minimise the amount of energy transferred to the neck in a misdirected tackle attempt. Low tackles, which are aimed near center of mass, are more effective in arresting the ball carrier's momentum and reduce the possibility of concussion to the attacking player as the tackle is aimed away from their head. However, this requires the tacklers to bend at the waist which could lead to a head, neck and torso alignment

2209 if they adopt bad technique (e.g. if fatigued or not wanting to be penalised for a high  
 2210 tackle). Additionally, together with the high possibility of head pocketing (i.e. head  
 2211 is constrained by the soft tissue of the stomach and large impact area) the tackler's  
 2212 neck would be required to arrest the momentum of the following body resulting in  
 2213 almost certain catastrophic injury during near cranial impacts. Although challenging  
 2214 to quantify the probability of these pocketing situations future computational and ex-  
 2215 perimental studies could evaluate the effects of the tackler's head contacting a more  
 2216 conforming surface of the stomach compared to the upper torso. Such a study would  
 2217 provide a more complete overview on the effect of tackle height technique with regards  
 2218 to possible concussive head and catastrophic neck injuries.

2219 Our computational study together with earlier theoretical work by Nightingale, et al.  
 2220 [96] provide additional evidence that hyperflexion is not the primary injury mechanism  
 2221 during rugby tackles. During posterior cranial impacts with flexed initial neck angles  
 2222 our study showed a combination of high compression, anterior shear and flexion loads  
 2223 in the lower cervical spine were generated before the neck exceeded  $-45^\circ$  of flexion. This  
 2224 demonstrates that during misdirected rugby tackles loading patterns associated with  
 2225 buckling and anterior facet dislocations are generated much earlier than when physio-  
 2226 logical neck flexion ranges are exceeded. Buckling does not itself cause injury (material  
 2227 failure) but it alters pre-injury neck kinematics and resulting loading modalities causing  
 2228 injury in the lower cervical spine. These alterations in intervertebral loading patterns  
 2229 help explain why injuries cannot be characterised by head motion alone [95, 163] which  
 2230 is an important consideration when relating field injuries to video analysis and players'  
 2231 recollections of the incident. Finally anterior dislocation injuries caused by the hyper-  
 2232 flexion of the entire cervical spine have been mostly disregarded [76, 77, 93] as *in vitro*  
 2233 experiments have not succeeded in generating them even under substantial loads (190  
 2234 Nm). Our results confirm that the term "*hyperflexion*" should cease to be used for the  
 2235 description of bilateral facet dislocation injuries under these conditions [92] as such a  
 2236 description may misguide injury prevention strategies in the game of rugby.

### 2237 6.5.3 Limitations

2238 Factors associated with the injury severity of a misdirected rugby tackle are many and  
 2239 all possible combinations that might be experienced on a rugby field cannot be fully  
 2240 replicated experimentally or computationally. Player internal factors such as experi-  
 2241 ence, physical maturity, fitness and technique [107, 143] and inciting event character-  
 2242 istics, such as the tackler and ball carrier approach velocities will all influence the risk  
 2243 of vertebral injury. Our study was conducted using a MRI-informed musculoskeletal

model of a rugby player which allowed for the prescription of task specific body kinematics and muscle forces closely representative of experimental conditions. A limitation of our approach is that neck muscle forces and initial angular velocities applied across all conditions were estimated from a single experimental neck position during a tackle. Ideally for each initial neck angle condition simulated in this study an estimation of muscle activations would have been experimentally estimated or optimised based on an *a priori* criterion. However, this was experimentally infeasible and outside the scope of this study. The chosen loading conditions for our study aimed to impact directions representative misdirected tackles. It should be noted that in reality impacts to the head would result in a shear loading component at and translation of the point of application that would change of the resulting impact force vector direction during the duration of the impact event. This is difficult to replicate in multibody models as contact models validated during such impacts should be used for this purpose. Therefore, it was assumed that point loads would be a reasonable representation for the short durations simulated (50 ms). However the use of contact models in these application should be investigated in the future. Finally, the use of multibody musculoskeletal models assumes that no plastic deformation is caused within the cervical spine during loading. This should be considered as this study was investigating injury mechanisms. Musculoskeletal models however cannot identify injury at a localised anatomical or material level (e.g. ligament tear, disc rupture or vertebral fracture) they can predict the overall dynamic response of the cervical spine in the time prior to injury.

The response of the cervical spine to axial head impacts has been previously shown with simplified finite element models that included rigid vertebrae and bushing elements to represent intervertebral joint behaviour [96, 22] similar to the present study. Although such models cannot identify specific locations or simulate injury they can be analyse experimental lab or on-field data to provide an initial appreciation of the cervical spine’s response to external impacts. This can be beneficial as patterns of internal loading and the spine’s response can be identified as impact parameters, such as neck angle and loading conditions, are changed. To better understand how the internal loading and resulting kinematic response of the cervical spine predicted by the musculoskeletal models during axial impacts results in the clinically observed injuries a successive step using finite element models should be completed. This step would utilise predicted kinematics (vertebral alignment and joint angular velocities) and muscle forces predicted by the musculoskeletal model, from representative experimental or on-field data, as boundary conditions in detailed finite element simulations to identify localised regions of stress and strain on cervical spine structures. Such finite element models could provide the specific identifiers of how cervical spine buckling leads to

2281 injury on a local vertebral level (e.g. joint dislocation, vertebral fracture, ligament tear  
2282 or disc burst).

## 2283 **6.6 Conclusion**

2284 In conclusion, the findings from our computational study indicate that the cervical  
2285 spine injuries observed in misdirected rugby tackles are not caused by a hyperflexion  
2286 mechanism. Posterior head impacts in when the neck was flexed produced patterns of  
2287 compression, anterior shear and flexion moment in the lower cervical spine indicative  
2288 of buckling and commonly observed anterior bilateral facer dislocation injuries. The  
2289 results of these simulations were guided by experimental data that informed the initial  
2290 joint angles, angular velocities, muscle forces and external loading conditions providing  
2291 high fidelity to the results. Although the musculoskeletal model used cannot identify  
2292 specific types of injury at a vertebral level the patterns identified from the predicted  
2293 dynamics suggest that a more extended neck reduces injury risk during axial rugby  
2294 impacts. This highlights the importance of the adoption of the correct tackling tech-  
2295 nique and inclusion of biomechanical analyses in injury prevention strategies to insure  
2296 the safety of the athletes in rugby tackling.



## Chapter 7

2297

## Epilogue

2298

The research presented in this thesis aimed to develop an integrated experimental and computational biomechanical framework for the analysis of cervical spine injury mechanisms in rugby. Initially, novel impact specific passive parameters of cervical spine intervertebral joints were estimated and validated. These parameters approximated the dynamic response of the cervical spine column to axial impacts. Secondly in order to provide a detailed biomechanical description of a rugby player the first athlete-specific musculoskeletal model that included MRI-informed muscle paths and strengths of a rugby player was created. The model was combined within a novel neuromuscular solution method to overcome previous experimental limitations and estimate physiological neck muscle activation patterns in preparation for rugby contact events. The estimated muscle activations were able to reproduce for the first time experimental net joint moments across the entire cervical spine. Finally, the musculoskeletal model incorporated the impact specific passive joint parameters and combined the physiological neck muscle activations with experimental kinematics and kinetics of rugby impacts in theoretical simulations. The simulations investigated combinations of loading conditions and neck angles during a tackle to determine their effect on internal loading of cervical spine joints. Through this study the first biomechanical evaluation of cervical spine injury in a sporting context was completed which could be incorporated in injury prevention research. The study concluded that the most likely cervical spine injury mechanism during misdirected rugby tackles is buckling and illustrated the effect of tackling technique on intervertebral joint loads.

2319

## 2320 7.1 Summary

2321 Although catastrophic cervical spine injuries are a rare phenomenon in rugby their  
2322 consequences to the quality of life of the individuals that suffer them is devastating  
2323 [47, 48, 19]. This is unfortunately mirrored by the considerable direct and indirect  
2324 financial costs associated to spinal injuries [46, 74]. Furthermore, the occurrence of  
2325 such injuries is a great concern to the reputation and the safety of the game which  
2326 puts pressure on governing bodies to mitigate their occurrence. Rugby law and policy  
2327 changes over the last two decades have been successful in reducing the incidences of  
2328 such injuries with a focus on protecting the head and neck areas of players. How-  
2329 ever, a lack of consensus has existed within the rugby community on the predominant  
2330 injury mechanism that causes the most commonly observed anterior bilateral facet dis-  
2331 location injuries in the lower cervical spine. The reason for this is that the intuitive  
2332 "hyperflexion" mechanism easily explains the phenotype of these injuries and has been  
2333 frequently used to describe them in a rugby setting. Furthermore, the body of quan-  
2334 titative evidence that otherwise supports buckling as primary injury mechanism has  
2335 been collected from controlled laboratory experiments, which it is argued do not accu-  
2336 rately represented the rugby specific situations the injuries are observed in. As rugby's  
2337 safety focus is now transitioning toward safeguarding players from concussions during  
2338 tackles, the aetiology and mechanisms of cervical spine injuries should also be taken  
2339 into account within new policies to ensure no unintended consequences are generated.  
2340 Therefore, the goal of this thesis was to provide a novel biomechanical platform that  
2341 allows for a more informed safety policy decision making in rugby.

2342 This thesis presents the first biomechanical evaluation of acute cervical spine injuries  
2343 caused by misdirected impacts within a sporting context. The framework simulates the  
2344 kinematic and kinetic conditions experienced during the injury situations and can help  
2345 in the identification of cause-effect relationships between the injury risk and injury risk  
2346 factors. A musculoskeletal modelling approach was chosen to allow for a more direct  
2347 integration of *in vivo* and *in vitro* experimental data representative of rugby tack-  
2348 ling scenarios. Previous studies investigating sporting head and neck injuries through  
2349 computational methods have either applied initial conditions (i.e. angular velocities,  
2350 muscle activations etc.) that are not highly representative of those experienced in the  
2351 sporting conditions [66, 87] or used passive multibody models that do not provide the  
2352 same physiological validity as musculoskeletal models [140]. The research presented in  
2353 this thesis integrated active musculoskeletal models with accurate experimental data  
2354 to guide biomechanical analyses and theoretical simulation studies. This was crucial  
2355 for the best replication of conditions that represented the applied environment under

investigation and the quality of the results.

2356

The first step to generate an impact-specific musculoskeletal model was to estimate the passive structural parameters that represented the viscoelastic response of intervertebral joints during axial impacts. The use of impact-specific parameters was key to replicate the response of the cervical spine to misdirected rugby impacts in the model. Previous lumped parameters used in models investigating acute neck injuries were not validated against high dynamic axial loading [37, 22, 96]. For this reason porcine cervical spine surrogates were loaded under sub-catastrophic axial impacts and their response was modelled to estimate their joints' viscoelastic properties. Multilevel specimens (C2 to C6) were selected to reduce the effect of experimental constraints on the end segments which has been hypothesised in previous literature. This allowed for two physiologically constrained intervertebral joints (C3-C4 and C4-C5) to be loaded dynamically which accounted for limitations in previous studies that used one or two functional units to investigate the viscoelastic response during static [84, 100] or quasi-static [124] loading. Specimen specific musculoskeletal models of the specimens were created from  $\mu$ CT scans and used in an optimisation procedure to identify joint viscoelastic parameters which were directly validated against the measured experimental kinematics.

2357  
2358  
2359  
2360  
2361  
2362  
2363  
2364  
2365  
2366  
2367  
2368  
2369  
2370  
2371  
2372  
2373

The results showed a large increase in axial stiffness values which was theorised to reflect viscoelastic and poroelastic behaviour of intervertebral discs under impulsive axial loads [34]. Increased compressive stiffness of the intervertebral joints under the large sub-catastrophic impulses ( $F_{max} = 3.0 - 4.8$  kN;  $dt = 5$  ms; Figure 4-4) applied to the specimens was expected as it logically follows results from incremental static [100, 84] and quasi-static [124] loading experiments. These studies have shown that human intervertebral joints display a non-linear increase in stiffness with applied loading. Although the use of porcine specimens in *Chapter 4* of the thesis remains an important consideration their stiffer response to axial impulses was as expected. Ideally human specimens could have been tested and should be considered in future investigations but for the purposes of this research porcine specimens were deemed a fair surrogate as they were tested in a structural rather than a functional manner. The work from *Chapter 4* allowed for the characterisation of cervical spine's structural response to axial impacts using linear lumped parameter viscoelastic elements. The accuracy of the larger axial stiffness values estimated was reflected in the validation stage as when previous literature values were tested model tracking errors increased by over 300% (Table 4.4 - 2<sup>nd</sup> and 4<sup>th</sup> Columns). These parameters can be incorporated in musculoskeletal models to study the response of the entire cervical spine to impacts. Importantly these pa-

2374  
2375  
2376  
2377  
2378  
2379  
2380  
2381  
2382  
2383  
2384  
2385  
2386  
2387  
2388  
2389  
2390  
2391

rameters are directly validated against large axial loads which allows musculoskeletal models to be used in impact analyses with confidence. Musculoskeletal models provide an important link between the analysis of initial experimental data and the use of more sophisticated finite element models for the detailed analysis of spinal structures [154]. Therefore this study provided estimates of lumped parameters that can be used in the development of an active musculoskeletal model for the analysis of cervical spine loading during sporting head impacts. These validated viscoelastic parameters describe the passive structural response of the cervical spine, however to obtain a complete dynamic representation of the cervical spine, estimates of muscle activations and resulting forces are necessary. This is a key step in the investigation of the dynamic response of the neck during impact events.

Estimation of muscle activations representative of those experienced during rugby contact events was a crucial step to generate physiological values of neck muscle forces. Experimental constraints regarding the ethical use of fine-wire EMG methods have prohibited the direct and detailed measurement of deep neck muscle activations during dynamic impact events. Ethical considerations are the primary reason why such studies have not been conducted. As major neurovascular pathways cross the neck and because impacts to the area occur in rugby contact events the use of fine-wire (indwelling) EMG has been limited to static and quasi-static tasks [15, 91]. Additionally limitations of using pure optimisation techniques for the estimation of neck muscle activations during impacts have provided limited understanding of muscle recruitment patterns during these events. Studies have shown that muscle activation estimates are sensitive to the objective criterion (e.g. mechanical or metabolic) chosen in the optimisation procedure [85]. For these reasons, an EMG-assisted optimisation methodology was used to provide the closest physiologically plausible estimation of muscle activations during dynamic *in vivo* experimental rugby tackling and scrummaging trials.

The EMG-assisted methodology combined with a calibrated MRI-informed musculoskeletal model of a rugby player estimated muscle forces that replicated experimental net joint moments in two planes of motion across the cervical spine. This was the first study in the literature to achieve net joint moment equilibrium across multiple neck joint levels. Solutions of muscle forces that generate equilibrium across the entire cervical spine system are important for evaluating intervertebral load transmission and muscle function. Estimation of muscle forces that generate correct net joint moments across all the intervertebral joints they span contribute to the dynamics of the entire cervical spine [37]. This is in contrast to the limited previous studies on the neck that estimate muscle activation and resulting muscle forces that generate moment

equilibrium at a single joint level [27, 28, 146]. These studies have provided accurate estimates of joint moments at a single level however do not consider the effect of the multi-articulate muscles at other joint levels. Estimates of muscle activations that generate single joint equilibrium are highly likely to produce muscle forces that result in discrepant and unreliable joint dynamics at the remaining levels they cross. Generating solutions for muscle force distribution across all the joints a neck muscle spans is important in cervical spine injury analysis as it will influence the propagation of loads down the cervical joints. Additionally, the EMG-assisted methodology replicated experimental neck muscle co-contractions about the cervical spine. Muscle co-contractions represent the stabilising effect of the neck musculature [15] and have been shown to reproduce more accurate joint load estimates than methods that do not include co-contractions. This study thus reproduced experimental net joint moments of the entire cervical spine by accurately estimating muscle activations during dynamic rugby impacts. The knowledge of how neck muscles activate just prior to rugby impacts could now be used to with the passive structural parameters estimated in *Chapter 4* to describe the complete dynamics of the neck during impacts through theoretical simulations.

The final study presented in this thesis aimed to answer the applied questions of what is the primary cervical spine injury mechanism in rugby, and how specific aspects of tackling technique are associated with the internal loads of the spine during misdirected impacts. A computational framework that closely replicated the biomechanical system of a tackler performing a tackle was developed by integrating the structural parameters from *Chapter 4* within the MRI-informed musculoskeletal model of *Chapter 5* and applying rugby tackle specific initial conditions for neck muscle activations, joint kinematics and impact forces. The combination of experimental *in vivo* and *in vitro* kinetic, kinematic and athlete specific data (anatomy, muscle activations and impact forces) generated simulations representative of misdirected tackles. To illustrate this with a more applied example the simulations aimed to replicate a tackler impacting the oncoming ball carrier with their head rather than their shoulder due to improper tackling technique (i.e. wrong positioning of the head and neck) or a misjudged tackling situation (e.g. ball carrier changed direction). The framework therefore closely replicated possible inciting events which is an important course of action for the identification of injury mechanisms [9] and in turn is a crucial component in injury prevention research [45, 149]. Results showed that cranial impacts, representative of “head-on” collisions, and flexed neck angles had the largest effects on maximal compression, anteroposterior shear and flexion moment loads in the lower cervical spine (specifically C5-C6 and C6-C7). Patterns of compression, shear and flexion moment loads dur-

2465 ing cranial impacts supported a previous computational study that also investigated  
2466 cervical spine joint loads with simulations of head-first falls [96]. Intervertebral joint  
2467 loads calculated from the simulations indicated that buckling is the most likely injury  
2468 mechanism that causes anterior bilateral facet dislocations in rugby tackling. Also,  
2469 this study clearly showed that more extended neck posture would reduce intervertebral  
2470 joint loads during misdirected impacts to the head.

### 2471 7.1.1 Contribution to the field of research

2472 The body of work presented in this thesis combined *in vivo*, *in vitro* and *in silico*  
2473 methods to develop novel and expand on existing methodological frameworks in order  
2474 to investigate acute cervical spine injury mechanisms in the applied setting of rugby.  
2475 Although the aims of this thesis were related to rugby the methodologies can be applied  
2476 to other events where high energy impacts to the head occur, such as other contact  
2477 sport and automotive roll-over accidents. Additionally the results of the *Chapter 6*  
2478 add to the quantitative experimental and computational evidence of cervical spine  
2479 buckling during compressive impacts [94, 96]. Overall the main outcome of this thesis  
2480 showed a pattern of decreased intervertebral loading with the neck in a more neutral  
2481 and extended posture. These results indicate the importance of tackling technique to  
2482 position the head and neck on the reduction of injury risk during misdirected rugby  
2483 tackles.

2484 The integration of *in vitro* spinal specimen drop tower testing and *in silico* analysis  
2485 allowed for the first time the estimation of intervertebral joint stiffness and damping  
2486 characteristics of intact cervical spines. The novelty of using spinal specimens with mul-  
2487 tiple intact intervertebral joints (C2-C3 to C5-C6) allowed for the two central joints  
2488 (C3-C4 and C4-C5) to be loaded without the experimental constraints which resulted  
2489 in a more physiological response to the applied load. Previous experimental studies  
2490 investigating intervertebral disc stiffness to compressive loads have used isolated discs  
2491 [84], single [84, 100] or two functional units [124] all of which impose experimental  
2492 end constraints, which are necessary for potting the specimens, directly at the inter-  
2493 vertebral level under investigation. It is possible that previous studies were limited to  
2494 single or two level analyses because of experimental limitations concerning the need to  
2495 mechanically measure joint displacement and applied load simultaneously. By using  
2496 an optimisation procedure and a multi-level spinal specimen in this study (*Chapter*  
2497 *4*) to inversely estimate intervertebral joints' stiffness and damping values previous  
2498 experimental limitations were circumvented. Finally the main outcome of this study  
2499 identified intervertebral joint axial stiffness values that were significantly higher than

previous studies (23100 vs 3924 kN/m) which was caused by the high loading rate applied to the specimens during compressive axial impacts. Further more this results supported previous evidence that loading rates above 75-90 N/s [108, 89] result in similar viscoelastic response of intervertebral discs. This was also shown in the sensitivity analysis where decreases in axial stiffness values of up to 50% of the optimum values did not increase tracking errors.

New neck muscle paths were defined in the musculoskeletal model after muscle volumes were segmented from MRI images of a academy level rugby player. These muscle paths were constrained using geometric wrapping surfaces that expanded on previous work by Vasavada et al. (2008) [151] and included new definitions for the trapezius muscles. The study presented in *Chapter 5* was the first study to create a musculoskeletal model personalised to the neck anatomy of a contact sport athlete. This model was used to estimate neck muscle activations that generated muscle forces resulting in joint moment equilibrium across the cervical spine. This was the first study to apply the EMG-assisted methodology of CEINMS [103] to estimate neck muscle activations across the cervical spine adding to the applicability of this method to the spinal region. Previous studies have been able to solve for muscle forces to generate moment equilibrium at single cervical and lumbar joint levels [6, 27, 28, 82] however the study presented in this thesis has provided a method to estimate the muscle forces across the cervical spine. This an important advancement firstly because muscle force estimates are not overfitted to produce moment equilibrium a single joint level which may produce over or under estimations at other cervical levels. Secondly this provides resulting neck joint forces across the cervical spine which are important for injury mechanism analysis as the affect the structural stability of the spinal column and the propagation of external impact forces.

The final study extended the contribution of this thesis from the field of biomechanics to the more applied area of injury prevention research in sport. A combination of *in vivo* and *in vitro* data was combined to provide the closest representation of possible injurious situations in misdirected rugby tackling. Previous applied research [85, 87, 66] investigating head and neck injuries in sport have applied arbitrary or approximate inputs to musculoskeletal models to simulate injurious situations. For this reason the study of *Chapter 6* created a framework that was used to investigate catastrophic cervical spine injuries and could be used in the future for other head and neck injuries in the field of injury prevention in contact sports and possibly automotive accidents. The results of this study contributed to the clarification that hyperflexion is most likely not the primary cervical spine injury mechanism but buckling that causes

2536 catastrophic injuries during misdirected rugby impacts. Furthermore the results rein-  
 2537 forced the coaching message that a flexed neck posture increases the risk of cervical  
 2538 spine injury during misdirected tackles. These results highlight the importance of cor-  
 2539 rect technique to be taught to players and the need for awareness of the consequences  
 2540 if it is not adopted during these rare high risk events. Finally the biomechanical inves-  
 2541 tigation also reiterates the importance of not bypassing the second stage (identification  
 2542 of injury mechanisms) in injury prevention research such as the van Mechalen [149] and  
 2543 TRIPP [45] models.

## 2544 7.2 Future outlook

2545 Considering the chosen methodologies of the thesis studies and the generated results  
 2546 inherent assumptions and limitations associated from the *in vitro*, *in vivo* and *in silico*  
 2547 methods should be considered. As highlighted in detail within each chapter (*Chapter*  
 2548 *4.5.3*, *Chapter 5.5.1*, *Chapter 6.5.3*) these limitations dictate the range of validity  
 2549 within which the developed models can be used and how conclusions can be drawn  
 2550 from their results. For this reason in each of the comprising chapters of this thesis  
 2551 the developed musculoskeletal models were used within ranges within which they were  
 2552 deemed valid and the results were interpreted considering the limitations of the methods  
 2553 used to generate them.

2554 In *Chapter 4* porcine cervical spine specimens (C2-C6) were used as surrogates to  
 2555 human cadaveric specimens. Although clear anatomical and thus functional differences  
 2556 exist between porcine and human cervical spines, porcine specimens do provide similar  
 2557 material and structural characteristics to humans [20, 116, 158]. The use of porcine  
 2558 or bovine specimens are readily available and provide an added benefit of obtaining  
 2559 a homogeneous sample that is not confounded by effects of degeneration caused by  
 2560 age usually found in human cadaveric samples [108, 95] which under impulsive loading  
 2561 would likely cause variability in specimen response. Additionally in the applied context  
 2562 of catastrophic sporting injuries people that are likely to sustain them are in their  
 2563 second and third decade of life compared to human specimens obtained from cadaveric  
 2564 donors with mean ages of 52 [95] and 87 [59] years old in previous studies. Another  
 2565 consideration in this study was the choice of loading rate applied to the specimens whose  
 2566 dynamic response was used to estimate the intervertebral joints' viscoelastic bushing  
 2567 parameters. During non-injurious drop tower tests cranial loads reached a maximum of  
 2568 4700 N with average loading rates of 800 kN/s over a 5 ms period. These loading rates  
 2569 are considerably higher than previous rates used to investigate the viscoelastic response  
 2570 of intervertebral joints and discs. Race et al. (2000) [108] tested human intervertebral



discs under loading rates of 0.09, 0.9, 9, 90, 900 and 9000 N/s and found no difference 2571  
in the stiffness response of the discs during loading rates above 90 N/s. This was also 2572  
supported by similar tests on bovine discs who did not identify significant differences 2573  
in disc stiffness above loading rates of 75 N/s [89]. For this reason the viscoelastic 2574  
characteristics identified in *Chapter 4* are deemed valid for use in axial impacts above 2575  
1 kN/s, also supported by the sensitivity analysis completed, however their response 2576  
to more eccentric loading should still be explored. 2577

A single participant was used in the study presented in *Chapter 5* where an MRI 2578  
informed musculoskeletal model was created and an EMG-assisted optimisation was 2579  
used to estimate levels of neck muscle activations to obtain cervical joint moment 2580  
equilibrium prior to rugby contacts. The use of a single subject and data collection 2581  
does limit the results of the study in terms of their transferability to a wider population 2582  
of rugby players. To provide a clearer description of the generalised neuromuscular state 2583  
of the neck before rugby impact events would require the application of the methods to 2584  
more than one participant. The aim of the study however was not to provide a general 2585  
description but to be able to extract information of physiologically plausible neck muscle 2586  
activations, and thus forces, in the lead-up and during rugby impacts. These can then 2587  
be used in theoretical simulations to provide internal loading (i.e. neck muscle forces) 2588  
extracted from *in vivo* measurements rather than *a priori* based assumptions. 2589

Similarly in *Chapter 6* the musculoskeletal model used and the initial internal loading 2590  
conditions (i.e. neck muscle activations thus muscle forces) of the forward simulations 2591  
are taken from a single subject (*Chapter 5*). Many intrinsic factors can predispose 2592  
athletes to neck injuries such as the length and the degree of lordosis of their cervical 2593  
spine. Coupled with extrinsic risk factors such as location, direction and magnitude of 2594  
the impact force as well as surface interaction between the two impacting bodies (i.e. 2595  
tackler's head and ball carrier's torso) can lead to a variety of resulting injuries under 2596  
seemingly similar conditions. This has been seen in multiple cadaveric experiments 2597  
with intact cervical spines [95, 59]. The use of the musculoskeletal model in the study 2598  
of *Chapter 6* therefore aimed to provide an understanding of the response of the cervical 2599  
spine to rugby specific impacts by identifying patterns in the resulting intervertebral 2600  
dynamics. Although specific loading tolerances of the neck will vary, which will dictate 2601  
when and where injuries occur, across a population of rugby players it is expected 2602  
the average response will be similar to the identified patterns of this study. For this 2603  
reason the conclusions based on the results of this study regarding the importance of 2604  
correct tackling technique are deemed to be valid. However in order to answer how 2605  
the identified injury mechanism of buckling results specifically into the most commonly 2606

2607 observed anterior bilateral facet dislocations further investigations using finite element  
2608 analyses should be conducted.

2609 The considerations outlined above together with the detailed limitations of each con-  
2610 ducted study in their respective chapters (*Chapter 4.5.3*, *Chapter 5.5.1*, *Chapter 6.5.3*)  
2611 define the range of validity of the model and the transferability of the results. Given  
2612 these considerations the following recommendations are made to build upon the devel-  
2613 oped models and the integrated research framework:

- 2614 • Further investigations should be carried out to gain a more complete understand-  
2615 ing of the multi-segmented cervical spine’s response under dynamic loads. In  
2616 *Chapter 4* porcine specimens were used in a neutral configuration under a single  
2617 impact load. Investigations should be completed with multi-segmented cervical  
2618 spine specimens in different configurations (e.g. flexion or extension) as this has  
2619 been shown to affect the dynamic response of intervertebral joints in the lumbar  
2620 region. Furthermore, application of varying loading rates would help clarify if  
2621 nonlinear descriptions of the intervertebral disc dynamics are necessary to repre-  
2622 sent intervertebral joints in musculoskeletal models under impacts. An additional  
2623 advancement would include a similar analysis with the use of human cadaveric  
2624 specimens. Although use of porcine specimens provides a more homogenous sam-  
2625 ple the different anatomy from that of a human spine may result in different  
2626 dynamic responses. However, for the purposes of injury mechanism analysis the  
2627 benefits of testing human spines might be less apparent during dynamic loading.  
2628 Access to kinetic and kinematic data from studies such as Ivancic (2012) [59] and  
2629 Nightingale et al. (1996) [95] could allow the application of the method presented  
2630 in *Chapter 4* to human cervical spine specimens.
- 2631 • The application of the EMG-assisted optimisation methodology to a cohort of  
2632 rugby players performing tackling and scrummaging trials would identify if the  
2633 recruitment strategies identifies in *Chapter 5* can be generalised to a wider popu-  
2634 lation. Although ethical approval is unlikely to be granted for the measurement  
2635 of detailed EMG during dynamic collision events such as those occurring in rugby,  
2636 the use of this methodology is encouraged for further analysis of existing detailed  
2637 datasets of neck muscle function under static and quasi-static movements. Fu-  
2638 ture studies should begin to focus on the estimation of neck muscle forces that  
2639 produce the required moment equilibrium across the entire cervical spine and not  
2640 a single intervertebral level. These studies will be fundamental in connecting ex-  
2641 perimental and computational methodologies to determine neck muscle function  
2642 during different events.

- Further development of the framework presented in *Chapter 6* would yield a powerful biomechanical tool for head and neck injury prevention research in sport. As wearable sensors become more common during sporting events and accident reconstruction from video analysis more robust, kinematic and kinetic data could be extracted from recorder injurious events and used as input for this framework to directly link field-based activities to resulting clinically observed injuries. A major advancement would be the ability to model the dynamic surface interactions between two colliding players. This would allow external loading conditions (impact forces) and loading constraints (point of application and direction) to be consistent with the relative configuration of the players' body positions, momentum and head positions. The incorporation of finite element methods could be adopted to model the interaction between a player's head and contacting surface during a misdirected impact to the head. Furthermore, outputs from the developed framework could be used to inform boundary conditions for further finite element analyses that provide detailed information of internal load distribution on specific cervical spine structures. The use of finite element models will be crucial in identifying how the identified buckling mechanism translates into injuries observed clinically at the vertebral level.

### 7.3 Conclusion

To summarise, an injury biomechanics framework that integrates experimental and computational methods was developed and used to investigate applied questions relating to cervical spine injuries observed in rugby. The integration of *in vivo* and *in vitro* data within this framework informed *in silico* methodologies which estimated impact specific structural parameters of the cervical spine, muscle activations experienced during rugby contact events, and intervertebral joint loads resulting from misdirected impacts. These results have combined biomechanical theories and methods regarding cervical spine injuries as well as injury prevention analysis to provide a complete biomechanical evaluation of the acute cervical spine injuries observed in rugby tackles.

This thesis has provided evidence that anterior facet dislocations in the lower cervical spine observed in rugby injuries, and specifically during tackling, are most likely a result of a buckling mechanism. This evidence supports the hypothesis put forward by Kuster et al. (2012) [67] that these injuries can be explained through biomechanical injury mechanisms caused by compressive axial loading and not by a hyperflexion mechanism [40]. Therefor it is reiterated that future clinical, biomechanical and epidemiology rugby research should cease to use the term "hyperflexion" for the description of these

2678 catastrophic injuries as it may misguide injury prevention research and the design of  
2679 future interventions in rugby or even other contact sports. A correct understanding of  
2680 the injury mechanism is crucial in an applied context such as the game of rugby because  
2681 the behaviours of players and coaches can directly determine risk factors associated with  
2682 these injuries. For example, the results of *Chapter 6* illustrate the effect of tackling  
2683 technique (related to player behaviour). Simulations showed that during misdirected  
2684 tackles to the head extended neck positions reduced overall intervertebral loads. This  
2685 supports the notion that the effects of playing technique and behaviour should be clear  
2686 to coaches and players to promote the understanding of injury causes and how their  
2687 actions may affect them.

2688 Future investigations into the biomechanics of injuries caused by collapsed scrums  
2689 should be completed by adopting the recommendations made in the previous section  
2690 of this chapter. The scrum as a set-piece is a more controlled environment than a  
2691 tackling (collision) situation, and direct policy and law changes would likely result in  
2692 improvements as have been seen in the past. Finally, as the current focus of injury  
2693 prevention research has shifted toward concussions this thesis has highlighted the im-  
2694 portance of injury biomechanics research, and the second stages of injury prevention  
2695 models (van Mechelen and TRIPP - Figure 1-3), on the mechanistic understanding of  
2696 injuries. A similar approach should be adopted for head injury prevention research  
2697 to gain a holistic understanding of their injury mechanisms in order to present well  
2698 informed intervention strategies reduce injury risk and mitigate unwanted side-effects.

2699 In conclusion, the integrated biomechanical framework developed in this thesis con-  
2700 tributed to the understanding of the aetiology and mechanisms of catastrophic spinal  
2701 injuries in rugby. The framework included new methods that combined experimental  
2702 data together with computational methodologies in order to investigate questions that  
2703 could not be answered solely by experimental or computational investigations. The  
2704 evidence put forward by this thesis supports buckling as the primary injury mechanism  
2705 of anterior bilateral dislocation in the lower cervical spine and that extended neck,  
2706 or "head-up", posture reduces dangerous intervertebral loading of misdirected tackles.  
2707 This body of work provides the first evidence-based biomechanical understanding of  
2708 rugby spinal injuries within an injury prevention model. The results of this work and  
2709 the developed framework can be used to better inform the process of injury prevention  
2710 models in order to provide the best informed decisions regarding head and neck safety  
2711 in the game of rugby and other contact sports.

## Appendix A

2712

## Appendix to Chapter 5

2713

### A.1 Estimation of maximal isometric force and definition of musculoskeletal model wrapping surfaces from MRI measurements

2714

2715

2716

Estimated  $F_{max}^{iso}$  derived from the segmented neck muscle volumes ranged between 60 and 260% of the population specific model values [23] with an average increase of 50% (Figure A-1) . Only rectus capitis posterior minor and obliquus capitis inferior MRI derived values of  $F_{max}^{iso}$  were reduced in relative to the baseline model. The MRI derived estimates of muscle  $F_{max}^{iso}$  were separated into their constituent MTU  $F_{max}^{iso}$  values relative to the baseline model and updated in the EMGaMRI model.

2717

2718

2719

2720

2721

2722

Some sub-regions of the neck musculature, which are defined in the musculoskeletal model as individual muscle-tendon units (MTUs), were not clearly identifiable from the MRI scans, subsequently their  $F_{max}^{iso}$  was scaled proportionally to the total  $F_{max}^{iso}$  of the original model's MTUs that comprised a whole muscle (Figure A-1). Left and right muscle strength was assumed equal in the model thus the average of the MRI derived  $F_{max}^{iso}$  values were prescribed to the MTUs.

2723

2724

2725

2726

2727

2728

The parametric wrapping surfaces included in the updated Rugby Model [23] were defined by measurements taken from segmented MRI imaging of muscle and bone structures whilst guided by methods detailed by Vasavada et al. (2008) [151]. Initially the raw DICOM image stacks were segmented in Mimics (v22, Materialise, Belgium) providing musculoskeletal geometries (from occiput to base of C7) of the front row rugby player in a neutral supine posture. Volume and centroid path measurements

2729

2730

2731

2732

2733

2734

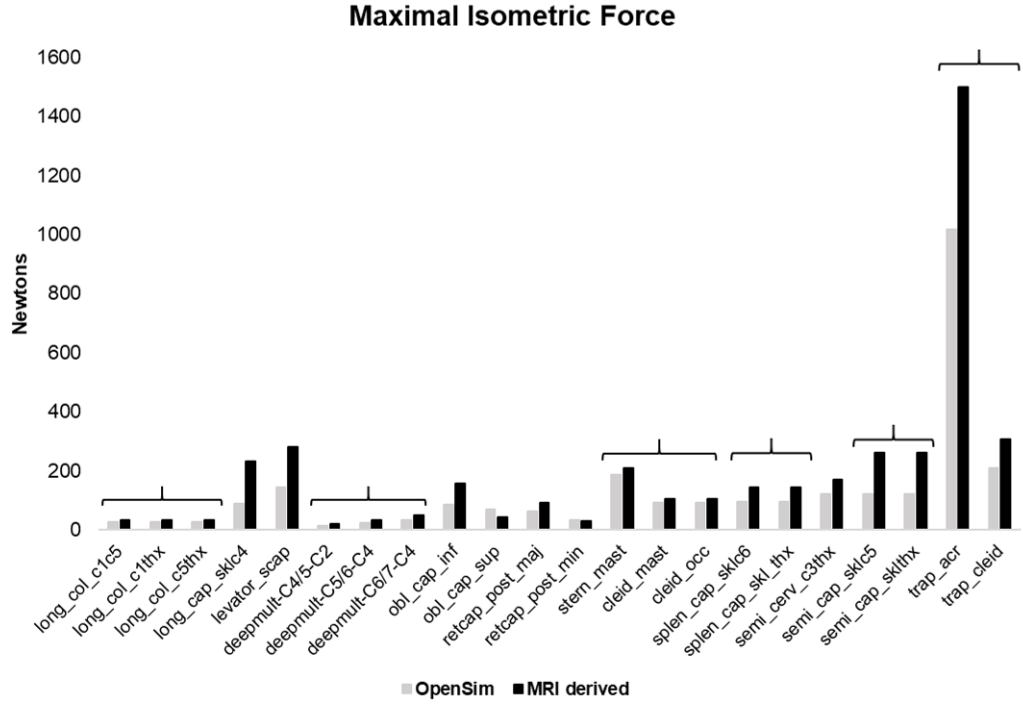


Figure A-1: Changes in model MTU maximal isometric force values ( $F_{max}^{iso}$ ) informed from segmented muscle volumes. Grey bars represent individual MTU  $F_{max}^{iso}$  values and black bars estimated values from MRI information. Multiple MTU under brackets are sub regions of an individual anatomical muscle (e.g. trap\_acr and trap\_cleid are both constituents of the *trapezius*). Naming of MTUs consistent with OpenSim models.

2735 were obtained from the segmented muscles. These data along with the segmented  
 2736 vertebral and skull geometries were then imported into Matlab R2017a (The Mathworks  
 2737 Inc., Natick MA, USA) were the parameters that would define the OpenSim wrapping  
 2738 surfaces could be estimated based on the techniques outlined by Vasavada et al. (2008)  
 2739 [151].

- 2740 • As stated in the main text of the study a single cylinder was defined at the centre  
 2741 of the C6 vertebrae [66]. Other than the identification of the C6 centre of mass  
 2742 the definition of this parametric cylinder was the same as in Kuo et al. (2019)  
 2743 [66].
- 2744 • A sphere was created with its origin located at the centre of mass of the C2  
 2745 vertebrae. Its radius was defined by averaging the shortest distances between  
 2746 the sphere's origin and centroid paths of the left and right *sternocleidomastoid*

muscles [151].

2747

- Two cylinders were defined one the left and one on the right posterolateral aspects 2748  
of the upper vertebral column. Initially the linear path of the of the left and 2749  
right *semispinalis capitis* muscles were recreated on the segmented geometries in 2750  
Matlab by virtually palpating the muscles' insertion on occiput then registering 2751  
the origin of the muscles to those points from the scaled OpenSim model. This 2752  
was initially completed because the thoracic region was not visible in the scans 2753  
and thus could not be virtually palpated in the segmented geometries. After 2754  
this the nearest *semispinalis capitis* centroid point to the C2 centre of mass was 2755  
identified. A perpendicular vector from this location to the linear muscle path 2756  
vector was then calculated that return the radius (magnitude of vector), centre 2757  
(location on linear muscle path vector) and orientation (long axis normal to the 2758  
plane defined by the radius and linear muscle path vectors) of the parametric 2759  
cylinder. The same was completed on both sides and the mean values were used 2760  
in the final model to reduce the effect of measurement errors. 2761
- Two tori were defined one on the left and one on the right posterolateral aspects 2762  
of the lower cervical spine. Their origins were defined from the *trapezius* muscle 2763  
centroid paths. A point of inflection was visually identified and registered to the 2764  
C7 centre of mass. This was the point where the centroid path progressed from a 2765  
mostly parallel path with respect to the transverse plane to a perpendicular path. 2766  
The tori's axes of revolution were aligned with the location of the acromion. The 2767  
same was completed on both sides and the mean values were used in the final 2768  
model to reduce the effect of measurement errors. 2769

The estimated parameters from these procedures were then used to define the para- 2770  
metric wrapping surfaces in OpenSim. Once the wrapping surfaces were defined the 2771  
model was prescribed maximal ranges of motion about single axis and motions com- 2772  
bining multiple axes to assess if muscle paths were stable. This was not the case for all 2773  
surfaces. Manual adjustments in OpenSim were made to the radii and distances of the 2774  
wrapping surfaces to maintain muscle path stability. During these manual adjustments 2775  
care was taken to maintain the original orientations and level of the surfaces in the 2776  
model. 2777

## 2778 A.2 Mapping of experimental excitations to muscle ten- 2779 don unit (MTUs) in CEINMS

2780 As detailed in the main body of the study muscle excitations were either constrained  
2781 or adjusted from measured EMG linear envelopes depending on their function and  
2782 if experimental measurements existed (Table A.1). This mapping was applied in the  
2783 CEINMS analysis of execution trials (Figure 5-2) and in Stage 2 of the calibration  
2784 process (Figure 5-4). During Stage 1 and 3 of the calibration process all excitations  
2785 were constrained to their mapped input signals.

Table A.1: The 96 muscletendon units (MTUs) used in the model with indication to which functional quadrant they were assigned to, experimental excitation signal they received as initial input (SCM = *Sternocleidomastoid* and UT = *Upper Trapezius*), if the mapped excitation signal was constrained (n=10) or adjusted (n=86) during the solution, if wrapping surfaces constrained the MTUs paths and the 44 MTUs'  $F_{max}^{iso}$  were scaled from MRI measurements.

Model Muscles	Functional quadrant	EMG input	Designation	Wrapping surface
cleid_mast	Right flexion	Right SCM	Prescribed	Anterior cylinder and Sphere
cleid_occ	Right flexion	Right SCM	Prescribed	Anterior cylinder and Sphere
stern_mast	Right flexion	Right SCM	Prescribed	Anterior cylinder and Sphere
long_cap_sklc4	Right flexion	Right SCM	Adjusted	N/A
long_col.c1c5	Right flexion	Right SCM	Adjusted	N/A
long_col.c1thx	Right flexion	Right SCM	Adjusted	N/A
long_col.c5thx	Right flexion	Right SCM	Adjusted	N/A
scalenus_ant	Right flexion	Right SCM	Adjusted	N/A
sterno_hyoid	Right flexion	Right SCM	Adjusted	N/A
omo_hyoid	Right flexion	Right SCM	Adjusted	N/A
sternothyroid	Right flexion	Right SCM	Adjusted	N/A
digastric_post	Right flexion	Right SCM	Adjusted	N/A
digastric_ant	Right flexion	Right SCM	Adjusted	N/A
geniohyoid	Right flexion	Right SCM	Adjusted	N/A
mylohyoid_post	Right flexion	Right SCM	Adjusted	N/A
mylohyoid_ant	Right flexion	Right SCM	Adjusted	N/A
stylohyoid_lat	Right flexion	Right SCM	Adjusted	N/A
stylohyoid_med	Right flexion	Right SCM	Adjusted	N/A

*Continued on next page*



Model Muscles	Functional quadrant	EMG input	Designation	Wrapping surface
cleid_mast_l	Left flexion	Left SCM	Prescribed	Anterior cylinder and Sphere
cleid_occ_l	Left flexion	Left SCM	Prescribed	Anterior cylinder and Sphere
stern_mast_l	Left flexion	Left SCM	Prescribed	Anterior cylinder and Sphere
long_cap_sk1c4_l	Left flexion	Left SCM	Adjusted	N/A
long_col_c1c5_l	Left flexion	Left SCM	Adjusted	N/A
long_col_c1thx_l	Left flexion	Left SCM	Adjusted	N/A
long_col_c5thx_l	Left flexion	Left SCM	Adjusted	N/A
scalenus_ant_l	Left flexion	Left SCM	Adjusted	N/A
sterno_hyoid_l	Left flexion	Left SCM	Adjusted	N/A
omo_hyoid_l	Left flexion	Left SCM	Adjusted	N/A
sternothyroid_l	Left flexion	Left SCM	Adjusted	N/A
digastric_post_l	Left flexion	Left SCM	Adjusted	N/A
digastric_ant_l	Left flexion	Left SCM	Adjusted	N/A
geniohyoid_l	Left flexion	Left SCM	Adjusted	N/A
mylohyoid_post_l	Left flexion	Left SCM	Adjusted	N/A
mylohyoid_ant_l	Left flexion	Left SCM	Adjusted	N/A
stylohyoid_lat_l	Left flexion	Left SCM	Adjusted	N/A
stylohyoid_med_l	Left flexion	Left SCM	Adjusted	N/A
trap_acr	Right extension	Right UT	Prescribed	Right torus
trap_cl	Right extension	Right UT	Prescribed	Right torus
deepmult-C4/5-C2	Right extension	Right UT	Adjusted	N/A
deepmult-C5/6-C3	Right extension	Right UT	Adjusted	N/A
deepmult-C6/7-C4	Right extension	Right UT	Adjusted	N/A
deepmult-T1-C5	Right extension	Right UT	Adjusted	N/A
deepmult-T1-C6	Right extension	Right UT	Adjusted	N/A
deepmult-T2-C7	Right extension	Right UT	Adjusted	N/A
iliocost_cerv_c5rib	Right extension	Right UT	Adjusted	N/A
longissi_cap_sk1c6	Right extension	Right UT	Adjusted	N/A
longissi_cerv_c4thx	Right extension	Right UT	Adjusted	N/A
obl_cap_inf	Right extension	Right UT	Adjusted	N/A
obl_cap_sup	Right extension	Right UT	Adjusted	N/A
rectcap_post_maj	Right extension	Right UT	Adjusted	N/A
rectcap_post_min	Right extension	Right UT	Adjusted	N/A
scalenus_med	Right extension	Right UT	Adjusted	N/A
scalenus_post	Right extension	Right UT	Adjusted	N/A
semi_cerv_c3thx	Right extension	Right UT	Adjusted	N/A
supmult-C4/5-C2	Right extension	Right UT	Adjusted	N/A

*Continued on next page*

Model Muscles	Functional quadrant	EMG input	Designation	Wrapping surface
supmult-C5/6-C2	Right extension	Right UT	Adjusted	N/A
supmult-C6/7-C2	Right extension	Right UT	Adjusted	N/A
supmult-T1-C4	Right extension	Right UT	Adjusted	N/A
supmult-T1-C5	Right extension	Right UT	Adjusted	N/A
supmult-T2-C6	Right extension	Right UT	Adjusted	N/A
semi_cap_sklc5	Right extension	Right UT	Adjusted	Right posterior cylinder
semi_cap_skltlx	Right extension	Right UT	Adjusted	Right posterior cylinder
splen_cap_sklc6	Right extension	Right UT	Adjusted	Right posterior cylinder
splen_cap_skltlx	Right extension	Right UT	Adjusted	N/A
splen_cerv_c3thx	Right extension	Right UT	Adjusted	N/A
levator_scap	Right extension	Right UT	Adjusted	N/A
trap_acr.l	Left extension	Left UT	Prescribed	Left torus
trap_cl.l	Left extension	Left UT	Prescribed	Left torus
deepmult-C4/5-C2.l	Left extension	Left UT	Adjusted	N/A
deepmult-C5/6-C3.l	Left extension	Left UT	Adjusted	N/A
deepmult-C6/7-C4.l	Left extension	Left UT	Adjusted	N/A
deepmult-T1-C5.l	Left extension	Left UT	Adjusted	N/A
deepmult-T1-C6.l	Left extension	Left UT	Adjusted	N/A
deepmult-T2-C7.l	Left extension	Left UT	Adjusted	N/A
iliocost_cerv_c5rib.l	Left extension	Left UT	Adjusted	N/A
longissi_cap_sklc6.l	Left extension	Left UT	Adjusted	N/A
longissi_cerv_c4thx.l	Left extension	Left UT	Adjusted	N/A
obl_cap_inf.l	Left extension	Left UT	Adjusted	N/A
obl_cap_sup.l	Left extension	Left UT	Adjusted	N/A
rectcap_post_maj.l	Left extension	Left UT	Adjusted	N/A
rectcap_post_min.l	Left extension	Left UT	Adjusted	N/A
scalenus_med.l	Left extension	Left UT	Adjusted	N/A
scalenus_post.l	Left extension	Left UT	Adjusted	N/A
semi_cerv_c3thx.l	Left extension	Left UT	Adjusted	N/A
supmult-C4/5-C2.l	Left extension	Left UT	Adjusted	N/A
supmult-C5/6-C2.l	Left extension	Left UT	Adjusted	N/A
supmult-C6/7-C2.l	Left extension	Left UT	Adjusted	N/A
supmult-T1-C4.l	Left extension	Left UT	Adjusted	N/A
supmult-T1-C5.l	Left extension	Left UT	Adjusted	N/A
supmult-T2-C6.l	Left extension	Left UT	Adjusted	N/A
semi_cap_sklc5.l	Left extension	Left UT	Adjusted	Left posterior cylinder

*Continued on next page*

Model Muscles	Functional quadrant	EMG input	Designation	Wrapping surface
semi_cap_sklthx_l	Left extension	Left UT	Adjusted	Left posterior cylinder
splen_cap_sklc6_l	Left extension	Left UT	Adjusted	Left posterior cylinder
splen_cap_sklthx_l	Left extension	Left UT	Adjusted	N/A
splen_cerv_c3thx_l	Left extension	Left UT	Adjusted	N/A
levator_scap_l	Left extension	Left UT	Adjusted	N/A

## 2786 **Appendix B**

## 2787 **Appendix to Chapter 6**

### 2788 **B.1 Supplementary results**

2789 This appendix include supplementary results of maximal flexion moments during cra-  
2790 nial impacts (Figure B-1) (CP, CC and CA) as well as maximal compressive, antero-  
2791 posterior shear and flexion moment loads during lateral impacts (LP, LMP, LMA and  
2792 LA).

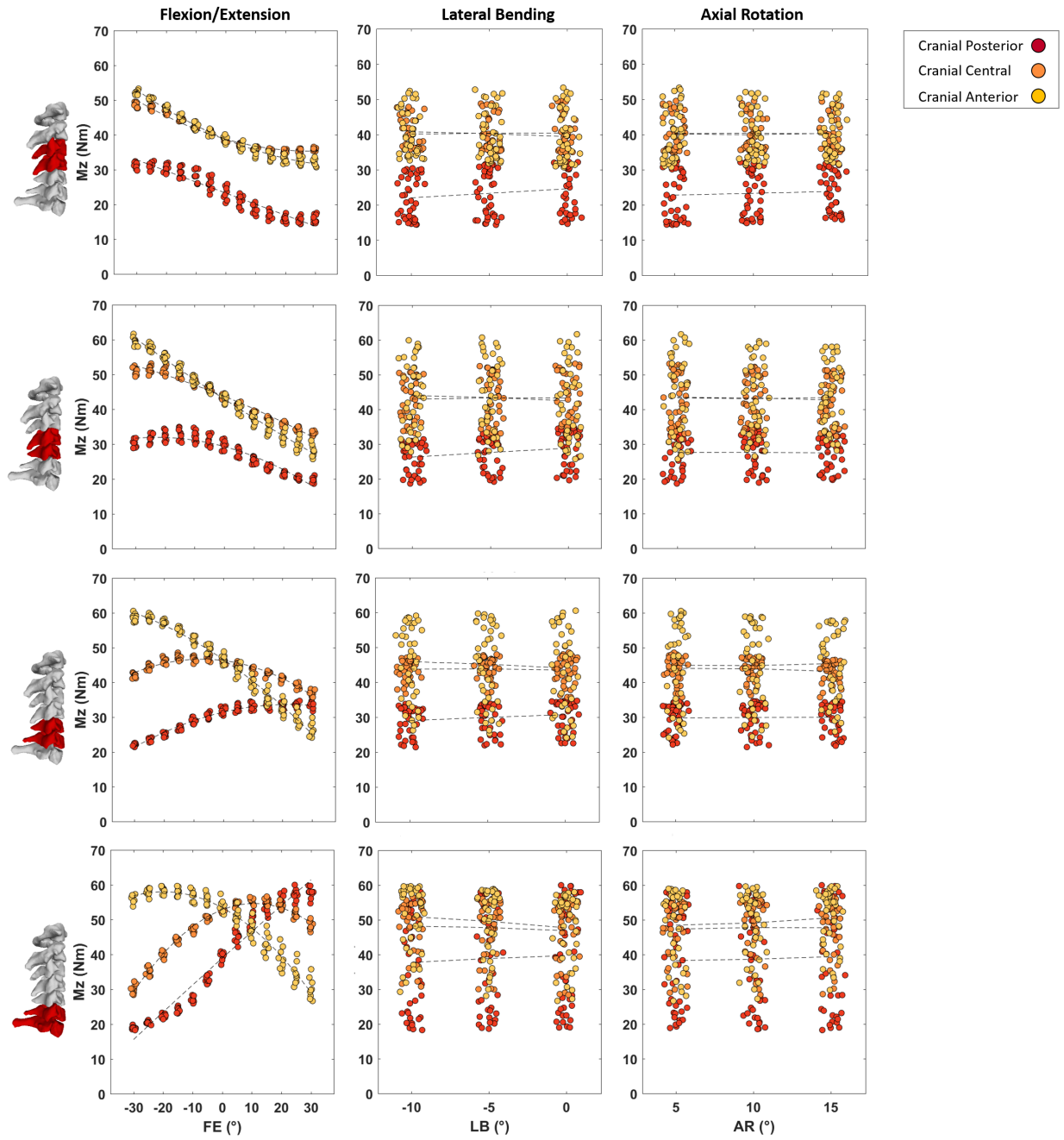


Figure B-1: Maximal flexion moment joint loads (Newton-meter) of C3-C4 (top row) to C6-C7 (bottom row) intervertebral joints plotted against  $5^\circ$  changes in Flexion(-)/Extension(+) (left column), Lateral Bending (centre column) and Axial Rotation (right column) during the cranial loading conditions (Cranial Posterior, Cranial Central and Cranial Anterior). In each subplot data points are spread slightly in each  $5^\circ$  bin on the horizontal axes for better visualisation.

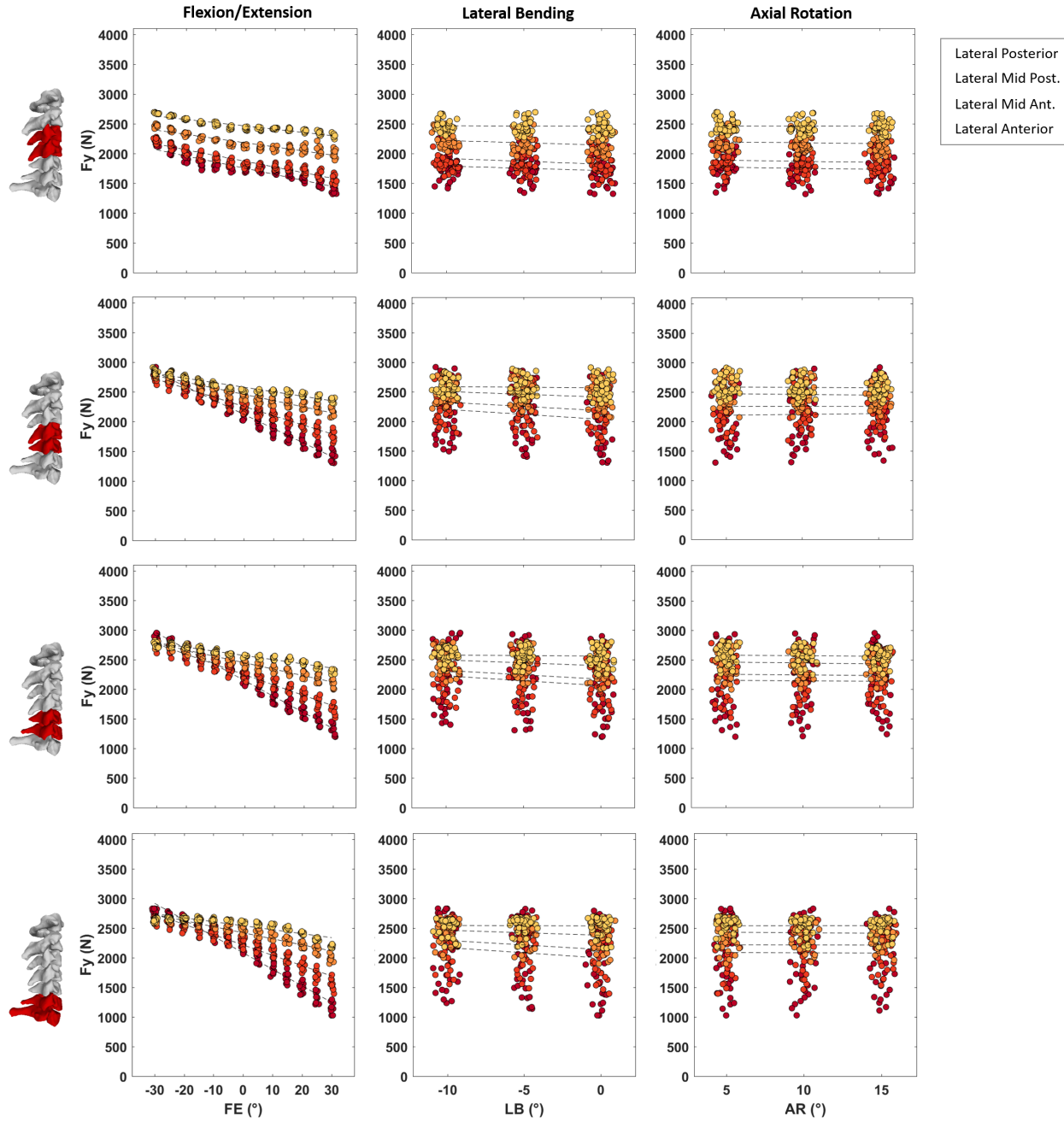


Figure B-2: Maximal compressive joint loads (Newton) of C3-C4 (top row) to C6-C7 (bottom row) intervertebral joints plotted against  $5^\circ$  changes in Flexion(-)/Extension(+) (left column), Lateral Bending (centre column) and Axial Rotation (right column) during the cranial loading conditions (Lateral Posterior, Lateral Mid Posterior, Lateral Mid Anterior and Lateral Anterior). In each subplot data points are spread slightly in each  $5^\circ$  bin on the horizontal axes for better visualisation.

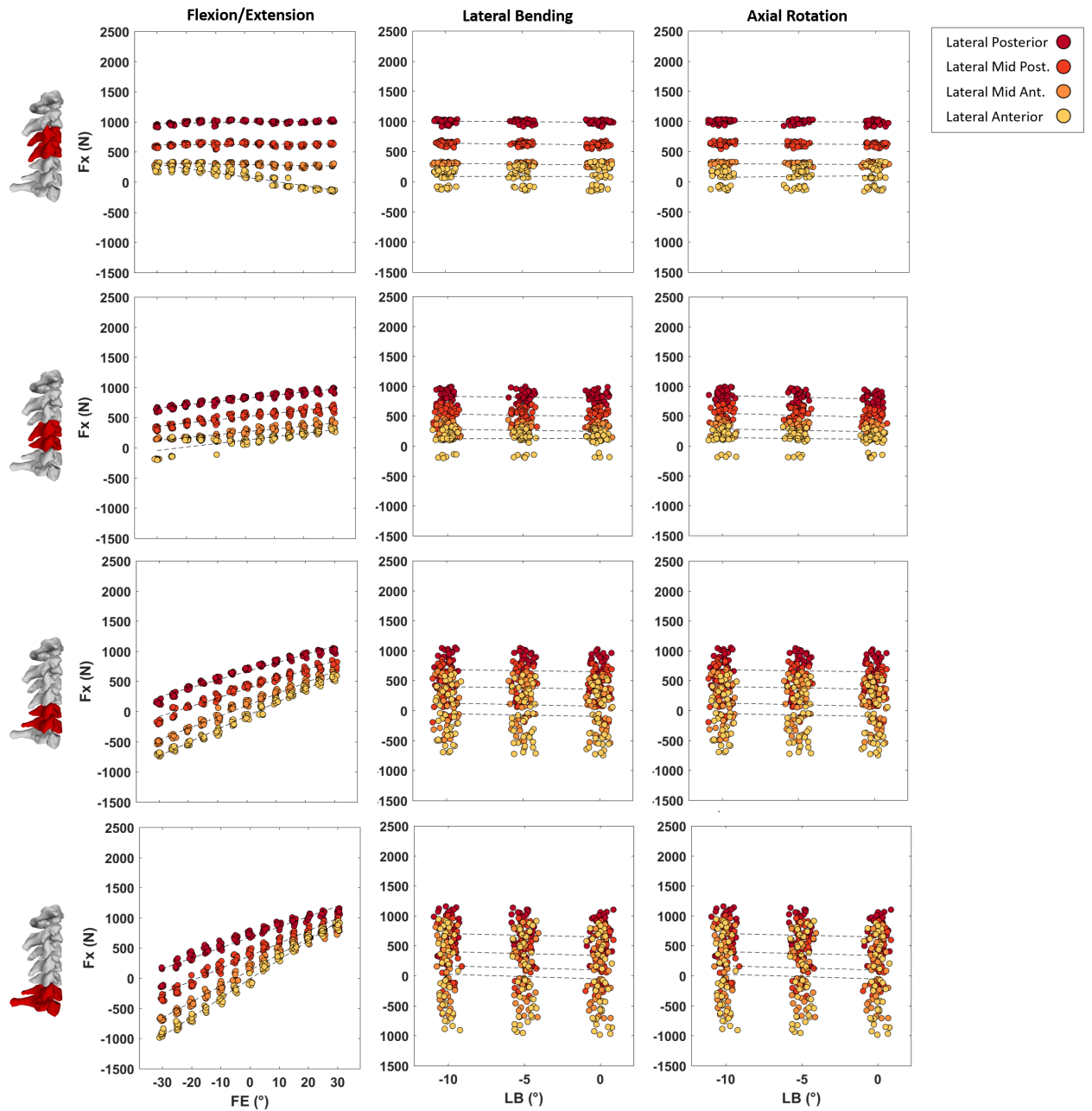


Figure B-3: Maximal anteroposterior shear joint loads (Newton) of C3-C4 (top row) to C6-C7 (bottom row) intervertebral joints plotted against  $5^\circ$  changes in Flexion(-)/Extension(+) (left column), Lateral Bending (centre column) and Axial Rotation (right column) during the cranial loading conditions (Lateral Posterior, Lateral Mid Posterior, Lateral Mid Anterior and Lateral Anterior). In each subplot data points are spread slightly in each  $5^\circ$  bin on the horizontal axes for better visualisation.

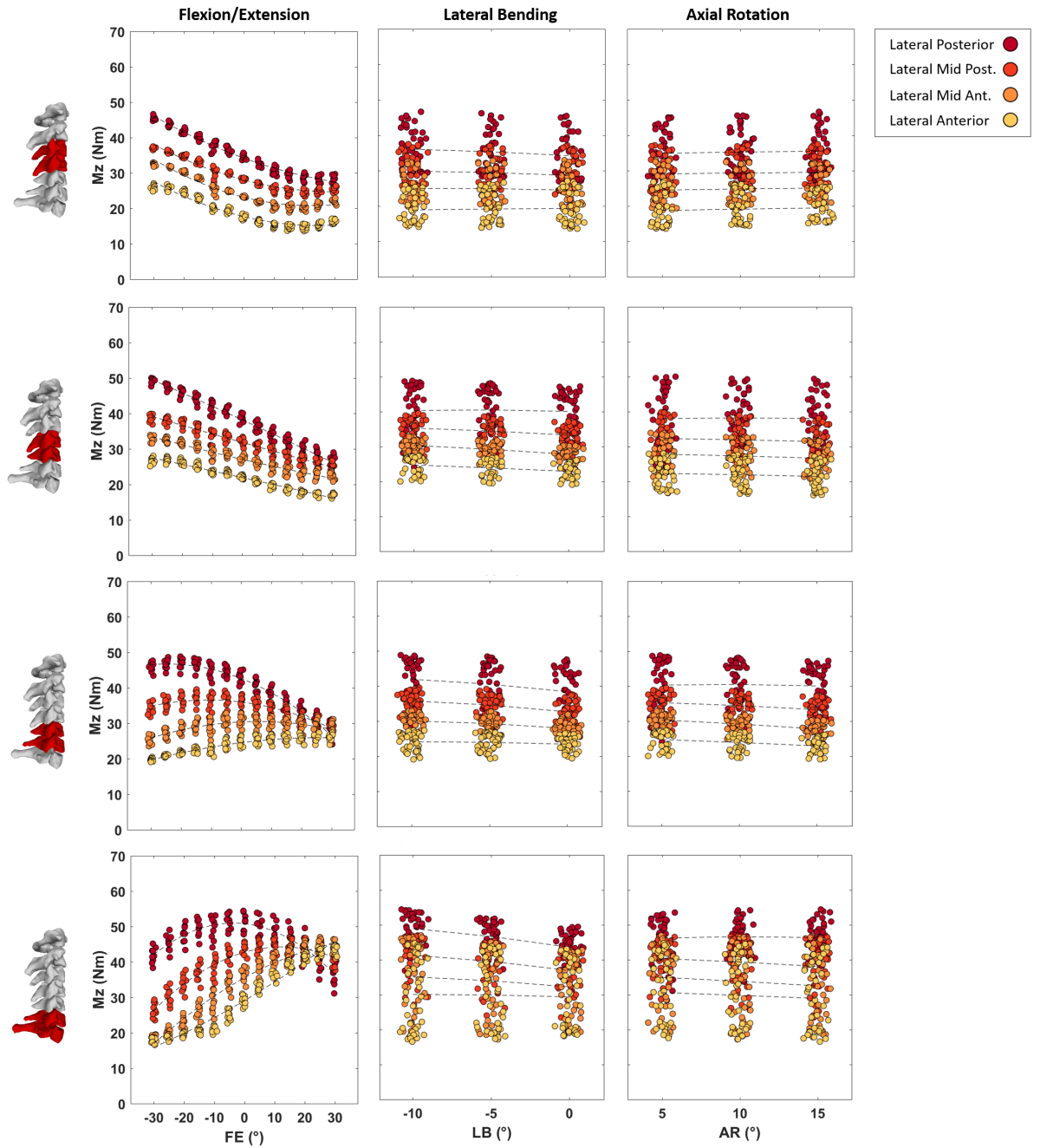


Figure B-4: Maximal flexion moment joint loads (Newton-meter) of C3-C4 (top row) to C6-C7 (bottom row) intervertebral joints plotted against 5° changes in Flexion(-)/Extension(+) (left column), Lateral Bending (centre column) and Axial Rotation (right column) during the cranial loading conditions (Lateral Posterior, Lateral Mid Posterior, Lateral Mid Anterior and Lateral Anterior). In each subplot data points are spread slightly in each 5° bin on the horizontal axes for better visualisation.



# Bibliography

2793

- [1] A. Ackery, C. Tator, and A. Krassioukov. A global perspective on spinal cord 2794  
injury epidemiology. *Journal of Neurotrauma*, 21:1355–1370, 2004. 2795
- [2] D. C. Ackland, Y.-C. Lin, and M. G. Pandy. Sensitivity of model predictions of 2796  
muscle function to changes in moment arms and muscle–tendon properties: A 2797  
monte-carlo analysis. *Journal of Biomechanics*, 45(8):1463–1471, 2012. 2798
- [3] D. C. Ackland, J. S. Merritt, and M. G. Pandy. Moment arms of the human neck 2799  
muscles in flexion, bending and rotation. *Journal of Biomechanics*, 44(3):475– 2800  
486, 2011. 2801
- [4] M. Alizadeh, G. G. Knapik, P. Mageswaran, E. Mendel, E. Bourekas, and W. S. 2802  
Marras. Biomechanical musculoskeletal models of the cervical spine: A systematic 2803  
literature review. *Clinical Biomechanics*, 71:115–124, 2020. 2804
- [5] J. Ambrósio and P. Verissimo. Improved bushing models for general multibody 2805  
systems and vehicle dynamics. *Multibody System Dynamics*, 22(4):341, 2009. 2806
- [6] N. Arjmand, D. Gagnon, A. Plamondon, A. Shirazi-Adl, and C. Larivière. A com- 2807  
parative study of two trunk biomechanical models under symmetric and asym- 2808  
metric loadings. *Journal of Biomechanics*, 43(3):485–491, 2010. 2809
- [7] J. Au, D. M. Perriman, M. R. Pickering, G. Buirski, P. N. Smith, and A. L. Webb. 2810  
Magnetic resonance imaging atlas of the cervical spine musculature. *Clinical* 2811  
*Anatomy*, 29(5):643–659, 2016. 2812
- [8] M. Badenhorst, E. Verhagen, M. I. Lambert, W. van Mechelen, and J. C. Brown. 2813  
‘in a blink of an eye your life can change’: experiences of players sustaining a 2814  
rugby-related acute spinal cord injury. *Injury Prevention*, 25(4):313–320, 2019. 2815

- 2816 [9] R. Bahr and T. Krosshaug. Understanding injury mechanisms: a key component  
2817 of preventing injuries in sport. *British Journal of Sports Medicine*, 39(6):324–329,  
2818 2005.
- 2819 [10] A. E. Bauman, J. J. McPhee, and P. H. Calamai. Application of genetic algorithms  
2820 to the design optimization of an active vehicle suspension system. *Computer  
2821 Methods in Applied Mechanics and Engineering*, 163(1):87–94, 1998.
- 2822 [11] R. J. Bauze and G. M. Ardran. Experimental production of forward dislocation  
2823 in the human cervical spine. *Journal of Bone Joint Surgery Br*, 60-b(2):239–45,  
2824 1978.
- 2825 [12] N. Bernstein. *The co-ordination and regulation of movements*. Pergamon Press,  
2826 Oxford, 1967.
- 2827 [13] S. S. Blemker, D. S. Asakawa, G. E. Gold, and S. L. Delp. Image-based muscu-  
2828 loskeletal modeling: Applications, advances, and future opportunities. *Journal  
2829 of Magnetic Resonance Imaging*, 25(2):441–451, 2007.
- 2830 [14] S. S. Blemker and S. L. Delp. Three-dimensional representation of complex muscle  
2831 architectures and geometries. *Annals of Biomedical Engineering*, 33(5):661–673,  
2832 2005.
- 2833 [15] J.-S. Blouin, G. P. Siegmund, M. G. Carpenter, and J. T. Inglis. Neural control  
2834 of superficial and deep neck muscles in humans. *Journal of Neurophysiology*,  
2835 98(2):920–928, 2007.
- 2836 [16] D. Brauge, C. Delpierre, P. Adam, J. C. Sol, P. Bernard, and F.-E. Roux. Clinical  
2837 and radiological cervical spine evaluation in retired professional rugby players.  
2838 *Journal of Neurosurgery*, 23(5):551, 2015.
- 2839 [17] J. H. M. Brooks, C. W. Fuller, S. P. T. Kemp, and D. B. Reddin. Epidemiology  
2840 of injuries in english professional rugby union: part 1 match injuries. *British  
2841 Journal of Sports Medicine*, 39(10):757, 2005.
- 2842 [18] J. C. Brown, M. I. Lambert, E. Verhagen, C. Readhead, W. van Mechelen, and  
2843 W. Viljoen. The incidence of rugby-related catastrophic injuries (including car-  
2844 diac events) in south africa from 2008 to 2011: a cohort study. *BMJ Open*, 3(2),  
2845 2013.
- 2846 [19] J. C. Brown, M. I. Lambert, E. Verhagen, C. Readhead, W. van Mechelen, and  
2847 W. Viljoen. The incidence of rugby-related catastrophic injuries (including car-

- diac events) in south africa from 2008 to 2011: a cohort study. *BMJ Open*, 3(2):e002475, 2013.
- [20] I. Busscher, J. J. W. Ploegmakers, G. J. Verkerke, and A. G. Veldhuizen. Comparative anatomical dimensions of the complete human and porcine spine. *European Spine Journal*, 19(7):1104–1114, 2010.
- [21] D. L. Camacho, R. W. Nightingale, J. J. Robinette, S. K. Vanguri, D. J. Coates, and B. S. Myers. Experimental flexibility measurements for the development of a computational head-neck model validated for near-vertex head impact. *SAE Transactions*, 106, 1997.
- [22] D. L. A. Camacho, R. W. Nightingale, and B. S. Myers. The influence of surface padding properties on head and neck injury risk. *Journal of Biomechanical Engineering*, 123(5):432–439, 2001.
- [23] D. Cazzola, T. P. Holsgrove, E. Preatoni, H. S. Gill, and G. Trewartha. Cervical spine injuries: A whole-body musculoskeletal model for the analysis of spinal loading. *PLoS One*, 12(1):e0169329, 2017.
- [24] D. Cazzola, E. Preatoni, K. A. Stokes, M. E. England, and G. Trewartha. A modified prebind engagement process reduces biomechanical loading on front row players during scrummaging: a cross-sectional study of 11 elite teams. *British Journal of Sports Medicine*, 2014.
- [25] D. Cazzola, B. Stone, T. P. Holsgrove, G. Trewartha, and E. Preatoni. Spinal muscle activity in simulated rugby union scrummaging is affected by different engagement conditions. *Journal of Medicine and Science in Sports*, 26(1600-0838 (Electronic)), 2016.
- [26] V. C. Chancey, R. W. Nightingale, C. A. Van Ee, K. E. Knaub, and B. S. Myers. Improved estimation of human neck tensile tolerance: reducing the range of reported tolerance using anthropometrically correct muscles and optimized physiologic initial conditions. *Stapp Car Crash J*, 47:135–53, 2003.
- [27] C.-H. Cheng, A. Chien, W.-L. Hsu, C. P.-C. Chen, and H.-Y. K. Cheng. Investigation of the differential contributions of superficial and deep muscles on cervical spinal loads with changing head postures. *PLOS ONE*, 11(3):e0150608, 2016.
- [28] H. Choi. Quantitative assessment of co-contraction in cervical musculature. *Medical Engineering and Physics*, 25(2):133–140, 2003.

- 2880 [29] J. Cholewicki and S. M. McGill. Emg assisted optimization: A hybrid approach  
2881 for estimating muscle forces in an indeterminate biomechanical model. *Journal*  
2882 *of Biomechanics*, 27(10):1287–1289, 1994.
- 2883 [30] J. Cholewicki, S. M. McGill, and R. W. Norman. Comparison of muscle forces and  
2884 joint load from an optimization and emg assisted lumbar spine model: Towards  
2885 development of a hybrid approach. *Journal of Biomechanics*, 28(3):321–331, 1995.
- 2886 [31] M. Christophy, M. Curtin, N. A. F. Senan, J. C. Lotz, and O. M. O’Reilly. On the  
2887 modeling of the intervertebral joint in multibody models for the spine. *Multibody*  
2888 *System Dynamics*, 30(4):413–432, 2013.
- 2889 [32] P. Cignoni, M. Callieri, M. Corsini, M. Dellepiane, F. Ganovelli, and  
2890 G. Ranzuglia. Meshlab: an open-source mesh processing tool. In *Eurograph-*  
2891 *ics Italian Chapter Conference*.
- 2892 [33] M. A. Correia, S. D. McLachlin, and D. S. Cronin. Optimization of muscle  
2893 activation schemes in a finite element neck model simulating volunteer frontal  
2894 impact scenarios. *Journal of Biomechanics*, page 109754, 2020.
- 2895 [34] J. J. Costi, A. I. Stokes, G. M. Gardner-Morse, and C. J. Iatridis. Frequency-  
2896 dependent behavior of the intervertebral disc in response to each of six degree  
2897 of freedom dynamic loading: Solid phase and fluid phase contributions. *Spine*,  
2898 33(16):1731–1738, 2008.
- 2899 [35] R. A. Cripps, B. B. Lee, P. Wing, E. Weerts, J. Mackay, and D. Brown. A  
2900 global map for traumatic spinal cord injury epidemiology: towards a living data  
2901 repository for injury prevention. *Spinal Cord*, 49:493, 2010.
- 2902 [36] G. Davico, C. Pizzolato, D. G. Lloyd, S. J. Obst, H. P. J. Walsh, and C. P.  
2903 Carty. Increasing level of neuromusculoskeletal model personalisation to investi-  
2904 gate joint contact forces in cerebral palsy: A twin case study. *Clinical Biome-*  
2905 *chanics*, 72:141–149, 2020.
- 2906 [37] E. de Bruijn, F. C. T. van der Helm, and R. Happee. Analysis of isometric cervical  
2907 strength with a nonlinear musculoskeletal model with 48 degrees of freedom.  
2908 *Multibody System Dynamics*, 36(4):339–362, 2016.
- 2909 [38] M. de Zee, D. Falla, D. Farina, and J. Rasmussen. A detailed rigid-body cervical  
2910 spine model based on inverse dynamics. *Journal of Biomechanics*, 40:S284, 2007.

- [39] S. L. Delp, F. C. Anderson, A. S. Arnold, P. Loan, A. Habib, C. T. John, E. Guendelman, and D. G. Thelen. Opensim: Open-source software to create and analyze dynamic simulations of movement. *IEEE Transactions on Biomedical Engineering*, 54(11):1940–1950, 2007.
- [40] C. R. Dennison, E. M. Macri, and P. A. Crompton. Mechanisms of cervical spine injury in rugby union: is it premature to abandon hyperflexion as the main mechanism underpinning injury? *British Journal of Sports Medicine*, 46(8):545, 2012.
- [41] A. T. Dibb, C. A. Cox, R. W. Nightingale, J. F. Luck, H. C. Cutcliffe, B. S. Myers, K. B. Arbogast, T. Seacrist, and C. R. Bass. Importance of muscle activations for biofidelic pediatric neck response in computational models. *Traffic Injury Prevention*, 14:116–127, 2013.
- [42] A. Falisse, G. Serrancolí, C. L. Dembia, J. Gillis, I. Jonkers, and F. D. Groote. Rapid predictive simulations with complex musculoskeletal models suggest that diverse healthy and pathological human gaits can emerge from similar control strategies. *Journal of The Royal Society Interface*, 16(157):20190402, 2019.
- [43] J. B. Fice, D. S. Cronin, and M. B. Panzer. Cervical spine model to predict capsular ligament response in rear impact. *Annals of Biomedical Engineering*, 39(8):2152–62, 2011.
- [44] J. B. Fice, G. P. Siegmund, and J.-S. Blouin. Neck muscle biomechanics and neural control. *Journal of Neurophysiology*, 120(1):361–371, 2018.
- [45] C. Finch. A new framework for research leading to sports injury prevention. *Journal of Science and Medicine in Sport*, 9(1):3–9, 2006.
- [46] D. D. French, R. R. Campbell, S. Sabharwal, A. L. Nelson, P. A. Palacios, and D. Gavin-Dreschnack. Health care costs for patients with chronic spinal cord injury in the veterans health administration. *The Journal of Spinal Cord Medicine*, 30(5):477–481, 2007.
- [47] C. W. Fuller. Catastrophic injury in rugby union. *Sports Medicine*, 38(12):975–986, 2008.
- [48] C. W. Fuller, T. Ashton, J. H. M. Brooks, R. J. Cancea, J. Hall, and S. P. T. Kemp. Injury risks associated with tackling in rugby union. *British Journal of Sports Medicine*, 44(3):159, 2010.

- 2943 [49] D. Gagnon, N. Arjmand, A. Plamondon, A. Shirazi-Adl, and C. Larivière. An  
2944 improved multi-joint emg-assisted optimization approach to estimate joint and  
2945 muscle forces in a musculoskeletal model of the lumbar spine. *Journal of Biome-*  
2946 *chanics*, 44(8):1521–1529, 2011.
- 2947 [50] P. Halldin and K. Brodin. Investigation of conditions that affect neck compression-  
2948 flexion injuries using numerical techniques. In *44th Stapp Car Crash Conference*  
2949 *(2000)*. The Stapp Association, nov 2000.
- 2950 [51] R. Happee, E. de Bruijn, P. A. Forbes, and F. C. T. van der Helm. Dynamic head-  
2951 neck stabilization and modulation with perturbation bandwidth investigated us-  
2952 ing a multisegment neuromuscular model. *Journal of Biomechanics*, 58:203–211,  
2953 2017.
- 2954 [52] T. L. Heiden, D. G. Lloyd, and T. R. Ackland. Knee joint kinematics, kinetics and  
2955 muscle co-contraction in knee osteoarthritis patient gait. *Clinical Biomechanics*,  
2956 24(10):833–841, 2009.
- 2957 [53] S. Hendricks, D. Karpul, and M. Lambert. Momentum and kinetic energy before  
2958 the tackle in rugby union. *Journal of sports science and medicine*, 13(3):557,  
2959 2014.
- 2960 [54] J. L. Hicks, T. K. Uchida, A. Seth, A. Rajagopal, and S. L. Delp. Is my model  
2961 good enough? best practices for verification and validation of musculoskeletal  
2962 models and simulations of movement. *Journal of Biomechanical Engineering*,  
2963 137(2):020905–020905–24, 2015.
- 2964 [55] H. X. Hoang, L. E. Diamond, D. G. Lloyd, and C. Pizzolato. A calibrated  
2965 emg-informed neuromusculoskeletal model can appropriately account for muscle  
2966 co-contraction in the estimation of hip joint contact forces in people with hip  
2967 osteoarthritis. *Journal of Biomechanics*, 83:134–142, 2019.
- 2968 [56] V. R. Hodgson and L. M. Thomas. Mechanisms of cervical spine injury during  
2969 impact to the protected head. *SAE Transactions*, pages 3792–3805, 1980.
- 2970 [57] T. P. Holsgrove, D. Cazzola, E. Preatoni, G. Trewartha, A. W. Miles, H. S. Gill,  
2971 and S. Gheduzzi. An investigation into axial impacts of the cervical spine using  
2972 digital image correlation. *The Spine Journal*, 15(8):1856–1863, 2015.
- 2973 [58] J. Hu, K. H. Yang, C. C. Chou, and A. I. King. A numerical investigation of  
2974 factors affecting cervical spine injuries during rollover crashes. *Spine*, 33(23),  
2975 2008.

- [59] P. C. Ivancic. Biomechanics of sports-induced axial-compression injuries of the neck. *Journal of Athletic Training*, 47(5):489–497, 2012.
- [60] P. C. Ivancic. Cervical spine instability following axial compression injury: A biomechanical study. *Orthopaedics and Traumatology: Surgery and Research*, 100(1):127–133, 2014.
- [61] M. Jager, de. *Mathematical head-neck models for acceleration impacts*. Thesis, 1996.
- [62] G. Jefferson. Fracture of the atlas vertebra. report of four cases, and a review of those previously recorded. *BJS (British Journal of Surgery)*, 7(27):407–422, 1919.
- [63] N. Karajan, O. Rohrlé, W. Ehlers, and S. Schmitt. Linking continuous and discrete intervertebral disc models through homogenisation. *Biomech Model Mechanobiol*, 12(3):453–66, 2013.
- [64] T. Kawasaki, Y. Tanabe, H. Tanaka, K. Murakami, N. Maki, H. Ozaki, D. Hirayama, M. Kunda, K. Nobuhara, T. Okuwaki, and K. Kaneko. Kinematics of rugby tackling: A pilot study with 3-dimensional motion analysis. *The American Journal of Sports Medicine*, 46(10):2514–2520, 2018.
- [65] A. Kian, C. Pizzolato, M. Halaki, K. Ginn, D. Lloyd, D. Reed, and D. Ackland. Static optimization underestimates antagonist muscle activity at the glenohumeral joint: a musculoskeletal modeling study. *Journal of Biomechanics*, page 109348, 2019.
- [66] C. Kuo, J. Sheffels, M. Fanton, B. Yu Ina, R. Hamalainen, and D. Camarillo. Passive cervical spine ligaments provide stability during head impacts. *Journal of The Royal Society Interface*, 16(154):20190086, 2019.
- [67] D. Kuster, A. Gibson, R. Abboud, and T. Drew. Mechanisms of cervical spine injury in rugby union: a systematic review of the literature. *Br J Sports Med*, 46(8):550–4, 2012.
- [68] M. Latash. There is no motor redundancy in human movements. there is motor abundance. *Motor Control*, 4(3):259–60, 2000.
- [69] M. L. Latash. The bliss (not the problem) of motor abundance (not redundancy). *Experimental Brain Research*, 217(1):1–5, 2012.

- 3007 [70] R. Ledesma, Z. D. Ma, G. Hulbert, and A. Wineman. A nonlinear viscoelastic  
3008 bushing element in multibody dynamics. *Computational Mechanics*, 17(5):287–  
3009 296, 1996.
- 3010 [71] B. B. Lee, R. A. Cripps, M. Fitzharris, and P. C. Wing. The global map for  
3011 traumatic spinal cord injury epidemiology: update 2011, global incidence rate.  
3012 *Spinal Cord*, 52(2):110, 2013.
- 3013 [72] D. G. Lloyd and T. F. Besier. An emg-driven musculoskeletal model to esti-  
3014 mate muscle forces and knee joint moments in vivo. *Journal of Biomechanics*,  
3015 36(6):765–776, 2003.
- 3016 [73] S. L. Lopes, E. Seminati, and C. Dario. Contact parameters for rugby tackling  
3017 simulations. European Society of Biomechanics, July 2017.
- 3018 [74] D. McDaid, A. L. Park, A. Gall, M. Purcell, and M. Bacon. Understanding and  
3019 modelling the economic impact of spinal cord injuries in the united kingdom.  
3020 *Spinal Cord*, 57(9):778–788, 2019.
- 3021 [75] S. McGill, D. Juker, and P. Kropf. Appropriately placed surface emg electrodes  
3022 reflect deep muscle activity (psoas, quadratus lumborum, abdominal wall) in the  
3023 lumbar spine. *Journal of Biomechanics*, 29(11):1503–1507, 1996.
- 3024 [76] H. J. Mertz and L. M. Patrick. Investigation of the kinematics and kinetics of  
3025 whiplash. *SAE Transactions*, 76:2952–2980, 1968.
- 3026 [77] H. J. Mertz and L. M. Patrick. Strength and response of the human neck. *SAE*  
3027 *Transactions*, 80:2903–2928, 1971.
- 3028 [78] M. Millard, T. Uchida, A. Seth, and S. L. Delp. Flexing computational muscle:  
3029 Modeling and simulation of musculotendon dynamics. *Journal of Biomechanical*  
3030 *Engineering*, 135(2), 2013.
- 3031 [79] L. Modenese, E. Ceseracciu, M. Reggiani, and D. G. Lloyd. Estimation of muscu-  
3032 lotendon parameters for scaled and subject specific musculoskeletal models using  
3033 an optimization technique. *Journal of Biomechanics*, 49(2):141–148, 2016.
- 3034 [80] L. Modenese, E. Montefiori, A. Wang, S. Wesarg, M. Viceconti, and C. Mazzà.  
3035 Investigation of the dependence of joint contact forces on musculotendon param-  
3036 eters using a codified workflow for image-based modelling. *Journal of Biome-*  
3037 *chanics*, 73:108–118, 2018.



- [81] T. B. Moeller and E. Reif. *Pocket Atlas of Sectional Anatomy. Computer Tomography and Magnetic Resonance Imaging*, volume Volume 3. Spine, Extremities, Joints. Thieme, Germany, 2007. 3038 3039 3040
- [82] D. D. Molinaro, A. S. King, and A. J. Young. Biomechanical analysis of common solid waste collection throwing techniques using opensim and an emg-assisted solver. *Journal of Biomechanics*, page e109704, 2020. 3041 3042 3043
- [83] N. Monteiro, M. Silva, J. Folgado, and J. Melancia. Structural analysis of the intervertebral discs adjacent to an interbody fusion using multibody dynamics and finite element cosimulation. *Multibody System Dynamics*, 25(2):245–270, 2011. 3044 3045 3046 3047
- [84] S. P. Moroney, A. B. Schultz, J. A. A. Miller, and G. B. J. Andersson. Load-displacement properties of lower cervical spine motion segments. *Journal of Biomechanics*, 21(9):769–779, 1988. 3048 3049 3050
- [85] J. Mortensen, M. Trkov, and A. Merryweather. Exploring novel objective functions for simulating muscle coactivation in the neck. *Journal of Biomechanics*, 71:127–134, 2018. 3051 3052 3053
- [86] J. D. Mortensen, A. N. Vasavada, and A. S. Merryweather. The inclusion of hyoid muscles improve moment generating capacity and dynamic simulations in musculoskeletal models of the head and neck. *PLOS ONE*, 13(6):e0199912, 2018. 3054 3055 3056
- [87] J. D. Mortensen, A. N. Vasavada, and A. S. Merryweather. Sensitivity analysis of muscle properties and impact parameters on head injury risk in american football. *Journal of Biomechanics*, page 109411, 2020. 3057 3058 3059
- [88] M. P. Nagarkar, G. J. Vikhe Patil, and R. N. Zaware Patil. Optimization of non-linear quarter car suspension–seat–driver model. *Journal of Advanced Research*, 7(6):991–1007, 2016. 3060 3061 3062
- [89] N. Newell, G. Grigoriadis, A. Christou, D. Carpanen, and S. D. Masouros. Material properties of bovine intervertebral discs across strain rates. *Journal of the Mechanical Behavior of Biomedical Materials*, 65(Supplement C):824–830, 2017. 3063 3064 3065
- [90] R. S. Newell, J.-S. Blouin, J. Street, P. A. Crompton, and G. P. Siegmund. The neutral posture of the cervical spine is not unique in human subjects. *Journal of Biomechanics*, 80:53–62, 2018. 3066 3067 3068

- 3069 [91] R. S. Newell, G. P. Siegmund, J.-S. Blouin, J. Street, and P. A. Crip-ton. Cervical  
3070 vertebral realignment when voluntarily adopting a protective neck posture. *Spine*,  
3071 39(15), 2014.
- 3072 [92] R. W. Nightingale, C. R. Bass, and B. S. Myers. On the relative importance  
3073 of bending and compression in cervical spine bilateral facet dislocation. *Clinical*  
3074 *Biomechanics*, 64:90–97, 2019.
- 3075 [93] R. W. Nightingale, B. J. Doherty, B. S. Myers, J. H. McElhaney, and W. J.  
3076 Richardson. The influence of end condition on human cervical spine injury mech-  
3077 anisms. In *SAE Technical Paper*. SAE International, 10 1991.
- 3078 [94] R. W. Nightingale, J. H. McElhaney, D. L. Camacho, M. Kleinberger, B. A.  
3079 Winkelstein, and B. S. Myers. The dynamic responses of the cervical spine:  
3080 Buckling, end conditions, and tolerance in compressive impacts. In *SAE Technical*  
3081 *Paper*. SAE International, 11 1997.
- 3082 [95] R. W. Nightingale, J. H. McElhaney, W. J. Richardson, and B. S. Myers. Dynamic  
3083 responses of the head and cervical spine to axial impact loading. *Journal of*  
3084 *Biomechanics*, 29(3):307–318, 1996.
- 3085 [96] R. W. Nightingale, J. Sganga, H. Cutcliffe, and C. R. Bass. Impact responses of  
3086 the cervical spine: A computational study of the effects of muscle activity, torso  
3087 constraint, and pre-flexion. *Journal of Biomechanics*, 49(4):558–64, 2016.
- 3088 [97] T. D. O’Brien, N. D. Reeves, V. Baltzopoulos, D. A. Jones, and C. N. Maga-  
3089 naris. In vivo measurements of muscle specific tension in adults and children.  
3090 *Experimental Physiology*, 95(1):202–210, 2010.
- 3091 [98] O. M. O’Reilly, M. F. Metzger, J. M. Buckley, D. A. Moody, and J. C. Lotz. On  
3092 the stiffness matrix of the intervertebral joint: Application to total disk replace-  
3093 ment. *Journal of Biomechanical Engineering-Transactions of the Asme*, 131(8),  
3094 2009.
- 3095 [99] W. H. Organization and I. S. C. Society. International perspectives on spinal  
3096 cord injury. Report 9241564660, World Health Organization and International  
3097 Spinal Cord Society, 2013.
- 3098 [100] M. Panjabi, J. Summers, R. Pelker, T. Videman, E. Friedlaender, and O. South-  
3099 wick. Three dimensional load displacement curves due to forces on the cervical  
3100 spine. *Journal of Orthopaedic Research*, 4(2):152–161, 1986.

- [101] M. M. Panjabi, J. J. Crisco, A. Vasavada, T. Oda, J. Cholewicki, K. Nibu, and E. Shin. Mechanical properties of the human cervical spine as shown by three-dimensional load- displacement curves. *Spine*, 26(24):2692, 2001.
- [102] L. Pitto, H. Kainz, A. Falisse, M. Wesseling, S. Van Rossom, H. Hoang, E. Papageorgiou, A. Hallemans, K. Desloovere, G. Molenaers, A. Van Campenhout, F. De Groote, and I. Jonkers. Simcp: A simulation platform to predict gait performance following orthopedic intervention in children with cerebral palsy. *Frontiers in Neurorobotics*, 13:54, 2019.
- [103] C. Pizzolato, D. G. Lloyd, M. Sartori, E. Ceseracciu, T. F. Besier, B. J. Fregly, and M. Reggiani. Ceinms: A toolbox to investigate the influence of different neural control solutions on the prediction of muscle excitation and joint moments during dynamic motor tasks. *Journal of Biomechanics*, 48(14):3929–3936, 2015.
- [104] E. Preatoni, D. Cazzola, K. A. Stokes, M. England, and G. Trewartha. Prebinding prior to full engagement improves loading conditions for front-row players in contested rugby union scrums. *Scandinavian Journal of Medicine and Science in Sports*, 26(12):1398–1407, 2015.
- [105] M. M. Priebe, A. E. Chiodo, W. M. Scelza, S. C. Kirshblum, L.-A. Wuermsier, and C. H. Ho. Spinal cord injury medicine. 6. economic and societal issues in spinal cord injury. *Archives of Physical Medicine and Rehabilitation*, 88(3, Supplement 1):S84–S88, 2007.
- [106] A. S. Przybyla, D. Skrzypiec, P. Pollintine, P. Dolan, and M. A. Adams. Strength of the cervical spine in compression and bending. *Spine*, 32(15):1612–1620, 2007.
- [107] K. L. Quarrie, R. C. Cantu, and D. J. Chalmers. Rugby union injuries to the cervical spine and spinal cord. *Sports Medicine*, 32(10):633–653, 2002.
- [108] D. A. Race, D. N. Broom, and D. P. Robertson. Effect of loading rate and hydration on the mechanical properties of the disc. *Spine*, 25(6):662–669, 2000.
- [109] E. Reboursiere, Y. Bohu, D. Retière, B. Sesboüé, V. Pineau, J. P. Colonna, J. P. Hager, J. C. Peyrin, and J. Piscione. Impact of the national prevention policy and scrum law changes on the incidence of rugby-related catastrophic cervical spine injuries in french rugby union. *British Journal of Sports Medicine*, 52(10):674–677, 2018.
- [110] O. Röhrle, J. Davidson, and A. Pullan. A physiologically based, multi-scale model of skeletal muscle structure and function. *Frontiers in Physiology*, 3:358, 2012.

- 3134 [111] J. A. Rihn, D. T. Anderson, K. Lamb, P. F. Deluca, A. Bata, P. A. Marchetto,  
3135 N. Neves, and A. R. Vaccaro. Cervical spine injuries in american football. *Sports*  
3136 *Medicine*, 39(9):697–708, 2009.
- 3137 [112] S. P. Roberts, G. Trewartha, R. J. Higgitt, J. El-Abd, and K. A. Stokes. The phys-  
3138 ical demands of elite english rugby union. *Journal of Sports Sciences*, 26(8):825–  
3139 833, 2008.
- 3140 [113] A. Saari, C. R. Dennison, Q. Zhu, T. S. Nelson, P. Morley, T. R. Oxland, P. A.  
3141 Crompton, and E. Itshayek. Compressive follower load influences cervical spine  
3142 kinematics and kinetics during simulated head-first impact in an in vitro model.  
3143 *Journal of Biomechanical Engineering*, 135(11):111003–111003–11, 2013.
- 3144 [114] M. Sartori, D. Farina, and D. G. Lloyd. Hybrid neuromusculoskeletal modeling to  
3145 best track joint moments using a balance between muscle excitations derived from  
3146 electromyograms and optimization. *Journal of Biomechanics*, 47(15):3613–3621,  
3147 2014.
- 3148 [115] L. Scheys, A. Spaepen, P. Suetens, and I. Jonkers. Calculated moment-arm  
3149 and muscle-tendon lengths during gait differ substantially using mr based versus  
3150 rescaled generic lower-limb musculoskeletal models. *Gait and Posture*, 28(4):640–  
3151 648, 2008.
- 3152 [116] R. Schmidt, M. Richter, L. Claes, W. Puhl, and H.-J. Wilke. Limitations of the  
3153 cervical porcine spine in evaluating spinal implants in comparison with human  
3154 cervical spinal segments: A biomechanical in vitro comparison of porcine and  
3155 human cervical spine specimens with different instrumentation techniques. *Spine*,  
3156 30(11):1275–1282, 2005.
- 3157 [117] F. P. Secin, E. J. Poggi, F. Luzuriaga, and H. A. Laffaye. Disabling injuries of  
3158 the cervical spine in argentine rugby over the last 20 years. *British Journal of*  
3159 *Sports Medicine*, 33(1):33–36, 1999.
- 3160 [118] L. H. S. Sekhon and M. G. Fehlings. Epidemiology, demographics, and patho-  
3161 physiology of acute spinal cord injury. *Spine*, 26(24S), 2001.
- 3162 [119] E. Seminati, D. Cazzola, E. Preatoni, and G. Trewartha. Specific tackling sit-  
3163 uations affect the biomechanical demands experienced by rugby union players.  
3164 *Sports Biomechanics*, 16(1):58–75, 2017.

- [120] E. Seminati, D. Cazzola, E. Preatoni, and G. Trewartha. Specific tackling situations affect the biomechanical demands experienced by rugby union players. *Sports Biomechanics*, 16(1):58–75, 2017.
- [121] M. Senteler, B. Weisse, D. A. Rothenfluh, and J. G. Snedeker. Intervertebral reaction force prediction using an enhanced assembly of opensim models. *Computer Methods in Biomechanics and Biomedical Engineering*, 19(5):538–548, 2016.
- [122] G. Serrancolí, A. L. Kinney, B. J. Fregly, and J. M. Font-Llagunes. Neuromusculoskeletal model calibration significantly affects predicted knee contact forces for walking. *Journal of Biomechanical Engineering*, 138(8), 2016.
- [123] A. Seth, J. L. Hicks, T. K. Uchida, A. Habib, C. L. Dembia, J. J. Dunne, C. F. Ong, M. S. DeMers, A. Rajagopal, M. Millard, S. R. Hamner, E. M. Arnold, J. R. Yong, S. K. Lakshmikanth, M. A. Sherman, J. P. Ku, and S. L. Delp. Opensim: Simulating musculoskeletal dynamics and neuromuscular control to study human and animal movement. *PLOS Computational Biology*, 14(7):e1006223, 2018.
- [124] M. Shea, W. T. Edwards, A. A. White, and W. C. Hayes. Variations of stiffness and strength along the human cervical spine. *Journal of Biomechanics*, 24(2):95–107, 1991.
- [125] M. A. Sherman, A. Seth, and S. L. Delp. Wha is a moment arm? calculating muscle effectiveness in biomechanical models using generalised coordinates. *Proceedings of the ASME 2013 International Design Engineering Technical Conferences and Computers and Information in Engineering Conference*, 2013:V07BT10A052, 2013.
- [126] G. P. Siegmund, J.-S. Blouin, J. R. Brault, S. Hedenstierna, and J. T. Inglis. Electromyography of superficial and deep neck muscles during isometric, voluntary, and reflex contractions. *Journal of Biomechanical Engineering*, 129(1):66–77, 2006.
- [127] G. P. Siegmund, J.-S. Blouin, M. G. Carpenter, J. R. Brault, and J. T. Inglis. Are cervical multifidus muscles active during whiplash and startle? an initial experimental study. *BMC Musculoskeletal Disorders*, 9:80–80, 2008.
- [128] P. Silvestros and D. Cazzola. Cervical spine injury in rugby scrummaging: is buckling the most likely injury mechanisms? Technical Group of Computer Simulation, 2017.

- [129] P. Silvestros, E. Preatoni, H. S. Gill, S. Gheduzzi, B. A. Hernandez, T. P. Holsgrove, and D. Cazzola. Musculoskeletal modelling of the human cervical spine for the investigation of injury mechanisms during axial impacts. *PLOS ONE*, 14(5):e0216663, 2019.
- [130] S. Sobue, T. Kawasaki, Y. Hasegawa, Y. Shiota, C. Ota, T. Yoneda, S. Tahara, N. Maki, T. Matsuura, M. Sekiguchi, Y. Itoigawa, T. Tateishi, and K. Kaneko. Tackler’s head position relative to the ball carrier is highly correlated with head and neck injuries in rugby. *British Journal of Sports Medicine*, 52(6):353, 2018.
- [131] B. D. Stemper, N. Yoganandan, and F. A. Pintar. Validation of a head-neck computer model for whiplash simulation. *Medical and Biological Engineering and Computing*, 42(3):333–338, 2004.
- [132] B. L. Suderman and A. N. Vasavada. Moving muscle points provide accurate curved muscle paths in a model of the cervical spine. *Journal of Biomechanics*, 45(2):400–404, 2012.
- [133] B. L. Suderman and A. N. Vasavada. Neck muscle moment arms obtained in-vivo from mri: Effect of curved and straight modeled paths. *Annals of Biomedical Engineering*, 45(8):2009–2024, 2017.
- [134] F. Taddei, S. Martelli, G. Valente, A. Leardini, M. G. Benedetti, M. Manfrini, and M. Viceconti. Femoral loads during gait in a patient with massive skeletal reconstruction. *Clinical Biomechanics*, 27(3):273–280, 2012.
- [135] Y. Tanabe, T. Kawasaki, H. Tanaka, K. Murakami, K. Nobuhara, T. Okuwaki, and K. Kaneko. The kinematics of 1-on-1 rugby tackling: a study using 3-dimensional motion analysis. *Journal of Shoulder and Elbow Surgery*, 28(1):149–157, 2019.
- [136] D. G. Thelen. Adjustment of muscle mechanics model parameters to simulate dynamic contractions in older adults. *Journal of Biomechanical Engineering*, 125(1):70–77, 2003.
- [137] G. J. Tierney, K. Denvir, G. Farrell, and C. K. Simms. The effect of tackler technique on head injury assessment risk in elite rugby union. *Medicine and Science in Sports and Exercise*, 50(3), 2018.
- [138] G. J. Tierney, K. Denvir, G. Farrell, and C. K. Simms. Does ball carrier technique influence tackler head injury assessment risk in elite rugby union? *Journal of Sports Sciences*, 37(3):262–267, 2019.

- [139] G. J. Tierney, J. Lawler, K. Denvir, K. McQuilkin, and C. K. Simms. Risks associated with significant head impact events in elite rugby union. *Brain Injury*, 30(11):1350–1361, 2016.
- [140] G. J. Tierney, C. Richter, K. Denvir, and C. K. Simms. Could lowering the tackle height in rugby union reduce ball carrier inertial head kinematics? *Journal of Biomechanics*, 72:29–36, 2018.
- [141] J. S. Torg, H. Pavlov, M. J. O’Neill, C. E. Nichols, and B. Sennett. The axial load teardrop fracture: A biomechanical, clinical, and roentgenographic analysis. *The American Journal of Sports Medicine*, 19(4):355–364, 1991.
- [142] J. S. Torg, J. Truex, Raymond, T. C. Quedenfeld, A. Burstein, A. Spealman, and I. Nichols, Claude. The national football head and neck injury registry: Report and conclusions 1978. *JAMA*, 241(14):1477–1479, 1979.
- [143] R. Tucker, M. Raftery, S. Kemp, J. Brown, G. Fuller, B. Hester, M. Cross, and K. Quarrie. Risk factors for head injury events in professional rugby union: a video analysis of 464 head injury events to inform proposed injury prevention strategies. *British Journal of Sports Medicine*, 51(15):1152, 2017.
- [144] G. Valente, G. Crimi, N. Vanella, E. Schileo, and F. Taddei. nmsbuilder: Freeware to create subject-specific musculoskeletal models for opensim. *Comput Methods Programs Biomed*, 152(Supplement C):85–92, 2017.
- [145] G. Valente, L. Pitto, D. Testi, A. Seth, S. L. Delp, R. Stagni, M. Viceconti, and F. Taddei. Are subject-specific musculoskeletal models robust to the uncertainties in parameter identification? *PLoS ONE*, 9(11):e112625, 2014.
- [146] M. Van den Abbeele, F. Li, V. Pomeroy, D. Bonneau, B. Sandoz, S. Laporte, and W. Skalli. A subject-specific biomechanical control model for the prediction of cervical spine muscle forces. *Clinical Biomechanics*, 51:58–66, 2018.
- [147] M. van der Horst. *Human head neck response in frontal, lateral and rear end impact loading : modelling and validation*. Thesis, 2002.
- [148] C. A. Van Ee, R. W. Nightingale, D. L. Camacho, V. C. Chancey, K. E. Knaub, E. A. Sun, and B. S. Myers. Tensile properties of the human muscular and ligamentous cervical spine. *Stapp Car Crash J*, 44(1532-8546 (Print)):85–102, 2000.

- [149] W. van Mechelen, H. Hlobil, and H. C. G. Kemper. Incidence, severity, aetiology and prevention of sports injuries. *Sports Medicine*, 14(2):82–99, 1992.
- [150] A. N. Vasavada, E. Hughes, D. D. Nevins, S. M. Monda, and D. C. Lin. Effect of subject-specific vertebral position and head and neck size on calculation of spine musculoskeletal moments. *Annals of Biomedical Engineering*, 46(11):1844–1856, 2018.
- [151] A. N. Vasavada, R. A. Lasher, T. E. Meyer, and D. C. Lin. Defining and evaluating wrapping surfaces for mri-derived spinal muscle paths. *Journal of Biomechanics*, 41(7):1450–1457, 2008.
- [152] A. N. Vasavada, S. P. Li, and S. L. Delp. Influence of muscle morphometry and moment arms on the moment-generating capacity of human neck muscles. *Spine*, 23(4):412–422, 1998.
- [153] D. C. Viano, A. I. King, J. W. Melvin, and K. Weber. Injury biomechanics research: An essential element in the prevention of trauma. *Journal of Biomechanics*, 22(5):403–417, 1989.
- [154] M. Viceconti, J. D. Humphrey, A. Erdemir, and M. Tawhai. Multiscale modelling in biomechanics. *Interface Focus*, 5(2), 2015.
- [155] M. Viceconti, S. Olsen, L.-P. Nolte, and K. Burton. Extracting clinically relevant data from finite element simulations. *Clinical Biomechanics*, 20(5):451–454, 2005.
- [156] J. P. Walter, A. L. Kinney, S. A. Banks, D. D. D’Lima, T. F. Besier, D. G. Lloyd, and B. J. Fregly. Muscle synergies may improve optimization prediction of knee contact forces during walking. *Journal of Biomechanical Engineering*, 136(2), 2014.
- [157] A. A. White and M. M. Panjabi. *Clinical biomechanics of the spine*. Lippincott Philadelphia, 1978.
- [158] H.-J. Wilke, J. Geppert, and A. Kienle. Biomechanical in vitro evaluation of the complete porcine spine in comparison with data of the human spine. *European Spine Journal*, 20(11):1859–1868, 2011.
- [159] S. Williams, G. Trewartha, S. Kemp, and K. Stokes. A meta-analysis of injuries in senior men’s professional rugby union. *Sports Medicine*, 43(10):1043–1055, 2013.



- [160] World Rugby. Year in review 2019. [https://www.world.rugby/documents/](https://www.world.rugby/documents/annual-reports) annual-reports, June 2020.
- [161] V. R. Yingling, J. P. Callaghan, and S. M. McGill. Dynamic loading affects the mechanical properties and failure site of porcine spines. *Clinical Biomechanics*, 12(5):301–305, 1997.
- [162] N. Yoganandan, M. Haffner, D. J. Maiman, H. Nichols, F. A. Pintar, J. Jentzen, S. S. Weinshel, S. J. Larson, and A. Sances. Epidemiology and injury biomechanics of motor vehicle related trauma to the human spine, 1989.
- [163] N. Yoganandan, F. A. Pintar, J. Sances, Anthony, J. Reinartz, and S. J. Larson. Strength and kinematic response of dynamic cervical spine injuries. *Spine*, 16, 1991.
- [164] F. E. Zajac. Muscle and tendon: properties, models, scaling, and application to biomechanics and motor control. *Critical reviews in biomedical engineering*, 17(4):359–411, 1989.